Final Report
DSE Group 12

Bramlage, Jasper	4790316
Catalán Pastor, Victoria	4838688
Dąbrowski, Mateusz	4844726
van Dijk, Arthur	4888022
Driever, Leonhard X.	4771362
Lubach, Sven	4788095
Pettersen, Øyvind B.	4810511
Roman, Karol	4873947
Tournoy, Aster Merel A.	4862031
Verbist, Joe	4772393

June 29, 2021
Delft, the Netherlands

TU Delft

(This page is intentionally left blank.)

Acknowledgements

Throughout the Design Synthesis Exercise for the Bachelor degree at the faculty of Aerospace Engineering at the Delft University of Technology, we received much relevant support.

First we would like to thank our supervisor Ronald van Gent, who provided us with the idea of the distributed propulsion bush plane and gave us the opportunity to design a state-of-the-art aircraft. His insight, knowledge and constructive feedback was extremely helpful during the entire project. The continuous guidance Mr. van Gent offered to us was of huge benefit to our project.

Furthermore, we would like to acknowledge the help of our tutors Colin van Dercreek and Kunal Masania, providing valuable insight to the project. We are very grateful they were always willing to answer our questions and provide us with feedback.

Finally, we would like to thank the friends and family of all of our team members for all the support and positivity they brought to the group.

Executive Summary

Bush planes are general aviation aircraft, that enable transportation to remote areas, where there is no infrastructure supporting regular aviation. Their main features are the taildragger configuration, a short take off and landing distance (STOL) and they offer the ability to land on rough terrain. Paradoxically, although they are the aircraft most directly related to nature, bush planes are often old, polluting and loud, and thus far from being environmentally friendly. To partially overcome these disadvantageous characteristics, Group 12 designed a state-of-the-art bush plane, using the principle of distributed propulsion, called the *Twin Puffin*.

In order to design a bush plane, first an understanding is required of the needs and desires of the stakeholders. For this, a market analysis is performed and from this it can be concluded that the aircraft will serve for three main purposes: transport, medical emergency missions and tourism. After obtaining the insight into the market of bush planes, all possible design options are listed. Pruning of unfeasible, unrealistic and inapplicable options is done to end up with seven aircraft concepts. From those concepts, the most suitable and promising is then selected. The aircraft is chosen to be a twin boom concept, therefore the name *Twin Puffin* was chosen for the design. Following, the design is worked out in detail, where all the subsystems are designed. The fuselage, the structure of the plane, the energy source, the wing, the propulsion system, the empennage, landing gear and electrical systems are designed and optimised, so the final aircraft design is finalised.

Inspired by Nature, the bush plane is named the *Twin Puffin*. 'Twin' following the distinctive twin-boom empennage, and the 'Puffin', from the bird with a stubby display and a master of short take-off and landing on the ocean cliff-sides, a real inspiration for a STOL aircraft. The featured twin boom empennage make aft loading of cargo or a medical stretcher easy. Furthermore, the distributed propulsion is placed on the wing's leading edge, allowing unobstructed view during all flight phases, solving the typical visibility issues of a traditional bush plane. The distributed propellers are powered by a hybrid engine using both electricity from batteries and power generated by an internal combustion engine that can run on diesel, jet fuel, and suitable types of biofuels. This allows for an increase in available power and a local reduction in the emissions and noise during electrically-powered take-off and landing. Furthermore, the distributed electric propulsion lead to excellent STOL characteristics, as the blown air over the wing allow for a large increase in lift at low speeds. Moreover, the *Twin Puffin* is primarily built of the sustainable material flax fibre composite, making the aircraft more environmentally friendly. The *Twin Puffin* is estimated to produce 70% less noise and 50% emission, compared to competing aircraft and is thereby a modern, impressively performing bush plane design.

Figure 1: CAD-render of the *Twin Puffin* in cruise.

Contents

Nomenclature

The following list describes all abbreviations used in the report, in alphabetical order, followed by a complete list of symbols.

Abbreviations

CAD	Computer-Aided Design
CS-23	Certification Specification 23
DOT	Design Option Tree
DPF	Diesel Particulate Filter
DSE	Design Synthesis Exercise
EASA	European union Aviation Safety Agency
EPC	Engineering, Procurement, Construction
FAA	Federal Aviation Administration
FEED	Front end engineering design phase
ICAO	International Civil Aviation Organisation
ICE	Internal Combustion Energy
ISA	International Standard Atmosphere
JIT	Just In Time
LFP	A Lithium Iron Phosphate battery
NCA	A Lithium Nickel Cobalt Aluminium battery
NCV	Net Calorific Value
NMC	A Lithium Nickel Manganese cobalt battery
NPRD	Non-electronic Parts Reliability Data
OEW	Operational Empty Weight
POS	Project Objective Statement
RAMS	Reliability, Availability, Maintainability,Safety
RPM	Revolutions per Minute
SPL	Sound Power Level
STOL	Short Take-Off and Landing
TBD	To-Be-Determined
USD	United States Dollar
VARI	Vacuum Assisted Resin Infusion

Greek Symbols

α	Angle of attack	deg
α_{0L}	Angle of attack at zero lift	deg
α_s	Stall angle of attack	deg
β	Prandtl-Glauert correction factor	–
δa_{max}	Maximum aileron deflection	m
$\Delta_{fus} C_{m_{ac}}$	Fuselage moment coefficient	–
η_0	y-coordinate of the shear centre	m
γ	Flight path angle	deg
Γ_{prop}	Propeller slipstream circulation	$m^2\,s^{-1}$
Γ_{wing}	Wing circulation	$m^2\,s^{-1}$
Λ	Sweep angle of the wings	deg
λ	Taper ratio	–
$\Lambda_{c/2}$	Half chord sweep wing	deg
$\Lambda_{c/4}$	Quarter chord sweep wing	deg
$\Lambda_{hingeline}$	Hinge line sweep wing	deg
Λ_{LE}	Leading edge sweep wing	deg
$\Lambda_{x/c}$	Sweep at chordwise location x	deg
μ	Airfoil efficiency:	–
μ_1	Moment coefficient estimation constant	–
μ_2	Moment coefficient estimation constant	–
μ_3	Moment coefficient estimation constant	–
μ_b	Non-dimensional mass for asymmetric motion	–
ω	rotational rate	s^{-1}
ρ_∞	Free stream air density	m
σ_y	Yield strength	Pa
τ	Aileron effectiveness	–
θ	Pitch angle	deg
ξ_0	x-coordinate of the shear centre	m
ζ	Damping ratio	–

Latin Symbols

$\dot{m}_{fuelflow}$	Mass flow of fuel	kg
$\frac{d\epsilon}{d\alpha}$	downwash gradient	–
MTOW	Maximum Take-Off Weight	N
$\tilde{x_{ac}}$	x-position of the aerodynamic centre	m
$\tilde{x_{cg}}$	x-position of the centre of gravity	m
$x_{le\tilde{mac}}$	x-position of the leading edge of the MAC	m
A	Aspect Ratio in section 6.5; Area in section 6.2	–
a	Propeller velocity increase factor	–
A_v	Vertical Tail Aspect Ratio	–
A_{eff}	Effective aspect ratio	–
A_{geo}	Geometric aspect ratio	–
b	Wing span	m
b	Wing span	m
b_v	Vertical tail span	m
b_f	Fuselage width	m
B_r	Boom area	m^2
C_d, C_D	Drag Coefficient	–
C_L	Lift Coefficient	–
C_m	Moment coefficient	–

c_t	wing tip chord length	m
C_{D_0}	Zero lift drag coefficient	–
C_{D_c}	Component drag coefficient	–
C_{D_i}	Induced drag coefficient	–
$C_{D_{mic}}$	Miscellaneous zero lift drag component	–
C_{Dr}	Radius dependent drag coefficient	–
$C_{L_{\alpha_{A-h}}}$	Aircraft lift slope without tail	–
C_{L_α}	Slope of the lift curve	–
C_{l_β}	Rolling moment due to sideslip angle.	–
$C_{L_{\delta a}}$	Rolling moment derivative w.r.t rolling rate	–
$C_{L_{aug}}$	Augmented lift coefficient	–
$C_{L_{max}}$	Maximum lift coefficient	–
C_{l_p}	Rolling moment derivative w.r.t rolling rate	–
C_{l_r}	Rolling moment due to yaw-rate	–
C_{Lr}	Radius dependent lift coefficient	–
C_{m_α}	Moment coefficient slope	$1/rad$
$C_{m_{0airfoil}}$	Moment coefficient at α =0	–
$C_{m_{ac_w}}$	Wing moment coefficient	–
$C_{m_{ac}}$	Aircraft moment coefficient	–
$c_{mac}, \bar{c}$	Chord length of mean aerodynamic chord	m
C_{n_β}	Yawing moment coefficient due to sideslip angle.	–
C_{n_r}	Yawing moment due to yaw-rate	–
C_{op}	Operating Costs	€
c_{root}	Root chord length	m
C_{Y_β}	Vertical force due to sideslip angle.	–
C_{Y_v}	Vertical force of vertical tail.	–
c_y	Chord length at position y	m
D	Drag	N
d	Propeller radius	m
D_i	Induced drag	N
D_{prop}	Propeller diameter	m
E	Young's modulus	Pa
e	Oswald's efficiency factor	–
E_m	Young's modulus of the matrix	GPa
E_r	Young's modulus of the reinforcement	GPa
E_u	Upper boundary of the Young's modulus in a composite	GPa
f	Volume fraction of the fibres	–
h	height	m
h_{cruise}	height during cruise	m
h_f	Fuselage height	m
I_{xx}	Moment of inertia along x-axis	m^4
I_{xy}	Product of inertia along xy-plane	m^4
I_{yy}	Moment of inertia along y-axis	m^4
J	Advance ratio	–
K_z	Non-dimensional moment of inertia around the z-axis	–
L'	Augmented lift per unit span	N/m
L'_∞	Unaugmented lift per unit span	$\mathrm{N\,m^{-1}}$
L/D	Lift to drag ratio	–
l_f	fuselage length	m
l_h	Distance between AC of wing and tail	m
L_{design}	Design lift	N
l_{fn}	Length wing nose to wing root	m
l_f	Length of the Fuselage	m
L_{wing}	Wing lift	N
M	Mach number in section 6.5, Moment in section 6.2	–
$m_{CO_2,sp}$	CO_2 Emissions per passenger per kilometre	$\mathrm{g\,pax^{-1}\,km^{-1}}$
$m_{CO_2/fuel}$	CO_2 Mass per Mass of Fuel	$\mathrm{g\,g^{-1}}$
m_{CO_2}	CO_2 Emissions	$\mathrm{g\,pax^{-1}\,km^{-1}}$
M_{Drag}	Moment due to drag	N m
$m_{fuel_{descent}}$	Fuel Mass at begin descent	kg
m_{fuel}	Fuel Mass	kg
m_{mto}	Maximum Take-Off Mass	kg
$m_{NO_x/J}$	NO_x Mass per Unit of Energy	$\mathrm{g\,pax^{-1}\,km^{-1}}$
m_{NO_x}	NO_x Emissions	$\mathrm{g\,pax^{-1}\,km^{-1}}$
$m_{payload}$	Payload Mass	kg
m_{start}	Mass before departure	kg
N_{1m}	Noise at 1 m distance	dB
N_{2500m}	Noise 2500 m downrange	dB
N_e	Number of engines	–
n_{pax}	Number of seats	–
n_{ult}	Ultimate load factor	–
P	Rolling rate	–
q	Dynamic pressure	Pa
q_∞	Free stream dynamic pressure	Pa
q_b	Basic shear flow	$\mathrm{N\,m^{-1}}$
q_{cruise}	Cruise dynamic pressure	Pa
q_{s0}	Shear flow at cut	$\mathrm{N\,m^{-1}}$
q_s	Shear flow	$\mathrm{N\,m^{-1}}$
R	Design Range	km
R	Range	km
r	distance from centre of rotation	m
S	Surface area	m^2
S_h	Surface area of the horizontal tail	m^2
S_x	Shear in x-direction	N
S_y	Shear in y-direction	N
S_{ref}	Reference wing area	m^2
s_{to}	Take-Off Distance at h=2500	m
S_{wet_c}	Component wetted area	m^2
S_{wf}	Flapped wing area	m^2

T	Thrust	N
t	thickness	m
t/c	Thickness to chord ratio	–
T_{prop}	Thrust per engine	N
V_c, V_{cruise}	Cruise Speed	$m\,s^{-1}$
V_h	velocity of the horizontal tail	$m\,s^{-1}$
V_x	Velocity in x-direction	$m\,s^{-1}$
V_x	Velocity in y-direction	$m\,s^{-1}$
V_∞	Free stream velocity	$m\,s^{-1}$
V_{climb}	Climb rate	$m\,s^{-1}$
V_{ep}	Propeller exit velocity	$m\,s^{-1}$
v_{max}	maximum deflection	m
V_{MC}	Minimum control speed	$m\,s^{-1}$
V_{stall}	Stall velocity	$m\,s^{-1}$
W/S	Wing loading	$N\,m^{-2}$
$W_{cruise,end}$	Weight at end of cruise	N
$W_{cruise,start}$	Weight at start of cruise	N
W_{mto}	Maximum Take-Off Weight	N
x_{ac}	x-position of the aerodynamic centre	–
x_r	x position of the boom	m
y_{mac}	y-position of the mean aerodynamic chord	m
y_r	y position of the boom	m

List of Tables

List of Figures

1 Introduction

The Twin Puffin distributed propulsion bush plane offers fast and easy transport, whenever remote and undeveloped areas lack the basic infrastructure to support regular aviation. Bush planes are general aviation STOL aircraft, used to transport people and goods to and from remote areas. Traditional bush planes show neither innovative features nor improve the existing noise and emission issues. To tackle these drawbacks, group 12 designed a state-of-the-art distributed propulsion bush plane, yielding in a modern, high-performing, short take-off and landing aircraft.

The objective of this report is to present the finalised conceptual design of the bush plane using distributed propulsion. To have a robust final design, the first step was to come up with possible design options. Based on an analysis of stakeholders and the corresponding requirements, multiple design concepts have been established and described in the Baseline Report [18]. Then a formal trade-off was performed between those selections to choose the most suitable design, as described in the Midterm Report [17]. The following design step is to design the chosen concept in depth, where the subsystems and the final product are defined in detail, which is the aim of this report.

The report is divided into three parts of different focus. Part I: Setting up the Design Space begins with Chapter 2, which provide a deeper insight into the project objective. The target market is analysed in Chapter 3. In this chapter, the current market of bush planes is studied, the competition of bush planes is examined, the possible new markets are analysed, the current and further use cases are listed. In Chapter 4, the requirements, based on the market analysis, are examined. Chapter 5 provides an in-depth explanation of the initial design steps, executed before the final design was created. Marking the beginning of Part II: Detailed Design Methods, in Chapter 6 the methods used for the design of the subsystems are explained. Following on this, the parameter and optimisation is explained in Chapter 7, where the definition of the objective function, the mission model tool, the optimisation of the aircraft parameters and the verification of the tool are discussed. The remainder of the report falls into Part III: FInal Aircraft Design: In Chapter 8, information regarding the final aircraft design is provided, where an overview of the parameters of the final design is given as well as the mission definition, the aircraft performance and the subsystem characteristics. Furthermore, the assessment of the aircraft design is discussed in Chapter 9. In Chapter 10, the continuation of the project is discussed. The methods for the product validation is analysed as well as the financial analysis, the scheduling of post-DSE activities and the production plan. Finally, a general conclusion is given in Chapter 11.

Part I:

Setting up the Design Space

2
Project Objectives

This chapter explains how the design of the distributed propulsion bush plane falls into the greater framework of the *DSE* of the TU Delft Aerospace Engineering bachelor's program. Presented in Section 2.1 is an explanation of the specific aims driving the project, and Section 2.2 outlines the depth to which the design process will be taken.

2.1. Aims of the Project

The Design Synthesis Exercise (DSE) is the final step for students to obtain their Bachelor's degree at the faculty of Aerospace Engineering at Delft University of Technology. During ten weeks, ten students are asked to provide an aircraft design, to get full experience in the field of *System Engineering*. The aim of project group 12 is to come up with a finalised design that provides the ability of transportation to remote areas and where infrastructure supporting general aviation is lacking. On the highest level, the design of the distributed propulsion bush plane is driven by the mission need statement, which is formulated to reflect the most generalised purpose that the aircraft shall serve. This statement is phrased as stated below.

> *The product shall provide remote communities with an affordable and dependable means of transportation to reach other communities, regardless of weather, altitude or infrastructure.* [18]

To fulfil this project effectively and with high quality, group 12 set up a strong group organisation both managerial and engineering wise. Therefore, the online communication was trouble-free, during those aforementioned ten weeks, and the project itself went effectively as possible.

2.2. Scope of the Project

The scope of the DSE of group 12 is to provide a detailed conceptual design of a bush plane using the principle of distributed propulsion, as an innovative idea to improve the noise and emissions of the rather outdated commonly-used bush planes. In addition, the project objective statement is defined to be the following.

> *Within 10 weeks, DSE Group 12 will design a bush plane that uses distributed propulsion, can carry a stretcher, and transport up to four passengers. [18]*

In order to meet the project objective statement, it is important to come up with a robust design, that fulfils the stakeholder needs and for which the technical and managerial risks are clearly analysed. The level of detail of the design of the *Twin Puffin* is as such that main key aspects are considered, but not yet ready for production. However, methods and plans of attack for other aspects, that are of less essence, are yet established.

3
Identification of Target Market

The identification of the target market is an inherent part of any project which highly affects the success of the project. It is vital to recognise where the product can be sold and under what conditions. Also, a profound understanding of the market helps to design a product that is more suitable for customers' needs, and hence will be more desired. To do so, the market analysis plays an important role in identifying and shaping the stakeholder requirements placed on the aircraft.

During the identification of the target market, three most relevant user cases arose: the transportation use, emergency/medical use and tourism. In the later sections of this chapter, reasoning is provided why it is deemed that the Twin-puffin may prove to be competitive among those applications.

In order to provide clear and comprehensive analysis of the target market, the chapter firstly assesses the current market for bush planes and then the competition of bush planes is analysed. Afterwards the benefit of distributed propulsion and its effect on the creation of new markets is explored. Finally, the identified use cases and their analysis are presented.

3.1. Assessment of Current Bush Plane Market

In order to show comprehensively how the Twin-Puffin can revolutionise the general aviation industry, first a brief analysis of the bush plane market is performed. Bush planes are known for their versatility and extensive applications thus, it is no surprise that in recent years they gained in popularity. In this section, the past development, current state, and the future prospects, of the market are presented with focus on the aspects related to the prospective user cases of the Twin-Puffin.

3.1.1. Popularity and Characteristics

Talking about popularity of the bush planes, it is imperative to mention the vast number of the societies of the unconventional planes enthusiasts. Sometimes referred to as 'backcountry flying' clubs, the societies are extremely vibrant and serve as great mediums to connect the pilots eager to exchange their ideas for plane improvements or destinations for excursions. Prominent examples of such societies are 'Backcountry Pilot'[1] or 'Canadian Bushplane Heritage Centre'[2].

Another premise portraying the popularity of the bush planes is the statistics for general aviation aircraft use in the US. In a special activity survey composed in 2013 by the Federal Aviation Administration (FAA) of the US, data on the population and its characteristics as well as the flying time of aircraft was gathered [3]. The report conveys how big the market is. In the US, it was estimated that the population of aircraft would be over 250 thousand with almost 200 thousand aircraft active. Also, the largest numbers of planes were observed in California, Texas and Florida, states, which apart from having largest number of inhabitants in the US, are also known for significant area sizes and natural parks to visit. Thus, the dependency between the landscape and the number of aircraft can be suspected.

Another very interesting conclusion that can be drawn from the report concerns the age of the population of general aviation aircraft in the US. The data gathered in the report suggests that over 110 thousand planes, which is 55% of the active aircraft are over 40 years old. Despite long life expectancy of aircraft, this premise may imply that large part of them may become obsolete in the upcoming years [3]. New technologies for aircraft are becoming increasingly common and some of them are already a necessity for safety as dictated by law. Thus, it could be suspected that a cavity will appear in a market of general aviation.

It is believed that despite the fact that the data was gathered for the entire general aviation market, it can still be representative for bush planes. The aircraft in the report were grouped in categories depending on their application and type. The group of particular interest for the bush plane market was the group of aircraft referred to as 'experimental' (believed to contain bush planes), which amounts to 12.5% of the entire population[3].

[1] URL https://backcountrypilot.org/base [cited 21 June 2021]
[2] URL https://www.bushplane.com/exhibits-online/bushplanes/ [cited 21 June 2021]

3.1.2. Demand

As implied in the Section 3.1.1, the market for bush planes is considerable. There exists number of bush plane enthusiasts and the number of such aircraft is large. However, it does not directly translate into a large demand on new bush aircraft. It is a very challenging task to accurately asses the demand on such a niche market and thus, is far beyond the scope of this paper. Nevertheless, some preliminary attempts to estimate the demand have been made and their results are presented in this subsection.

It is often the case that old utility aircraft are acquired to be transformed into bush planes, making it difficult to keep track of the sales and population of bush planes. Fortunately, there also exist companies that are primarily occupied with building bush planes and those can help measuring the demand with their sales records. One notable example of such a company is 'CubCrafters'[3]. This company manufactures small, high quality and high performance bush planes and is widely renowned. As it could be seen in the Table 3.1 the total number of aircraft sold by the 'CubCrafters' amounts to almost one hundred pieces which is a rather unimpressive number.

Another example of a manufacturer producing small general aviation aircraft is 'Diamond'[4]. Despite the fact that those are not usually suitable for bush plane type application, the records of their sales still can be representative for the market that is close to the bush plane one. In the Table 3.2 it is showed that the producer sold more than three thousand of two of their models piston single engine aircraft in the last 25 years.

3.1.3. Sustainability

The aspect of sustainability is becoming increasingly important in aviation nowadays. Despite that, the current bush plane market is not well adjusted to the latest standards on emissions. As explained in the previous sections, the vast majority of bush planes are old aircraft and their designs are often negligent with respect to the efficiency. Currently, most bush planes use large reciprocating engines with large propellers. This constitutes to high CO2 and noise emissions. The fact that the conventional bush planes poorly adhere to the latest standards on sustainability, may in near future contribute to their decline. In most developed countries, aviation authorities consider implementing rules that would ban operation of high polluting aircraft, which could have a sever effect on the current bush planes population.

3.2. Analysis of competition

To further investigate the target market for the *Twin Puffin*, it is crucial to perform an analysis of what is deemed to be the potential competition. This is meant to help understand the dynamics of the market and to determine key parameters of the product so that it satisfies the market needs. For that reason, an extensive overview of the main aircraft competing with the *Twin Puffin* in general aviation aircraft has been created. Furthermore, trends in the market value of the main competitive aircraft are analysed and additional requirements for the *Twin Puffin* are determined.

3.2.1. Main Competitive Aircraft

The aircraft identified as direct competition for the *Twin Puffin* are of similar class in terms of size and performance. They have been split into two main categories the *Taildraggers*, and the *Tricycles*. Data for these reference aircraft is shown in Table 3.1 and Table 3.2 [5]. Traditionally, the taildraggers have been associated with performance characteristics important for missions performed by Bush Planes. These include STOL capabilities, high rate of climb, and robust, simple to repair design. On the other hand, the tricycles selected for the market overview have characteristics important for transportation needs.

Table 3.1: Overview of competition in the General Aviation Market (taildraggers).

	AC 7ECA Citabria Aurora	*AC 8GCBC Denali Scout*	*AC 8KCAB Xtreme Decathlon*	*Aviat Husky A-1*	*Cub Crafters Top Cub CC18*	*Cub Crafters XCub CC19*	*Maule M-4 (O-360-C1F)*	*Maule M-7-235B*
Sold [#]	5238	-	6000	650	74	20	474	500
Range [Nmi]	556	680	509	695	495	695	821	800
Climb speed [m/min]	226	435	457	457	244	457	305	457
Cruise speed [kts]	100	113	129	122	110	126	120	139

[3]URL http://cubcrafters.com/ [cited 28 June 2021]
[4]URL https://www.diamondaircraft.com/en/ [cited 28 June 2021]
[5]URL https://customer-janes-com.tudelft.idm.oclc.org/janes/home [cited 4 June 2021]

Table 3.1: Overview of competition in the General Aviation Market (taildraggers).

	AC 7ECA Citabria Aurora	*AC 8GCBC Denali Scout*	*AC 8KCAB Xtreme Decathlon*	*Aviat Husky A-1*	*Cub Crafters Top Cub CC18*	*Cub Crafters XCub CC19*	*Maule M-4 (O-360-C1F)*	*Maule M-7-235B*
Stall speed [kts]	46	43	51	37	42	40	35	35
Noise [dB]	-	74.4	76.8	75.1	83	79.3	81.9	73.2
Price [kUSD]	155	290	295	360	285	335	160	290
MTOW [kg]	794	975	816	1021	1043	1043	1043	1134
Age [years]	60	47	51	32	17	5	60	40
OEW [kg]	508	644	599	578	544	552	633	728
Take-off roll [m]	321	217	292	122	177	52[6]	214	183
Usable mass [kg]	286	331	217	443	499	491	410	406

Table 3.2: Overview of competition in the General Aviation Market (tricycles).

	Beechraft Bonanza 36	*Cessna 172S SP Skyhawk*	*Cessna 182T Skylane*	*Cirrus SR20*	*Cirrus SR22 G5*	*Diamond DA20 Katana*	*Diamond DA40NG DS.*	*Piper PA-28 Cherokee*	*Tecnam P2010*
Sold [#]	17000	44000	25000	1500	6200	1000	2200	33000	30
Range [Nmi]	847	518	820	627	925	703	948	629	545
Climb speed [m/min]	375	223	282	252	387	203	215	201	240
Cruise speed [kts]	165	124	140	155	142	122	125	117	137
Stall speed [kts]	59	48	49	56	60	45	60	48	52
Noise [dB]	-	77.2	81.1	82	85	66.5	71.4	74.2	77.6
Price [kUSD]	890	390	490	595	755	235	460	360	350
MTOW [kg]	1656	1157	1406	1383	1633	800	1310	975	1160
Age [years]	75	65	65	22	20	27	24	61	10
OEW [kg]	1193	744	891	964	1022	525	900	559	710
Take-off roll [m]	584	497	462	677	330	500	397	244	595
Usable mass [kg]	463	413	515	419	611	275	410	416	450

Looking at the reference aircraft of Table 3.1 and Table 3.2, there are two aircraft that shall be used as main reference points when directly comparing the *Twin Puffin* to its competition. These two aircraft are the taildragger *Cub Crafters Top Cub* and the tricycle *Cessna 172S SP Skyhawk*.

3.2.2. Analysis of Aircraft Value

The full database of reference aircraft shown in Table 3.1 and Table 3.2 is furthermore used to analyse the relation between the key performance characteristics, such as range or cruise speed, and the market value of an aircraft. Such a relation will be essential when creating the final *Twin Puffin* design and wanting to quantitatively judge the relative value of different design options. The results presented here will thus be applied for the definition of the optimisation objective function in Section 7.3.2.

The method used to analyse the reference data follows the observation that aircraft, especially within the same family of aircraft, will increase in price with increasing (advertised) performance. To complete the statistical analysis, the aircraft database in Table 3.1 and in Table 3.2 are concatenated and combined in a linear regression model. The division between taildragger and tricycle aircraft is maintained as it became clear from advertised performance that taildragger aircraft are mostly valued for their STOL-performance, while tricycle aircraft where mostly advertised with performance values such as range, and cruise speed. In the following analysis, the regression is done twice to differentiate these type of aircraft. Landing distance and climb rate

[6] This value corresponds to the take-off run (without taking into account the distance to overcome a 50 ft

were used as basis functions for the taildragger aircraft, while cruise speed, range, and useful load formed the basis functions for the tricycle configuration aircraft.

The initial idea was to use quadratic or exponential basis functions for the regression, to include the effect of diminishing returns, but this proved inaccurate as the discovery was made that the comparison of retail price to these performance parameters formed a plane when placed in a scatter plot. The basis functions were therefore limited to a monomial basis of just a constant and first term. The basis functions are summarised in Table 3.3, where the superscripts $tail$ and tri indicate that the basis functions were used for the taildragger and tricycle aircraft, respectively.

Table 3.3: The basis functions used in the regressional analysis of the aircraft retail prices.

SYMBOL	*DESCRIPTION*
	Taildragger
φ_0^{tail}	Constant term.
φ_1^{tail}	Take-off distance, over 50 ft obstacle [m].
φ_2^{tail}	Climb rate at sea-level [m min^{-1}].
	Tricycle
φ_0^{tri}	Constant term.
φ_1^{tri}	Cruise speed at 75% power [kts].
φ_2^{tri}	Useful load [kg].
φ_3^{tri}	Range [Nmi].

The goal of the regression is to form two equations of the type as seen in Equation 3.1, one for each undercarriage configuration. For M basis functions, and N data points, the dot product of the basis is functions is defined as in Equation 3.2, and the matrix equation, with f the vector of retail values of the associated aircraft, is as seen in Equation 3.3 [31].

$$\phi(\mathbf{x}) = \sum_{i=1}^{M} a_i \varphi(\mathbf{x}) \qquad (3.1) \qquad \langle \varphi_k, \varphi_j \rangle = \sum_{i=1}^{N} \varphi_k(x_i)\varphi_j(x_i) \qquad (3.2)$$

$$\begin{bmatrix} \langle \varphi_1, \varphi_1 \rangle & \cdots & \langle \varphi_1, \varphi_M \rangle \\ \vdots & & \vdots \\ \langle \varphi_M, \varphi_1 \rangle & \cdots & \langle \varphi_M, \varphi_M \rangle \end{bmatrix} \begin{bmatrix} \hat{a}_1 \\ \vdots \\ \hat{a}_M \end{bmatrix} = \begin{bmatrix} \langle f, \varphi_1 \rangle \\ \vdots \\ \langle f, \varphi_M \rangle \end{bmatrix} \qquad (3.3)$$

After solving for $\mathbf{a} = [\hat{a}_1, \cdots, \hat{a}_M]$, for each of the aircraft types, using the associated values in the aircraft database, the least-squares approximations are of the form seen in Equation 3.4. The value of a potential aircraft design can then be assessed using the function shown in Equation 3.5. It is the summation of the two least-square approximations for each of the landing gear configuration types, using the associated basis functions in Table 3.3

$$\hat{\phi}(\mathbf{x}) = \sum_{i=1}^{M} \hat{a}_i \varphi_i(\mathbf{x}) \qquad (3.4) \qquad F(\mathbf{x}) = \hat{\phi}^{tail}(\mathbf{x}^{tail}) + \hat{\phi}^{tri}(\mathbf{x}^{tri}) \qquad (3.5)$$

Figure 3.1 and Figure 3.2 work to illustrate the results of the regression, compared to a scatter plot of the used database. They highlight the linear correlation exploited to form the objective function. Note that for representation purposes, the regression shown in Figure 3.2 is not the same regression completed for the objective function, but an analysis conducted using the same tool for one less dimension.

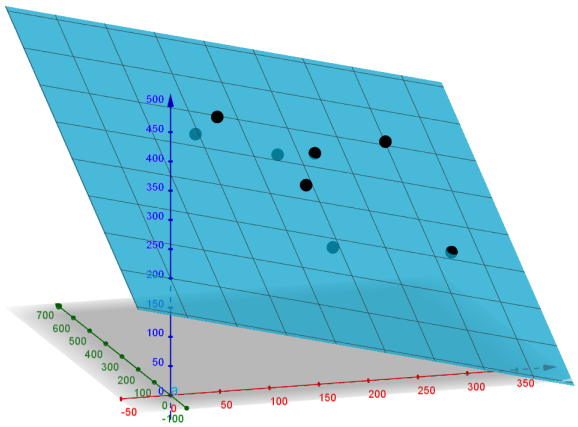

Figure 3.1: A 3D-plot of take-off distance (x), climb rate (y), and retail price (z), together with the least-squares estimate, showing the linearity of their correlation.

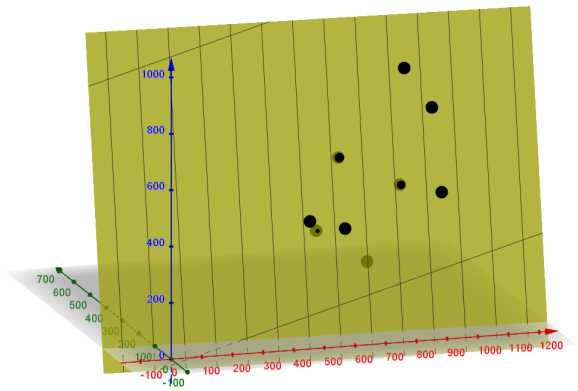

Figure 3.2: A 3D-plot of range (x), cruise speed (y), and retail price (z), together with the least-squares estimate, showing the linearity of their correlation.

3.2.3. Market Requirements

In order to make a successful product, it is important to have an overview of what the potential customers demand. To find this information, the characteristics of established competitive designs where studied. The specific parameters of interest are the aircraft usable weight (which includes payload and fuel weight) and the number of passengers that the aircraft can carry. The metric used to judge which values for these parameters are most prominent among the competition is the number of aircraft sold per year. The aircraft data[7] is graphically summarised in Figure 3.3.

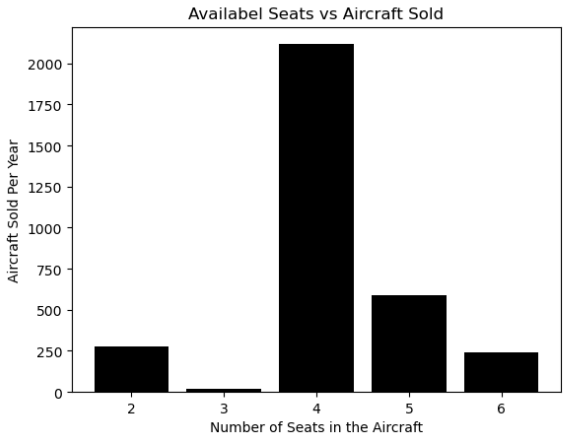

(a) Seats available plotted against aircraft sold per year

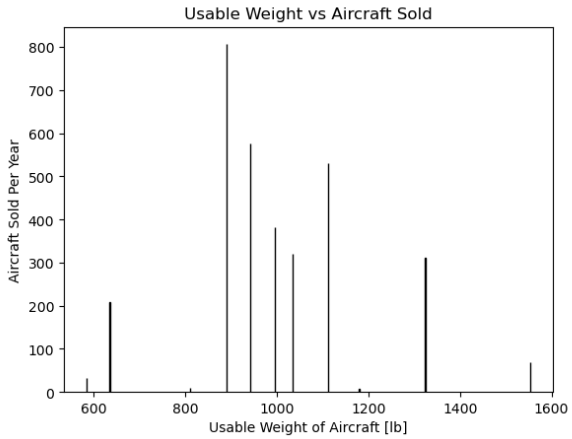

(b) Usable weight plotted against aircraft sold per year

Figure 3.3: Graphical representation of the data collected for a set of competitive reference aircraft

As follows from Figure 3.3a, the majority of competitive aircraft have four seats, facilitating one or two pilots and two or three passengers. For the subset of taildragger reference aircraft, which closer reflect the market of traditional bush planes, the most common number of seats is two. However, limiting the assessment of competition to traditional bush planes alone, would neglect that this to-be-designed distributed propulsion bush plane is intended for applications going beyond those of traditional bush planes. Should fewer seats be required, when operating in the same market as traditional bush planes for example, it will easily be possible to remove two seats and thereby free up more mass and volume for cargo transportation.

The usable weight of the aircraft indicates the difference between maximum take-off weight and operational empty weight, indicating the mass available for fuel, crew, passengers, and cargo. From Figure 3.3b it follows that the majority of sold aircraft have a usable weight in the range of 900 lb to 1100 lb (410 kg to 500 kg).

[7] URL https://shop.janes.com/Yearbooks-IHS/All-the-World-s-Aircraft/ [cited 19 May 2021]

Consequently, to accommodate for the apparent demand of the bulk of the market, the aircraft shall be designed such that it facilitates a usable weight corresponding to 500 kg.

Therefore, the analysis of the competition has brought forward two additional requirements that the *Twin Puffin* will have to meet in order to be more successful on the market. Firstly, requirement *TP-MA-1* states that the aircraft will have to be able to facilitate up to four seats. Secondly, *TP-MA-2* shall require that the aircraft is able to facilitate a usable mass of at least 500 kg.

3.3. Advantages of Distributed Propulsion

The undisputed advantage of the *Twin Puffin* as compared to the older generation bush planes is the ground-breaking improvement of the propulsion system. The use of distributed propulsion is a flagship feature of the *Twin Puffin* and is believed to provide it with advantages over its competitors described in the Section 3.2. In this section, the specific benefits of the distributed propulsion and their possible effects on the market are explored. In few words, the most notable effects are better STOL performance, greater efficiency, and 'lower noise to surrounding communities'[30].

3.3.1. Controllability

Controllability of aircraft is always of vital importance for the mission. It affects the safety, which is always the highest priority. Thus, the special attention is drawn to this aspect and full advantage of distributed propulsion is taken to maximise it.

Because of the improved controllability of the aircraft, missions can take place at less accessible locations. It allows the *Twin Puffin* for steeper ascends, descends and sharper turns. These features make it nimble and more attractive to fly. It can have an effect on the market, as *Twin Puffin* would be able to reach destinations where agility is required.

Another plausible advantage of having better controllability is being more adapted to urban aviation. The prospects of urban mobility for aircraft are becoming increasingly realistic and achievable, and it is suspected that agility may be a key factor in the prospective rules regarding flying in urban areas. That has to do with the fact that while distributed propulsion would make the *Twin Puffin* quieter than the competition, it is still desired to be able to climb and descent as quickly as possible to further reduce the noise footprint.

3.3.2. Lift Improvement

The distributed propulsion has another notable advantage, namely the improvement of the lift coefficient. Thanks to energising the airflow over the wing by the series of propellers, the lift experienced by the aircraft is dramatically higher.

The result of improved lift value for the aircraft is lower stall speed. This means that the aircraft can fly slower, which again may be a desired property for aircraft potentially operating in urban environment. Also, sightseeing flights can improve in quality when the flights around an object of interest can occur with lower speed. More information on this subject is provided in Section 6.4.

3.3.3. Improvement of STOL characteristics

STOL, short take-off and landing characteristics are what defines a bush plane. Thus, improving those characteristics is more than desired from the *Twin Puffin*. Thanks to the concept of the distributed propulsion applied in the aircraft, the lift of the aircraft is increased as explained in the previous section. 'Spanwise high lift via high-aspect-ratio trailing-edge nozzles for vectored thrust providing powered lift, boundary layer control, and/or supercirculation around the wing, all of which enable short take-off capability'[30]. This has crucial importance for the short runway requirement during take-off and landing.

The possibility of taking off and landing at a very short runway can prove to be important for operating at rough terrain in mountains or small airports located in cities.

3.3.4. Reduction in Noise

The noise limitations is the main factor that limits access of many aircraft into noise sensitive areas, such as urban residential areas or natural inhabitants of particular national or regional performance. Due to the fact that distributed propulsion offers substantial improvements in terms of total noise produced by 'better integration of the propulsion system with the airframe [30] the aircraft could be expected to operate at more noise sensitive areas.

3.3.5. Maintenance

Final advantage of the distributed propulsion mentioned in this section is its effect on maintenance. The distributed propulsion enables 'high production rates and easy replacement of engines or propulsors that are small and light'[30]. Because of the small size and large number of the motors, each motor is relatively inexpensive.

Thus in case of failure of one it can be easily replaced. Electric motors are also widely available, thus the replacement work does not need to be delayed by timely delivery of a rare part as it is sometimes the case with traditional propulsion. Nevertheless, the increase in number of engines does contribute to increase in complexity of the system. For that reason, the effect of this advantage of distributed propulsion is expected to be smaller than outlined in Kim et al. (2019) [30].

3.3.6. Reduction in Emissions

Distributed propulsion offers substantial improvements in terms of efficiency of the propulsive subsystem. For that reason, it offers lower emissions per kilometre travelled per passenger in the plane. The advantages of this is not only having more sustainable aircraft but also making the flight cheaper as less fuel is required.

3.4. Market for the *Twin Puffin*

The predictions about the size of general aviation market, and consequently the predictions regarding the market for the *Twin Puffin*, are outlined in this section. Due to the fact that many bush planes are rather old designs, it is difficult to predict the demand for those. For that reason, market for the *Twin Puffin* is predicted using data for piston engine aircraft, due to their comparable size and performance. Because the *Twin Puffin* is capable of performing missions typical for normal general aviation aircraft, this approach is deemed as applicable. To present the market for the *Twin Puffin* comprehensively, firstly the market trends and characteristics are presented. Subsequently, they are followed by assessment of what is deemed to be a realistic market share achievable for the *Twin Puffin*.

3.4.1. General Market Trends

Figure 3.4 presents market trends in the general aviation sector[3]. Over the last 20 years it can be seen that the number of flown hours remained rather constant. Lack of incline can be partially explained by the stagnant economy in many countries as a repercussion of the recession of 2008. However, even though the hours flown did not increase significantly, they are still considerable. On that figure, particular attention shall be brought to the 'Fixed Wing Piston' aircraft, because those aircraft are usually of the similar size to the *Twin Puffin*. For the past 20 years, the number of hours flown by this category remained almost unaffected and they still account for approximately half of the total hours flown by the general aviation. Thus, the market for the *Twin Puffin* may seem to be stable.

However, the question that remains to be answered are trends in the demand for small general aviation aircraft in the next 10 - 20 years. As said previously, the market is significant, however current fast converting aircraft industry may bring some changes. Again, to inspect that, the Figure 3.4 can be of help.

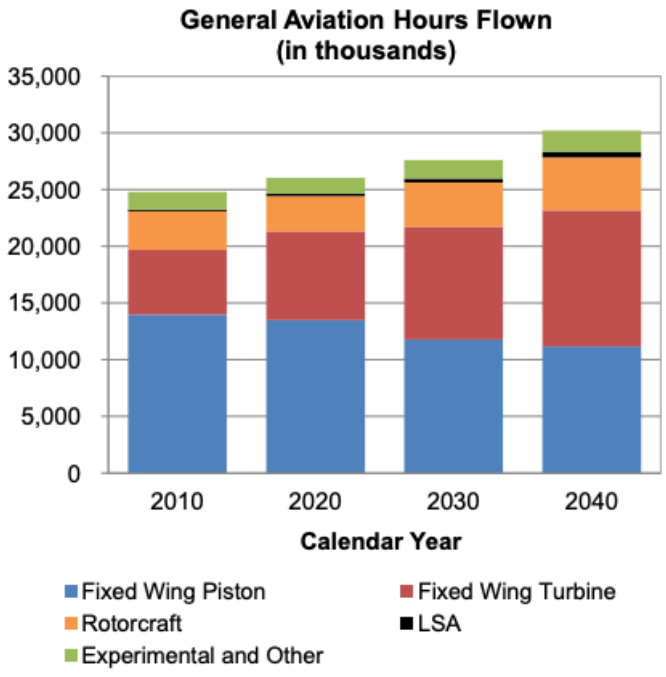

Figure 3.4: Predictions about the size of the general aviation market.

While the total number of hours flown by general aviation aircraft is excepted to increase, that figure will

actually decrease for fixed wing piston engine aircraft. The primary reason for that decline is believed to be the environmental concerns as the 'Fixed Wing Piston' category poorly addresses the sustainability aspect. It is expected that the air-authorities around the world (most significantly for the *Twin Puffin* in the US and Europe) in near future are going to implement more strict rules on CO2 emissions for aircraft[8]. Also, as an effect of the environmental concerns, unnecessary flights are burdened with a social stigma known as 'flight shaming'. This phenomenon is also believed to have significant influence on the decline in the category[9]. For those reasons, the 'Fixed Wing Piston' will experience an decline in the upcoming years.

At this point however, fortunately for the *Twin Puffin*, the resemblance between this project and the 'Fixed Wing Piston' aircraft is no longer valid. This is because of the dramatically more efficient and 'eco-friendly' design of the *Twin Puffin*. Potentially, the *Twin Puffin* can prove to remain competitive as it limits the CO2 and is built with sustainability in mind. Thus, the decline in the 'Fixed Wing Piston' market does not necessarily mean that the *Twin Puffin* will become obsolete.

3.4.2. Achievable Market Share

The global market for aircraft of similar size as the *Twin Puffin* can be estimated as approximately 1250 aircraft sold each year [3]. However, the *Twin Puffin*, being a new product, will initially lack recognition among its competitors, leading lower demand. Thus, a realistic sales rates need to be assessed. This can be done with the help of the current distribution of the aircraft sold per year, per manufacturer. Figure 3.5 [10] presents the market share of biggest general aviation aircraft companies.

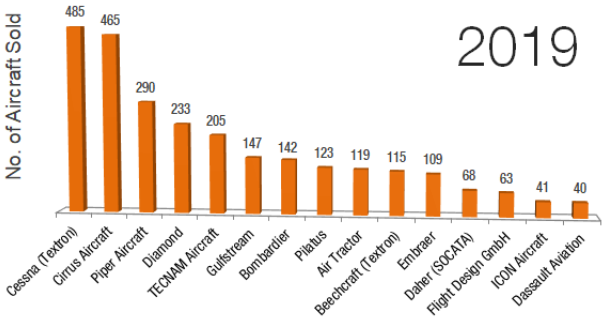

Figure 3.5: Current market share of specific companies

The biggest players (Cessna and Cirrus Aircraft) both have a share of around 17%, while plenty of smaller manufacturers have a share of almost 5%, for example the Beechcraft. It is unrealistic to expect that the *Twin Puffin*, being a new player on a well established market, will quickly get a market share comparable to the biggest manufacturers. That assumption holds despite many advantages that the *Twin Puffin* has related to the concept of distributed propulsion. Therefore, it is assumed for the *Twin Puffin* that it will take 5% of the market share in the Piston Engine Aircraft Market. That yields a yearly demand of roughly 60 aircraft.

This suggests that yearly demand for the *Twin Puffin* for small general aviation aircraft is likely to be smaller than 60. From now on it is therefore going to be assumed at 55 aircraft per year.

3.4.3. Urban Mobility and Night Flying

As partially portrayed in the preceding section, Section 3.3, the advantages of the design of the *Twin Puffin* can be exploited in order to adhere to new markets that are usually not accessible for bush planes. This section describes briefly two relevant alternative markets and is followed by a section on one more.

Thanks to the low noise and emissions standards, the *Twin Puffin* aircraft can be considered as top tier eco-aircraft among current competition. Together with agility and favourable STOL characteristics, it can be a great contender for prospective market of operating in urban areas. Based on the reasoning provided in this section, there also is a strong premise that there is sufficient demand for night flying [11].

[8] URL https://www.edf.org/climate/aviation [cited 22 June 2021]
[9] URL https://www.bbc.com/news/business-49890057 [cited 22 June 2021]
[10] URL http://fi-aeroweb.com/General-Aviation.html [cited 15 June 2021]
[11] VFR night flight with illuminated take off and landing sites

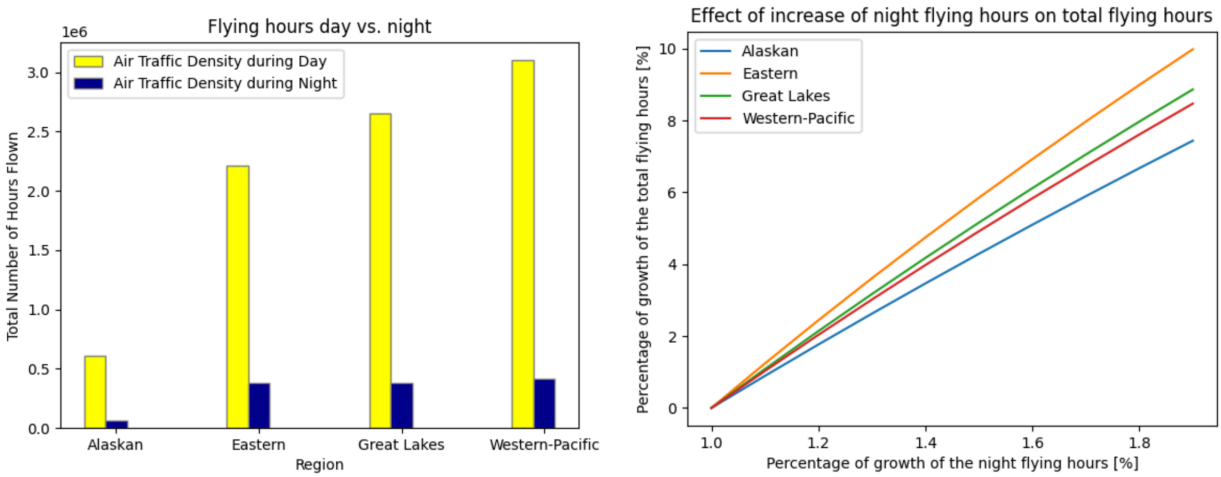

(a) Hours flown during day and night by region.

(b) Regional Variation of Increase in Night and Total Flying hours.

Figure 3.6: Graphical representation of total number of general aviation aircraft sold in 2000 - 2019 and market share of main producers in 2019.

In the report from FAA released in 2013, number of hours flown during night and day is given [3]. Four most representative regions were chosen and presented in the Figure 3.6a. A trend can be observed that independent of region, the number of hours flown during night is significantly lower than during day. In total, for the entire area of the US, flights during the night account only for 13% of all flights [3]. There are a few factors that cause that, primarily, flights during nights are less popular as people are less eager to travel. However, it is suspected that it is not the only limiting factor. Important issue is the noise restriction around urban areas during late hours. A great number of aircraft cannot simply operate at those hours due to their high noise levels. Fortunately for the *Twin Puffin*, the distributed propulsion offers much lower noise levels that could satisfy the noise restrictions.

In plots in Figure 3.6a and Figure 3.6b the relation between the night flown hours and the total hours is portrayed. It is evaluated that for different regions the increase in night flown hours has different effect on the total hours, as in different regions the flying at night has different popularity. However, as the graph in the Figure 3.6b shows, the difference is only significant when the market is increased by a large value. For the smaller increase, the differences between regions are irrelevant. Furthermore, the Figure 3.6b shows in a continuous way, the effect of increase of the night flying hours on the total flying hours, where this is clearly visible. Thus, the conclusion can be drawn that in the Eastern region the market may prove to be the most lucrative as the total market will increase by the most. The *Twin Puffin* could be a good answer to such an increase.

Due to all those aforementioned advantages, the Twin Puffin is likely to have a bigger share in the market than as it was predicted above. The effects of distributed propulsion on the demand for the aircraft is very difficult to estimate. For that reason, it will be assumed at 60 again from this point.

3.4.4. Eco-sightseeing

Not rarely, the sightseeing flights occur at the natural locations of wilderness. Often air tourism is organised above such locations as Coral Reefs in Australia or Amazon Rainforest in Brazil, sites that are especially endangered to degradation by high levels of pollution like CO2. Fortunately, the *Twin Puffin* aircraft perfectly addresses this problem as with curbed emissions and low noise it poses little threat to the precious natural environment.

3.5. Identified Use Cases

The extensive analysis of the use cases for a bushplane with distributed propulsion has been performed for the purposes of the DSE Group 12 Midterm Report [17]. The key aspects of that analysed are included below.

”The use cases reflect markets and thus groups of potential clients. Understanding these markets and the ways in which the aircraft will be used by future clients is essential in order to determine suitable stakeholders and requirements, which will be done in Chapter 4.

Due to the combination of a bush plane concept with distributed propulsion, a number of special use cases can be defined. These stem from the market gap that the aircraft aims to fill. Given that the bush plane market is quite saturated[12] expensive new, or older, proven, and cheaper aircraft, the market that this design will be aimed

[12]URL https://www.forbes.com/sites/erictegler/2021/04/28/prices-for-new-general-aviation-aircraft-may-be-pricing-pilots-out-of-the-

at is the transition across urban controlled airspace and rural areas or remote nature. This defines the specific use cases which are centred around urban areas where the reduced noise and emission, in comparison to normal bush planes, allow this design to be used more frequently at night or over populated areas with reduced impact.

Three major use cases have been identified for the bush plane. These are summarised and explained in Table 3.4.

Table 3.4: The identified major use cases of the conceptual aircraft with explanation and reasoning.

Use Case	*Mission*	*Explanation*	*Justification of the Demand*
Transportation (TA)	**Cargo Delivery**	Delivery of goods and for personal transport in urban and remote areas.	Many bush planes perform cargo delivery role, thus the market is deemed to be significant.
	Remote Transport and Charter	Delivery vehicle of goods and resources to remote locations and the delivery of goods from remote locations.	In locations with no infrastructure, with significant distances and large payload to be carried, drones are often found insufficient and not versatile enough. Thus, a sustainable aircraft able to land at rough terrain with access only to popular diesel fuel can satisfy such market.
Emergency Medical Services (EMS)	**Evacuation**	From the POS, the aircraft will be able to transport a stretcher, such that it is usable for medical evacuation.	On many continents people live in remote areas, far from healthcare. As statistics in Australia show, the percent of 'age-standardised potentially avoidable deaths' for very remote areas is 0.25% as compared to 0.1% for major cities[13]. Thus, the need for a faster and more popular mode of medical transport within the remote areas in Australia is more than apparent.
	Medicine Delivery	Connection between the medical and the transportation use case.	In the event of a natural disaster (e.g. hurricanes or earthquakes) there are no suitable conditions for landing of conventional aircraft, thus the delivery of medicine could be impaired. An aircraft with STOL characteristics and good visibility could address this issue.
	Search and Rescue	Due to the good visibility and low stall speed, the aircraft will be suitable for search and rescue missions.	There are rescue organisations that perform around 100 operations per year[14]. The use of helicopter is thus uneconomical, and a cheaper suitable aircraft would be much desired.
Tourism (TO)	**Air Touring**	"Tour" by air: travelling far instances with multiple stops and flying above a city.	Air touring occurs often at wilderness (e.g. Safari, Coral Reef, Antarctica) where wildlife could be threatened by old polluting aircraft. Thus, there is a need to replace them with a more sustainable plane.
	Exploration	Fly around and land to explore an area.	Areas of exploration are often of a sensitive nature, so low pollution levels are desired.
	Scientific Experiments	Fly over the area of interest to perform the scientific experiments.	This market is deemed to be smaller. However a low-cost aircraft is always important to decrease the cost of the entire mission. Also, the increased visibility will be of use.

3.5.1. Further Use Cases

The use cases presented in Table 3.4 are those from which stakeholder requirements will be derived. However, there are also additional use cases that should be kept in mind. These use cases are uncertain markets with limited potential and are thus not focused on. The limited relevance of these user groups means that their needs do not need to be considered in the derivation of the requirements and that they do not impact the design of the

market/?sh=861df853722a [cited 4 May 2021]

[13]URL https://www.aihw.gov.au/getmedia/0c0bc98b-5e4d-4826-af7f-b300731fb447/aihw-aus-221-chapter-5-2.pdf.aspx [cited 26 May 2021]

[14]URL https://mountainrescueaspen.org/about/ [cited on 26 May 2021]

bush plane. Nonetheless, after the completion of the design, it should be investigated if, without further design modifications, the created design is also suitable for sales in these markets. The identified possible secondary markets are stated below.

1. **Sub-urban mobility** In small cities, the low noise, short take-off and landing, low operating cost, and good visibility characteristics of the aircraft could allow it to be used as an urban mobility solution. It is especially interesting for night-time transportation due to the low noise emissions.
2. **Research** Research that is noise sensitive, such as the observation of animals, is an ideal candidate for the bush aircraft. It is quiet and offers good visibility.
3. **Military** The low noise characteristic would allow extraction, insertion (possibly parachuting) of special forces personnel and covert resupply in foreign territory as well as covert reconnaissance of a foreign military base.
4. **Policing** The low cost, good visibility, and low stall speed characteristics of the proposed aircraft could enable it to be used for policing and border control, as an alternative to helicopters.
5. **Hunting** Aerial vehicles are may be used for hunting purposes, especially when the prey is considered a pest. An example of this would be boar hunting in the United States. The advantage of using this plane would be the low noise and potentially good visibility.
6. **Crop Dusting** Aircraft have been, and are still, used for applying pesticides and fertiliser to large fields of crop. In addition, they can also be used for the seeding of the crop. The main concerns with such use of an aircraft are the unwanted spread of the aforementioned chemicals. To limit this, the aircraft flies close to the crop which means they are close to obstacles. Here good visibility and low stall speeds are key for the safety of the pilot and machine.
7. **Precision Firefighting** Due to the low stall speed and good visibility, the aircraft could function as a high-precision firefighting aircraft when converted into a water landing capable platform.
8. **Premium, fast, aerial package delivery**. For long range package transportation, the final distance to the customer can take the most time, especially in rural areas. With the large payload volume, good visibility and short take-off and landing distances, the proposed aircraft could function as a premium, short-range, and fast delivery platform.
9. **Optionally Piloted Flight** the possibility of including a fly by wire system in the design would allow advanced computer control of the vehicle. At a time when regulations allow it, this would enable the aircraft to become a quiet and efficient, autonomous, urban-and-beyond method of transport.

A lot of bush planes that are currently in use for some of the applications identified in this section have been built in the twentieth century, which means that they have lower performance, are less efficient and have higher emissions compared to modern day aircraft. Therefore, it is expected that there will be notable demand for the novel distributed propulsion aircraft. Initial production is aimed at ten units per year, but it is expected that demand will continue to grow as the importance of reduced emissions and noise pollution increases." [17].

3.6. Functional Analysis of Key Use Cases

The diagrams for Functional Analysis of the Use Cases have been created for the purposes of the DSE Group 12 Baseline Report. For clarity, those results are also included in this work. The Functional Break-down Structure is presented on Figure 3.7, and Functional Flow Diagram of the Bush Plane can be seen on Figure 3.8 and Figure 3.9.

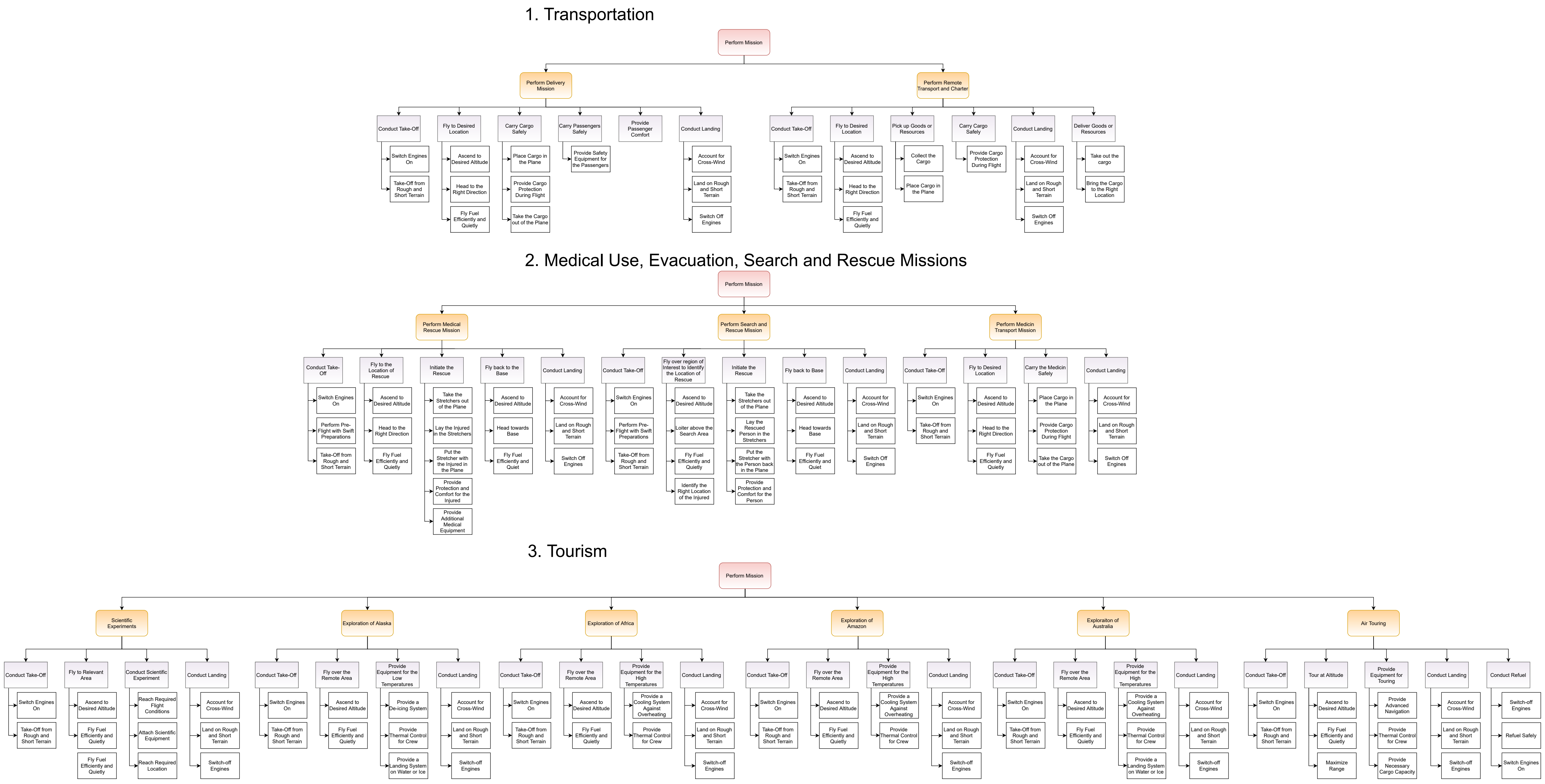

Figure 3.7: Functional Break-Down Structure

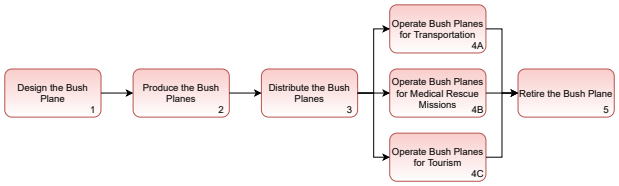

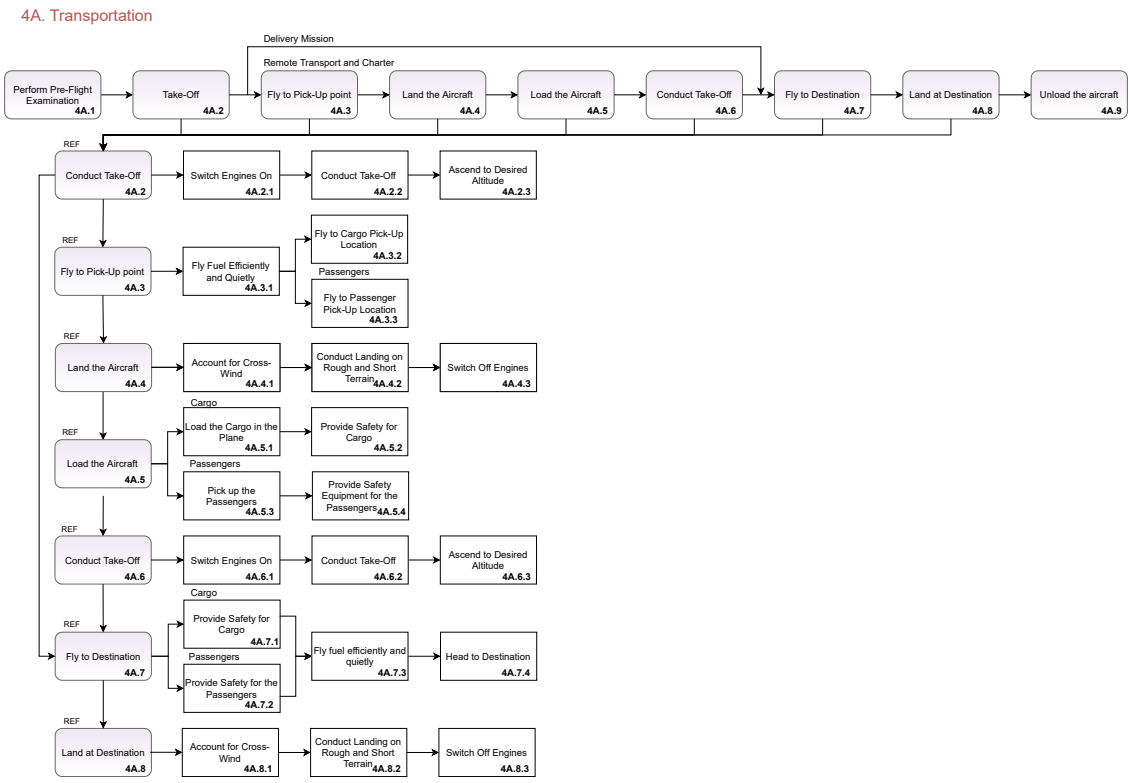

Figure 3.8: Functional flow diagram of the bush plane.

4B. Medical Use, Search and Rescue and Medicin Delivery

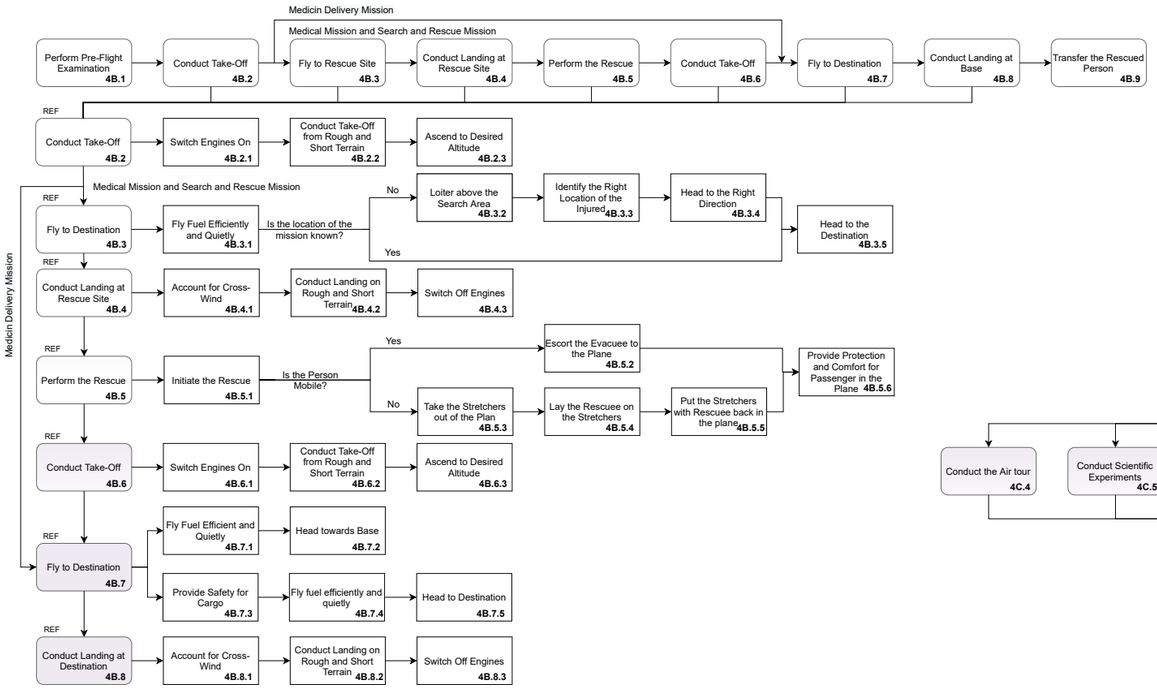

4C Tourism

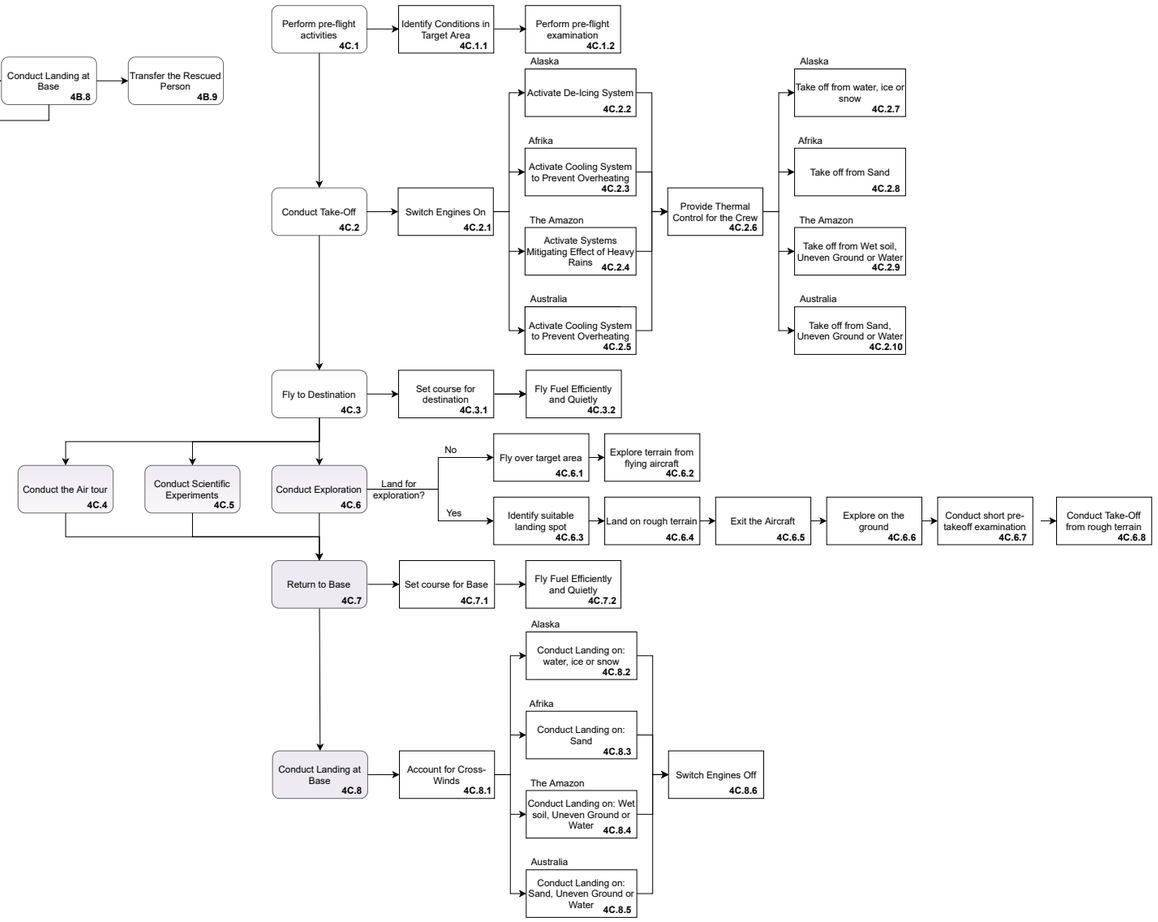

Figure 3.9: Functional flow diagram of the bush plane.

4
Requirements

This chapter provides the stakeholder, system and subsystem requirements and outlines the process used to find them. This process starts in Section 4.1, which presents the stakeholder requirements that follow from Chapter 3. Then, the stakeholder requirements are translated into system requirements in Section 4.2, from which the subsystem requirements are found and presented in Section 4.2.

4.1. Stakeholder Requirements

The stakeholder requirements presented in Table 4.1 flow directly from the market analysis presented in Chapter 3. For one thing, this includes the general market requirements derived in Section 3.2.3. Most stakeholder requirements, however, are a direct consequence of either the general market trends, the specific advantages that can be achieved using distributed propulsion, or the analysis performed for the different aircraft use cases in Section 3.6.

Table 4.1: Main requirements driving the design, following from the stakeholder analysis.

Tag	*Requirement*	*Relevance*
TP-AP-01	The aircraft shall fit within an 15 m by 15 m square floorplan.	Key
TP-MA-01	The aircraft shall be able to carry up to four passengers including the pilot.	Key
TP-MA-02	The aircraft shall have a usable mass of 500 kg.	Key
TP-USER-01	The aircraft shall have a take-off roll of less than 100 m at an ISA density equivalent to 2500 ft and 35 °C.	Driving
TP-USER-02	The aircraft shall have a landing roll of less than 100 m at an International Standard Atmosphere density equivalent to 2500 ft and 35 °C.	Driving
TP-USER-03	The aircraft shall be capable of taking off from Type I runways (unprepared gravel and sand).	Driving
TP-USER-04	The aircraft shall be capable of landing on Type I runways (unprepared gravel and sand).	Driving
TP-USER-05	The aircraft shall be able to perform all pre-flight actions (except fueling) and take-off without any external equipment.	Key
TP-USER-06	The aircraft shall have a cruise speed of at least 100 kts.	Key
TP-USER-07	The aircraft shall have a range of at least 500 Nmi.	Key
TP-USER-08	The aircraft shall use distributed propulsion.	Driving
TP-USER-09	The aircraft propulsion shall use electrically powered engines.	Driving
TP-USER-10	The aircraft shall be able to transport one stretcher.	Driving
TP-USER-11	The aircraft shall comply EASA CS-23 requirements.	Driving
TP-USER-12	More than 80% of the aircraft material shall be reused at the end of life.	Driving
TP-USER-13	The aircraft shall have at least a 50% emissions reduction compared to the *CubCrafters Top Cub*.	Driving
TP-USER-14	The aircraft shall have at least a 70% noise reduction compared to the *CubCrafters Top Cub*.	Driving
TP-USER-15	The aircraft retail cost shall be below 500,000€ when 10 units/yr are produced.	Key

4.2. System Requirements

From the stakeholder requirements outlined in Section 4.1 the system requirements were derived. This process involves translating requirements from the stakeholder vocabulary into technical vocabulary. If multiple stakeholder requirements refer to the same system characteristic, they are combined into the same system requirement.

Table 4.2: System requirements.

Tag	Requirement	Reasoning	Verification by...
		Structure	
TP-SYS-01	The length of the aircraft shall not exceed 15 m.	Maximum allowed by airports.	Inspection
TP-SYS-02	The width of the aircraft shall not exceed 15 m.	Maximum allowed by airports.	Inspection
TP-SYS-03	The structure shall withstand the required loading with a safety factor of 1.5.	Necessary to avoid structural failures.	Analysis
		Noise	
TP-SYS-04	The SPL at one meter of the aircraft shall be less than 136 dB	30% of the value estimated for the *CC Top Cub*.	Analysis
TP-SYS-05	The aircraft noise level 2500 m down range at maximum climb rate shall be lower than 76-88 dB.[1]	ICAO Annex 16, chapter 10.	Analysis
		Emissions	
TP-SYS-06	The total emissions of the aircraft shall not exceed a value of 0.095 kg/pax/km	50% of the CO_2 emissions of the *CC Top Cub*.	Analysis
		Usable Mass	
TP-SYS-07	The usable mass of the aircraft shall be of at least 500 kg.	From the market analysis. Includes both payload and fuel.	Analysis
TP-SYS-08	The mass of the payload shall be of at least 380 kg.	From the market analysis. Two (90 kg) passengers + 200 kg.	Analysis
		Performance	
TP-SYS-09	The take-off roll of the aircraft shall be of 100 m or less, at an ISA density equivalent to 2500 ft and 35 °C.	From the user requirements. To ensure good STOL performance	Simulation
TP-SYS-10	The landing roll of the aircraft shall be of 100 m or less, at an ISA density equivalent to 2500 ft and 35 °C.	From the user requirements. To ensure good STOL performance	Simulation
TP-SYS-11	The climb speed with all engines operative shall be at least 1.2 times the take-off stall speed.	From CS 23.65.A.4.	Simulation
TP-SYS-12	The climb gradient with all engines operative shall be of at least 8.3%.	From CS 23.65.A.	Simulation
TP-SYS-13	The climb speed with one engine inoperative shall have a minimum value of 1.2 times the take-off stall speed.	From CS 23.67.A.1.	Simulation
TP-SYS-14	When flying at 1.2 times the take-off stall speed, the aircraft shall have a positive climb gradient.	To ensure adequate climb performance	Simulation
TP-SYS-15	The cruise speed of the aircraft shall be of at least 51.4 m/s.	A cruise speed greater than 100 kts.	Simulation
TP-SYS-16	The stall speed of the aircraft shall have a maximum value of 25 m/s.	Stall speed of the *CC Top Cub* taken as reference.	Simulation
TP-SYS-17	The aircraft shall be able to fly for at least 926 km, non-stop.	Minimum range of the bush plane.	Simulation
		Aerodynamics	
TP-SYS-18	The Lift-to-Drag ratio with engines inoperative shall be at least of 7.	About an 80% of the Lift-to-Drag ratio of comparable aircraft.	Analysis
		Stability & Control	
TP-SYS-19	The aircraft shall be trimmable at all points during the flight.	It should be possible to make the C_m equal to 0.	Analysis
TP-SYS-20	The aircraft shall be longitudinally statically stable.	C_{m_α} should be negative for an increase in angle of attack.	Analysis

Table 4.2: System requirements.

Tag	Requirement	Reasoning	Verification by...
TP-SYS-21	The value of C_{m_α} shall be negative at all times during flight.	C_{m_α} must be negative (not too low or too high) for the aircraft to be longitudinally statically stable.	Analysis
TP-SYS-22	The aircraft shall have vertical static stability throughout the whole mission.	The aircraft should recover from a disturbance causing a yaw moment.	Analysis
TP-SYS-23	The aircraft shall be laterally statically stable.	It should be able to counteract a disturbance causing a rolling moment.	Analysis
TP-SYS-24	The aircraft shall be recoverable when entering deep stall.	Necessary to ensure safe flying	Analysis
TP-SYS-25	The aircraft shall be recoverable when entering spin.	Necessary to ensure safe flying	Analysis
TP-SYS-26	The aircraft shall be controllable on ground.	Necessary to ensure safe flying	Analysis
	Cost		
TP-SYS-27	The retail cost of the aircraft shall not be more than 500,000€.	From the user requirements. Necessary for ensuring the aircraft remains commercially competitive	Analysis
	Energy		
TP-SYS-28	The battery shall be able to store backup energy to use it in case of failure of the generator at any point during flight.	TO enable a more controlled descent than if no power was available	Analysis

4.3. Subsystem Requirements

Following from the system requirements, several subsystem requirements were obtained. These are shown in Table 4.3, and identify the main aspects that each of the parts of the aircraft need to comply with.

Table 4.3: Subsystem requirements.

Tag	Requirement	Verification by...
	Wing Subsystem	
TP-SYS-WNG-01	The wingspan shall not exceed 15 m.	Inspection
	Propulsion Subsystem	
TP-SYS-PROP-01	The engines shall be able to deliver enough thrust during cruise to achieve force balance.	Analysis
TP-SYS-PROP-02	The engines shall be able to deliver sufficient thrust during take-off to surpass drag and achieve the required climb rate.	Analysis
TP-SYS-PROP-04	The engines shall be able to provide a sufficient torque using differential thrust during take-off and landing to minimise taildragger characteristics.	Analysis
	Energy Source Subsystem	
TP-SYS-EN-01	The battery shall be able to carry enough extra energy for the aircraft to be able to return safely to the airport in case of ICE failure at take-off.	Analysis
TP-SYS-EN-02	The battery shall be able to carry sufficient extra energy for the aircraft to be able to land safely in case of ICE failure at any point during the mission.	Analysis
	Structure Subsystem	
TP-SYS-STR-01	The aircraft length *(fuselage + booms)* shall not exceed 15 m.	Inspection

[1] The required maximum value inside the indicated range is computed depending on the maximum take-off weight of the aircraft.

Table 4.3: Subsystem requirements.

Tag	*Requirement*	*Verification by...*
TP-SYS-STR-02	The fuselage shall have the capacity for carrying at least four seats.	Inspection
TP-SYS-STR-03	The fuselage shall be able to carry a stretcher.	Inspection
TP-SYS-STR-04	The usable volume of the fuselage shall be of at least 2 cubic metres.	Inspection
TP-SYS-STR-05	The structure of the aircraft shall be able to withstand a maximum loading of 6g.	Analysis
TP-SYS-STR-06	The structure of the aircraft shall be able to withstand a minimum loading of -4g.	Analysis
	Landing Gear Subsystem	
TP-SYS-LG-01	The landing gear shall be able to withstand impact loads of up to 5g.	Analysis
TP-SYS-LG-02	The tail landing gear shall be able to withstand up to 10% of the maximum aircraft weight.	Analysis
TP-SYS-LG-03	The angle between the most forward position of the centre of gravity and the main landing gear shall be greater than 15 degrees.	Analysis
TP-SYS-LG-04	The angle between the most aft position of the centre of gravity and the main landing gear shall be smaller than 25 degrees.	Analysis
TP-SYS-LG-05	The lateral angle between the highest centre of gravity position and one of the wheels of the main landing gear shall exceed 25 degrees.	Analysis
TP-SYS-LG-06	The clearance angle between the main landing gear and the most outward propeller shall be of more than 20 degrees.	Analysis
TP-SYS-LG-07	The clearance angle between the main landing gear and the wing tip shall be of more than 20 degrees.	Analysis
	Empennage Subsystem	
TP-SYS-EMP-01	The horizontal stabiliser shall be able to create a moment sufficiently large in order to trim the aircraft.	Analysis
TP-SYS-EMP-02	During deep stall, the horizontal tail shall not be shadowed by the wake of the main wing.	Analysis
TP-SYS-EMP-03	During take-off and landing, a rudder deflection shall be able to produce a large enough force so as to minimise taildragger characteristics.	Analysis
TP-SYS-EMP-04	The vertical tail shall be able to keep the aircraft straight for crosswinds of at least 0.2 times the stall speed of the aircraft.	Analysis
TP-SYS-EMP-05	The vertical tail shall be able to counteract the torque produced when at least half of the engines in one wing are inoperative (round up).	Analysis
TP-SYS-EMP-06	During spin, at least one third of the rudder shall be outside of the wake produced by the horizontal stabiliser.	Analysis

5
Initial Design Steps

This chapter outlines the initial design steps that were taken to decide on the general aircraft and energy source concepts and find initial values. First, the design options are generated in Section 5.1 after which the corresponding trade-offs are performed. In Section 5.2 the resulting preliminary design is presented.

5.1. Considered Design Options

For the both the general aircraft concept as the energy source(s), trade-offs are performed. First, seven different strawman concepts are compared, followed by four different types of energy sources.

5.1.1. Strawman Concepts

Prior to selecting the main concepts that would enter the trade-off, all possible design choices were taken into account by creating several DOT). These accounted for all features of the aircraft. However, in order to perform a preliminary design, only the DOTs containing the characteristics which would influence the aircraft's performance the most were taken into account (*fuselage shape*, *wing arrangement*, *empennage*, *engine placement* and *landing gear*). The engine concept was limited to propeller-type, as it was required that the aircraft used distributed electrical propulsion. [17]

First, the options that were unfeasible or unrealistic were eliminated. From the remaining ones, more than 100 different configurations could be achieved. However, some design choices were deemed non-feasible, and were removed as well. For example, low-wing configurations were discarded due to the insufficient ground clearance. Some empennage types were not considered as ground clearance would also be lacking in case that the design was to be a taildragger aircraft. Moreover, other options were discarded, such as having a canard or tandem wing configuration, due to its moment arm being too short as the center of gravity is located quite far forward. [17]

In the end, seven inherently different designs were chosen for further analysis, summarised in Table 5.1, and illustrated in Figure 5.1. They cover all feasible parts of the top-level DOT. This way, the analysis is broadened and can realise a design that incorporate aspects from all the strawman concepts [18]. Note that in Figure 5.1, the strut bracing for the 'pusher'-concept and the 'piper'-concept are not purposefully braced. [17]

Table 5.1: Major design characteristics of the different strawman concepts. [18]

Concept	*Fuselage Shape*	*Wing Arrangement*	*Empennage Configuration*	*Engine Placement*	*Landing Gear Configuration*
Twin-boom	Box-shape, transpa- rent cockpit, aft loading	High-wing	Twin-boom	Leading edge	Quad-gear
Pusher	Cigar-shape, transpa- rent cockpit, front loading	High-wing	Conventional	Trailing edge	Taildragger
Piper	Box-shape, loading on side	High-wing	Conventional	Leading edge	Taildragger
V-tail	Tadpole-shape, aft loading	High-wing	V-tail	Leading edge	Tricycle
Fuselage	Tadpole-shape, aft loading	High-wing	T-tail	Fuselage	Tricycle
Split	Cigar-shape, transparent cockpit, front loading	High-, biplane-wing	Conventional	Trailing edge	Taildragger
Blended-Wing-Body	Blended in the wing	Blended wing body, sweep	Vertical tail only	Leading edge	Taildragger

'Twin-Boom'-concept The 'twin-boom-concept, has the defining feature of a twin-boom empennage design. The two vertical tails follow up from the aft of the fuselage structure and connect at the top with a horizontal tailplane. The twin-boom empennage allows for easy access to payload from behind the aircraft. [18]

'Pusher'-concept For the 'pusher'-concept, the distributed propellers promote a more aft centre of gravity and therefore a more agile aircraft. Additionally, the propellers are moved away from the cockpit, so the pilot is not in immediate danger in case of blade-off failure. With a conventional tail, loading must be done at the front, either by a side-door or by the transparent front opening up as a hatch door. [18]

'Piper'-concept The 'piper'-concept design is based on the design of the Piper J-3 Cub aircraft, with the propulsion moved from a front propeller, to distributed propellers along the aircraft's leading edge. The idea is that the tip of both wings are equipped with a bigger engine, with the goal to provide thrust during cruise. The wings are then loaded with smaller engines, to improve aerodynamic properties of the wing during take-off and landing. The loading of payload is possible by way of a hatch along the side of the fuselage, behind the pilot. [18]

'V-tail'-concept The 'V-tail'-concept design is characterised by a V-tail empennage. The empennage is mounted with additional propulsion, in addition to leading edge distributed propellers. To allow for very aft propulsion systems without altering the centre of gravity too much, a V-tail is utilised to reduce the necessary tailplanes from three to two. Loading of payload is by way of a loading ramp at the aft of the cockpit. [18]

'Fuselage'-concept The 'fuselage'-concept utilises propulsion distributed around the fuselage, and a T-tail to avoid turbulent air from the propellers. This is the only concept that does not use propulsion distributed along the wing. Loading of payload is by loading the ramp at the aft of the cockpit. [18].

'Split'-concept For the 'split'-concept, the engines are placed on top of the wing surface towards the trailing edge, and they are ducted. This design was inspired by the Lilium concept - an electric regional air vehicle[1]. Loading must be done at the front, with either a side-door or front-hatch. [18].

'Blended-Wing-Body'-Concept A seventh concept design was added to the list of strawman concepts. Due to the desirable properties the concept design offers, the 'Blended-Wing-Body'-concept is qualified for further trade-off. The concept is characterised by no apparent fuselage, to take advantage of the idea that the entire aircraft can be used for effective lift production and aerodynamic characteristics' enhancement, leading to an increase in the lift over drag ratio of 24% [15]. The oversized winglets at the wing tips will additionally serve as vertical stabilisers. [17]

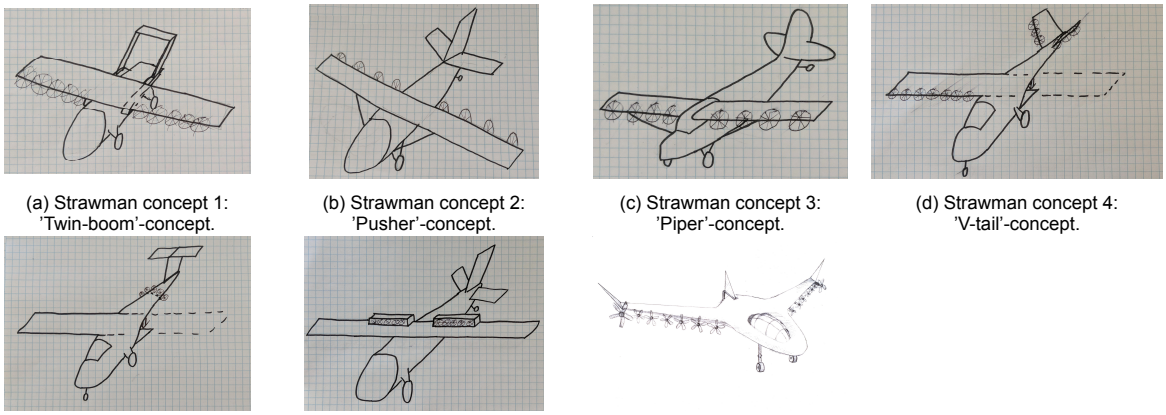

(a) Strawman concept 1: 'Twin-boom'-concept.

(b) Strawman concept 2: 'Pusher'-concept.

(c) Strawman concept 3: 'Piper'-concept.

(d) Strawman concept 4: 'V-tail'-concept.

(e) Strawman concept 5: 'Fuselage'-concept.

(f) Strawman concept 6: 'Split'-concept.

(g) Strawman concept 7: 'Blended-Wing-Body'-concept.

Figure 5.1: Sketches of the seven strawman concepts.

5.1.2. Selection of Strawman Concepts

From the driving requirements, explained in Chapter 3, it is possible to distinguish designs that outperform others in terms of relevant characteristics. These desirable characteristics are translated into selection criteria. There are two types of criteria: quantitative, for which the concepts can be numerically compared and qualitative criteria, for which an analysis is needed. Each of the criteria are weighted, reflecting the relative importance, with scale: 1 - minor importance, 2 - limited importance, 3 - important, 4 - very important, and 5 - essential. The different selection criteria, together with their weights are shown in Table 5.2. [17]

[1] URL https://lilium.com/jet [cited 11 May 2021]

Table 5.2: Selection criteria, tags and weights for the strawman trade-off

Selection Criteria	*Assessment Type*	*Weight*
Noise at 1 m distance	Calculation	5
Operational Empty Weight	Calculation	4
Aerodynamic Efficiency	Calculation	4
Wing Loading	Calculation	3
Fuel Mass	Calculation	3
Ease of Ground Operations	Qualitative	3
Usable Volume	Qualitative	2
Visibility	Qualitative	1

In order to compare the different strawman concepts quantitatively, an initial sizing tool was built. For the qualitative criteria, an analysis was performed. After performing the formal trade-off, a sensitivity analysis was done. First, the sensitivity to parameters was studied. By evaluating the apparent weaknesses of each design and applying proposed fixes, the trade-off was updated. Secondly, the weights of the criteria were adapted for each use case, explained in Section 3.6. From the sensitivity analysis, it was shown that the most suitable concept is the 'twin-boom'-concept and that this concept is chosen for further design.

5.1.3. Energy Source Concepts

With a driving requirement stating that the aircraft must be environmentally friendly, it is important to find a suitable energy source. The concepts deemed viable are discussed below. Additional concepts that were identified, but deemed unviable were nuclear power and solar power.

Lithium-Ion Battery The first energy source concept is a lithium-ion battery. The advantages of using these batteries are that they directly provide the electrical energy, resulting in high efficiency. Next to that, they have no emission during operation. Because no fuel is being burned, the centre of gravity of the aircraft does not change. Therefore, the aircraft can be designed for the optimal position of the centre of gravity. However, lithium-ion batteries have poor performance properties with respect to weight and volume. The average specific energy and the average energy density equal $180\,\mathrm{W\,h\,kg^{-1}}$ and $400\,\mathrm{W\,h\,l^{-1}}$ respectively [24]. [17]

Internal Combustion Engine The ICE concept is based on the idea of having the required power supplied purely by a fossil fuel engine. The engine is used much like an engine would be in a car, except that the mechanical work is converted to electricity which is used by the electric motors. This has the advantage that no battery is required, which keeps the weight of the aircraft down. Furthermore, the ICE is a well developed technology. The ICE has a long history in aviation, with the first heavier than air aircraft using an ICE [2]. The fuel used has high specific energy, in the order of $45\,\mathrm{MJ\,kg^{-1}}$. Fossil fuels also have a well established distribution network, in contrast to other energy sources. A disadvantage is that these energy dense fuels emit gasses harmful to the environment when burned. This can be mitigated by using biofuels (fuel derived from biomass) or electrofuels (green electric energy stored in the chemical bonds of liquid or gas fuels), which are drop-in replacements, leading to no net emissions at the detriment of increased fuel cost. Another disadvantage of ICE engines is that they have relatively low thermal efficiency compared to the alternatives. Diesel engines have a peak thermal efficiency of around 45 %, which is further reduced by turning the mechanical energy into electric energy [1]. [17]

Hybrid The hybrid concept is an ICE with a supplementary battery. The engine is used as a generator for electricity. The battery is used to supplement power when needed, for example during take-off and landing. The battery can be recharged from external power sources on the ground, and it is recharged by the generator during the flight. The advantage of the hybrid is that the engine can run at peak efficiency, causing a reduction in emissions compared to the pure ICE concept. Biofuels and electrofuels can also be used to further reduce the net missions. Furthermore, the noise is reduced since part of the power is delivered by the battery. The disadvantage of the hybrid is the added mass and volume of the battery. This is especially crucial for a STOL concept since mass is directly related to take-off and landing distances.

Fuel Cell The fuel cell concept is based on the idea of using a Proton-exchange membrane (PEM) fuel cell, which uses hydrogen as an energy source. The highly compressed hydrogen is stored in high pressure tanks. The fuel cell is responsible for delivering the power to the engines. Advantages of fuel cells include that they only produce water as a byproduct and that they are energy efficient, with efficiencies up to 65 % [39]. Here

[2] URL https://wright.nasa.gov/airplane/eng03.html [cited 16 May 2021]

the emissions and efficiency of the required infrastructure are not considered. Furthermore, fuel cells produce negligible noise emissions, since no combustion takes place. Finally, hydrogen has very high specific energy of 120 MJ kg^{-1}. A disadvantage is that hydrogen has poor energy density, at sea level a kilogram of hydrogen has a volume of 11 m^3. Straightforward calculations then show that hydrogen is less energy dense than fossil fuels, even when stored at 700 bar. Furthermore, there are a limited amount of hydrogen station compared to other energy sources. [17]

5.1.4. Selection of Energy Source

To be able to select the most viable energy source for the design, seven selection criteria were determined. They are listed in Table 5.3. As with the Strawman trade-off criteria, they can be divided into quantitative and qualitative categories. It is also shown which weight each criterion is given in the trade-off, to indicate the relative importance of the criteria.

Table 5.3: Selection Criteria for the Energy Source Trade-Off

Selection Criteria	*Assessment Type*	*Weight*
Fuel Availability	Qualitative	5
Mass	Calculation	4
Noise	Qualitative	3
Emissions	Qualitative	3
Operating Cost	Calculation	3
Acquisition Cost	Calculation	1
Required Volume	Calculation	1

For the quantitative criteria, a tool has been made to approximate some preliminary values for each design option. For the qualitative criteria, the different concepts were studied and compared. After the trade-off is finished, a sensitivity analysis is performed. Firstly, the sensitivity to parameter changes was studied, where it is investigated whether changing the main assumptions, based on six different scenarios, have much influence on the trade-off. Secondly, similarly to the trade-off of the aircraft concept trade-off, the weights of the criteria were adapted to account for the different use cases, described in Section 3.6. From this analysis, it can be concluded that the hybrid system performs the best and is therefore chosen to be the energy source of the bush plane.

5.2. Preliminary Design

The selected design is a twin-boom aircraft, with distributed propulsion. The bush plane has a hybrid diesel-electric propulsion system. It has been called the ”Twin-Puffin” to emphasise the twin booms that are crucial to the use cases. An illustration of the concept design is shown in Figure 5.2 and the key characteristics of the design are provided in Table 5.4.

The aircraft has leading edge distributed propulsion, causing better aerodynamic performance i.e. a higher maximum lift coefficient, a higher lift over drag ratio and lower noise and emissions. Having the propellers on the leading edge allows for a transparent cockpit, which increases the visibility of the pilot significantly. The hybrid diesel-electric power source allows for an increase in available power during take-off and landing, by using the battery. This also allows for a reduction in noise and emissions during operations. It also offers the operator the option to further reduce emissions by using electrofuels or biofuels. The bush plane features a twin boom empennage with a horizontal tail between the tips of the vertical tails, allowing the aircraft for aft loading. The landing gear has a taildragger configuration. This provides the ability to land on remote, unprepared ground. Finally, the fuselage is box-shaped, to have more usable space within the cabin. [17]

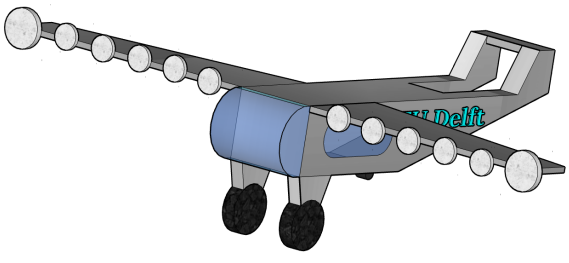

Figure 5.2: Preliminary aircraft design

Table 5.4: Preliminary characteristic values.

Parameter	*Symbol*	*Value*	*Unit*
Payload mass	$m_{payload}$	400	kg
Seats	n_{pax}	4	-
Range	R	926	km
Cruise speed	V_{cruise}	100	knots
Noise at 1 m distance	N_{1m}	115	dB
CO_2 emissions	$m_{CO_2,sp}$	84	g/pax /km
Operating costs	C_{op}	1.9	cents/pax/km

Part II:

Detailed Design Methods

6

Subsystem Design Methods

This chapter explains the different design methods that will be used to design the various aircraft subsystems. Starting with the design of the fuselage in Section 6.1, the chapter discusses the design methods for the aircraft structure (Section 6.2), the energy source (Section 6.3), the design for lift augmentation (Section 6.4), the wing (Section 6.5) the propulsion system (Section 6.6), the empennage (Section 6.7), the landing gear (Section 6.8), and finally the electrical and aircraft control systems (Section 6.9). At the end of the chapter Section 6.10 summarises the outcomes of the different subsystem design methods. It is important to note that in many cases, the design methods for one subsystem may rely on the outcomes of the design results for other subsystems. Even if these relations form loops with no clear starting point, this is no issue as the methods will be combined in one iterative auto-updating program.

6.1. Design of the Fuselage

As the fuselage shall be able to carry passengers comfortably, a robust fuselage design should be designed. In the following section, the design of the fuselage of the *Twin Puffin* is explained. First, in Section 6.1.1, the design of the cross-section is demonstrates, where first the shape is carefully selected through trade-off and then the dimensions of the design are computed. Then in Section 6.1.2, the design of the side view of the fuselage is defined.

6.1.1. Design of the Cross-Section

Shape of the Cross-Section The first step in designing the fuselage, is deciding upon the cross-sectional shape. For this, the overall shape of the fuselage has to be selected. Two main options are suitable for the shape of the non-pressurised fuselage of the bush plane: a frustum shape or a tadpole shape. The main advantage of having a tadpole shape is that it produces less drag compared to the frustum shape. However, the frustum design is more suitable for the bush plane, due to the fact that this shape is more spacious, less expensive to produce, stronger and stiffer than the tadpole design [25]. Therefore, it is chosen that the bush plane has a frustum shape. This frustum fuselage can have various cross-sectional shapes so a trade-off has to be performed to select the most optimal shape. In this trade-off, several shapes were analysed and compared to each other: these shapes are the hexagon, the rectangle and two trapezoids. Initial sketches of these different cross-sectional shapes can be seen in Figure 6.1.

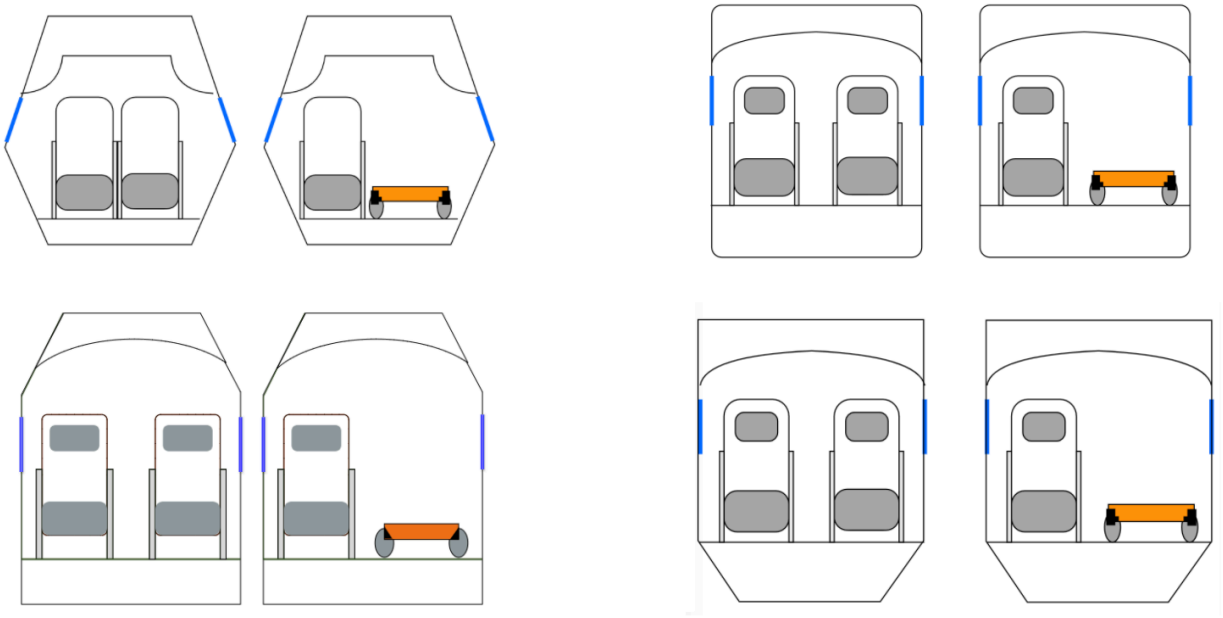

Figure 6.1: Sketches of different fuselage shapes

To perform the trade-off, the selection criteria need to be listed, weighted and analysed for each fuselage shape. As weight is one of the most crucial factors in the aerospace industry in order to achieve green aviation, the structural weight (S.W.) was chosen to be the most important criteria, and thereby weighted with a factor of five [71]. Another selection criteria is the ease of maintenance (E.O.M.) and is weighted with a factor of four. The ease of maintenance was chosen to be a selection criteria because it can significantly affect the costs during the operation phase of the aircraft [35]. Next to that, the ease of production (E.O.P.) is also a selection criteria and has a weight of three. This criteria is taken since it can highly affect the cost of the bush plane [13]. A fourth criteria is the usable volume (V), which is weighted with a factor of two. This is a selection criteria because one of the main use cases of the bush plane is transport. Lastly, the comfort of the passengers (C.) are taken into account for the selection, since the bush plane is designed for tourism. An overview of the selection criteria is given in Table 6.1.

Table 6.1: Selection criteria for the fuselage shape

Tag	*Criteria*	*Weight*
S.W.	Structural weight	5
E.O.M.	Ease of maintenance	4
E.O.P.	Ease of production	3
V	Usable volume	2
C.	Comfort for the passenger	1

To perform the formal trade-off, the different selection criteria are qualitatively compared for the possible shapes of the fuselage. The different shapes are received a colour for each selection criteria. The combinations of scores and colours are excellent - green, good - blue, correctable deficiencies - yellow, and unacceptable - red. To accommodate for colourblind readers, the colours are also indicated with their first letter.

Since less complex structures result in lower structural weights (S.W.), the hexagonal shape was said to be unacceptable, the trapezoids good and the rectangular shape excellent. The ease of maintenance (E.O.M.) increases when the parts in the fuselage are easily accessible. The hexagon walls are not easy to access due to there complex shape and has therefore correctable deficiencies. The rectangular fuselage is easy to access and is therefore good in terms of ease of maintenance. The trapezoid with the extra added part on top has a similar accessibility as the rectangular shape, so therefore it scores good. However, the trapezoid with the extra part on the bottom is easier to access from below and therefore it scores excellent. Similarly to the selection criteria of the structural weight, the ease of production (E.O.P.) is dependent on the complexity of the structure. Therefore, the hexagon is scored unacceptable, the rectangle is scored excellent and the trapezoids are good. The usable volume (V) are good for both the hexagon and the rectangle and excellent for the trapezoids, as they have an extra voluminous part, either below or on top of the cabin. For the comfort of the passengers (C.) , the hexagon scores excellent due to the extra shoulder width the passenger has. For other configurations, there is still comfort provided and therefore they are scored good. The trade-off matrix,

with the scores mentioned above, can be seen in Table 6.2

Table 6.2: Trade-off matrix of the cross-sectional shape

	S.W.	E.O.M.	E.O.P.	V	C.
Hexagon	[R]	[Y]	[R]	[B]	[G]
Rectangle	[G]	[B]	[G]	[B]	[B]
Trapezoid 1	[B]	[B]	[B]	[G]	[B]
Trapezoid 2	[B]	[G]	[B]	[G]	[B]

From the trade-off table, in Table 6.2, it can be noted that the rectangular shape scores the best and is therefore the most suitable choice for the cross-sectional shape of the fuselage.

Dimensions of the Cross-section The next important step in the design of the cross-section is to provide the dimensions of the cross-section of the fuselage. To dimensionalise the cross-section, the dimensions of the objects that will be placed in the fuselage have be researched. The main objects needed are the chairs, the stretcher, the ICE and the battery, with enough clearance. If the aircraft is used for medical rescue missions, two seats behind one another, are removed so a stretcher can easily be placed instead. Roskam provides an insight in the dimensions of a passenger seat [51]. However, the dimension of the seat width of 420 mm, given in the book of Roskam are rather outdated, so therefore, an updated seat width of 542 mm was used such that 95% of the world's population would fit into the passenger seats [50]. However the seat width was updated, the total height of the chairs, the overhead space and the seat height were sufficient and therefore stayed 990 mm, 216 mm and 216 mm, respectively [51]. For the dimensions of the stretcher, research was done on stretchers used in helicopters. A height of 204 mm and a width of 575 mm was found [1]. The dimensions of the ICE based on commonly used ICEs and the dimensions of the batteries were roughly estimated through preliminary calculations, performed in the Midterm Report [17]. The dimensions found for the ICE are 400 mm height x 1000 mm width x 1100 mm length and the battery has an estimated volume of 18 L [17]. dimensions for the clearance were defined to be 51 mm [51]. The only clearances that differ from the standard 51 mm are the space between the chairs and the space between the stretcher and the chair, those are defined to be 64 mm and 31 mm respectively. A sketch of the objects that go into the fuselage, together with their dimensions are sketched in Figure 6.3

For the ICE and batteries, a formal trade-off was performed for the positioning of them as their weight and dimensions are relatively large. The different options for the positions is shown in Figure 6.2.

Figure 6.2: Options for the positioning of ICE and battery

The trade-off of the positioning is based on four selection criteria: the safety in case of fire (S.C.F.), the effect on the longitudinal stability (L.S.), ease of maintenance (E.O.M.) and the structural weight (S.W.) which can differ due to the thickness of the firewalls. An overview of the different selection criteria, their tag and weight are provided in Table 6.3

Table 6.3: Selection criteria for the positioning of ICE and battery

Tag	*Criteria*	*Weight*
S.C.F.	Safety in case of fire	5
L.S.	Effect on longitudinal stability	4
E.O.M.	Ease of maintenance	3
S.W.	Structural weight	3

The safety in case of fire parameter can differ with the location of the ICE and batteries. When placing both systems very near to each other, chances are higher that when one of the two systems is on fire, then

[1] URL https://www.majorsafety.com/products/junkin-lightweight-stokes-basket-rescue-stretcher, [cited 25 May 2021]

the other one lights fire too. Therefore, the the first two positioning options are marked as unacceptable. For the longitudinal stability it is preferable to have the systems higher up, so there won't be a constant nose down moment created. So, the first option is marked with correctable deficiencies. When placing both the ICE and the batteries on top or the ICE on top and the batteries on the side, the criteria is marked as excellent. When placing either the ICE on top and batteries at the bottom or the batteries on top and ICE at the bottom, the stability is rather neutral and therefore it is marked as good. For the ease of maintenance, it is easier to reach the ICE and battery from below, therefore, when placing both the batteries and the ICE at the bottom, it is scored as excellent. When the systems are placed on top, it is still relatively easy to access and therefore, for the second option, third option and fourth option, they are marked as good. When placing the batteries on the sides, it is marked as having correctable deficiencies, since for that case, there are three sides to be checked for failure, making the maintenance less easy. The structural weight differs due the thickness of the firewalls that are needed to separate the passengers from the ICE and batteries. Next to that, there might be added structural weight due to the ducting fan, that is needed for ground clearance. In case of fire, safety must be provided, so the passengers are separated from the batteries and ICE in means of a firewall. Due to ground clearance reasons, the ICE is preferred to be on top, so there is no ducted fan needed. The first option is marked as having correctable deficiencies, since the fan needs ducting. The second system on the other hand, is marked as excellent, since it has the ICE on top and there is only one fire wall needed. The third system is also marked as excellent since the ICE is on top. The fourth positioning option, is marked as unacceptable, since there are two firewalls needed and the ICE is below the cabin. The final option is also marked as unacceptable, since there are three fire walls needed. In Table 6.4, the trade-off matrix is shown for the positioning of the battery and the ICE.

Table 6.4: Trade-off matrix of the positioning of ICE and battery

	S.C.F.	L.S.	E.O.M.	S.W.
option 1	[R]	[Y]	[G]	[Y]
option 2	[R]	[G]	[B]	[G]
option 3	[B]	[B]	[B]	[B]
option 4	[B]	[B]	[B]	[R]
option 5	[G]	[G]	[Y]	[R]

From Table 6.4, it can be seen that the only positioning option that is does not contain any unacceptable properties is the one where the ICE is on top and the batteries below. Moreover, it is decided that the ICE will be placed within the wing box. The ICE, however, might not fit in the wing box and therefore, there will be a bubble on top of the wing box to fit the ICE.

From this, the fuselage width and height can be defined. The height, without the ICE system and the width of the fuselage equal 1410 mm and 1250 mm respectively. The height of the ICE system, together with the according clearances equal 412 mm, resulting in a total fuselage height of 1822 mm. To have an overview of the dimensions, a sketch is provided in Figure 6.3.

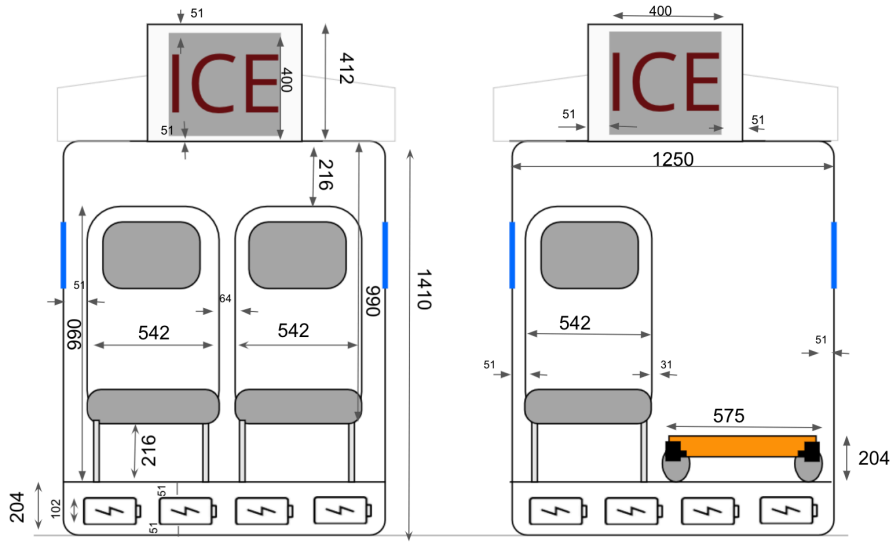

Figure 6.3: Sketch of the cross-section with dimensions

6.1.2. Side View of the Fuselage

After the cross-sectional view is determined, the side view of the fuselage can be designed. In order to design the side view of the fuselage, the length has to be determined. This is done by establishing the lengths of the items that need to fit in the cabin. Using the dimensions from Roskam it is found that the chair depth equals 600 mm, for comfortable passenger seats and the space between the chairs was taken to be 762 mm [51]. The length of the ICE is taken to be 1100 mm, as explained in Section 6.1.1. For the battery, a length of 1000 mm was taken initially, to provide enough space for shifts in the centre of gravity and to provide the possibility for iterations of the size of the batteries. Next to those items also a stretcher needs to fit properly into the cabin. For the dimension of the stretcher, a standardised stretcher used in helicopters was taken as reference and has a length of 2050 mm [2]. From the dimensions of these items, the length of the fuselage was esitmated to be 4000 mm, where the cockpit, cabin and tailcone have a length of 1200 mm, 1400 mm and 1400 mm respectively. An overview of the dimensions of the side view of the cross-section is given in the sketch in Figure 6.4.

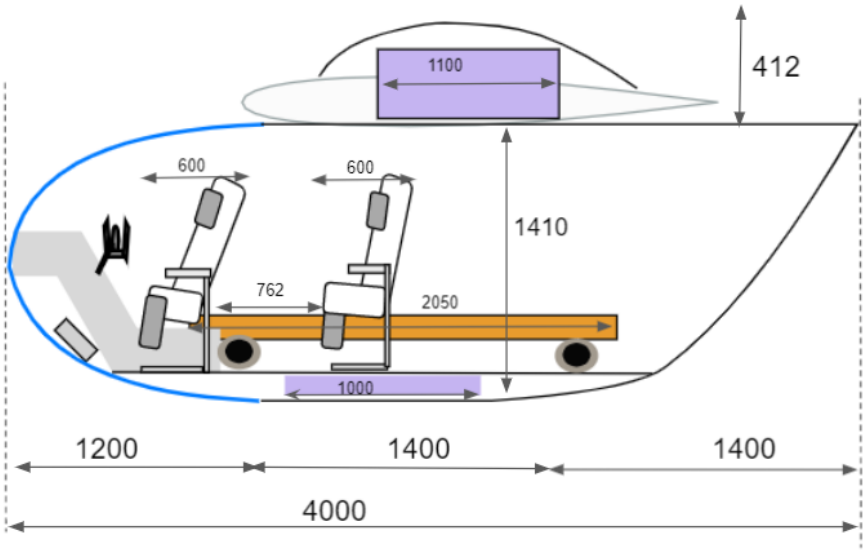

Figure 6.4: Sketch of the side view of the fuselage with dimensions

6.1.3. Cockpit Design

To dimensionalise the cockpit, the standard dimensions of Roskam were used [51]. These dimensions can be seen in the sketch in Figure 6.5. One of the requirements was to provide enough visibility. Therefore, the nosecone is made from transparent material and the computer system is such that it obstructs the least view as possible. A preliminary sketch of the view of the pilot can be seen in Figure 6.6.

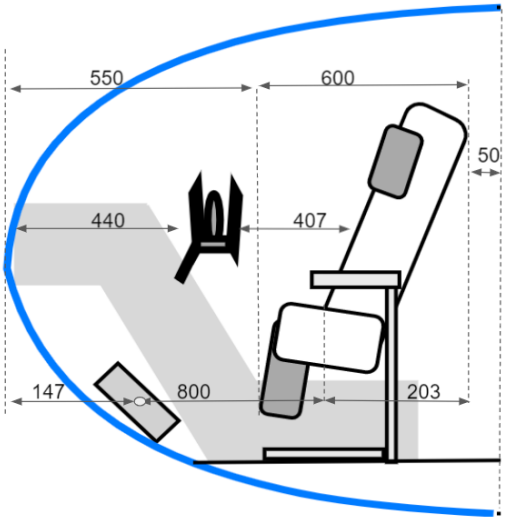

Figure 6.5: Sketch of the side view of the cockpit with dimensions

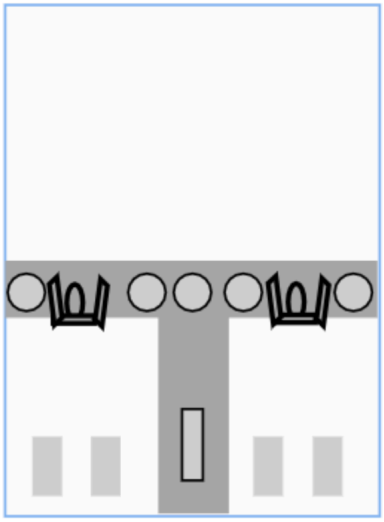

Figure 6.6: Sketch of the cockpit view

[2] URL https://www.majorsafety.com/products/junkin-lightweight-stokes-basket-rescue-stretcher, [cited 25 May 2021]

6.2. Design of the Structure

During operation the aircraft will be submitted to large, varying, loads. As mentioned in Section 4.3, a requirement states that the aircraft shall be able to sustain load factors up to $n = 6$. In the following section, a method to find a preliminary design of the airframe and wing structure will be presented, analysed for this load factor. Following the analysis of Megson, one of the critical load cases for the airframe structure is a steady pull-up manoeuvre at maximum load factor [34]. This is the design load case considered for this initial estimate of the airframe design, and will provide a reasonable estimate for the critical external and internal loads carried by the aircraft.

6.2.1. Structural Design

The major load-carrying element in the aircraft is an airframe, where a combination of longitudinal stringers, thin metal skin, and transverse frames supply load-carrying capabilities in all directions. In the load case considered, the skin will largely carry the shear force on its own. The shear force from the empennage also induces a bending moment in the fuselage, which will be carried by the stringers. The transverse frames are positioned in the fuselage to transfer shear loads from the skin, into the airframe shell, and also to reduce the effective length for buckling under compressive stresses. Therefore, the transverse frames will be important to analyse for critical stresses. Due to brevity, the buckling is not considered in detail, but the distribution of transverse frames rather set to five along the fuselage.

To provide an initial analysis of the internal loads of the aircraft, the shear flow distribution around a transverse frame is calculated using an idealised cross-section of the fuselage. Figure 6.7 shows this idealised fuselage cross-section featuring eight, evenly distributed booms, representing stringers, around the rectangular shape of the fuselage. The top-left and top-right booms have an area of $B_1 = 1000\text{mm}^2$, and the remaining half that, at $B_2 = 500\text{mm}^2$. The larger booms at the top extend to the twin-boom empennage, and will therefore be the main load-carrying stringers of the airframe.

The two governing equations for shear flow in closed sections are seen in Equation 6.1 and Equation 6.2. Using these, an analysis of the shear flow distribution of the idealised cross-section will be done to give an initial idea of the internal stresses carried by the airframe.

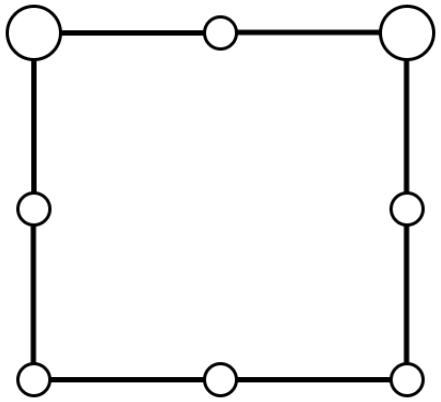

Figure 6.7: The idealised fuselage cross-section, featuring 8 booms with attaching skin, in a rectangular shape.

$$q_s = -\left(\frac{S_x I_{xx} - S_y I_{xy}}{I_{xx} I_{yy} - I_{xy}^2}\right)\sum_{r=1}^{n} B_r x_r - \left(\frac{S_y I_{yy} - S_x I_{xy}}{I_{xx} I_{yy} - I_{xy}^2}\right)\sum_{r=1}^{n} B_r y_r + q_{s,0} \quad (6.1)$$

$$S_x \eta_0 - S_y \xi_0 = \oint p q_b ds + 2A q_{s,0} \quad (6.2)$$

The stringers in Figure 6.7, running along the fuselage, will connect at the front of the cockpit providing protection in the event of impact on landing. With a transparent cockpit, the pilot and passengers are also more exposed to the environment, like branches or, more critically, rocks and wires, on the landing roll. By bringing the structural stringers around the front, to the nose, any debris or obstacles will be moved away from the pilot and payload without the added weight of additional protection.

$$\frac{d^2 v}{dx^2} = \frac{-M}{EI} \quad (6.3)$$

Another critical aspect of the structural design is the internal loading diagrams of the wings. The deflection of the wings will be computed using Equation 6.3, with the Young's Modulus E following the material selection, and I, the moment of inertia of the final wing cross-sectional area. A strut can be placed under the wing, reducing the effective length of the wing, and in turn reducing the required structure in the wing root.

6.2.2. Material Selection

In order to determine the structural properties of the bush plane, a suitable material, for the general structure, should be selected. Given the requirement that 80% of the material used in the bush plane shall be reusable

at the end of life, several environmental friendly materials were studied and compared in order to perform a formal trade-off. In this section, information is provided regarding the selection of the most suitable material.

Material Options The first step in choosing the optimal material is listing suitable and environmental friendly materials. As aluminium alloys show a good performance for the recyclability criteria, three aluminium alloys that are commonly used in aircraft are analysed and taken into account for trade-off. Due to the properties regarding recycling, energy can be saved up to 95% and around 75% of the aluminium ever made is still in circulation [3]. The aluminium alloys taken for the trade-off are Al2024, which is commonly used in aerospace for parts where a high strength-to-weight ratio is needed [4], Al2014, widely used for high strength structures in the aerospace industry and defence sector [5], and Al6061, commonly used for the construction of aircraft structures like wings and fuselages [4]. Next to aluminium alloys, also several natural fibre composites are studied and considered for further trading-off. Natural fibres are green materials having a fully degradable and renewable aspect and their growth does not release toxic gases but captures carbon dioxide instead. However, the recycling of the composite itself is rather tough as the matrices are usually thermosetting embedded. One way to solve this issue is the shredding of the material to ruse them as fillers in the production of products, where fillers are usually added, like calcium carbonate or silica, which have the same or even better material properties compared to the initial composite [11]. Therefore, there are four natural fibre composites taken into account, all having an epoxy resin. Flax fibre composite is considered for the trade-off due to its cost-effectiveness and its mechanical properties being comparable to those of glass fibre composites [67]. Also, flax seeds supply linseed oil, which can be used for the production of the epoxy resin, making it an even more efficient option [23]. Bamboo fibre composite is also considered because of its light weight and high strength properties [2]. Next to that, basalt fibre composite is analysed because of its high E-modulus, high strength and elastic behaviour [22]. Finally, also cotton fibre composite is studied for the trade-off, because of the high strength and fracture toughness it offers [5].

Selection Criteria To perform the trade-off, selection criteria should be defined and weighted. Hereby, both qualitative, for which an analysis is required, and quantitative criteria, for which calculations are required, are defined. As the material should be light weighted, stiff and strong to carry the loads, the specific stiffness (S.E.) and the specific strength (S.S.) are chosen to be Quantitative selection criteria and weighted with a factor of five. In these criteria, the weight is included as the specific stiffness and specific strength are defines as the ratio over the material density. Next to the specific strength and stiffness, also the environmental impact (E.I.) due to the production of that material is a qualitative selection criteria and weighted with a factor of four. Because the cost of the material (C.) influences the total price of the aircraft, the cost per kilogram material is considered to be a quantitative selection criteria with a weight factor of three. Lastly, the damage tolerance of the material (D.T.) is taken into account as a qualitative selection criteria, as it influences the lifetime and the maintenance cost of the bush plane. Table 6.5 provides an overview of the selection criteria, together with their tag, assessment type and weight.

Table 6.5: Selection criteria for the material selection

Tag	*Criteria*	*Assessment Type*	*Weight*
S.E.	Specific stiffness	Calculation	5
S.S.	Specific strength	Calculation	5
E.I.	Environmental impact	Qualitative	4
C.	Cost per kg of material	Calculation	3
D.T.	Damage tolerance	Qualitative	2

Formal Trade-off With the selection criteria mentioned in Table 6.5, the different aluminium alloys and natural fibre composites can be compared. For the quantitative selection criteria, the material properties were taken from the Grants Edupac 2020[6]. However, since the material properties of the composite depends on the fibre fraction, all four natural fibre composites are said to have 40% fibre volume fraction and an epoxy matrix for the sake of comparison. Given the latter, the composite's properties, like the young's modulus and ultimate strength, can be computed using the rule of mixture, given in Equation 6.4 [6].

$$E_u = fE_r + (1 - f)E_m \tag{6.4}$$

[3]URL https://www.recyclenow.com/recycling-knowledge/how-is-it-recycled/cans [cited 14 June 2021]
[4]URL https://www.aircraftspruce.com/catalog/mepages/aluminfo.php [cited 14 June 2021]
[5]URL https://web.archive.org/web/20190920071009/https://www.smithmetal.com/2014a.htm [cited 14 June 2021]
[6]URL https://www.ansys.com/products/materials/granta-edupack, accessed 22/06/2021

In Equation 6.4, E_u is the upper boundary of the composite material property, f is the volume fraction of the fibres, the E_r is the property of the fibre reinforcement, and the E_m is the property of the matrix. When applying Equation 6.4, the material properties of the natural fibre composites are calculated. The overview of the quantitative results is provided in the trade-off matrix in Table 6.6. Note that only the upper boundary was considered for comparison in the trade-off table. For the qualitative selection criteria, the material needs to be studied. The environmental impact (E.I.) depends on the way of producing the specific materials. To produce one tonne of aluminium, 17,000 kWh of energy is required [12]. Therefore, the environmental impact of aluminium alloys are marked as having correctable deficiencies. When creating aluminium using renewable energy, this deficiency can be corrected. The environmental impact of the natural fibres on the other hand however, is marked as excellent as the material captures carbon dioxide when growing. The second qualitative selection criteria is the damage tolerance. Aluminium alloys show good behaviour in terms of corrosion, fatigue, as its fatigue limit is defined to be $10^7 - 10^8$ cycles. Therefore aluminium alloys are marked as excellent for the trade-off. Natural fibre composites show less favourable properties for damage tolerance. However the ultimate strength is significantly reduced after impact, the value of the Young's modulus is barely affected [53]. Since the stiffness property almost remains unchanged, the damage tolerance of natural fibres is marked as acceptable. Basalt reinforced composite however shows unacceptable damage tolerance behaviour, due to basalt being brittle [27]. In Table 6.6, the trade-off table is given.

Table 6.6: Trade-off matrix of the material selection

	S.E.	S.S.	E.I.	C.	D.T.
Al 2024	27.9 [G]	28.6 [Y]	[Y]	2.64 [B]	[G]
Al 2014	27.6 [G]	113 [G]	[Y]	2.64 [B]	[G]
Al 6061	25.8 [G]	53.5 [B]	[Y]	2.5 [G]	[G]
Flax fibre	17.5 [B]	100.5 [G]	[G]	2.54 [G]	[B]
Bamboo fibre	8.54 [Y]	48.2 [B]	[G]	2.51 [G]	[B]
Basalt fibre	20.9 [B]	720.9 [G]	[G]	2.81 [Y]	[R]
Cotton fibre	4.02 [R]	92.8 [G]	[G]	3.17 [Y]	[B]

From Table 6.6, it can be seen that the only material without unacceptable properties nor correctable deficiencies is the flax fibre reinforced composite, using epoxy as matrix. Therefore, this was chosen to be the main material for the *Twin Puffin*.

Selected Material From the trade-off it can be seen that flax fibre composite, with epoxy as matrix, is the most suitable material for the design of the bush plane. However, to prevent failure, the flaws and risks of this material should be clearly addressed. The first issue that can be acknowledged is the decrease in material properties of the natural fibres due to moisture [8]. Therefore epoxy was chosen as resin. The epoxy functions as water-resistant coating to protect the fibres from moisture [60]. One additional solution is an additional coating on the natural fibre composite, by immersing the fibres in a solution of ethanol and silane coupling and then adding nano TiO2 coating to the material [48]. Furthermore, composites show undesirable behaviour when subjected to shear. One possible way to increase the shear performance is by using pyramidal lattice cores, which can be seen in Figure 6.8 [65].

Furthermore, there are two different options to be considered for the epoxy resin. Either natural epoxy can be used or synthetic epoxy. The natural variant is more environment friendly, since it can be made from the linseed oil that can be abstracted from the flax seed used for the flax fibre. BioPoxy 36 has been found to be an ecologically friendly option with similar properties to what was assumed for the material trade-off [7]. Therefore, as it maintains high performance but allows for a more environmentally friendly design, natural epoxy will be used as resin for the selected flax fibre composite.

[7] URL https://ecopoxy.cdn.prismic.io/ecopoxy/ba9819ca-f76e-40fe-838c-88b62db8954a_TDS-BioPoxy-36.pdf [cited 25 June 2021]

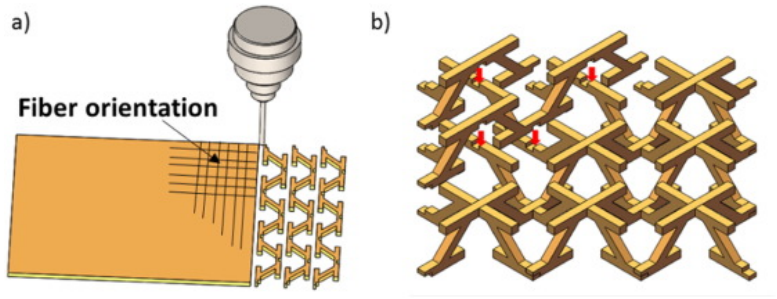

Figure 6.8: Pyramidal lattice structures with orientation [65, Fig 3]

6.3. Design of the Energy Source

In order to provide the aircraft with sufficient electric energy for the mission, careful attention had to be drawn to the design of the energy source. The energy system design was one of the biggest challenges for the project as it not only had to satisfy the demanding propulsion requirements, but also adhere to the environmental concerns. Thus, the need for an unconventional, state of the art system became crucial for the success of the project.

From an extensive research on energy acquisition types it became apparent that the most realistic option is to implement a hybrid system that would comprise an internal combustion engine (ICE) suited for electricity generation and energy storage in a form of batteries. The hybrid layout is a compromise between low emissions, low weight, and reliable high power output. In the two subsequent subsections, the ICE and batteries choices are explained. Afterwards, the trade-off between them is presented. Finally, an overview of the integration of the entire system is given.

6.3.1. ICE

It was decided during the design process that the ICE generator would be the primary source of power for the aircraft as it would be operating at highest efficiency at all times. Thus, a large generator was needed. During the research phase, two major options to implement a generator arose. One option is to acquire a complete engine-generator system as provided by manufacturers and the second option is to choose separately a combustion engine and a generator. The first approach is simpler as it does not require integration systems, however, it also confines the flexibility of the design as there is a limited number of such generators on the market. Also, it is believed that by choosing two separate components, the weight can be lowered.

For the ICE, it is preferable if it can run on low quality fuel. As the aircraft is supposed to operate in remote areas, the fuel supply is often limited. Thus, a widely available fuel was sought that is available even in distant communities. From the research it was found that car fuel is indeed very common and is relatively cheap and easy to operate. Either a diesel or petrol engine suffices for the mission. Diesel, offers slightly higher energy density but requires glow plugs to be operational in low temperatures and can be less environmental friendly due to exhaust gasses and particle emissions in the case that a catalytic converter and diesel particulate filter aren't used. Additionally, diesel is the most common fuel for military, agricultural, and construction vehicles while diesel generators are the primary source of electricity in Alaska [8]. On the other hand, petrol is more expensive and less accessible than diesel in remote areas. Finally, diesel and aircraft grade kerosene, such as Jet-A, are in fact so similar that in many engines one could use them interchangeably with few side effects. On top of these conventional options, sustainable fuels can also be used to reduce the net emissions. Sustainable aviation fuel will become much more widely available in the coming years, and will therefore increasingly available to the operators of the aircraft. Sustainable Aviation Fuels (SAF), also referred to as bio fuels, can be used in conjunction with regular fossil fuels, called blended SAF. Current SAF are certified up to 50% as drop in replacements, a number which is to rise to 100% [9]. Therefore the existence of multi-fuel aircraft engines that will take mixtures of diesel, kerosene and SAF are no surprise, a selection of multi fuel and more high performance Jet-A engines are shown in Table 6.7

The following Table 6.7 presents all the viable options of ICE that were considered and their parameters which were important criteria for the trade-off are provided. Naturally, more aspects, as explained above in this section, were considered.

[8]URL https://www.eia.gov/energyexplained/diesel-fuel/use-of-diesel.php [cited 21 June 2021]
[9]URL https://www.flightglobal.com/flight-international/how-sustainable-fuel-will-help-power-aviations-green-revo
143044.article [cited 21 June 2021]

Table 6.7: Diesel-Kerosene fuel engine options. The realistic power is actually the estimated power at FL100 when an economical cruise setting of 65% peak power is used [10][10]

Name	*Power [kW]*	*Realistic Power [kW]*	*Weight [kg]*	*Dimensions LxWxH [m]*
Continental CD-135[11]	99	61.1	134	8.2 x 7.8 x 6.4
Continental CD-155[12]	114	70.9	134	8.2 x 7.8 x 6.4
Continental CD-170[13]	125	78.0	156	8.2 x 7.8 x 6.4
Austro Engine AE300[14]	123.5	77.0	186	7.4 x 8.6 x 5.7
Safran SR305[15]	169	94.8	106.6	8.3 x 9.3 x 7.5

6.3.2. Batteries

As mentioned in above sections, the ICE is to be sized to operate at all times at highest efficiency. Thus as a result, the batteries are to be sized for take-off and climb support with enough reserves in case the ICE fails. For selecting the appropriate battery type for the mission, the driving property is the specific energy. However, there are also other aspects of batteries that were investigated, for instance toxicity or resistance to abuse.

The research that had been performed prior to the batteries was firstly focused on the specific energy. As the weight of the aircraft is a very sensitive parameter, the batteries with the lowest specific energy were discarded from the considered options very early.

Another aspect that was of crucial importance for batteries to be used for an aircraft, is the depth of discharge and number of useful cycles. As the aircraft is meant to operate with limited access to maintenance and in general supplies, the batteries need to be able to last long and without loosing too much of their maximum capacity. Replacing the batteries should not happen more often than every second serious ICE maintenance. Thus, this criteria narrowed down the considered selection of batteries types even more.

As this entire project aims to redefine the sustainability of a small general aviation aircraft, a special emphasis during the selection of batteries was placed on the toxicity and recyclability. It is commonly known that some types of batteries use nickel and cadmium extensively, which are undeniably linked to harmful effects on environment. Also, certain batteries are suitable for recycling, which is a very desirable aspect and was treated as a great advantage of a battery. All these aspects were taken into consideration when selecting the battery type for the project.

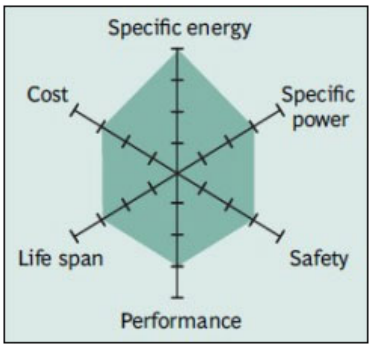

Figure 6.9: Web-plot displaying the characteristics of a lithium nickel manganese cobalt battery (NMC) [9, Fig 7]

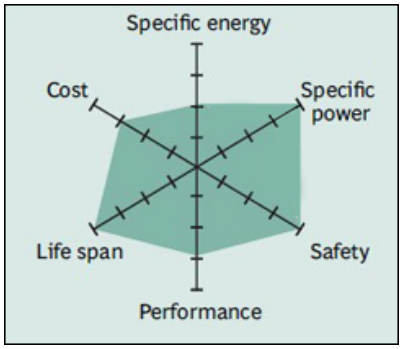

Figure 6.10: Web-plot displaying the characteristics of a lithium iron phosphate battery (LFP) [9, Fig 9]

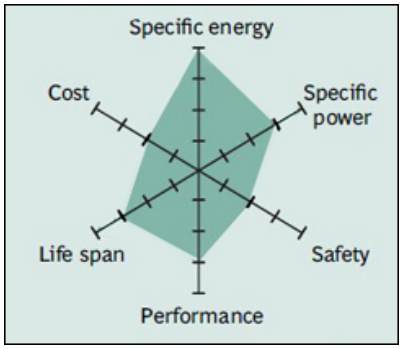

Figure 6.11: Web-plot displaying the characteristics of a lithium nickel cobalt aluminium battery (NCA) [9, Fig 11]

From the above reasoning, few battery types were selected that adhere to the desired standards. Most notably Lithium-Ion batteries of NMC and LFP types. Apart from providing relatively high specific energy, they are suitable for recycling, do not use excessively harmful substances, and allow for many charging cycles. Additionally, they have an advantage that they can confined into small cells and as a result, arranged freely in the fuselage. Instead of one cumbersome battery, it is possible to have many smaller ones. There are almost no limits to their distribution, which means that they can fill up dead space in the fuselage or can be placed somewhere in order to alter the location of the centre of gravity. This should also allow for sufficient safety shielding to be included in battery packs to keep the batteries and the aircraft safe. Although lithium ion battery cells like NCA can also have cost and safety concerns.

For future applications of batteries in the aircraft industry, lithium polymer batteries are a very promising

[11] URL `http://www.continental.aero/diesel/engines/cd135.aspx` [cited 21 June 2021]
[12] URL `http://www.continental.aero/diesel/engines/cd155.aspx` [cited 21 June 2021]
[13] URL `http://www.continental.aero/Continental_CD-170_Jet-A_Engine/` [cited 21 June 2021]
[14] URL `https://www.austroengine.at/uploads/pdf/mod_products9/AE330FactSheet.pdf` [cited 21 June 2021]
[15] URL `https://www.smaengines.com/sites/snecma_sma/files/fiche_sma_sr_305_engine_bat_0.pdf` [cited 21 June 2021]

concept. They provide even higher specific energy values and are flexible, which also simplifies the arrangement in the fuselage. However, as of today, they suffer from inflation issues and low cycles. This technology is still under development and fortunately for the aircraft industry, it is expected to overcome these issues in near future.

6.3.3. Energy Acquisition Sizing

As already introduced in the preceding subsections, the ICE was tasked with energy provision mostly for the cruise as it would operate at all times with the RPM suited for the most efficient energy production. The batteries however are meant to power the take-off. This task division has many advantages, primarily, the weight of the entire system can be relatively low, as most of the energy is to be delivered by the ICE. Lower weight is thus due to the fact that the specific energy stored in fuel is much higher than the specific energy stored in batteries. Thus, if majority of the energy is to be provided by the ICE, which uses fuel, the energy stored in batteries can be lower, meaning that the total mass of the system also drops significantly.

However, having a more powerful engine has also certain undesired outcomes. As majority of energy is to be produced by the ICE, the shear size of it needs to be larger and as a result, heavier. A bigger engine may pose a problem to the structure of the aircraft. Initially, the engine was assumed to take place above the fuselage, however, if it is too heavy and big, the predefined engine bay may prove to be too small for a big engine and the structural support may be too weak. Thus, there are constraints in choosing the ICE. Another example of such constraints is the increase in emissions. While batteries are assumed to be charged with electricity at the location of the take-off with sustainable energy sources, the ICE burns fossil fuel such as diesel or petrol leading to emission of exhaust gasses. Thus, a bigger engine is linked to higher emissions. For these reasons, there is a pressing incentive to choose an engine which is smaller.

Having introduced the dilemmas in ICE and battery selection, now the method to size the energy acquisition system can be presented. In order to choose an appropriate combination of the ICE and batteries that would deliver the desired performance for the mission, an optimising tool was set up. This tool takes as inputs different engine options, specific energy of fuels and batteries and the required power for the mission. The following Table 6.8 summarises the inputs.

Table 6.8: Summary of inputs needed for the sizing of the energy acquisition system

Inputs to the Tool	*Description*
ICE Options	Power, mass and type of fuel
Battery Properties	Specific energy, energy density
Power Required Climb	-
Power Required Cruise	-
Thrust Cruise	-
Maximum Thrust	Maximum thrust while taking-off

In the ICE category two previously considered variants of generators are present: the complete generators and the generators that are assembled from separately available parts. For the assembled generators, the mass that is considered, is the mass of engine, electric generator and interrelating systems.

Firstly, the tool takes the value for the power required for the mission and based on the duration of the mission it translates it into energy that needs to be provided. Knowing the specific energy of given fuel and power of a given ICE, the tool verifies if the engine is sufficient for the mission. Then, the energy system sizing tool evaluates the amount of fuel needed for the mission, returning its mass and volume.

Afterwards, having determined if the ICE suffices for the cruise, the tool starts the analysis of the batteries required for the climb. It calculates the energy that needs to be stored in batteries based on the power required during the take-off. However, unlike the ICE options, which are discrete, the battery sizing can be done almost continuously. Batteries increase their energy capacity with very small increments, thus for the sake of this analysis the tendency can be assumed to be continuous. Moreover, their energy storage can be assumed to scale linearly with mass. Thus, as a result of the aforementioned reasoning, any battery energy requirement can be satisfied. Based on the energy that needs to be stored in batteries, the mass of them is determined using the specific energy value given for the battery type.

After evaluation of the ICE options and sizing the batteries accordingly to the climb requirements, the tool applies redundancy and safety margins. Thus, the ICE, which provides power and energy for the most pessimistic scenario, requiring the highest power, is only deemed acceptable. Also, additional amount of fuel is added for redundancy. Then, the same is done with the batteries, they are sized again to have bigger capacity in order to account for even more unforeseen events (e.g. longer climb, difficult conditions). When the initial sizing based on the power requirements is completed, the tool proceeds with other constraints, namely: ICE size and weight, emissions rates and noise. Firstly, the tool needs to verify if the requirement of the emission rates and noise is satisfied. The stakeholders demand that the aircraft curbs the emissions by 50% and noise

by 70% with respect to the reference aircraft. Thus the tool evaluates the emissions of the selected ICE unit. The CO2 emissions are based on energy of the fuel, which then is related to the specific energy. Thus, having the mass of the fuel burnt during flight, it is sufficient to determine the mass of the CO2 emitted. Also, the noise is evaluated and verified under the noise requirements. If the mass of the resulting energy acquisition unit does not adhere to the desired standards, the research on engines is broadened and the evaluation is iterated for newly found engines. If no available engines are sufficient to meet the CO2 requirements, that means that the design needs to settle with the biggest engine that does, and compensate the lack of energy provided by it with additional batteries. Thus, the initial idea to run the ICE on most efficient RPM and size the batteries for take-off only is redefined. The batteries would need to be present for cruise as well. However, it is not desired as more batteries introduce additional weight.

Another constraint under which the chosen ICE is analysed is the size and weight. As already mentioned, the engine bay described in the Section 6.1.1 is confined. Thus, the ICE needs to adhere to the assigned maximum dimensions and weight. In case it does not, the same procedure is applied that was used in case of too high emissions.

In addition to the ICE generator used to produce cruise and some climb energy, during descent, some or all of the propellers can also be used to harvest part of the potential energy while still in the air. This is beneficial as any in flight charging capability would allow for a reduction in heavy battery capacity as well as increasing overall energy efficiency of the aircraft. According to Sinnige et al. it's possible to use normal propellers with electric motors to generate electric power with an efficiency of up to 8.5% during descent at an ideal propeller rotational speed. This additional energy generation source is useful for reducing overall weight and ensuring some additional energy for the powering of high lift augmenting distributed propulsion.

6.3.4. Integration of the System

Having selected a combination of ICE and batteries, the integration between them needs to be designed. Specifically, in order to keep all energy sources compatible, all system power will be taken from or converted into electric power. So that the ICE will be attached to a high efficiency, full scale, electrical generator to produce electrical power.

Firstly, for electrical system integration, it is necessary to use an additional generator to attach to the ICE in case a complete engine/generator system isn't chosen. The generator that would then be used for this energy conversion task was specifically designed for the purpose. Honeywell's 200 kW capable generator has an efficiency of up to 90% and is designed for use in future electric propulsion aircraft with a small form factor and low weight [11]. Either way the engine/generator and the battery will need to individually provide the necessary power to the power distribution unit for all systems to operate at least on an emergency level in order to provide necessary safety and redundancy while together in nominal operation the power as described in previous sections needs to be provided.

Furthermore, during descent, the propellers on the wing tip which aren't able to fold for drag reduction will be employed to generate power. The nature of electric motors means that they are capable of not only producing kinetic energy but also turning it back into electrical power, in fact, many electric motors certified for aviation use are capable of this as a feature. For this reason windmilling of the tip mounted propellers on descent will be used to generate additional power to recharge the batteries without the use of the internal combustion engine in preparation for landing battery power draw.

6.4. Design for Lift Augmentation

One of the key aspects of using distributed propulsion is that it allows for higher lift generation. The placement of propellers along the wing leading edge energises the flow over the lifting surfaces behind it, thereby leading to higher aerodynamic forces than could otherwise be achieved at the same flight conditions. As this lift augmentation combines the properties of the wing and the propulsion subsystems, it must be analysed first before either of the two subsystems can be designed. This section first presents the general implication that designing for lift augmentation has on the propulsion system, before discussing the method used to model lift augmentation and explaining how the high lift propellers are optimised for their purpose.

6.4.1. Use of Propellers for Lift Augmentation and for Cruise

For the *Twin Puffin*, two different types of propellers shall be used: one pair of large wing tip propellers for cruise, combined with a set of smaller high lift propellers distributed along the wing leading edge. During cruise, lift augmentation is not required and the primary focus of the propulsion system is to provide sufficient thrust to balance the drag. During takeoff and landing, however, the concept of distributed propulsion allows for significant lift increases that lower the aircraft stall speed and improve its STOL characteristics.

[11] URL `https://aerospace.honeywell.com/content/dam/aerobt/en/documents/learn/products/electric-power/brochures/N61-2024-000-000_200kw-Generator_v2.pdf` [cited 20 June 2021]

Because the need for lift augmentation aligns with the different mission phases, dividing the propulsion system between cruise and takeoff/landing means that the propellers can be optimised for their respective flight conditions. On the one hand, the large wingtip propellers will be optimised for the relatively higher speeds during cruise. On the other hand, the high lift propellers will be designed for operation at low speeds and must comply with the prescribed thrust and diameter values determined in Section 6.4.3. Therefore, the use of different propellers for different purposes will allow for an overall more efficient aircraft.

6.4.2. Modelling Lift Augmentation

A common approach to modelling the effects of lift augmentation is to find an expression for the local increase in lift per unit span, which can then be applied selectively to the blown areas of the wing. As shown in Equation 6.5, a very simple method to calculate this lift augmentation factor is to equate it to the ratio of dynamic pressures for the blown versus the unblown wing. However, the method is inaccurate and fails to account for important parameters such as the propeller radius. As argued by Patterson and German, this method is thus deemed insufficient for estimating the effective lift augmentation [43].

$$\frac{L'}{L'_\infty} = \frac{q}{q_\infty} \tag{6.5}$$

Patterson and German also present an alternative, more elaborate analytical method that takes into consideration a larger set of design parameters [43]. However, the method was found to be insufficiently stable when larger ranges of input values are considered. While this second method was thus also found to be inadequate for the task at hand, it nonetheless put forth the design considerations that lift augmentation is enhanced when the distance between the propellers and the wing leading edge and the ratio of propeller radius to wing chord are increased. Although, these effects are not quantified in the lift augmentation method used for the design of the *Twin Puffin*, they are backed up by Patterson et.al. using simulation results [44] and are thus incorporated in the design as much as possible. Specifically, they support the choice of a high aspect ratio, which given the required wing surface area reduces the wing chord, and favour the design of placing the engines on booms in front of the wing.

The lift augmentation method selected for the design of the wing is that provided by Patterson et.al. in a later paper. Shown in Equation 6.6, the method is based on semi-empirical findings and determines the lift augmentation using the propeller radius, here referred to as d, and the ratio a of velocities in front of and after the propellers [45].

$$\frac{L'}{L'_\infty} = \left(1 - 0.18909\left(a/d^2\right) + 0.04883\left(a/d^2\right)^2 - 0.00479\left(a/d^2\right)^3\right) \cdot \left(\frac{V_{ep}}{V_\infty}\right)^2 \tag{6.6}$$

6.4.3. Optimisation of High Lift Propellers

With the method for predicting lift augmentation selected, it is then possible to identify the optimum combination of propeller strength, size, number, and placement. To do so, it has been identified that these parameters will be limited by the available space on the wing as well as the total thrust required. As thrust is limiting, the choice has been made to not use the two most outboard engines on the wing tips during flight phases where lift augmentation is desired. This is so because only half the wake of the wing tip engines streams over the wing, making them inefficient in terms of lift generation. Thus, when lift augmentation is desired, all thrust will be generated by the inboard engines, which have all of their energised wake flowing over the wing. Following from this choice of not using the wing tip engines for lift augmentation is that the available space on the wing leading edge is limited to the total span of the wing, minus the width of the fuselage, minus a safety margin of 15% fuselage width between the cabin and the most inboard propeller tip, and minus half the diameters of the engines on the wing tips. Another factor that must be considered in order to find the optimum number and sizes for the propellers is the airspeed for which the system shall be optimised. As lift augmentation is most crucial during slow flight, for instance at landing and takeoff, the system shall be sized for operating at ten percent above stall speed under sea level conditions.

To find the best number and size of propellers, it is then necessary to connect the thrust per propeller, which is simply the total thrust divided by the number of engines, to the ratio *a* of the velocity generated by the propeller to the free stream velocity. As this is the flight regime of interest for the lift augmentation system, the free stream velocity is set to equal 110% of the aircraft stall speed. As is shown in Equation 6.7 and Equation 6.8, this is done using the results of actuator disc theory [63].

$$V_{ep} = \sqrt{\frac{8T_{prop}}{\pi D_{prop}^2 \rho_\infty} + V_\infty^2} \tag{6.7}$$

$$\left(a/d^2\right) = \frac{4V_{ep}}{V_{inf}D_{prop}^2} = \frac{4}{V_\infty D_{prop}^2}\sqrt{\frac{8T_{prop}}{\pi D_{prop}^2 \rho_\infty} + V_\infty^2} \tag{6.8}$$

The parameter a/d^2 can then be calculated by using the different options for the propeller radius. Knowing this parameter then allows the calculation of the local lift increase. However, it is essential to realise that the parameter of interest is not the maximum local increase in lift, but rather the lift augmentation of the total wing. Thus, the parameter used to compare the different options is the local increase ratio in lift per unit span, weighted by the total fraction of the wing area that is blown by the high lift propellers. This concept is illustrated using the two half-wings in Figure 6.12. Even though the option on the left has a higher local lift increase, the greater fraction of blown area (indicated by the shaded region of the wings) means that the option on the right leads to a higher total lift increase.

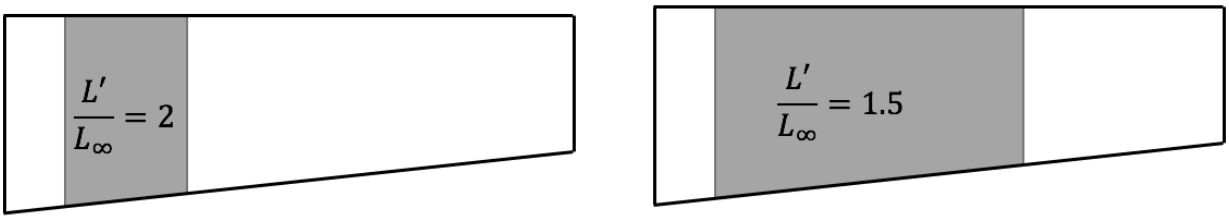

Figure 6.12: Effect of blown wing fraction on total lift augmentation

Accounting for all feasible possibilities of propeller number and size leads to the results displayed in Figure 6.13. The graph is based on sample values of a total thrust of 3000 N and a stall speed of 18 m/s at sea level. The number of engines considers even numbers only, as the aircraft is desired to be symmetric and have the same number of propellers on both wings. It is important to note that not the entire domain of engine numbers and propeller sizes produces feasible values. For one thing, no lift augmentation values are provided in case that the combination of engine number and propeller radius exceeds the available space. As a limiting scenario, propellers are assumed to be placed tip-to-tip, a placement choice that will be explained in more detail in Section 6.5. The other scenario where no values are returned is when the combination of parameters leads to a too high a/d^2 value that exceeds the domain of the lift augmentation method.

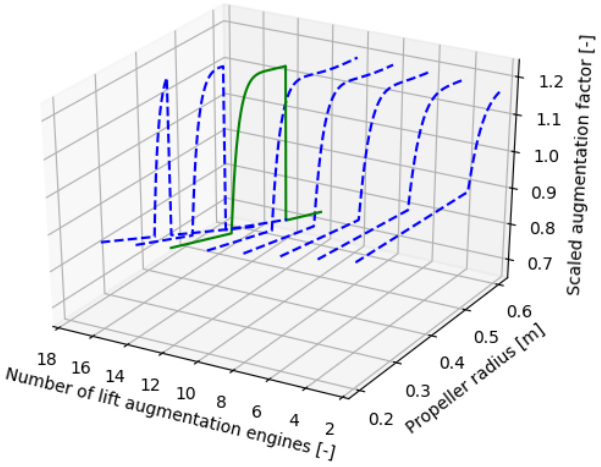

Figure 6.13: Scaled wing lift augmentation factor for different combinations of propeller size and number.

Based on the results of Figure 6.13, which will be iteratively re-calculated as values for total thrust and stall speed are updated, it is possible to identify the optimum combination of propeller size and number. For

the example shown in Figure 6.13, this optimum lies on the continuous green curve at a total of 14 high lift propellers (excluding the propellers on the wing tips) with a diameter of 0.824 m each. Consequently, the thrust per propeller can also be found. The results of the design for lift augmentation are then used in Section 6.5 and Section 6.6 for the design of the wing and the individual propellers. Furthermore, the same method as discussed here will be applied to identifying the optimum propeller parameters for the blowing of the horizontal tail, which is discussed in greater detail in Section 6.7. There, the propeller radius will be known, so instead the optimal number of propellers as well as the optimal thrust per propeller will be known.

6.5. Design of the Wing

The design of the wing is tightly interlinked with the overall aerodynamic properties of the aircraft and is thus in direct relation with the aircraft stability and performance. This section presents the methods used to design the different aspects of the wing, starting with the wing planform and continuing with the airfoil selection, the lift and drag characteristics, the use of high lift devices, the effect of lift augmentation, the aerodynamic moments, the aileron sizing, and the wing mass.

6.5.1. Wing Planform

Two key parameters are taken as inputs to the design of the wing planform: the wing area and the wing span. Both values follow from the overall optimisation of aircraft parameters, and can thus be sized for. In addition, choices have to be made regarding a set of other geometric parameters, which are explained below.

Taper Ratio Though the wings of bush planes such as the Piper Cub reference aircraft are often untapered, the use of wing taper is not unheard of for aircraft this size, for instance, the Cessna 172 Skyhawk reference aircraft [12]. For the wing of the *Twin Puffin*, a taper ratio of 0.7 has been selected. This value strikes the balance between drag efficiency and structural as well as lift augmentation considerations. On one hand, a taper ratio of 0.7 is low enough that the lift distribution over the wing is still largely elliptical[14], which increases the Oswald efficiency factor and therefore reduces the level of induced drag. On the other hand, the taper ratio is high enough that the difference between tip and root chord is sufficiently modest and the length of the root chord is not excessive. Too large a root chord could otherwise lead to problems with the structural integration into the fuselage and, as discussed in Section 6.4, it would reduce the beneficial effects of lift augmentation.

Sweep In general, the main purpose of using swept wings is to increase the wing critical Mach number. The disadvantages of swept wings are the increase in structural weight of the wing due to torsional forces acting on the planform and the decrease of maximum lift coefficient of the wing [14]. As the low Mach number at which the *Twin Puffin* will be flying means that sweep is not necessary, a straight wing with zero leading edge sweep will be used. This is furthermore beneficial as it will ease the mounting of the propellers on the wing leading edge, avoiding the issue of propellers potentially striking the swept leading edge [14]. It must be noted that, due to the inclusion of wing taper, the sweep will have non-zero negative values at all other chordwise positions. However, due to the high wing aspect ratio and modest taper, the angles remain small.

Dihedral Normally, dihedral is used to mitigate the influence of sideslipping turbulence, as aircraft with a dihedral angle will naturally return to a stable position [14]. However, there are numerous disadvantages of using it for a bushplane, including increased drag, reduction in roll capabilities and potential problems with ground clearance for the propellers. The dihedral for a high-wing configuration aircraft has to be pointed downwards to provide the aforementioned advantage and might therefore cause issues regarding the ground clearance. Thus, a wing without dihedral is used.

Twist Though complicating the manufacturing of the wing, twist is found on the wings of many aircraft including small simple reference aircraft such as the Cessna 172 Skyhawk [13]. Whereas untwisted wings typically suffer from the wing tips stalling before the wing roots, the use of twist to achieve a lower geometric angle of attack at the wing tips allows for the desired scenario of the wing root stalling first [14]. However, though the topic was investigated, it was deemed that an accurate design of wing twist goes beyond the scope of this report. It is thus left for later design stages. Importantly, the neglect of wing twist at this point of the design process is feasible as it does not affect any of the other considered design methods.

[12] URL https://aerotoolbox.com/intro-wing-design/ [cited 22 June 2021]
[13] URL https://www.boldmethod.com/learn-to-fly/aircraft-systems/how-wing-washout-makes-your-airplane-and-wings-more-stable-in-flight/ [cited 20 April 2021]
[14] URL brightspace.tudelft.nl, Course AE2111-II, *Systems Design*, accessed 2021-06-22.

With the aforementioned inputs and selected parameters, it is possible to calculate the remaining wing geometry. Parameters such as the geometric aspect ratio, the average chord, and the root and tip chord can be found using commonly known geometric relations. Noteworthy are the important equations for the sweep at different chordwise positions and the chord length at different spanwise positions. Shown in Equation 6.9, the former is necessary to calculate the wing sweep at locations such as the quarter chord or the hinge line. The latter, shown in Equation 6.10 is necessary to determine the chord lengths behind the distributed propulsion propellers, which is necessary in order to calculate the blown area of the wing.

$$\Lambda_{x/c} = tan^{-1}\left(tan\left(\Lambda_{LE}\right) - \frac{2c_{root}(x/c)(1-\lambda)}{b}\right) \tag{6.9}$$

$$c_y = c_{root}\left(1 - \frac{2y}{b}(1-\lambda)\right) \tag{6.10}$$

Two further geometric parameters that are of interest are the length of the mean aerodynamic chord and the spanwise location of the mean aerodynamic chord, which are calculated in Equation 6.11 and Equation 6.12 respectively. Due to the unswept leading edge of the wing, the position of the leading edge of the mean aerodynamic chord is the same as the position of the leading edge of the root chord.

$$c_{mac} = c_{root}\frac{2(1+\lambda+\lambda^2)}{3(1+\lambda)} \tag{6.11}$$

$$y_{mac} = \frac{b(1+2\lambda)}{6(1+\lambda)} \tag{6.12}$$

6.5.2. Airfoil Selection

With the wing planform defined, it is then time to select a suitable airfoil. Due to the iterative nature of the calculations used to design this aircraft, it would not be suitable to simply select one airfoil and then use it no matter how the total aircraft design might change. Instead the airfoil should be selected based on the design lift coefficient, which follows from the design lift required at cruise. Thus, as the aircraft mass or wing area can change, so can the design lift coefficient and a different airfoil needs to be selected. Overall, the airfoil selection can be divided into the five the steps explained below.

Find Airfoil Database First, a database of ten suitable airfoils with different design lift coefficients, spanning the reasonable range of anticipated design lift coefficients, has been created. For all airfoils, the design lift coefficient has been determined by considering the airfoil lift coefficient at which the airfoil drag coefficient is minimised. In addition to having been selected for their desirable design lift coefficients, all airfoils have been picked such that they offer high maximum lift coefficients and high stall angles, properties that are important for STOL aircraft. All airfoil characteristics have been determined externally by using the *XFOIL* program at a suitable Reynold's number[14].

Calculate Total Design Lift With the airfoil options determined, the next step is to identify the desired design lift coefficient. The desired overall design lift is calculated as shown in Equation 6.13, where a factor of 1.1 is applied to account for potential negative lift from the aircraft tail [14].

$$L_{design} = 1.1\frac{1}{q_{cruise}}\frac{W_{cruise\ start} + W_{cruise\ end}}{2S} \tag{6.13}$$

Model Lift Augmentation During Cruise The value found using Equation 6.13 is, however, the total wing design lift and includes the effects of lift augmentation. While the inboard high lift engines are not used during cruise and thus do not cause any lift augmentation for most of the wing, there still is a small amount of lift augmentation at the wing tips. This is caused by half of the slipstream of the wing tip cruise propellers flowing over the wing behind them and locally increasing the generated lift. For the selection of the airfoil it is necessary to filter out the effects of this lift augmentation and find the unblown design lift coefficient of the wing.

To model the effects of lift augmentation during cruise, the lift augmentation method presented in Section 6.4 is used. The diameter of the wing tip engines, the thrust per engine, and the cruise conditions are all known, meaning that the lift augmentation factor can directly be calculated by using Equation 6.6, Equation 6.7, and Equation 6.8. This lift augmentation factor is then applied to the wing region behind the propeller, leading to an augmented lift distribution over the wing. The augmented lift distribution is then scaled such that the total area under the curve equals the design lift calculated using Equation 6.13.

[14]URL http://airfoiltools.com/ [cited 22 June 2021]

Calculate the Unblown Design Lift Coefficient Finally, the effects of lift augmentation are removed from the distribution without changing the scaling of the distribution. Thus, when the area under the distribution is re-computed, a smaller value than the original design lift is found. This is the unblown design lift, the value necessary for the selection of the most suitable airfoil. Subsequently, the division by the wing area and the freestream dynamic pressure at cruise allows the determination of the unblown wing design lift coefficient - the design lift coefficient for which the geometric wing shape shall be designed. As the wing does not have any leading edge sweep, this wing design lift coefficient also equals the desired airfoil design lift coefficient [15].

Choose the Best Airfoil With the desired airfoil design lift coefficient thus determined, the airfoil from the database, for which desired and actual design lift coefficient are closest to one another, is selected. In addition to determining the geometry of the wing cross-section and the wing thickness-to-chord ratio, the chosen airfoil also provides important aerodynamic parameters such as the airfoil stall angle and maximum lift coefficient.

6.5.3. Lift and Drag Characteristics

With the wing airfoil selected and geometry determined, it is then possible to investigate the wing lift and drag characteristics. The section first explains how to determine the effective aspect ratio, before discussing the lift slope, the maximum lift coefficient and stall angle of attack for clean aircraft configuration, the zero lift drag coefficient, and the induced drag.

Effective Aspect Ratio Whereas the geometric aspect ratio follows directly from the wing area and span, the effective aspect ratio also takes into consideration aerodynamic effects. For the *Twin Puffin*, the wing effective aspect ratio depends on the flight phase. During takeoff and landing, the large engines on the wing tips do not produce any forward thrust, so they do not have an impact on the wing tip vortices. Because the space is occupied by the wing tip engines, there are also no winglets mounted on the wing. Thus, during takeoff and landing the effective aspect ratio simply equals the geometric one.

During cruise, however, the operation of the wingtip engines means that the inboard swirling wing tip vortex is partially counteracted by the rotation of the propeller slipstream. As illustrated in Figure 6.14, this effect only holds when the propellers on the wing tips are outboard-rotating such that propeller slipstream and wingtip vortex rotate in opposite directions.

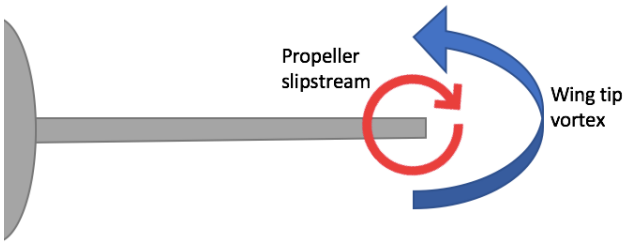

Figure 6.14: Wing tip vortex reduction caused by outboard rotating wing tip engines

The effect of increasing the effective aspect ratio using outboard-rotating wingtip propellers is discussed in parts by Snyder and Zumwalt. They present the relation shown in Equation 6.14, which links the strength of the propeller slipstream vortex to the engine thrust, the wing lift, and the wing circulation [58].

$$\Gamma_{prop} = \Gamma_{wing} \frac{T_{prop}}{L_{wing}} \tag{6.14}$$

From lifting line theory of subsonic aerodynamics it follows that the induced drag is proportional to the circulation of the wing tip vortices, which according to the model of vortex filaments together equal the total wing circulation. Thus, the equation linking the propeller slipstream circulation to the wing circulation can be used to calculate the reduction in effective wing tip vortex and consequently the reduction in induced drag. Equation 6.15 shows the proportionality statements for both the induced drag under regular conditions, and the induced drag in case of a wing tip engine with thrust. Given that the induced drag is proportional to the inverse of the aspect ratio, an equation for the effective aspect ratio as a function of the geometric aspect ratio and the wing tip engine thrust can be derived. This equation is shown in Equation 6.16. It is important to note that the results achieved with this method are on a sufficiently similar scale to the experimental findings of Sinnige et.al. (2019) [56].

[15]URL brightspace.tudelft.nl, Course AE2111-II, *Systems Design*, accessed 2021-06-22.

$$D_i \propto \Gamma_{wing} \Longrightarrow D_{i_{new}} \propto \Gamma_{wing} - \Gamma_{prop} \Longrightarrow D_{i_{new}} \propto \Gamma_{wing} \left(1 - \left(\frac{T}{L}\right)_{cruise}\right) \tag{6.15}$$

$$A_{eff} = \frac{A_{geo}}{1 - \left(\frac{T}{L}\right)_{cruise}} \tag{6.16}$$

Lift Slope With the effective aspect ratio determined, it is then possible to calculate the wing lift slope using the applicable DATCOM method [21]. In order to do so, it must first be confirmed that the aircraft indeed falls into the category of high aspect ratio wings, which given the straight leading edge of the wing and the taper ratio of 0.7 means that the geometric aspect ratio must be greater than approximately 3.5. As will be verified during the design process, this criterion is always met for the *Twin Puffin*. Therefore, it is possible to use the DATCOM method presented in Equation 6.17, where β is the commonly known Prandtl-Glauert correction factor calculated using the free-stream Mach number, and η is the airfoil efficiency with values around 0.95.

$$\frac{dC_L}{d\alpha} = C_{L\alpha} = \frac{(2\pi)A}{2 + \sqrt{4 + \left(\frac{A\beta}{\eta}\right)^2 \cdot \left(1 + \frac{\tan^2 \Lambda_{c/2}}{\beta^2}\right)}} \tag{6.17}$$

Maximum Clean Lift Coefficient and Stall Angle of Attack

The wing maximum lift coefficient can be calculated using the airfoil lift coefficient and the wing geometry. For this, the applicable DATCOM method, shown in Equation 6.18, is used. The fraction $\frac{C_{L\max}}{C_{l\max}}$ is obtained from a table of DATCOM reference values and, for an unswept leading edge, equals 0.9 [21]. It should be noted that in the equation the common convention is used that a capital L indicates the wing lift coefficient, whereas a lower case l indicates the airfoil lift coefficient.

$$C_{L\max} = \left[\frac{C_{L\max}}{C_{l\max}}\right] C_{l\max} \tag{6.18}$$

Related to the maximum lift coefficient is the wing stall angle of attack, which can be estimated using the DATCOM method shown in Equation 6.19 [21]. Here, $C_{L\max}$ is obtained from Equation 6.18, $C_{L\alpha}$ is calculated using Equation 6.17, and α_{0L} is the zero lift angle of attack which is the same for both the wing and the airfoil.

$$\alpha_s = \frac{C_{L\max}}{(C_{L\alpha})} + \alpha_{0L} \tag{6.19}$$

Drag Coefficient

The method used to determine the zero lift coefficient of the aircraft is shown in Equation 6.20[16]. The method is based on the principle of summing up the zero lift drag contributions of the different aircraft components. For the *Twin Puffin*, the relvant components are the wing, the fuselage, and both the horizontal and vertical tail. The standard drag contribution values of each component, C_{D_c} are taken from an empirical set of reference values that the method provides for multi-engine propeller aircraft. For this class of aircraft the method furthermore defines $C_{D_{mic}}$ as a further 15% in zero lift drag coefficient [16]. Finally, the $C_{D_{mic}}$ is assumed as extra 15% to account for other zero drag contributions, e.g. additional flow disturbances due to usage of rivets.

$$C_{D_0} = \frac{1}{S_{\text{ref}}} \sum_c C_{D_c} S_{wet_c} + C_{D_{mic}} \tag{6.20}$$

With the effective aspect ratio of the *Twin Puffin* known for the different flight phases, the remaining parameter necessary in order to calculate the induced drag for various lift coefficients is the Oswald efficiency factor. Shown in Equation 6.21, the used method is the semi-empirical relation presented by Howe, which takes into consideration the key geometric parameters of the wing [40]. The dependence of Equation 6.21 on the Mach number means that it is important to re-calculate the Oswald efficiency factor based on the flight condition of interest. Using the Oswald efficiency factor, the induced drag can then be calculated using Equation 6.21.

$$e = \frac{1}{(1 + 0.12 \cdot M^2)\left(1 + \frac{0.142 + f(\lambda) \cdot A \cdot (10 \cdot t/c)^{0.33}}{(\cos \Lambda_{c/4})^2} + \frac{0.1 \cdot (3N_e + 1)}{(4 + A_{eff})^{0.8}}\right)} \tag{6.21}$$

[16] URL brightspace.tudelft.nl, Course AE2111-II, *Systems Design*, accessed 2021-06-22.

$$C_{D_i} = \frac{C_L^2}{\pi A_{eff} e} \tag{6.22}$$

With both zero lift and induced drag coefficients known, the total drag coefficient can simply be found by taking the sum of the two components. Subsequently, the lift-over-drag ratio can be found by dividing the lift by the drag coefficient. Importantly, it must be ensured that all parameters are calculated for the correct mission phase and flight conditions.

6.5.4. High Lift Devices

Through increasing the maximum achievable lift coefficient, high lift devices play an essential role in further improving the STOL characteristics of an aircraft. For this reason, they are of particular importance for bush planes such as the *Twin Puffin*. Out of the many high lift device options available, single slotted slaps were selected as the most suitable choice for the *Twin Puffin*. This is due to the fact that they result in a substantial increase in maximum lift coefficient while maintaining relatively simple design, which is valued for bush planes. Compared to the even simpler plain flaps, single slotted flaps offer an additional increase of 0.4 in lift coefficient, while not adding a large additional amount of complexity [16]. Compared to more advanced options such as Fowler or double-slotted flaps, the single slotted option reduces the necessary system complexity and system mass. The usage of leading edge high lifting devices was deemed as unpractical due to distributed propulsion being mounted on the leading edge. As a result, if leading edge high lift devices were to be used, their total length would be small as it is not possible to have slots at the location where propellers are placed.

A key factor in how effective high lift devices are is the flapped area, so the fraction of the wing area that is either covered by flaps or is right in front of flaps. To maximise this reference flapped wing area S_{wf}, the entire trailing edge of the wing is equipped with extendable flaps. A 10 % margin is left at both the wing tip and at the intersection of the wing and the fuselage to avoid interfering with the structure of the wing tip engines and to remove the risk of a moving flap scratching the fuselage. To further increase the effectiveness of the high lift devices, a high value should be selected for the ratio of flap chord to wing chord. This value is either limited by the rear spar of the wing structure or the maximum feasible value, which is found to be 0.4[16]. The rear spar is placed by considering the location of the front spar (which is set at 20 % of the chord to account for the space required for the leading edge engine systems), and the length of the ICE and generator, which at the wing root have to fit between the spars. If this is farther back, the rear spar is placed at 55% of the chord. An additional margin of 5% of the chord length is then included behind the rear spar to ensure that there is enough space for the flap actuation mechanisms, and any remaining distance is available for the potential placement of flaps.

The effect of the slotted flaps on the wing maximum lift coefficient and zero lift angle of attack can be calculated using Equation 6.23 and Equation 6.24 respectively. With single slotted flaps deflecting up to $40\,\mathrm{deg}$, the airfoil lift coefficient increase $\Delta C_{l\max}$ is 1.04 during takeoff and 1.3 during landing. The change in zero lift angle of attack, $\Delta\alpha_{0L}$, is $-10\,\mathrm{deg}$ for takeoff and $-15\,\mathrm{deg}$. As flap deployment will not change the overall wing surface area (as would for example be the case for Fowler flaps) the lift slope does not change [16].

$$\Delta C_{L\max} = 0.9\Delta C_{l\max}\frac{S_{wf}}{S}\cos\Lambda_{hinge\ line} \tag{6.23}$$

$$\Delta\alpha_{0L} = (\Delta\alpha_{0L})_{\text{airfoil}}\ \frac{S_{wf}}{S}\cos\Lambda_{hinge\ line} \tag{6.24}$$

6.5.5. Lift Augmentation

One of the unique aspects of the *Twin Puffin* is that the use of distributed propulsion allows for further notable increases in lift during takeoff and landing. To model this, the optimised propeller thrust and size found in Section 6.4 are used.

With the propeller size and number known, it remains for the propellers to be placed in spanwise direction along the leading edge. Accounting for the elliptic-like nature of the wing lift distribution, lift augmentation will be most effective in the region close to the wing root. Thus, the high lift propellers are placed as far inboard as possible. Due to this reason, and to avoid small regions of very turbulent flow over the wing, the propellers are distributed in such a manner that in spanwise direction there is no gap between propeller tips. To avoid possible prop-on-prop strikes, every second propeller is slightly moved forward, leading to a propeller separation in chordwise direction.

The starting point for the calculation of the lift augmentation is the scaled lift distribution of the unblown wing. Elliptical in nature (a reasonable assumption due to the wing taper ratio of 0.7), the area under the distribution equates to the free stream dynamic pressure multiplied by the wing area and the applicable lift coefficient. Next, with the propeller characteristics known, it is possible to use Equation 6.6 to Equation 6.8 to find the lift augmentation factor behind each propeller. These lift augmentation factors are then applied to the unblown lift distribution, leading to local increases in wing lift. The procedure is similar to that used in the airfoil selection, with the difference that here the total area under the lift distribution is already scaled. Figure 6.15 shows an example of the unaugmented and augmented lift distributions for a half wing of an aircraft flying at sea level

[16] URL brightspace.tudelft.nl, Course AE2111-II, *Systems Design*, accessed 2021-06-22.

conditions at a velocity of 18 m/s, 3000 N of thrust, seven lift augmentation engines per wing, and flaps in takeoff position. The vertical lines indicate the spanwise locations of the lift augmentation propellers. As the lift distribution is shown for takeoff, only the inboard lift augmentation engines are active but the engines at the wing tips are not. Thus, there is no change in the lift distribution at the wing tips.

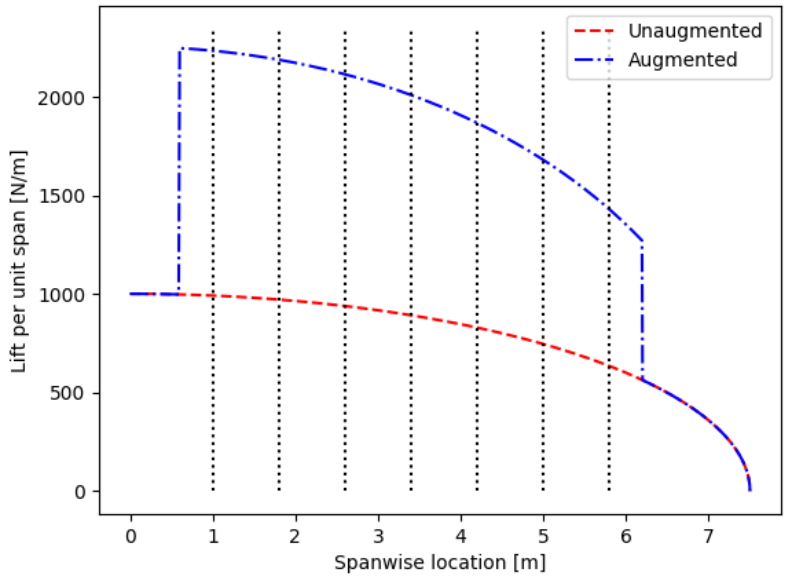

Figure 6.15: Unaugmented and augmented lift distribution for a half wing at sea level conditions at a velocity of 18 m/s, 3000 N of thrust, and flaps in takeoff position

The total augmented lift can then be found by numerically integrating the augmented lift distribution. Subsequently, this value can be converted to an augmented lift coefficient. Defined in this report as is shown in Equation 6.25, the augmented lift coefficient is calculated using the free stream dynamic pressure and the total integral of the augmented lift distribution. Using the augmented lift coefficient allows for an easy way to integrate the effects of lift augmentation into conventional calculations: whenever the aircraft performance is considered during flight phases where lift augmentation is active, the augmented lift coefficient can simply be used instead of the unaugmented one. It is important to note that the level of achievable lift augmentation depends on both the airspeed and the atmospheric conditions, and thus the augmented lift coefficient has to be re-calculated for different flight phases and altitudes. Furthermore, the change in lift coefficient also leads to a change in lift slope, which can be easily calculated by scaling the lift slope by the same factor by which the lift coefficient increased.

$$C_{L_{aug}} = \frac{\int_{-b/2}^{b/2} L'(y)\delta y}{q_\infty} \tag{6.25}$$

6.5.6. Ailerons

To ensure aircraft controlability, the wing design methods must also account for the sizing of the ailerons. Making use of the results of previous design steps, it has been decided to use flaperons and thereby combine the functions of flap and aileron into one mobile surface. Removing the need for an additional separate mobile surface on the wing trailing edge, the use of flaperons means that there is more space for trailing edge high lift devices, allowing for a higher maximum lift coefficient. The wing trailing edge flaps are thus split between a part solely used as high lift devices, and a part used for both high lift and for aircraft manoeuvring.

With the flaps already designed, sizing the aileron thus corresponds to identifying the spanwise limits at which the flaps are designated to be flaperons. As ailerons are more effective the farther outboard they are placed, the outboard limit is simply taken to equal the previously explained outboard limit of the flaps. What

remains to be identified is the inboard limit. To find this inboard limit, three equations must be considered[17]. Where the combination of capital C and lower case l now indicates the aircraft rolling moment derivative, Equation 6.26 and Equation 6.27 relate the wing properties to the rolling moment derivative for different aileron deflections and rolling moments respectively. The equation connecting these two parameters is Equation 6.28, where P is the minimum required roll rate. As follows from CS23 certification, the *Twin Puffin* is required to be able to perform a roll of $60\,\mathrm{deg}$ in five seconds or less. With all parameters apart from the aileron inboard limit b_1 known, it is then possible to combine Equation 6.26 to Equation 6.28 and solve the resulting cubic equation. With the aileron inboard limit thus found, the ailerons are completely defined.

$$C_{l_{\delta a}} = \frac{2c_{l\alpha}\tau}{S_{ref}b}\int_{b_1}^{b_2} c(y)y\,dy \tag{6.26}$$

$$C_{l_P} = -\frac{4\left(c_{l\alpha} + c_{d_0}\right)}{S_{ref}b^2}\int_0^{b/2} y^2 c(y)\,dy \tag{6.27}$$

$$P = -\frac{C_{l_{\delta a}}}{C_{l_P}}\delta a_{\max}\left(\frac{2V}{b}\right) \tag{6.28}$$

6.5.7. Aerodynamic Centre and Moments

For the proper determination of aircraft stability and control characteristics, it is important to determine both the location of the wing aerodynamic centre and the aerodynamic moment about this point. Using the methods of Torenbeek, the chordwise position of the mean aerodynamic centre shall be estimated using Equation 6.29 [61]. Using the wing taper and zero leading edge sweep, the position of the aerodynamic centre of the wing alone, $\left(\frac{x_{ac}}{\bar{c}}\right)_w$, is found to be 0.24. As follows from the relevant reference values provided by Torenbeek, the unswept leading edge of the wing means that the shift in wing aerodynamic centre is negligible [61]. All other elements of Equation 6.29, which account for the effects of the fuselage on the aerodynamic centre position, can then be calculated using the aircraft geometry.

$$\frac{x_{ac}}{\bar{c}} = \left(\frac{x_{ac}}{\bar{c}}\right)_w - \frac{1.8}{C_{L_{\alpha_{A-h}}}}\frac{b_f h_f l_{fn}}{S\bar{c}} + \frac{0.273}{1+\lambda}\frac{b_f c_g\left(b-b_f\right)}{\bar{c}^2\left(b+2.15b_f\right)}\tan\Lambda_{c/4} \tag{6.29}$$

With the position of the aerodynamic centre thus known, it is possible to then determine the moment coefficient about the aerodynamic centre. For a clean aircraft configuration, the moment coefficient is given as shown in Equation 6.30.

$$C_{m_{ac}} = C_{m_{ac_w}} + \Delta_{\text{fus}}\, C_{m_{ac}} = \mathrm{Cm}_{\text{0airfoil}}\,\frac{\mathrm{A}_{\text{eff}}\cos^2\Lambda_{LE}}{\mathrm{A}+2\cos\Lambda_{LE})} - 1.8\left(1-\frac{2.5b_f}{I_f}\right)\frac{\pi b_f h_f I_f}{4S\bar{c}}\alpha_0 \tag{6.30}$$

Furthermore, an additional calculation must be performed when considering the moment coefficient during takeoff and landing when the flaps are deployed. Using the method presented by Torenbeek, Equation 6.31 shows the change in moment coefficient coming into effect when the flaps are used. The relevant parameters μ_1, μ_2, and μ_3 are found using reference data provided by Torenbeek [61]. However, it must be noted that this value quantifies the change in moment coefficient about the quarter chord point, not the aerodynamic centre. Thus, using the previously calculated aerodynamic centre location and Equation 6.32, the flap contribution to the moment coefficient must first be translated from being about the quarter chord to being about the aerodynamic centre. Finally, the value found using Equation 6.32 can then be added to the value found using Equation 6.30, giving the total wing moment coefficient during takeoff and landing.

$$\Delta C_{m_{c/4}} = -\mu_1\mu_2\Delta C_{l_{\max}} + 0.7\frac{A}{1+2/A}\mu_3\Delta C_{l\,\max}\tan\Lambda_{c/4} \tag{6.31}$$

$$C_{m_{ac}} = C_{m_{c/4}} - C_L\left(0.25 - \frac{x_{ac}}{\bar{c}}\right) \tag{6.32}$$

6.5.8. Weight Estimation

The final wing parameter that remains to be determined is the wing weight. For this, the Roskam Cessna method shall be used as shown in Equation 6.33 [51, part V, p67]. It is important to note that, as the method is semi-empirical, it is essential that the correct units are used. Thus, W_{TO} must be given in lb, and the S must be given in ft^2.

$$w_{wing} = 0.04674 \cdot W_{TO}^{0.397} \cdot S^{0.360} \cdot n_{ult}^{0.397} \cdot A_{geo}^{1.712} \tag{6.33}$$

[17] URL brightspace.tudelft.nl, Course AE2111-II, *Systems Design*, accessed 2021-06-22.

6.6. Design of the Propulsion System

This section provides an overview on how the aircraft is to be propelled. As the objective of the project is to design, a plane with distributed propulsion, the only viable option for propulsion are electrical motors with fans. This chapter delves into the sizing process of the distributed propulsion for the project. Aspects such as number of propellers, their power, and geometric properties are explored in the succeeding sections. Firstly, however, the theory behind the sizing process is explained.

6.6.1. Thrust of Electric Motors

In order to achieve the final design of the electric motors, first the sizing of them had to be performed. Such sizing allowed to establish the required torque in engines, number of engines and their distribution. The driving requirement during sizing was the power that had to be provided throughout the mission. With adherence to that, an optimisation tool was set up that would return the number of engines, their configuration on the wings and the torque.

From the input of the power required for flight, the thrust requirement was derived. Firstly, prior to the optimisation of the entire propulsive system, the tool needed for relating thrust with torque of the engine is presented.

Realising that a propeller blade is nothing else but a rotating wing, lift and drag equations were applied to derive thrust. Assuming that the rotation of the blades is constant, for the given torque of the engine, the only force counter acting the moment is the drag. The infinitesimal drag component acting on a given section of the blade can be given as follows in the Equation 6.34.

$$dD = \frac{1}{2}\rho V^2 S C_D \tag{6.34}$$

This equation is dependant on the distance r, measured from the centre of rotation. V linearly increases with r, S can be expressed with thickness of the blade multiplied by infinitesimal length dr, and C_D can vary as the airfoil is different along the blade. Using an assumption that the thickness t is constant and the airfoil profile changes linearly with r ($\frac{dC_D}{dr} = C_{Dr}$), an expression for the total moment due to drag on one blade can be forged as showed in the Equation 6.35.

$$M_{Drag} = \int_R r dD = \frac{1}{2}\rho\omega^2 C_{Dr} t \int_0^R r^4 dr \tag{6.35}$$

As mentioned previously, the only moment countering the torque is the moment caused by the drag. As the Equation 6.35 is given for one blade, the equilibrium equation for the entire propeller will become the Equation 6.36.

$$Torque = 2 \cdot M_{Drag} \tag{6.36}$$

Using both relations from the Equation 6.35 and Equation 6.36, the rotational rate ω can be derived, which is be later useful in thrust derivation.

$$\omega^2 = \frac{Torque \cdot 5}{\rho C_{Dr} t R^5} \tag{6.37}$$

In a very similar fashion to the above reasoning, a lift analysis of the blade is perpetrated in order to obtain the estimate of the value for thrust. However, as drag was related with torque by moments, the lift and thrust are forces. Using the infinitesimal lift force from the Equation 6.38 the total lift for the blade can be assessed as in the Equation 6.39, where the same assumptions are applied as in the above drag reasoning. Also, heeding that the thrust of the propeller consists of two blades, thrust will take the form presented in the Equation 6.40

$$dL = \frac{1}{2}\rho V^2 S C_L \tag{6.38}$$

$$L = \int_R dL = \frac{1}{2}\rho\omega^2 C_{Lr} t \int_0^R r^3 dr \tag{6.39}$$

$$Thrust = 2 \cdot L \tag{6.40}$$

The only unknown in the Equation 6.39 is the rotational rate ω. This however can be taken from the drag drag - torque analysis in the Equation 6.37. Thus finally the thrust of the propeller can be related with the torque of the engine as presented in the Equation 6.41.

$$Thrust = Torque \cdot \frac{5}{4} \cdot \frac{1}{R} \cdot \frac{C_{Lr}}{C_{Dr}} \tag{6.41}$$

The relation from the Equation 6.41 shows what may seem to be a counter-intuitive dependency at first. The thrust decreases with the increasing radius, thus size of the blade. This however, can be simply explained by comparing the Equation 6.35 and Equation 6.39. The equations are much alike, however drag scales with r^5 while the lift scales with r^4, hence, the larger blade will have higher influence on drag than on lift.

However, the aforementioned reasoning is merely based on theory. Thus in order to translate it into useful tool suited for real world, additional constraints are needed. As it is presented in the Equation 6.37, decreasing the radius of the propeller R, increases the rotational rate ω drastically. From aerodynamic analysis it is known however, that propeller becomes inefficient when any part of the blade enters the trans-sonic range. The highest velocity at the blade occurs at the tip and hence the minimum radius R should be such that the rotational rate ω does not make the velocity of the tip exceed $0.85Mach$. Thus, this sets a limit on how much the R could be decreased.

In addition to that, there is also a constraint on the highest allowable RPM for the electric motors. Most electric motors operate at a useful range of up to 3000 RPM. Again, the radius of the blade should be sized such that the ω does not exceed the highest allowable rotational velocity for the engines as this could lead to their failure or malfunction.

Another, crucial reason why the propellers' blades should not be too small is the incentive for the distributed propulsion along the wing. The propellers, in order to be useful for providing the advantage of the locally increased airspeed over the wing, naturally need to be larger than the thickness of the wing. During the design it was chosen that they must be at the very least 10% thicker than the thickness of the wing at the root.

Thus, whereas initially it may have seemed that the lowest possible fan is the best choice for the design, in reality a number of constraints that speak against it arise.

Furthermore, from the Equation 6.41 it can be concluded that in order to maximise the thrust delivered with a propeller the ratio of $\frac{C_{Lr}}{C_{Dr}}$ ought to be maximised, which is an expected result.

6.6.2. Airspeed After the Propeller

The second piece of theory that is needed for the calculations regarding the propellers is a so called 'Disk Theory'. This theory uses the aerodynamic momentum conservation equation to relate the airspeed in front and behind the propeller with the thrust that it is providing. The momentum equation is applied along a control volume of a 'disk' that is of size of a wheel with the radius of the propeller This theory is very useful for evaluation of the airspeed over the wing and thus the advantage of the distributed propulsion and augmented lift that was covered in the late sections.

The result of the 'Disk Theory' can be stated through the Equation 6.42.

$$\delta p = \frac{1}{2}\rho(V_e^2 - V^2) \tag{6.42}$$

To apply the 'Disk Theory' into the thrust considerations, it needs to be realised that δp in nothing else as the lift produced by the propeller, meaning thrust. Thus, it is possible to evaluate the velocity after the propeller V_e as a result of the thrust, which was evaluated in the Section 6.6.1 and velocity of the aircraft V, with the use of the equation Equation 6.43.

$$V_e = \sqrt{\frac{2T}{\rho A_d isk} + V^2} \tag{6.43}$$

6.7. Design of the Empennage

In this section, the methods used for designing the tailplane of the Twin-Puffin are outlined and justified. First, the sizing of the horizontal stabiliser is presented, showing how its area and dimensions are selected, as well as the constraints for vertical positioning of the tail. Then, the design of the vertical plane is tackled, explaining the different scenarios which constrain its area and the sizing methods applied.

6.7.1. Horizontal Tail Sizing

The first step of the horizontal tail design is finding its required area. This is done by creating a loading diagram as seen in Figure 6.16a, finding the possible variation in centre of gravity. The two loading conditions considered are, first, four passengers placed in the assigned seats, with no cargo, and second, one pilot with 300 kg of cargo. The 300 kg is divided across two sections of the cargo hold, separated in two equal parts, each rated for a maximum 150 kg. This division is done to avoid too much cargo far aft in the aircraft. The result is a most forward and most aft centre of gravity with an added 2% MAC margin in each direction. This loading diagram is repeated for a variation in wing-position, and a plot showing the cg-range as a function of the location of the wing leading edge follows as in Figure 6.16b.

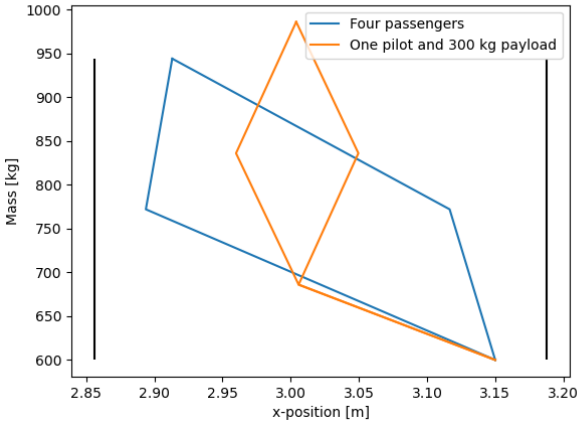

(a) An example of a loading diagram showing two loading conditions; one pilot and 300 kg of payload, and one pilot with three passengers. Dark, vertical lines mark the c.g.-range, highlighting the applied margin of 2% MAC.

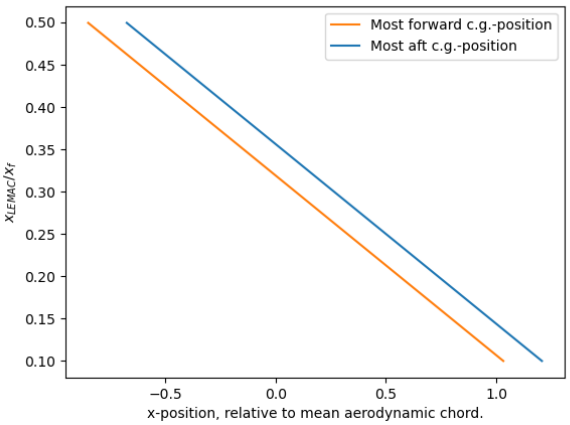

(b) An example of a wing positioning diagram, showing the variation of c.g.-range and location with varying X_{LEMAC}.

Figure 6.16: Examples of the diagrams used to compare c.g.-ranges for varying wing position.

Now that the loading of the aircraft is known, it can be compared to the stability and controllability requirements to optimise the wing position for a minimum required horizontal tail size. The requirements on stability follows from the static equations of stick-fixed stability, with an applied 5% MAC margin to account for other constraints such as stick-free, and control-feel constraints[18]. The equation for the neutral stability curve is given in Equation 6.44.

The controllability requirements follow the requirement on trim for the aircraft. From TP-SYS-19 in Table 4.2, the aircraft shall be trimmable in static flight condition, i.e. the tail contribution to the aircraft moment must be able to counter-act the moment from the fuselage, wing, and propulsion[19]. The relevant equation can be seen in Equation 6.45.

For both Equation 6.44 and Equation 6.45, $\left(\frac{V_h}{V}\right)^2 = 1$, as the twin-boom tail configuration, seen in Figure 6.18, places the horizontal tail plane sufficiently high to avoid any perturbing effects of the local wind speed from the wing. The aerodynamic parameters follow from the analysis in Section 6.5.3.

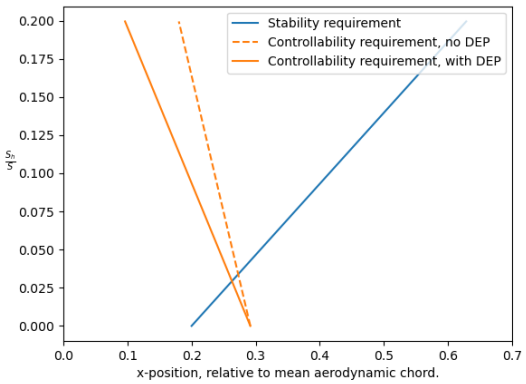

Figure 6.17: An example of a scissor plot of the aircraft design, also highlighting the effect of distributed electric propulsion (DEP) on the horizontal tail.

$$\bar{x}_{cg} = \bar{x}_{ac} + \frac{C_{L_{\alpha_h}}}{C_{L_{\alpha_{A-h}}}} \left(1 - \frac{d\varepsilon}{d\alpha}\right) \frac{S_h l_h}{S\bar{c}} \left(\frac{V_h}{V}\right)^2 - 0.05 \quad (6.44)$$

$$\bar{x}_{cg} = \bar{x}_{ac} - \frac{C_{m_{ac}}}{C_{L_{A-h}}} + \frac{C_{L_h}}{C_{L_{A-h}}} \frac{S_h l_h}{S\bar{c}} \left(\frac{V_h}{V}\right)^2 \quad (6.45)$$

By combining the wing positioning diagram in Figure 6.16b with the scissor plot in Figure 6.17, a position of X_{lemac} can be found such that S_h/S is at a minimum. An iterative method is applied as shifting wing position naturally varies the loading diagram, and in turn the diagrams themselves.

What becomes clear is that the extremely low stall speeds mean the tailplane becomes largely ineffective on the critical landing approach. The horizontal tail will have to be fully moving, but as can be seen by the dashed line in Figure 6.17, the controllability requirement for a fully moving horizontal tail is still very limiting following

[18]URL brightspace.tudelft.nl, Course AE3211-I, *Lecture 4: Requirement Analysis and Design principles for A/C stability & control (Part 1)*
[19]URL brightspace.tudelft.nl, Course AE3211-I, *Lecture 5: Requirement Analysis and Design principles for A/C stability & control (Part 2)*

the low flight velocities. The proposed solution is to let the horizontal tail, like on the main wing, be blown by electrically powered fans to increase its effective lift, even at low speeds. As is shown by the continuous line in Figure 6.17, this will ease the requirement on controllability.

To simplify the structure, and also provide benefit to the vertical tail, the two additional propellers are placed in the intersection between the horizontal and vertical tail. These additional propellers are limited in size by the distance between the vertical tails, thus the dimensions are fixed, and the applied thrust is optimised to achieve the largest lift augmentation over the tail. The method used to determine the level of lift augmentation is the same as discussed in Section 6.4. With these added effects, the horizontal tail size can be kept at a sufficiently low level.

6.7.2. Horizontal Tail Geometry

Once the area required for the horizontal tail is obtained, its dimensions can be specified. What is already known of its location is that the horizontal tail will run across the twin booms, connecting both vertical tails, and it will be located as far up as possible to facilitate the aft loading.

As the horizontal stabiliser is situated in between the two vertical tails (which are located at the end of the booms), it was decided that its shape will resemble a rectangle. This means that sweep angle was chosen to be zero, as was also the case for the dihedral.

The airfoil selected for this horizontal tail was the NACA 0009. The factors leading to this decision were obtained from Torenbeek's preliminary tailplane design [61, p.327]. One of the basic requirements was that the airfoil selected should have a high lift coefficient slope (c_{l_α}). Moreover, (approximately) symmetrical airfoils are used, in order to allow for the production of both upward and downward lift. Lastly, airfoils with thickness-to-chord ratios of about 9 to 12% are frequently used for the horizontal stabiliser.

Once all parameters are selected, and the required surface area can be computed by following the procedure explained above, the dimensions of the horizontal tailplane can also be obtained.

As a first estimation, the horizontal stabiliser is determined to be bounded by the two vertical tails, this meaning that (at first) its span equals the distance between the booms. From this span, the average chord is computed. This will coincide with the mean aerodynamic chord (as well as with the root and tip chords), as the shape of the horizontal tail is chosen to be rectangular.

However, as the rudder is a moving surface, it is not possible for the horizontal stabiliser to cover it. This is why its chord has a maximum value which is dependent on the vertical position of the horizontal tail, as observed in Figure 6.18. In case that the average chord computed previously exceeds this value, the span will be recalculated to be enough to provide the required surface area, while having the maximum allowed chord. Then, the new span will be larger than the distance between the aircraft booms, and the horizontal stabiliser will stick out of the area enclosed by the vertical tails, as visualised in the drawing.

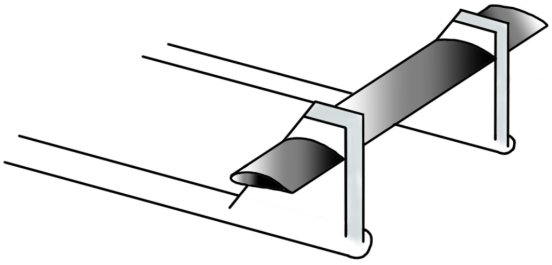

Figure 6.18: Horizontal tail design.

As previously mentioned, the deep stall characteristics of the aircraft will influence the vertical positioning of the horizontal stabiliser. It is known that its maximum location given by the vertical tail geometry will be at the point in which the rudder starts occupying the entire chord at the tip of the fin. However, it will also need to be checked whether this positioning is the right one.

This will be done by checking whether the bush plane can still be controllable for deep stall or not. When this situation occurs, the horizontal stabiliser should not be inside of the wake of the wing, as otherwise aircraft controllability is not achieved. Moreover, in case that most of the horizontal tail is located in between of the vertical fins, the wake produced by the fuselage during deep stall will also need to be taken into account, constraining even more the vertical position of the horizontal stabiliser.

Furthermore, the weight of the vertical and horizontal tails are computed using Class-II estimation methods [51]. Once this is found, the centre of gravity of the complete empennage is estimated by assuming the centre of gravity of each of the tails being at 40% of the chords.

6.7.3. Vertical Tail Sizing

As for the horizontal tail, before the geometry can be specified, the vertical tail area must be found. For this, three different requirements on the design were identified. First, the area would have to satisfy the certification requirements on aircraft handling in crosswind. The second requirement is the requirement of static directional stability, and finally, what is expected to be the most critical, the requirement following a one-engine-inoperative condition.

Per requirements TP-USER-11 and TP-SYS-EMP-04 in Section 4.3, the aircraft must be able to sustain an approach track, at less than 5° bank angle, during crosswind. The crosswind to size for is either 20% of

stall speed, or 20 knots, whichever is larger. Then, the value of C_{n_β} is estimated using the fuselage shape and wing size. This is equated against the induced C_{Y_v} of the vertical tail, including the lift augmentation from the added empennage propellers following the horizontal tail design, and solved for the required vertical tail size for equilibrium. The vertical tail will have an aspect ratio below 1.8. Its lift slope is assumed to be equal to $\frac{\pi}{2} \cdot A_v$, an estimation valid only for very low aspect ratio wings[20].

To ensure static directional stability, the C_{n_β} of the entire aircraft must be positive, i.e. the aircraft yaws towards the aircraft heading. Following the analysis of Torenbeek, the analysis of directional stability is difficult, but a quick sizing method is given, showing a relationship between vertical tail size and the estimated C_{n_β} contribution of the fuselage [61, Fig. 9-24]. Directional stability of the aircraft is critical in cruising flight, so the blowing of the vertical tail from the empennage-mounted propellers is not relevant for this computation.

The final requirement is the one-engine-inoperative condition. In the case of distributed electric propulsion, this critical condition is assumed to be equivalent to losing one quarter of the available engines. The most critical engines to lose are naturally the most out-board engines of the wing. The induced moment following the asymmetric propulsion will then be counter-acted by the, still available, propellers along the wing. The induced moment, together with C_L, W, and l_v, form a parameter that can be compared to the method of Torenbeek for the required S_v/S for the one-engine-inoperative condition [61, Fig. 9-22].

6.7.4. Vertical Tail Geometry

Once the area required for the vertical tail is obtained, its dimensions can be computed. However, several parameters needed to be chosen first, according to aircraft design conventions. Firstly, the general shape of the vertical tail needs to be decided upon. The most conventional design was followed, selecting the configuration shown in Figure 6.19 with a more trapezoidal shape.

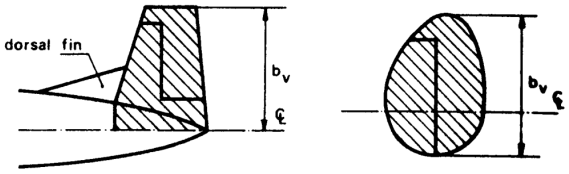

Figure 6.19: General design of the vertical tail [61].

As it can be observed from the left drawing in Figure 6.19, the rudder will run from about 20% of the tail height until its top. At the tip, it occupies the whole chord, helping in moment counteracting on the hinge line when the rudder is deflected. Moreover, the chord of the rudder was chosen to be 30% of the average chord of the fin with a maximum deflection of 25 degrees, being these approximate limits for its design [61, p.335].

The position of the horizontal tailplane with respect to the vertical tail also needs to be defined, as this will determine the structural rigidity required for the vertical fin. In order to allow for better loading of the aircraft, the preferred location of the horizontal stabiliser will be on the upper part of the vertical tailplane, which will need to provide enough support for it. However, its exact position will be determined by the deep stall conditions of the aircraft, which will be further explained in the following subsection.

The next thing to select was the airfoil. As the lift force produced by the vertical tail is required to be identical for the same angle of sideslip in both directions, the airfoil needs to be symmetrical. Usually, vertical tailplane sections have a thickness of about 12% of their chord [61, p.339]. Hence, the airfoil chosen for the fin was NACA 0012.

Since the taper ratio of the vertical fin does not affect lateral stability significantly, a value close to one can be chosen (meaning that the root cord and the tip chord will have similar dimensions) [61, p.339]. Then, in order to achieve a more stiff structure (since the horizontal tail will have to be carried by the fin), while also reducing the weight, a taper ratio of 0.7 was selected in the design.

The last parameter to be defined was the aspect ratio. A low value is required in order to provide rigidity to the vertical tail, without excessively increasing the weight. Moreover, in order to reduce the possibilities of vertical tailplane stall, a moderate aspect ratio is recommended (A_v < 1.8), together with a positive sweep angle in the leading edge of the fin [61, p.332] (coming inherently with the selected general design, as the trailing edge was defined to be perpendicular to the root and tip chords). Hence, taking all these into consideration, an aspect ratio of 1.2 was selected for the vertical tail.

By using all these specifications, the vertical tail can be sized applying the same simple geometry relations used in the main wing of the aircraft. However, it needs to be noted that now the span has a slightly different notation, as it is not anymore the distance between both tip chords, but the distance between the root and tip chords.

[20]URL brightspace.tudelft.nl, Course AE3211-I, *Lecture 9: Lateral and Ground 2021*, accessed 2021-06-14.

Since the horizontal stabiliser will be positioned on the higher part of the vertical tail, this will be favourable for controllability, as when the aircraft enters spin it will still be recoverable. As it can be observed in Figure 6.20, when during spin, the wake of the horizontal tail can cover the rudder. According to Torenbeek [61, p.53], at least one third of the rudder needs to be outside of the wake of the horizontal tail while this takes place, in order for the aircraft to be able to recover. Although this is assumed to be the case for this bush plane (due to the similarity with the bottom right design), it will be checked once the final design is completed.

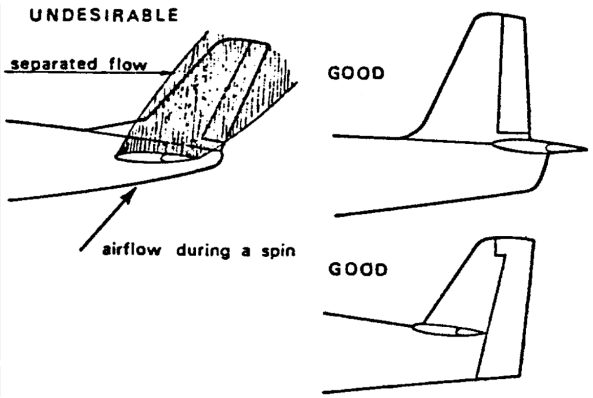

Figure 6.20: Effectiveness of the rudder during a spin. [61]

6.7.5. Wing Positioning and Iteration

Closely connected to the empennage sizing is the positioning of the main wing of the aircraft. Combining the loading diagram, scissor plot, and wing-positioning diagram, seen in Figure 6.16a, Figure 6.17 and Figure 6.16b respectively, the optimal location for the wing can be found to minimise the required horizontal tail area. However, moving the main wing of the aircraft has serious implications on many parameters, like tail length and most notably the shift in the centre of gravity at operative empty weight. Moving the wing to the optimal position completely changes the initial parameters for that optimisation, and an iteration is necessary.

The iteration continuously equates the stability and controllability requirements, optimally places the wing, and updates the aircraft parameters. This continues until the wing shifts less than 1% of the total fuselage length between two iterations. This iteration ensures the true optimal wing position is found, and the horizontal tail is iterated to the absolute minimum while still ensuring all requirements are fulfilled.

In the end, the design of the empennage and positioning of the wing can be completed for any variation of aircraft parameters while ensuring the fulfilment of the requirements, making it ready for the optimisation following in Section 7.3.

6.8. Design of the Landing Gear

The next step on the design process is to position the landing gear. The method followed in order to achieve this goal was based on the one presented by Roskam [51]. In Figure 6.21, the angles acting as constraints for this positioning are presented.

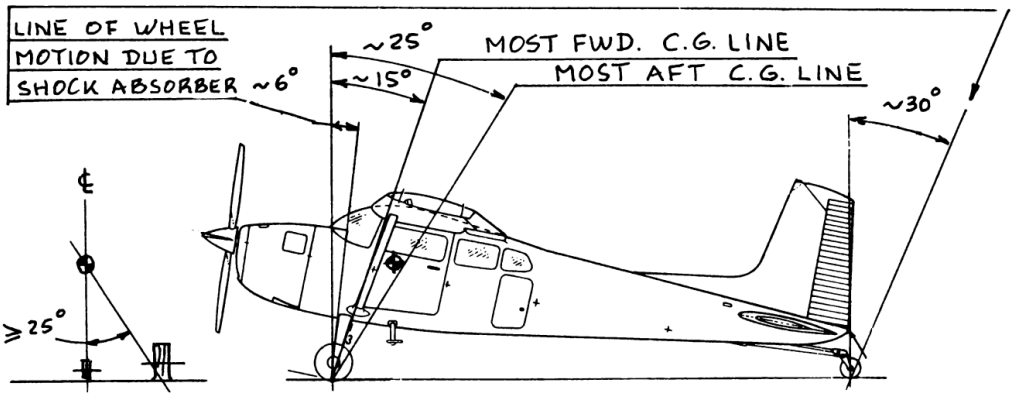

Figure 6.21: Tail landing gear layout requirements.[51]

The longitudinal and vertical positions of the main landing gear can be computed by following these constraints. From the drawing, it is observed that the centre of gravity of the aircraft needs to be located in between approximately 15 to 25 degrees with respect to the point at which the main landing gear touches the ground. In case that the center of gravity is located forward, the aircraft will not be able to achieve a favourable attitude for taking off. Moreover, braking while landing will also be an issue in this case, as the main wheels should create a tail-down moment, which will be more difficult as the centre of gravity moves closer to the landing gear.

It needs to be noted that, for this case, the longitudinal location of the tail wheel will be fixed by the aircraft length. Its position will be given by the most aft point on the lower part of the vertical tail . Two wheels will be placed, making the landing gear have a quasi-quad configuration. However, the aircraft still recognised as a

taildragger, due to it still presenting all of its characteristics. For this design, it is then required that the vertical fins extend downwards, so as to be able to place small wheels on them and touch the ground.

This landing gear configuration was chosen due to the short fuselage length, which would compromise the stability of the aircraft on ground. Moreover, this design option also allowed for the tail wheels being smaller, as it was expected that a single tail wheel at the back of the fuselage would need to extend further back (or be quite tall) in order to keep up with the main landing gear at such a short distance from it, an aspect that would affect its structural rigidity, thus making it heavier. Another advantage was the fact that then the fuselage could have a more tapered and smooth end, instead of it being practically a box in order to allow the tail wheel to be properly attached.

Once this is fixed, the vertical position of the tail wheel can be computed. For this, the inclination angle of the bush plane needs to be decided upon. Usually, this angle is constrained between 10 and 15 degrees. In this case, in order to facilitate the loading of the aircraft, the inclination angle is required to be as small as possible. Hence, a value of 10 degrees was selected. By using this value, the location of the tail landing gear can be computed.

Finally, the separation between the wheels of the main landing gear needs to be found. Here another constraint was used. Again, from the drawing, a 25-degree angle between the centre of gravity location and the point in which the wheel touches the ground, is given to be the minimum required for the aircraft to not tip sideways. Moreover, it is also checked that there is enough clearance between the wing and propellers, and the ground, choosing a minimum angle of 20 degrees for this.

6.9. Design of Electrical and Aircraft Control Systems

For the design of the electrical and aircraft control systems, three systems will be considered: the power distribution, the interactions between aircraft hardware and data flows, and the software. This section first outlines the general principles that are considered for all three categories. Then special attention is paid to the aircraft control system, and it is explained which system type is selected as the best option.

6.9.1. General Design Principles

Spanning across all the categories of systems discussed here is the need for redundancy and reliable operations. No where in the systems shall the successful operation of the aircraft be put at risk by a single point of failure. This includes both physical points of failure, such as a wire breaking, and software malfunctions.. Simultaneously, it is important to not be overly redundant, as this would lead to an overly complex system and unnecessarily increase parameters such as the aircraft weight. To determine how much redundancy is applicable for different parts of the electrical and aircraft control systems, two aspects must be assessed: how high is the likelihood of a failure occurring and how severe would the consequences of a failure be. Based on this assessment, it is then identified how much redundancy must be included at the different points of the systems in order to ensure safe operations.

6.9.2. Selection of Aircraft Control System Type

Before the aircraft hardware and data flow diagram can be designed, it is necessary to decide which kind of system shall be used to control the aircraft. Here, the three most feasible options shall be discussed and traded off. The first option is a conventional mechanical system that uses cables and struts to pass on the control forces from the pilot stick to the aircraft mobile surfaces. This is the tried and tested kind of system used in traditional aircraft and many smaller modern planes. The second kind of system is an augmented version of the first type. While mechanical connections are still used to pass on the control forces, electric motors are included that can push and pull on the cables and struts. Thereby, the control forces input using the pilot stick can be augmented on the basis of a computer-controlled system. Such a type of system is used for autopilots in general aviation aircraft [21]. As for the *Twin Puffin* the capabilities of the system will be expanded to allow for both remote piloting and the modification of manual pilot stick inputs, the type of system has been dubbed as ”augmented autopilot”. The third and final option is the use of a fly-by-wire system. Removing the need for mechanical connections between the pilot stick and the control surfaces, fly-by-wire uses wires and electric signals to pass on the information from the pilot to the actuators moving the aircraft mobile surfaces. While fly-by-wire is typically used in military fighters and larger aircraft, it shall also be considered as an option for the *Twin Puffin*.

To qualitatively trade off between the three options, selection criteria and corresponding criteria weights must be determined. The first and most important criterion is safety and reliability. It must be possible to ensure that the aircraft can be operated safely even in case of individual components failing. Although given enough resources and system complexity, all systems can be made sufficiently reliable, the criterion shall assess the inherent level of safety of the three options relative to one another. Due to safety being of utmost importance in

[21] URL https://www.banyanair.com/garmin-gfc-600-digital-autopilot/ [cited 28 June 2021]

aviation, this criterion is awarded the maximum weight of five. With a weight of four, a nonetheless still important criterion is the feasibility of using the system for remote piloting of the aircraft. Directly connected to this, and thus judged using the same criterion, is the ability to augment pilot control inputs. While not necessary, these aspects are desirable as they will allow flying the aircraft without a pilot and, if a pilot is present, will make flying easier, more comfortable, and more efficient. The third criteria is ease of maintenance. With bush planes such as the *Twin Puffin* operating under often harsh climate conditions, maintenance is essential in ensuring that all systems work as intended. As bush planes need to be maintained without large amounts of auxiliary maintenance infrastructure, it is important that maintenance is easy to perform. Thus, this criterion is weighted with a three. The fourth and fifth criteria of interest are the system mass and cost. Though both are of relevance for the design of the *Twin Puffin*, they are of less importance than the first three criteria and are both weighted with a two.

The five selection criteria, their tags, and their weights are summarised in Table 6.9. All criteria are assessed in a qualitative manner and designs are judged on a fourfold scale of green - excellent, blue - good, yellow - correctable deficiencies, and red - unacceptable. The scoring of each design option for the different selection criteria is individually explained in Table 8.3 and all scores are presented in Table 6.11.

Table 6.9: Selection criteria for the control system selection

Tag	*Criteria*	*Weight*
S.&R.	Safety and reliability	5
R.P.&C.A.	Remote piloting and control augmentation	4
E.M.	Ease of maintenance	4
S.M.	System mass	2
S.C.	System cost	2

Table 6.10: Explanation of the scoring of the different design options for each criterion

Criteria	*Conventional Mechanical System*	*Augmented Autopilot*	*Fly-by-Wire*
S.&R.	Being tried and tested and used across many existing aircraft, the conventional mechanical system is deemed to have good reliability. Using two cables or struts in parallel for each control surface, good redundancy can easily be achieved. Furthermore, system failure can be predicted using well-established structural models	The augmented autopilot is even more reliable than the conventional mechanical system. It retains the same ease of adding redundancy, but also means that the aircraft can be remotely steered in case of the pilot experiencing health issues and not being able to fly anymore. Importantly, the system can still be manually controlled in case of power loss	The fly-by-wire system scores poorly in terms of reliability. In addition to being susceptible to wires breaking, the functioning of the system can be impaired through software issues. A sufficient system of backup power supply will be required, as a full loss of power would leave the aircraft uncontrollable, even with a pilot on board
R.P.&C.A.	The conventional mechanical system scores as unacceptable for this category as neither remote piloting, nor augmentation of control inputs is possible	Both remote piloting and the computer-aided augmentation of control inputs is possible using the augmented autopilot system	Both remote piloting and the computer-aided augmentation of control inputs is possible using a fly-by-wire system

Table 6.10: Explanation of the scoring of the different design options for each criterion

Criteria	*Conventional Mechanical System*	*Augmented Autopilot*	*Fly-by-Wire*
E.M.	The physical cables and struts used in a conventional mechanical control system are easy to inspect. Flaws and potential points of failure can often be identified visually and faulty parts can easily be exchanged	The same ease of maintenance holds for the augmented autopilot as for the conventional mechanical system. However, the inclusion of the electrical engines makes the process a bit more complicated	Maintenance is more difficult for fly-by-wire systems. For electric wires, flaws are typically internal and are less easy to detect. In case a connection is found to be faulty, it can be difficult to detect where exactly the problem lies. Furthermore, rather than one central set of electric engines having to be maintained, it will be necessary to maintain an entire set of actuators that are distributed across the aircraft (partly in difficult-to-reach places)
S.M.	Though the inclusion of the electric engines for control input augmentation makes the augmented autopilot system heavier than its conventional mechanical counterpart, the difference is expected to be rather small. Thus, both options are scored equally well		Though unlike the other options the fly-by-wire system does not require rather heavy structural parts, it is expected to be heavier. This is because of the many actuators required at each of the aircraft mobile surfaces.
S.C.	As it requires only structural but no electric components, the conventional mechanical system is deemed to be cheap	The augmented autopilot will be more expensive than the conventional mechanical system, as the additional cost of the electric engines has to be accounted for	Due to the high number of electric components, which are more expensive than the mechanical alternatives, the fly-by-wire system is expected to be rather costly

Table 6.11: Trade-off matrix for the control system selection

	S.&R.	**R.P.&C.A.**	**E.M.**	**S.M.**	**S.C.**
Conventional mechanical system	[B]	[R]	[G] [B]	[B]	[G]
Augmented autopilot	[G]	[B]	[B]	[B]	[B]
Fly-by-wire	[Y]	[B]	[Y]	[Y]	[Y]

Based on the trade-off results shown in Table 6.11, it is clear that the most suitable type of system for the control of the *Twin Puffin* is the augmented autopilot. Thus the specifics of this type of system will be used to design the electrical and control systems for the aircraft.

6.10. Subsystem Design Method Outcomes

This section summarises the outcomes of the various subsystem design methods discussed throughout this chapter. It is these outcomes that are used for the calculations of Chapter 7 and largely define the final aircraft design presented in Chapter 8. The specific outcomes of each method are found in Table 6.12

Table 6.12: Subsystem Design

Outcome	*Method*
	Design of the Fuselage
Cross-section shape	Through trade-off the most optimal shape was selected
Cross-section dimensions	By placing the dimensionalised objects in the fuselage and designing for the most efficient space use
Side-view shape	Chosen to enable the possibility of aft loading

Table 6.12: Subsystem Design

Outcome	*Method*
Side-view dimensions	By placing the dimensionalised objects in the fuselage and designing for the most efficient space use
	Design of the Structure
Load carrying structure	Using a structural analysis of an idealised boom structure
Main aircraft material	Through formal trade-off, the most suitable material was selected
	Design of the Energy Source
ICE choice	Selection based on requirements and available engine specifications
Battery Sizing	Based on performance deficits between the ICE power and required power in certain flight situation as well as efficiency concerns
	Design for Lift Augmentation
Number and diameter of high lift engines	The optimal number and size for the high lift propellers has been determined to maximise lift augmentation given the available space and thrust
	Design of the Wing
Wing planform	Designed using the surface area and taking into account structural and aerodynamic considerations
Wing airfoil	Selected to match the unblown design lift coefficient of the wing
Drag parameters	The determination of the zero-lift drag coefficient, the effective aspect ratio, and the Oswald efficiency factor then allow finding drag values for any given lift coefficient
Lift parameters	The achievable lift coefficients and slopes have been found for the clean, the flapped, and the blown configurations of the aircraft
Aileron size	minimum size found to meet the roll requirements
Aerodynamic moments	Determined for different aircraft configurations
Wing weight	Estimated using a semi-empirical approach
	Design of the Propulsion System
Electric motor choice	Selection based on requirements and available engine specifications and efficiency ranges
Propeller sizing	Inputting diameter and performance requirements into JavaProp and altering the geometry for
	Design of the Empennage
Vertical fin dimensions	The surface area was computed accounting for crosswinds and the one-engine inoperative case, and then the vertical tail was sized accordingly.
Horizontal stabiliser dimensions	It was sized such that the surface area could guarantee stability and controllability of the aircraft, and then its dimensions were computed according to the vertical tail dimensions and the distance between the fins.
	Design of the Landing Gear
Landing gear positioning	Following Roskam's conventions [51], and also guaranteeing a sufficient clearance angle for the wings.
	Design of the Electrical and Aircraft Control System
Aircraft control system	The augmented autopilot system, combining the advantages of conventional and fly-by-wire systems, has been selected as the best option

7

Parameter Calculation and Optimisation

This chapter explains how the subsystem design methods of Chapter 6 are combined to create an aircraft design (Section 7.1), how the performance of such as design is analysed (Section 7.2), and how the optimisation ensures that the aircraft design most valuable to the customers is found (Section 7.3). Section 7.4 explains how the software used during the project is verified.

7.1. Aircraft Design

Before the aircraft can be scored or even analysed, it must first be designed. The software structure implemented is shown in Figure 7.1. The aircraft design process takes in the following high level design variables: fuel mass, cruise speed, wing area, thrust available at cruise, thrust available at take-off and landing, aircraft length, and x-position of the batteries. With these input parameters, and a set of default parameters, the aircraft design loop can start. It begins with the design of the propulsion system (the motors and propellers), Section 6.6, followed by the design of the power system (battery and generator sizing), Section 6.3. Then, the sizing of the wing, and aerodynamic analysis is performed, Section 6.5 and Section 6.4. Subsequently the fuselage mass is estimated (its shape is fixed, but depending on the load factor and aircraft weight, the fuselage weight changes), Section 6.1. Thereafter, the empennage is sized and the wing and landing gear are positioned, Section 6.7. Finally, the operating empty weight and centre of gravity are calculated.

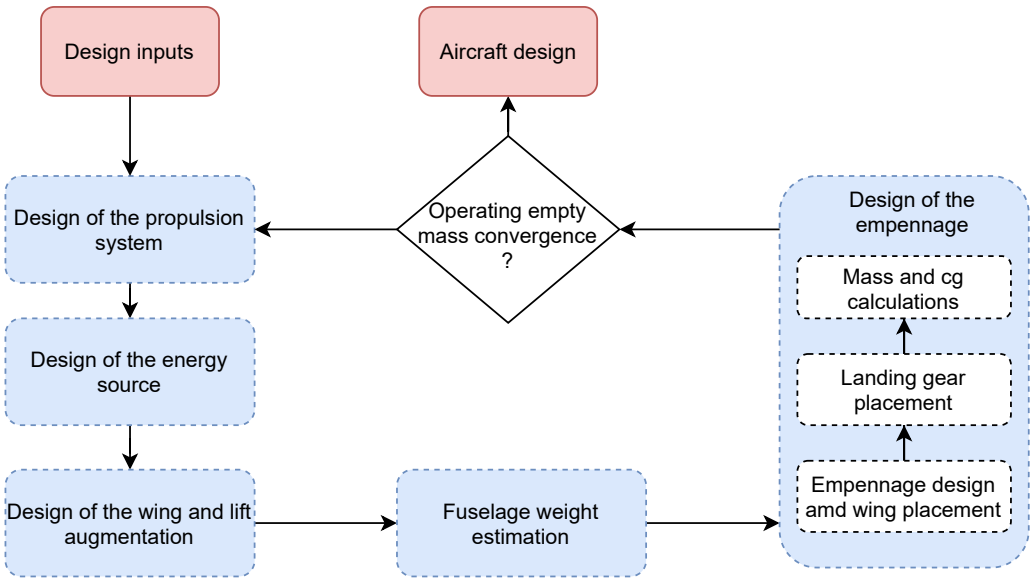

Figure 7.1: Structure of the final design calculations

Once the blue blocks of Figure 7.1 are run, the subsystem masses are summed and compared to the initially estimated operating empty mass. If the different is larger than 1%, the loop keeps running. However, if the difference is less than 1%, the loop ends and the aircraft design is returned. In effect, by combining the parametric subsystem design tools explained in Chapter 6, a tool that takes in high level input parameters and returns an aircraft is created.

7.2. Mission Model tool

To analyse aircraft performance, the Mission Model was derived and implemented. It was chosen over the simple mathematical equations taught in the bachelor due to the novel nature of the aircraft. Especially the atypical lift augmentation and hybrid power source are not easily taken into account using simple mathematical relations. As a result of this added complexity, a discrete simulation of an aircraft performing a mission profile was derived and implemented.

The Mission Model simulates, in two dimensions, the complete flight of an aircraft from take-off to landing. It takes a designed aircraft as input, and simulates a desired mission profile. During the simulation, the aircraft changes velocity, angle of attack, pitch angle, thrust, mass (decreases due to fuel flow), and state (in the state machine). The assumptions made in the model are presented in Table 7.1 and the inputs and outputs are provided in Table 7.2.

Table 7.1: List of assumptions.

Tag	*Assumption*	*Explanation*
A-1	Flat and non-rotating earth	This allows the model to have as reference frame a non-rotating fixed flat surfaced. In effect, the aircraft moves in a two dimensional plane.
A-2	The fuselage does not produce lift	The assumption is made that the lift produced is negligible compared to both the drag produced by the fuselage and the lift produced by the tail and wing.
A-3	The vertical tail produces no forces in the z direction.	While the drag of the vertical is considered (it is included with the horizontal tail drag), it is assumed that the vertical tail produces no 'lift'.
A-4	Only the constant dynamic friction due the ground forces is taken into account.	Only a constant friction force related to the normal force is taken into account, neglecting velocity dependent ground-related friction.
A-5	The wing has no twist and has a linear taper	This is an assumption made for the ground effect estimation to be valid, and is what the wing ended up becoming.
A-6	power available is constant throughout the flight	The power available from the generator varies with altitude. Rather than adapting it with altitude, a conservative estimate was made that the power available is constant and equal to the power available at cruise altitude.
A-7	The centre of pressure of the fuselage does not move	The (simplified) drag force created by the fuselage has a point of application: the centre of pressure. This centre of pressure is assumed to not move with either angle of attack or mission phase. This assumption is made because the centre of pressure is estimated calculating the variation in it location requires more advanced analysis. This assumption is deemed acceptable due to the combination of relative low force and small excepted variation in centre of pressure.
A-8	Constant mass fuel flow in the generator	During the entire flight, the generator is normally set to produce the same power, which is slightly above what is required to fly during cruise. This extra power is used to recharge the batteries. However, once the batteries are charged, the throttle setting can be slightly reduced. The reduction in mass fuel flow is assumed to be small. This assumption is deemed acceptable as using the higher value provides a conservative estimate
A-9	The lift and drag coefficients are idealised	Without performing a advanced aerodynamic analysis of the whole aircraft, the wing, tail and fuselage aerodynamic coefficients can only be estimated. The calculation of these parameters is explained in Section 6.5.

7.2.1. Model Structure

This subsection explains the general structure of the model, as shown in Figure 7.2. After setting up the initial model, a loop starts. First the forces and moments are calculated, they are used to find the acceleration and then update the state variables. With these new state variables, the state machine can be updated, the controller provides new outputs and visualisation and logging are performed.

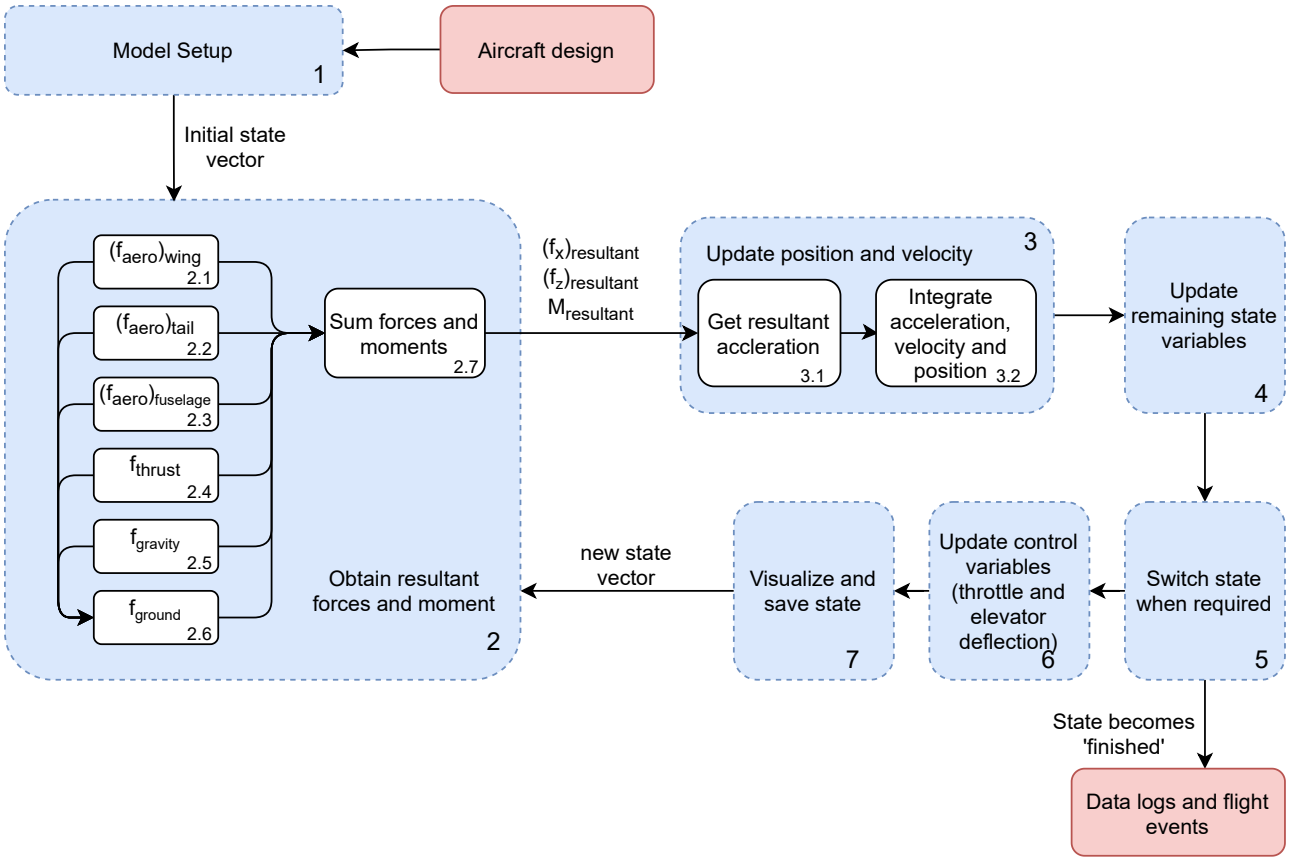

Figure 7.2: Structure of the Mission Model

Table 7.2: Inputs and outputs

Inputs	***Outputs***
• The points of application of all forces. This includes the centre of gravity, the location of the landing gear, the positions of the engines, the aerodynamic centre of the wing and horizontal tail, and the centre of pressure for the fuselage.	• Special events (such as take-off, reaching cruise, turning off distributed propulsion engines, ...)
• Functions that provide the wing and tail lift, drag and moment coefficients for a given thrust, angle of attack, mission phase, air density, airspeed, and elevator deflection.	• Time series of the airspeed (total, as well as in the x and z directions)
• Available thrust during take-off, cruise and landing. •The (constant) mass fuel flow of the generator. •Operating empty mass, payload mass and fuel mass. •Dynamic rolling friction coefficient both for take-off (no brakes) and landing (full brakes). • The desired cruise altitude and cruise speed.	• Time series of the angle of attack and flight path angle •Time series of the elevator deflection. •Time series of all forces and moments • Wing area, horizontal tail area, wing root chord and tip chord, and wing aspect ratio. • Time series of the x and y position of aircraft → altitude and range

Model States To model the different behaviour of the aircraft during different parts of the flight, a state machine is implemented. It is a software construct that applies different logic (in this case different physics and controller behaviour) depending on which state it is in (in this case the different flight phases, Figure 7.3 and 2 extra). The model has ten states: not started, ground, rotate, take off, climb, cruise, descent, approach, landing roll, and finished. The state of the model changes the physics (the ground force is only present in ground, rotate, and landing roll), the controller behaviour, the available thrust (during cruise only the main engines are available), and aerodynamic behaviour (due to the distributed propulsion). When applicable, state transitions, as explained

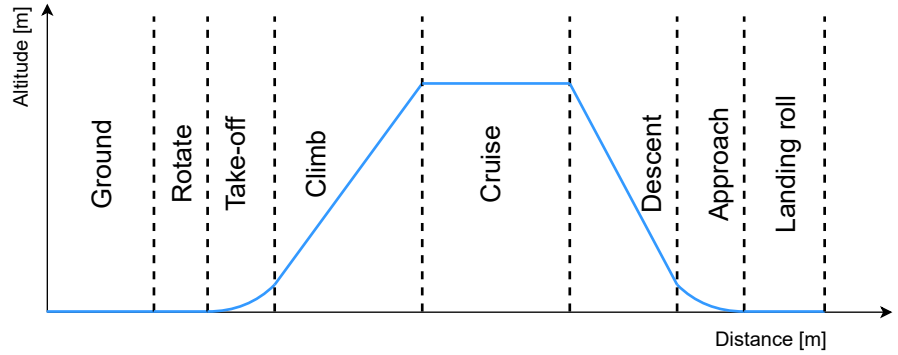

Figure 7.3: Visual representation of the relationship between the state of the state machine and the flight phase

in Table 7.3, are performed. Transition to the finished state can occur for many different reasons, such as going outside the flight domain, having flown a certain amount of time, or when the desired values have been found.

Table 7.3: State transitions

Initial State	*Condition*	*Subsequent State*
Ground	$v > 1.2 \cdot v_{stall}$	Rotate
Rotate	Predicted $(f_{ground})_z$ pulls down (rather than pushing up)	Take-off
Take-off	$h > 100m$	Climb
Climb	$h > h_{cruise}$	Cruise
Cruise	$m_{fuel} < m_{fuel\ descent} + m_{margin}$	Descent
Descent	$h < 100m$	Approach
Approach	$h <= 0$	Landing roll

State vector To handle the changing of state variables a state vector is used. It holds the x and z position(x and z), velocity in x and z direction (v_x and v_z), total velocity (v), aircraft mass (m), time (t), pitch angle (θ), flight path angle (γ), angle of attack (α), air density (ρ), throttle, total thrust, elevator deflection ($\delta_{elevator}$) and the state. The parameters that are not updated by the controller or related to position/velocity are updated by Equation 7.1. The state vector holds varying values (thus not fixed parameters such as the wing area) that affect the forces and moments, inform the controller's decisions, and inform state switching.

$$
\begin{aligned}
m &= m_{start} - \int_{t_0}^{t} \dot{m}_{fuel\ flow} dt \\
V &= \sqrt{V_x^2 + V_z^2} \\
\gamma &= \arctan(V_z / V_x) \\
\alpha &= \theta - \gamma
\end{aligned}
\tag{7.1}
$$

Integration To update the velocity and velocity of the simulated aircraft, an integration mechanism is necessary. The variables that need to be updated using integration are the velocities (linear: v_x, v_z, and angular: ω), and position (linear: x, z and angular: θ). For this, Adams-Bashfort integration is used. It is a linear multistep method, which means it uses information from multiple time steps to approximate an integral increment. Equation 7.2 shows how the y-value at time $n+5$ is calculated using the y-value at timestep $n+4$ and previous function calls (which in our case are the derivatives), with h the timestep.

$$
\begin{aligned}
y_{n+5} = y_{n+4} + h\,(& \frac{1901}{720} f(t_{n+4}, y_{n+4}) - \frac{2774}{720} f(t_{n+3}, y_{n+3}) \\
& + \frac{2616}{720} f(t_{n+2}, y_{n+2}) - \frac{1274}{720} f(t_{n_1}, y_{n+1}) + \frac{251}{720} f(t_n, y_n)
\end{aligned}
\tag{7.2}
$$

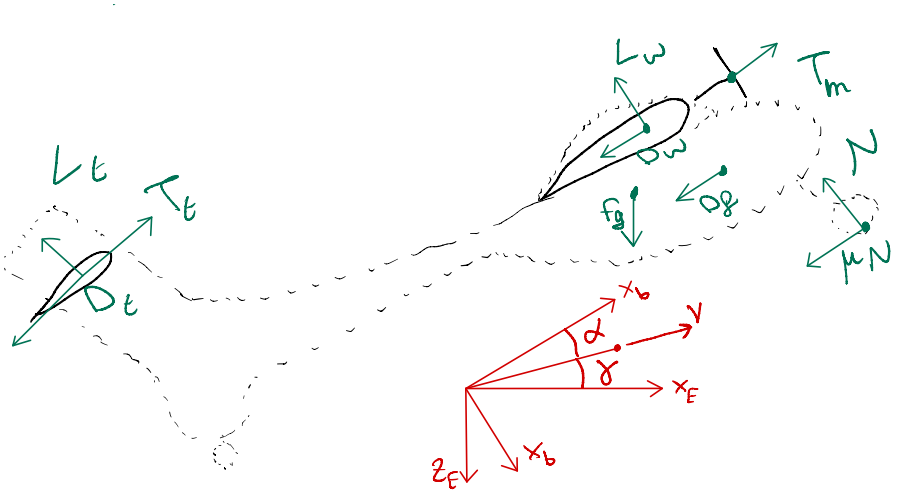

Figure 7.4: The free body diagram of all forces implemented in the model and the reference frame chosen.

Data logging and visualisation Auxiliary features such as data logging and visualisation were implemented both to simplify debugging and increase trust in the final result. For this, the state vector and all forces and moments are logged at each time steps. This data is presented after the simulation in a plot. During the simulation however, also a real-time visualisation of the aircraft is presented which is used to find potential issued with the model.

7.2.2. Forces and moments

This subsection explains how the resultant forces and moments are obtained, represented by block 2 in Figure 7.2. The mathematics of the model rely on Euler's laws of motion in two dimensions, Equation 7.3. The model is in the Earth-frame (subscript "E"), but it contains forces that are in the body frame (subscript "b"). The mass moment of inertia, I, is estimated using the relation explained in [36, p 103], Equation 7.6.

$$ma_{x_E} = \sum F_{x_E} \tag{7.3}$$

$$ma_{z_E} = \sum F_{z_E} \tag{7.4}$$

$$I\alpha = \sum M_{c.g.} \tag{7.5}$$

$$I = (0.4 \cdot m^{1/3} + 1)^5 \tag{7.6}$$

To use Equation 7.3, all forces and moments must be combined. For the forces, this means converting them into the earth frame, and the summing them. For the moments, the points of applications are taken from the aircraft design, which are given in the body frame. Therefore, the summing of moments is performed by first transforming the forces to the body frame, calculating the moments around the relevant point, and the summing them up. When the aircraft is on the ground, this rotation point is the front wheels, and when in the air, the rotation point is centre of gravity. To perform the transformations and moment calculations, a single function was written, rather than repeatedly performing this manually, preventing sign and reference frame errors. As a result, there is no single expression for a_{x_E}, a_{z_E} and α, as these are found computationally.

Gravity The force of gravity is modelled as a forced in the positive z direction (towards the centre of the earth) with a magnitude of mg, acting on the centre of gravity, Equation 7.7. When the aircraft is in the air, this force creates no moment (as the point of rotation is the centre of gravity), but when on the ground, it creates a positive moment (pitch up) around the front main wheels.

$$F^E_{grav} = mg \tag{7.7}$$

Aerodynamic The resultant aerodynamic force on the wing, horizontal tail, and fuselage are decomposed in the body frame along the tangential and normal directions, Equation 7.8. The fuselage is assumed to produce no lift, and the vertical tail is neglected (as this simulation is in 2D). The tangential direction is in parallel to x_b, while the normal direction points in the opposite direction of z_b. The lift and drag coefficient functions are provided by the aerodynamic analysis explained in Section 6.4. Note that the horizontal tail forces forces are given with respect to the horizontal tail area and airspeed.

$$
\begin{aligned}
(F_{aero}^{x_b})_{wing} &= -\frac{1}{2}\rho V^2 S C_{L_{wing}}(\alpha, T_{main}, \rho, V_\infty, state) \\
(F_{aero}^{x_b})_{tail} &= -\frac{1}{2}\rho V^2 S C_{L_{tail}}(\alpha, T_{tail}, \rho, V_\infty, state, \delta_{elevator}) \\
(F_{aero}^{z_b})_{wing} &= -\frac{1}{2}\rho V^2 S C_{D_{wing}}(\alpha, T_{main}, \rho, V_\infty, state) \\
(F_{aero}^{z_b})_{tail} &= -\frac{1}{2}\rho V^2 S C_{D_{tail}}(\alpha, T_{tail}, \rho, V_\infty, state, \delta_{elevator}) \\
(F_{aero}^{z_b})_{fuselage} &= -\frac{1}{2}\rho V^2 S C_{D_{tail}}
\end{aligned}
\tag{7.8}
$$

AS the take-off performance of the aircraft is a central point of the design, ground effect was also accounted for. It was taken into account using lifting line predictions which are described in Equation 7.9 and Equation 7.10 for lift and induced drag respectively, [47]. These equations are applicable for untwisted tapered wing, with taper ratios between 0.3 and 1.0 and aspect ratios between 4 and 20.

$$
\begin{aligned}
\frac{[C_L(\alpha)]_h}{[C_L(\alpha)]_\infty} &= 1 + \delta_L \frac{288(h/b)^{0.787}\exp[-9.14(h/b)^{0.327}]}{A_{eff}^{0.882}} \\
\delta_L &= 1 - 2.25\left(\lambda^{0.00273} - 0.997\right)\left(A_{eff}^{0.717} + 13.6\right)
\end{aligned}
\tag{7.9}
$$

$$
\begin{aligned}
\frac{(C_{Di}/C_L^2)_h}{(C_{Di}/C_L^2)_\infty} &= 1 - \delta_D \exp\left[-4.74(h/b)^{0.814}\right] \quad - (h/b)^2 \exp\left[-3.88(h/b)^{0.758}\right] \\
\delta_D &= 1 - 0.157\left(\lambda^{0.775} - 0.373\right)\left(A_{eff}^{0.417} - 1.27\right)
\end{aligned}
\tag{7.10}
$$

In Equation 7.9 and Equation 7.9, h is the distance between the wing and the ground, b is the wingspan, λ is the taper ratio, and A_{eff} is the aspect ratio. The output of these equations are multiplication factors applied to the lift coefficient and the induced drag coefficient.

Thrust The main thrust force is controlled through a throttle setting (between 0 and 1), while the tail engines are either on or off depending on the aircraft state. In the equation below, T_{max} is the maximum thrust available and t is the throttle setting.

$$
(F_{thrust})_{main} = \begin{cases} t \cdot (T_{max})_{\text{TO and L}} & \text{if state in (ground, rotate,} \\ & \text{take-off, approach, landing-roll)} \\ t \cdot (T_{max})_{cruise} & \text{else} \end{cases}
$$

$$
(F_{thrust})_{tail} = \begin{cases} T_{max\ tail} & \text{if state in (ground, rotate, take-off, approach)} \\ 0 & \text{else} \end{cases}
$$

Ground Forces When the aircraft is on the ground, it experiences both a normal force and a friction force, which disappear once the aircraft is in the air. The normal force is usually defined as the difference between the lift and the weight of the aircraft: $N = L - W$. However, in this model, it will be calculated from the sum of all other forces in the z_E direction, such that there is no movement in the z direction. Once this predicted force becomes negative, the model changes from ground state into air-state and both components of the forces are set to zero. Note that this force is in the Earth frame, just like gravity, while the other forces are in the body frame.

$$
F_{ground}^{x_E} = -\mu N \tag{7.11}
$$

$$
F_{ground}^{z_E} = -N \tag{7.12}
$$

7.2.3. Obtaining performance values using the model

The purpose of the model presented is to estimate the performance of a given aircraft. The simulation can be started in different flight phases. This allows the model to estimate a variety of performance parameters that are relevant to other tools that are used to design the aircraft or that are relevant to requirement verification.

It was decided to find the majority of theses parameters using a simulation as opposed to analytical and empirical formulae, since the *Twin Puffin* is a unique aircraft with unique features. It was feared that the aforementioned formulae would not estimate the performance of the design with satisfactory accuracy.

The procedures used to estimate the most pertinent performance characteristics are explained in the following sections. In order to perform these procedures, a simple controller was developed. The controller can gets information from the previously described state vector. In addition it also has information on the resultant forces and moment acting on the aircraft.

The controller can however only alter four variables. These variables are the throttle, elevator deflection, pitch, and angular velocity. The angular velocity is partially controlled because it is not possible to get it to be exactly zero. This is also true for the horizontal and vertical acceleration, however the vertical and horizontal are less sensitive to small errors than the attitude of the aircraft. The controller has two main functions. The first being the attitude control and the second being the velocity control. The former achieves the desired flight path angle by increasing the pitch of the aircraft. By setting the pitch of the aircraft, the simulation automatically converges to the corresponding angle of attack and flight path angle. When the desired flight path angle has been achieved, it tries to achieve moment equilibrium by deflecting the elevator.

The latter adjusts the throttle setting of the aircraft. With use of the resultant forces the simulation will increase or decrease the throttle as required. Since the vertical and horizontal acceleration are not under control of the controller, the simulation has a velocity margin when it stops adjusting the throttle. When the difference between the target velocity and the actual velocity increases beyond this margin, the controller activates again.

Stall Speed To find the stall speed of the aircraft, the standard mathematical technique, shown in Equation 7.13, was only used as a starting point, after which a computational technique was implemented. This is because the standard equation does not take into account that the lift and weight vectors are not aligned at $\alpha = \alpha_{max}$, the effect of thrust (significant for this aircraft due to the high maximum thrust), and the lift force produced by the tail (which can be positive or negative).

$$W = L = \frac{1}{2}\rho V^2 S C_L \quad \rightarrow \quad V_{stall} = \sqrt{\frac{2W}{\rho S \left(C_L\right)_{max}}} \tag{7.13}$$

The algorithm works iteratively, trying to a fly at a certain velocity and then determining the aircraft stalls or not. If the aircraft doesn't stall, the velocity is reduced and the test is repeated, otherwise, the previous velocity is returned. The test starts with setting the velocity is set, angle of attack of 14°, maximum thrust (which depends on the state, which itself depends on the altitude), the correct density (given the altitude) and mass. Then, for each velocity, the elevator setting is found that puts the moment closest to zero, and a check ensures that the tail can change the sign of the resultant moment, verifying that the attitude can be maintained. With the aircraft now in a pitch stable state, the resultant forces are observed: if the aircraft accelerates down, the aircraft is assumed to be stalling.

Take-off Distance To simulate the take-off of the aircraft, the simulation starts in the *ground* state. To simplify the simulation, it is assumed that the aircraft is held at zero degrees of pitch. This is a fair assumption considering the pitch down moment the engines produce and the added controllability due to the blown tail. From this position, the aircraft is accelerated using full throttle of the cruise engines only. For take-off the DEP is also active, it is turned on when the aircraft approaches v_{stall}. The v_{stall} value in question is calculated with the DEP active.

The simulation showed that the DEP provided high lift, even at low angle of attacks, also leading to high drag during take-off. It was found that the activation of DEP during the take-off procedure was favourable over activating the DEP at the start of the take-off.

The aircraft is set to rotate when its velocity has reached 1.2 v_{stall} [52]. During rotation, the elevator is deflected to generate a pitch up moment. This is done until a climb gradient of a minimum of 4° is achieved. By deflecting the elevator, it also shows that the tail can create a sufficient moment to pitch the aircraft up, despite the large pitch down moment of the engines. The take-off is considered finished when the aircraft climbs past 15 m altitude with respect to the ground. This leads to results for the take-off roll distance and take-off run distance.

Landing Distance The landing procedure is more complex than the other mission phases. It was therefore opted to use an analytical landing procedure, as described by Ger J.J. Ruijgrok in 2013, to estimate the airborne phase of the landing procedure[52]. The airborne phase starts at 15 metres, the screen height, altitude and end at touchdown after the flare.

The glide slope during approach is found using Equation 7.14[52]. Here the lift drag and thrust to weight ratio determine the approach steepness.

$$\gamma = \arcsin(\frac{C_D}{C_L})_A - \frac{T}{W} \tag{7.14}$$

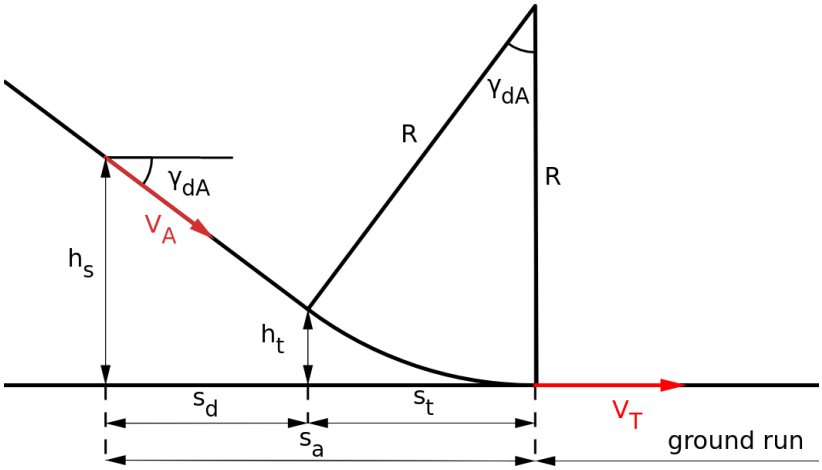

Figure 7.5: Diagram depicting the landing manoeuvre [52].

The flare is modelled using a circle, the radius of which is found using Equation 7.15[52]. Here the approach velocity at the start of the flare and the load factor during the flare determine the radius of the flare. With the radius of the flare, the horizontal and vertical distance travelled during the flare can be found with Equation 7.16 and Equation 7.17, respectively[52]. The horizontal distance between the flare point and the screen height can then easily be determined using the found glide slope during approach.

$$R = \frac{V_A^2}{g(n_a - 1)} \tag{7.15}$$

$$s_t = R\gamma_{dA} \tag{7.16}$$

$$h_t = \frac{1}{2} s_t \gamma_{dA} \tag{7.17}$$

During the approach a velocity of 1.3 v_{stall} is used as this is the minimum velocity stipulated by most airworthiness regulations[52]. Furthermore, the glide slope is set with 70 % throttle and a maximum value of 8°. The maximum load factor during the flare is set to be 1.1. With these parameters the airborne distance can be approximated.

The ground roll distance is estimated by simulating the aircraft on the ground. Doing this allows the braking to take into account the variable normal force the aircraft experiences due to the reduction in lift throughout the procedure. The braking of the aircraft is simulated using an increased dynamic roll resistance of 0.3, which is a conservative estimate. This is done since the aircraft is prone to tipping forward whilst braking. The cruise engines are not set to produce negative thrust, as the aircraft should be able to stop within 100 m using brakes only. The DEP is however active since they are required for the short landing. Furthermore, it is assumed that the flare only arrests the vertical velocity and that the horizontal velocity remains unchanged.

Maximum Climb Angle The maximum climb angle is an important performance parameter, since it indicates if the aircraft can clear an obstacle in its flight path. The maximum climb angle is found by starting the simulation at a pressure altitude of 2500 ft . The aircraft is given an initial velocity of 50 m s^{-1} with a throttle setting of 95 %. The DEP is turned off during this simulation. The altitude is chosen as the climb angle is most important after take-off, and from the requirements the aircraft should be able to meet its take-off performance at this altitude.

The aircraft has an initial flight path angle of 0°. The aircraft pitch is then increased with increments of 0.1°. The simulation then waits for the forces to be in equilibrium again. When this is the case, the pitch is further increased. When the maximum climb angle has been surpassed, the aircraft will not be able to return to equilibrium and the maximum climb angle is found. It is verified that the elevator can create a sufficient moment to achieve the pitch that the aircraft is flying at.

Rate of Climb The maximum climb speed is found using the methods described by Ger J.J. Ruijgrok in 2013[52]. The equations used are Equation 7.18 and Equation 7.19. It is found that the optimal velocity is 28.9 m s^{-1}, regardless of power setting.

$$RC_{max} = \frac{P_a}{W} - \sqrt{\frac{W}{S}\frac{2}{\rho}\frac{1}{\frac{C_L^3}{C_D^2}}} \tag{7.18}$$

$$v_{optimal} = \sqrt{\frac{W}{S}\frac{2}{\rho_0}\frac{1}{C_{L_{optimal}}}} \tag{7.19}$$

For the rate of climb, two values shall be found. First of all, a derated climb rate is calculated using the regular power available from the generator and the batteries. Here, the ICE continues to operate at optimum efficiency, such that emissions are relatively low. The derated climb rate can thus also be considered as the ”green” climb rate.

The other value to consider is the maximum achievable climb rate. Here, the power available is further increased by operating the ICE at its maximum power output setting. The increase in available power then allows for significantly better climb performance. However, this improved climb rate comes at an ecological cost: when operating at maximum power, the ICE no longer operates at its optimum point, so the engine efficiency decreases and the emissions increase. Furthermore, operating the engine at high RPM settings above its design point increases noise pollution.

Power Required During Cruise To estimate the power the generator needs to provide, the aircraft is put at the selected cruise altitude with the initial velocity set to the desired cruise velocity. The aircraft is then set to maintain its altitude, by targeting a flight path of 0°, and target cruise velocity.

In order to keep the simulation streamlined with an iterative process, the setup of the state is kept minimal. This can lead to some initial instability and oscillations of the flight path, velocity, throttle, and altitude. To minimise the effect of these simulation artefacts, the simulation waits until the aircraft is stable within margins.

This is done by verifying that the sum of forces in horizontal and vertical direction are stable and close to zero. Furthermore it is verified that the flight path angle is also close to zero. To ensure that the found power required corresponds to cruise conditions, the density is set to the density at cruise. This negates the effect of possible altitude changes due to initial flight path instabilities.

Once the aircraft is stable, the power required can easily be found using the power setting of the engine. Using this value the engine can be sized for cruise and in addition it is also used to size the battery of the aircraft.

Energy Required Climb Phase The energy required during the climb phase encompasses the energy used from the start of the take-off until the cruise altitude has been reached. The aircraft takes off as described earlier and then proceeds to climb at the maximum rate of climb until it reaches the cruise altitude.

The energy used is estimated using the power setting of the aircraft. During the take-off procedure the throttle is set to 100 % as this setting is considered to be take-off power. During the climb phase the throttle is set to 95 % to simulate the maximum continuous power setting. During the climb phase the simulation also switches off the DEP once an altitude of 100 m is achieved. This decreased the drag the aircraft experiences and is akin to retracting high lift devices on conventional aircraft. With the time step and the power setting, the total energy used can be estimated.

In addition the simulation also verifies that the aircraft is capable of performing the climb profile selected. It does this by verifying that the aircraft does not stall and by verifying that the tail can provide the required moment to hold the aircraft at its specified attitude. Since the tail is fully moving, it is also verified that the elevator does not stall.

The numeric outputs of the simulation are the energy used when the cruise altitude is reached, the mass of the aircraft at the start of the cruise, and the time it takes to climb to cruising altitude. The qualitative outputs are that the aircraft can perform the set climb procedure and that the elevator can control the aircraft.

Energy Required During Cruise and Cruise Range The energy required during cruise is found by starting the simulation at the cruise altitude with an initial velocity equal to the selected cruise velocity. The flight path angle is set to 0°. The aircraft is set to maintain both its cruise velocity and the initial flight path. In order to accommodate for simulation artefacts of slight altitude oscillations due to small non-zero flight path angles, the density is set to the cruise altitude density.

During the cruise, the power required is integrated with respect to time to find the energy used during every time step. From the energy used and the efficiency of the powertrain, the used fuel mass can be calculated. This fuel mass is subtracted from the mass of the aircraft. When the fuel mass reaches a set value, fuel needed for descent, landing, and reserve fuel, the cruise phase ends.

The numeric outputs of this simulation are the cruise range, the energy required for the cruise phase, and the mass at the end of the cruise.

Noise The calculation of noise is complicated in aircraft design and is usually an involved process to do accurately. Usually experimental procedures are employed but based on statistics some more general empirical estimations can be made that can quantify sound pressure levels even with the limited information available at the current theoretical design stage. These empirical relations are taken from both Simons and Snellen as well as Fink. To estimate the total noise output, the noise produced by the primary elements of the aircraft is calculated individually and then combined to give a final sound pressure level (SPL). The motor and exhaust

noise as well as each of the propellers' noise is calculated by Simon and Snellen [54]. The Noise of the overall airframe was then calculated with Fink [20].

After calculating all of the individual component sound pressure levels, they need to be added correctly. When calculating in decibels this becomes more difficult, so instead, each decibel value will be converted to a noise power level. The reference power is 10^{-12} W for 0 dB and with this and Equation 7.20 the total noise at one meter distance can be computed. To calculate the noise at other distance, the phenomena that sound pressure decreases with distance by $\frac{1}{r}$ can be employed[1].

$$SPL_1 = 10\log\left(10^{\frac{SPL_{1,E}}{10}} + 10^{\frac{SPL_{1,P}}{10}} + 10^{\frac{SPL_{1,AF}}{10}}\right) \tag{7.20}$$

7.3. Optimisation

The goal of optimisation is to design the aircraft such that it maximises the objective function outlined in Section 7.3.2. For this optimisation, the aircraft design and analysis modules are combined into one function that takes as input high level design parameters and outputs a value estimation. This one tool is then used by the Nelder-Mead optimisation algorithm to maximise the projected value, hereby finding the optimal design.

7.3.1. Optimisation structure

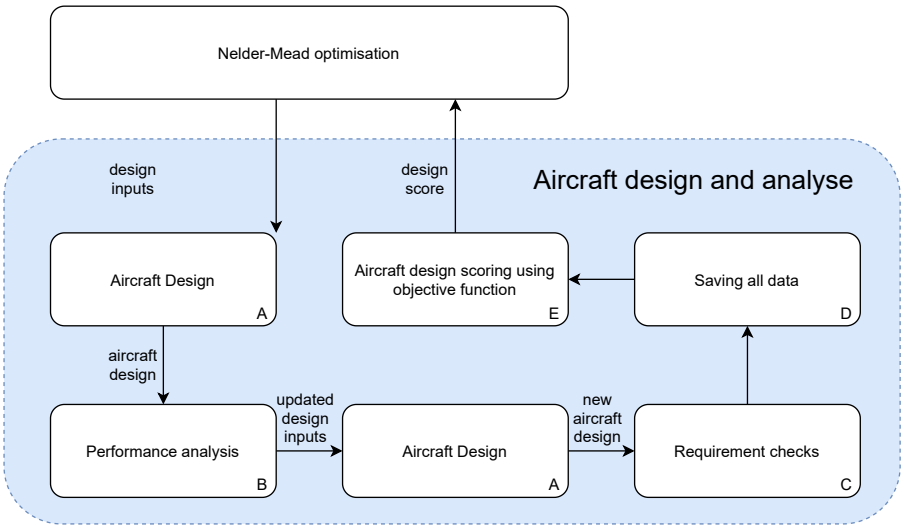

Figure 7.6: Code structure for optimisation

The aircraft design and analysis, Figure 7.6, starts by designing the aircraft given high level design parameters, block A. Then, the aircraft's performance is analysed, block B. After analysing the performance of the aircraft, certain parameters such as the energy required to climb and the power during cruise are updated, following which the aircraft is designed again. Due to computational time restrictions, this redesigning only occurs once. After that, the aircraft requirements are checked, in block C. Then, all information computed is saved, block D for further analysis. Finally, the final design is scored using the objective function described in Section 7.3.2, block E. Hereby, an aircraft is designed using high level input parameters, and scored.

Requirement check During the loop, the requirements are checked to ensure that only suitable aircraft are considered during the optimisation. If any requirements fail, the aircraft is given the worst possible score, to force the optimisation to move in a different direction. The requirements checked are only those related to parameters that are computed in the code, such as take-off and landing roll, cruise velocity, and climb gradient.

7.3.2. Definition of the Objective Function

The methods outlined in Chapter 6 to design each specific subsystem of the aircraft have a lot of inter-dependencies between them. For example, the size of the wing depends on the lift that the aircraft has to produce, which is a parameter influenced by all the subsystems. Similarly, geometric parameters of the wing determine the value of induced drag during flight, which in turn create requirements on the propulsion subsystem. The aforementioned inter-dependencies are accurately described by the concept of snowball effect - where an increase or decrease in one of the design parameters results in variation of many other parameters.

[1]URL `http://www.sengpielaudio.com/calculator-SoundAndDistance.htm` [cited 29 June 2021]

The aircraft, being the outcome of the sizing and designing model, has to comply with several requirements and constraints, as outlined in Chapter 4. However, several similar but nonetheless different designs would be able to satisfy the same list of requirements, especially given a limited number of driving requirements. For that reason, it is necessary to establish an optimisation framework that judges different possible design configurations relative to one another. For this, the analysis performed in Section 3.2.2 is used. The outcome of said analysis was the regression function stated in Equation 3.5, which finds an approximate measure for the market value achievable for different aircraft designs. The method takes as inputs the take off distance, the climb rate at sea level, the cruise speed at 75% power, the useful load, and the range.

The statistical aircraft value prediction of Section 3.2.2 shall thus be used as an objective function for the optimisation program. This will make it possible to score different aircraft designs on the basis of how well their specific combination of performance values is expected to allow them to perform on the market. As the objective function is the summation of the two approximations of retail price, it will have combined error measures, and should not be used for any extrapolation of retail price beyond the realistic range that the gathered data lies in. The error should not play into the optimisation accuracy, as only the relative measure of importance of the performance parameters is of value in the objective function.

7.3.3. Optimisation algorithm

To optimise the input parameters and search for the optimal design, the Nelder-Mead algorithm was chosen. It was chosen for its stability and its lack of requirement of derivatives on the function to be optimised (in this case, the design and analyse block, is very complicated).

Nelder-Mead optimisation works by slowly moving from an initial guess towards the higher function output values. It is hereby susceptible to getting stuck in local maxima. The algorithm start by transforming the initial input of n variables into n+1 linearly independent points, forming a simplex. Then, it evaluates each of the points with the to-be-maximised function, ranking the points from best to worst. Then a new point is calculated, and evaluated, discarding the worst option. Depending on the result, a different new point is calculated, and evaluated, and the worst is discarded. Slowly, the simplex moves towards a maximum of the function. When the difference in function evaluation between all points is sufficiently small, the loop ends and the final point is found.

7.3.4. Running the optimisation

Running the optimisation for different starting points, combining all values, and plotting the operating empty mass against the total take-off thrust results in Figure 7.7. The points are coloured in accordance with their value from the objective function and are scored on a relative scale from zero to one. The higher the score, the higher the predicted value of the aircraft is. Further information about how the model was run and why is provided in Section 9.1.

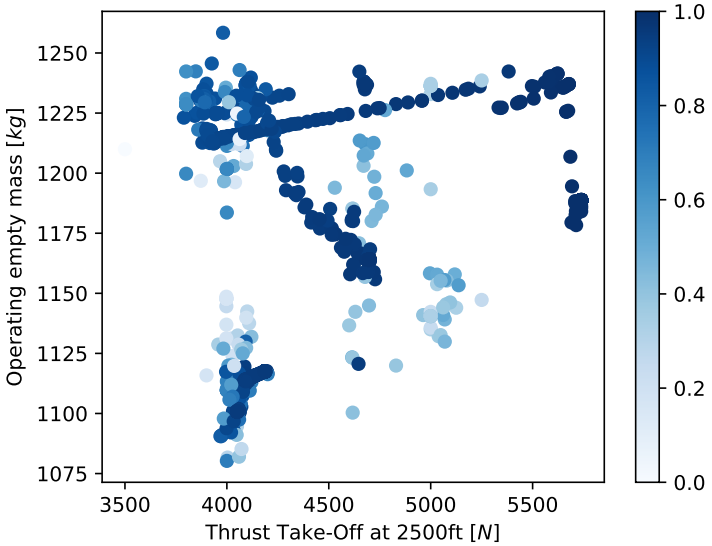

Figure 7.7: Results from the optimisation run

7.4. Verification

Multiple verification tests are applied to ensure the quality of the software used for parameter calculation and optimisation. These verification methods are described and examples of verification tests are listed below.

Verification by Manual Calculations - Type I This method is used when verifying formulae or relations which themselves are considered valid. The method solely confirms that the equation has been translated into code correctly. The verification is performed by choosing input parameters for the equation and using these in manual calculations. Then the output of the program is compared to the manually found result. The difference should be negligible and only due to the numerical nature of the computer.

Verification by Acceptable Range - Type II This method is complementary to the method described prior. The method does not confirm that the values are correct, it confirms that the obtained results are not out of the ordinary. This is important when important parameters are for example estimated using statistical relationships or relations that are based on assumptions. If the verification fails it indicates that the data base of the statistical relationship is not representative of the design or that the assumptions do not hold for the examined design.

This is also a useful tool when verifying functions that return large numbers such as the Reynold's number. When the difference between the expected value and the output is several orders of magnitude smaller than the total magnitude of the expected value, the output is still acceptable.

Verification by Limits - Type III This method is important to ensure that outputs have realistic values. When limitations of a function are known such as, assumptions made for analytical expressions, range limits for interpolation, or diverging accuracy, it is important that this is handled accordingly. This is done by identifying these limitations and purposefully targeting them by means of verification and confirming that the outputs remain realistic or exceptions are raised.

Verification by Visual Inspection - Type IV This method is used for large data sets, since it is difficult to go through every data point individually. The best course of action is to plot theses data sets and verify that the shape of the graph has the features, the shape, and the magnitude as expected. This method can also identify outliers in large data sets to narrow down the issue.

Furthermore, this method can be using statistical relations. For example when sizing subsystems using reference subsystems. The performance of the designed subsystem can differ in performance from the reference data, but it will most likely be close to the other reference points in the plot.

Verification by Inverse Calculation - Type V This method is used when subsystems are chosen or designed based on a set of performance requirements using complex logic. This type of verification is performed by letting the the program choose or design a subsystem based on performance requirements. The subsystem is then manually analysed to verify that the performance requirements are met with the intended margins. This verification is very important when many different functions or even classes interact to produce an output. It verifies that the individual verified functions and classes work together as intended.

Verification by Prediction - Type VI This method is used to verify that calculations work as intended. It is performed by predicting how the output should change by increasing, decreasing, or changing parameters. To verify that the code works as intended, the predicted change is compared to the change in output. Depending on the accuracy of the method, a margin of error can be allowed for.

Verification Examples Some examples of verification used in the code for the design of the *Twin Puffin* are shown in Table 7.4. These examples are a subset of the total verification tests performed. They are considered the more important functions and are therefore shown.

Table 7.4: This table elaborates on which functions have been verified, how they were verified, and what type of verification was used.

Function	*Explanation*	*Type*
	Stability and Control	
Potato Diagram	The mass of the passengers was increased and it was verified that the corresponding potato becomes wider	VI
Potato Diagram	Final point of loading diagram should equal payload mass + OEW	IV
Scissor Plot	For Sh/S = 0, the neutral point is equal to the aerodynamic centre	III
Horizontal Tail Sizing	Manually detach horizontal tail from vertical tail and check that it will automatically placed at the closest vertical tail location	III
Wing Placement	Moving the location of the OEW centre of gravity forward also moves the wing placement forward	VI
Tail Sizing	Reducing the moment arm of the tail will increase the tail size.	VI

Table 7.4: This table elaborates on which functions have been verified, how they were verified, and what type of verification was used.

Function	*Explanation*	*Type*
Class I Weight Estimation	It is checked that the the location of the design is close to the reference aircraft	IV
	Aerodynamics	
Airfoil Selection	With the chosen airfoil, find its optimal C_l range and verify that this matches with the input $C_{l_{des}}$	V
Wing Geometry	Check that the tip chord cannot be larger than the root chord	III
Oswald Efficiency	It is verified that the formula was correctly input using manual calculations.	
Oswald Efficiency	The Oswald efficiency factor should be between 0.65 and 0.8	II
Lift Over Drag	The lift over drag factor should be between 10 and 20	II
Moment Coefficient	The moment coefficient of the wing should be negative	II
Aerodynamic Centre	Should be located between 0.2 and 0.3 chordwise location	II
Lift Augmentation	It is verified that the formula was correctly input using manual calculations.	I
Lift Augmentation	Lift augmentation factor is between 1 and 2	II
	Propulsion	
Engine Placement	It is checked if the engines overlap.	III
Propeller Size	It is checked that the propellers are larger than the airfoil for lift augmentation.	III
Propeller Tipspeed	It is checked that the propeller tip does not enter the drag divergence regime	III
Engine RPM	It is checked that the engine RPM is not lower than 1000 RPM	II
Battery Mass	The battery mass estimation is checked using manual calculations	I
Engine Mass	It is verified that the engine mass is located on the interpolation graph	IV
Propeller Mass	It is verified that the engine mass is located on the interpolation graph	IV
Noise Estimation	It is verified that the formula was correctly input using manual calculations.	I
Noise Estimation	Increase number of blades to check if noise decreases.	VI
Noise Estimation	Increase blade diameter to check if noise increases.	VI
Noise Estimation	Increase engine power to check if noise increases.	VI
	Mission Model	
Gravity Force	It is checked that the gravity force has the right magnitude and direction	I
Wing Forces	It is checked that the forces have the right magnitude and direction	I
Wing Forces	It is checked that changing the dynamic pressure has the expected effect on the lift	VI
Wing Forces	It is checked that changing the wing area has the expected effect on the lift	VI
Wing Forces	The lift over drag ration is checked to see if the value is reasonable.	II
Horizontal Tail	The same verification is done as for the main wing	-
Ground Force	It is checked that the ground force does not accelerate the aircraft when standing still.	III
Ground Force	It is checked that the normal force decreases when lift increases	VI
Stall Speed	It is checked that the stall speed is similar to the stall speed found using the standard formula. This is done by setting a conservative and optimistic stall speed using the standard formula	II
	Miscellaneous	
ISA Calculator	The temperature output is checked by manual calculations.	I
ISA Calculator	The pressure output is checked by manual calculations.	I
ISA Calculator	The density output is checked by manual calculations.	I
Vector Calculations	The moment calculations around different reference points are verified using manual calculations.	I
Vector Transform	The transformed vectors are verified using manual calculations.	
Vector Transform	It is checked that a vector transform A $\longrightarrow$ B $\longrightarrow$ A results in the initial vector	III
Adam-Bashforth	It is checked that the integration error decreases with increasing number of nodes	VI

Part III:

Final Aircraft Design

8

Final Aircraft Design

Having explored all the design options and introduced all the tools needed for sizing of the aircraft, finally the ultimate form of *Twin Puffin* can presented. This chapter focuses on portraying all of the most important features and properties of the final design. It comprises eight sections that comprehensively and in-detail describe what were the results of design methods presented in the Chapter 6. Firstly, a general overview is given, where the most important values for stakeholders are given. Then, the proceeding sections treat different subsystem and the specifics of the performance of the *Twin Puffin*. Furthermore, subsequent subsections elaborate on the integration of the systems inside the aircraft.

8.1. Overview of the Final Design

The effect of all the design procedures and efforts is the complete design of the *Twin Puffin*. The goal of this section is to provide a sort of a general summary of its final shape. The most important properties are provided here and the general integration of the aircraft's systems is presented. A general overview of the aircraft is presented in Section 8.1.1. The dimensions of the aircraft are presented in Section 8.1.2. The performance of the aircraft is summarised in Section 8.1.3. The masses of the major subsystems are listed in Section 8.1.4. The values in Section 8.1.2 to Section 8.1.4 stem from the total parametrisation of the aircraft found in Table A.1.

8.1.1. General Overview

A render of the *Twin Puffin* is presented in Figure 8.1. Based on this figure some preliminary conclusions can be drawn.

Figure 8.1: Front view of the *Twin Puffin*

The most notable feature of the *Twin Puffin* is the distribution of the propellers along the wings. The foremost advantage of which being the lift augmentation described in Section 6.4,but also a high potential thrust and overall unparalleled short take-off opportunities.

Another apparent conclusion that can be easily drawn from the drawing concerns the agility of the *Twin Puffin*. As the propellers are mounted far from the fuselage, it can be suspected that the potential yawing moment can be significant. Also, concerning the dynamic performance, an anti-tip over system for landing could be easily implemented. Since the propellers are placed on the leading edge, above the centre of gravity, in an event of potential tipping over while abrupt breaking during landing, the propellers can provide reverse thrust that would stabilise the aircraft.

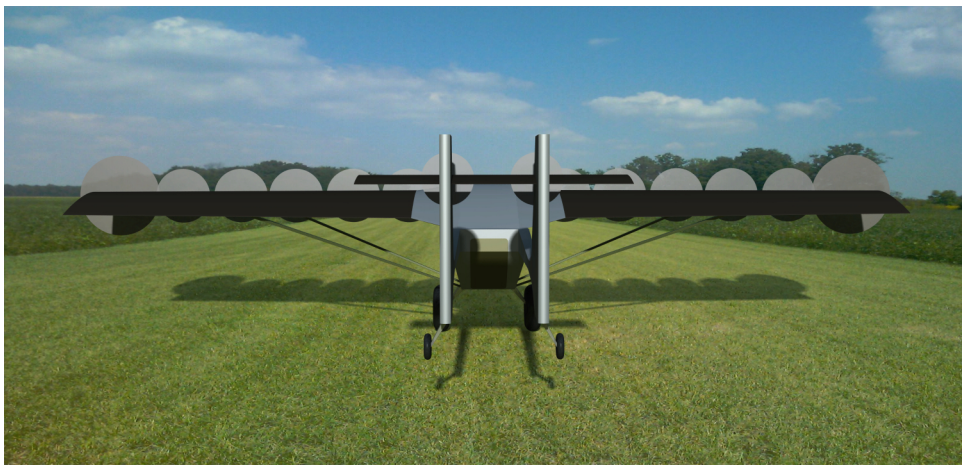

Figure 8.2: Rear view of the *Twin Puffin*

As the Figure 8.2 portrays, the *Twin Puffin* does not have only one door as most conventional aircraft, but two. This seemingly irrelevant feature, in reality can prove to be of vital importance for potential customers. The 'rear hatch' makes loading of the aircraft easier than it would be through a hatch on the side. It is especially convenient for loading stretchers. This advantage is exclusively possible due to the twin boom construct.

Furthermore, the *Twin Puffin* was able to marry two concepts of taildragger and twin boom in an unprecedented way. This unconventional design allows to elicit the advantages of both concepts without introducing any disadvantages. Thus, the benefit of having a taildragger aircraft with high initial α prevails.

Lastly, the cockpit is another characteristics that distinguishes the *Twin Puffin* among its competitors. It is entirely translucent, which not only provides stunning views during cruise but primarily allows the pilot to navigate safely during taxiing as the visibility is not hindered, unlike in a conventional taildragger. It is also worth mentioning that the cockpit is strengthened with rods creating a shall like structure, that in case of an accident protects the pilot.

8.1.2. Dimensions of the aircraft

Having achieved the final design of the aircraft, its most relevant dimensions can now be presented. A summary of, what are deemed, the most interesting geometric values can be visualised in the Table 8.1.

Table 8.1: Geometric values.

Parameter	*Symbol*	*Value*	*Unit*
Wing Area	S	28.14	m^2
Wing Span	b	15	m
Root-Chord	c_r	2.21	m
Tip-Chord	c_t	1.55	m
Aircraft Length	l_f	8.95	m
Cabin Length	l_f	4	m
Cabin Width	w_f	1.3	m
Cabin Height	h_f	1.41	m

What definitely can be surprising from the above data is the length of the wignspan. However, it needs to be mentioned that those wings are longer than for competitors as they are meant to fully take advantage of the distributed propulsion. Above that, most competitors of the *Twin Puffin* provide only space for two or even one passenger. Thus, the *Twin Puffin's* wing could have been anticipated to be longer and bigger.

Another aspect worth mentioning is the fuselage, which is quite long. Despite the fact that not full length of it is useful for passengers or cargo, it still can provide comfortable alternative to other competitors of the *Twin Puffin*.

8.1.3. Characteristic values for performance and aerodynamics

In the Table 8.2, the most important properties related to the performance of *Twin Puffin* are presented.

Table 8.2: Key characteristic values.

Parameter	*Symbol*	*Value*	*Unit*
Payload Mass	$m_{payload}$	400	kg
Seats	n_{pax}	4	-
Design Range	R	1247	km
Cruise Speed	V_{cruise}	54.9	$m\,s^{-1}$
Take-off Ground roll at 0 ft	s_{to_0}	61.0	m
Take-off Ground roll at 2500 ft	$s_{to_{2500}}$	65.2	m
Landing Roll at 0 ft	s_{land_0}	87.8	m
Landing Roll at 2500 ft	$s_{land_{2500}}$	94.5	m
Noise at 1 m Distance	N_{1m}	116.4	dB
Noise at 2500 m Downrange	N_{2500m}	87.8	dB
CO_2 emissions	$m_{CO_2,sp}$	56.76	g/pax /km
Operating Costs 800 h	$C_{op_{800}}$	150	$USDhr^{-1}$
Operating Costs 500 h	$C_{op_{500}}$	190	$USD\,hr^{-1}$
Maximum Take-off Mass	MTOW	1781	kg
Operative Empty Mass	OEW	1201	kg
Design Fuel Mass	m_{fuel}	106	kg
Wing Loading	W/S	350	$N\,m^{-2}$
Cruise Lift-to-Drag Ratio	$(L/D)_{cruise}$	12.2	-
Stall Speed *(clean)*	V_{stall}	24.3	m/s
Derated climb Rate	V_{climb}	2.16	m/s
Maximum climb Rate	V_{climb}	3.59	m/s
Climb Angle	γ	7.11	deg

What especially should be pointed out from the Table 8.2 is that the MTOW. It is fairly high, however it needs to be noted that it does not hinder the characteristics such as range, emissions, stall speed or required runway length which are still very positive. The required landing and take-off distance is kept far below the minimum required runway length in order for the aircraft to be considered STOL. Also, important for sustainability, the mass of CO2 emitted per passenger per kilometre is kept very low for the aircraft of this size and capabilities. Thus, to conclude, the seemingly high weight does not pose a problem for the *Twin Puffin*, which still achieves (or even outperforms) its goals.

8.1.4. Masses of the subsystems

Firstly, the overview of the masses in the aircraft is given. The Table 8.3 presents the weights as given per aircraft component, rounded to the nearest whole kg. This section also delves more in depth into how the masses are relevant for the design.

Table 8.3: Component weights of the final aircraft design.

Component	*Mass [kg]*
Battery	52
Electric engines	152
Empennage	221
Fixed Equipment	103
Fuselage	169
Generator	151
Undercarriage	54
Wing	368

Counter to what might have been expected out of the energy acquisition system, the final result for the weight of the batteries is rather limited. For most electric propelled aircraft the weight of batteries is substantial, however due to the powerful ICE-generator in the *Twin Puffin*, the battery weight was narrowed down.

It is also important to take a note of the low mass of the electric engines. This mass is a sum of weight of all propellers, where only two bigger engines are sized for cruise and ten smaller ones for the advantage of the lift augmentation. This division mean fewer larger engines are required, leading to a reduction in total mass of the propulsion subsystem.

The heaviest components of the aircraft are the wings. This result was expected as the design, in simple words, was optimised in order to provide the highest lift and explore the full advantage of the distributed

propulsion. Since, for highest lift and lowest drag the most slender wings are needed, a high aspect ratio, A was desired. High aspect ratio introduces more weight as it leads to a larger wing span for the same area. For larger wing spans, the required structural support in the wings for the larger bending moments add significant weight, which occurs despite the 'bending relief' introduced by the weight of the engines on the leading edge.

8.1.5. Aircraft Noise

The noise analysis is based on the method presented in Section 7.2.3 and leads to the estimated decibel levels of noise produced by the aircraft in various sections of flight. Using the empirical methods primarily based on Simons and Snellen [54] these calculations are likely to have some errors in them. Therefore this methodology is applied consistently from this point onward in finding noise values to provide a better comparison between the *Twin Puffin* and other bush planes. Upon analysis of real versus estimated values, the calculated values are overestimates. So the values seen at ICAO Annex 16 noise certification altitude in Figure 8.3 being below the requirement makes this a safely surpassed requirement [14].

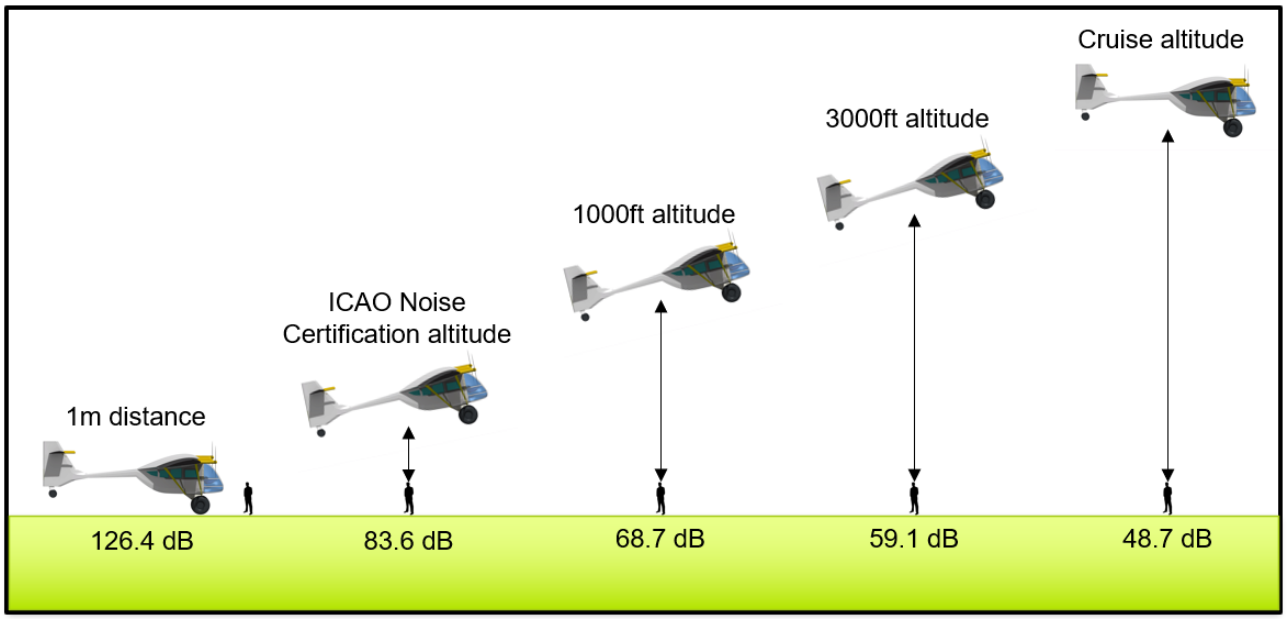

Figure 8.3: Diagram displaying the change in noise measured in decibels in various sections of flight

8.1.6. Auxiliary aircraft systems

The designing process for the Twin Puffin also took into consideration the aircraft auxiliary systems. While these systems are not directly related to the aircraft performance, they are nonetheless important for ensuring the proper operation of the plane. The auxiliary systems of interest are the climate control system, the de-icing system, and the tires of the landing gear.

Climate control is necessary in order to ensure that the pilot and passengers are kept within a comfortable range of temperatures. The Twin Puffin is expected to be used for a wide range of applications and operate in geographic regions ranging from cold Alaska to the deserts of Australia. Thus, both the scenario where the cabin interior must be cooled and the scenario where it must be heated have to be considered. For cooling, it shall be possible to partially redirect the oncoming flow of air into the cabin. This can be done using a set of ventilation slots at the front of the aircraft. For heating, use shall be made of the ICE exhaust gasses. By optionally channelling these exhausts around the fuselage, rather than directly expelling them, part of the waste heat trapped in the gas can be recuperated and used in a meaningful way. Illustrated in Figure 8.4, the climate control system thus works as an example of how the dual use of resources can lead to an integrated design that is more efficient as a whole. In the figure, blue arrows indicate the cold oncoming airflow and red arrows indicate heat from the exhaust gases.

The aircraft de-icing system, shown in Figure 8.5, is based on a similar principal to the heating of the aircraft cabin. If necessary, it shall be possible to redirect the hot ICE exhaust gases to the propellers mounted on the wing leading edge. Streaming out at the base of the propellers, the exhaust gases will be blown over the wing, thereby removing ice and snow. To ensure that the tail control surfaces are also sufficiently de-iced, exhaust vents are also included ahead of the aircraft empennage. Furthermore, use is made of the waste heat generated by the electric high power connections running to the wing-mounted engines. The heat generated by these connections will warm the surface and interior of the wing, thereby further de-frosting the structure.

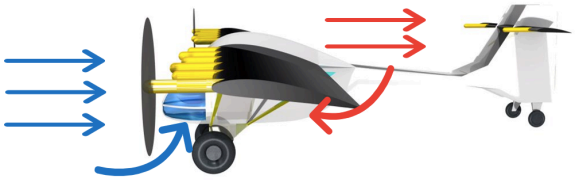

Figure 8.4: Climate control system

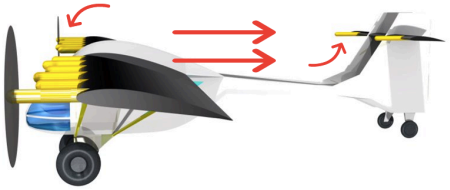

Figure 8.5: De-icing system

The specific choice of landing gear tires is, of course, dependent on the context and application for which the Twin Puffin shall be used. In those cases where the aircraft mostly operates on semi-prepared runways, smaller tires may be sufficient. If, however, the plane is to be landed in very rough terrain, large tundra wheels will be necessary. Furthermore, if desired, it will be possible to mount more unique landing gear attachments. While the design of these attachments exceeds the scope of this design phase, the three major options have been identified. The possible use of skis and floats will allow the aircraft operator to take off and land in an even wider range of places. With four attachment points available, mounting these attachments is facilitated by the quad-taildragger configuration of the Twin Puffin landing gear. The third landing gear option of interest are airless tires. Based on innovative technology, these tires may lead to an increase in aircraft cost, but would provide benefits such as removing the risk of tires popping.

8.2. Operational Procedures

This section outlines the operational procedures associated with the different flight stages of the aircraft. First, it is explained how exactly the pilot interacts with the aircraft controls. Next, the operational procedures for the three major flight phases, namely *take-off*, *cruise*, and *landing*. Then, special operational scenarios are investigated: the stall procedures, the velocity-height diagram, the procedures in case of power loss, and the procedures in case one or more propellers are lost. Across all operational scenarios it holds that at any moment where a propeller is not in use, it is folded up to reduce the aircraft drag.

8.2.1. Pilot-Aircraft Interaction

As will be explained in greater detail in Section 8.9, the pilot can control the aircraft through five distinct types of control inputs: the stick forces (including the forces applied to the rudder pedals), the braking forces, the flap setting, the throttle setting, and the autopilot setting. The throttle setting is divided into two components: the throttle setting for the lift augmentation engines, and the throttle setting for the wing tip cruise propellers. The types of control settings hold for both manual piloting (when a pilot is present on board of the aircraft) and remote piloting.

Across all flight stages, the pilot is assisted in their flying of the aircraft by the flight director system, which augments control inputs as necessary to find the optimal balance between the use of the mobile surfaces and the use of differential thrust settings for the individual engines. This is possible, as the aircraft engines are electric and are controlled using a digital engine control software. The computer-controlled engine management system also means that during manoeuvres such as take off or emergency cases such as the failure of the tail engines, the propulsion system can react immediately by changing engine thrust settings without having to wait for the pilot input. This makes flying easier under regular circumstances and safer in emergencies.

8.2.2. Take off

For take off, special procedures have been designed on when to use which of the distributed propulsion engines of the aircraft. This allows the aircraft to be most effective in its use of distributed propulsion, leading to the short achievable take off distances. Overall, take off is divided into two phases: acceleration and lift off.

As the name suggests, the first take off phase of acceleration is purely concerned with speeding up the aircraft. For this it is desired that drag is minimal, meaning that low lift coefficient values are needed in order to reduce the induced drag. Thus, the aircraft is accelerated by the wing tip engines only, while the lift augmentation engines are kept idle. The most direct drag-reducing consequence of this is that there is no lift augmentation yet, which significantly reduces the aircraft lift coefficient and thus the induced drag. Furthermore, induced drag is reduced as the use of the wing tip engines increases the effective aspect ratio. Finally, drag is reduced by not yet deploying the high lift devices.

The acceleration phase lasts until the aircraft reaches its augmented stall speed, where the lift off phase begins. Importantly, the aircraft will not automatically lift off at this velocity, as it is still in clean configuration without lift augmentation. Once this speed is reached, however, all power is diverted from the wing tip engines to the lift augmentation engines which, combined with deploying the flaps, lead to an immense increase in lift coefficient. This allows the aircraft to detach from the ground and start climbing. The lift augmentation propellers and deflected flaps continue to be used until the aircraft has accelerated to a sufficient velocity that

the extremely high lift coefficients used during take off are no longer necessary.

8.2.3. Cruise

During cruise, the primary objective is to minimise the aircraft drag. For this objective, the aircraft is operated using only the wing tip engines. Primarily, this is done to reduce the induced drag by increasing the effective aspect ratio of the wing: the more thrust is generated by the wing tip engines, the weaker the wing tip vortex and the lower the induced drag will be. Furthermore, the use of the wing tip engines is more efficient as they are primarily designed for efficiency at high speeds, as contrasted to the lift augmentation propellers that are designed for providing high thrust at low speeds. Lift augmentation is not necessary during cruise.

8.2.4. Landing

For the landing of the Twin Puffin, four phases can be identified. The first phase is the descent from cruise altitude. Here the aircraft is manoeuvred to the desired landing site, ideally in gliding flight where the wing tip propellers are used in a windmilling configuration that recharges the aircraft batteries.

Phase two begins once the landing site is approached. Here, the aircraft fully deploys its flaps and slows down to the unblown stall speed (the stall speed with flaps deployed but lift augmentation not used). As lift augmentation is not yet desired but thrust will be necessary to control the aircraft behaviour, the aircraft is propelled by the wing tip engines.

Phase three of the landing begins once the aircraft passes below the height of 50 ft (an explanation of why this number is selected is presented in the stall procedures and the discussion of the velocity height diagram). Here, thrust begins to be produced by the lift augmentation engines, which leads to a further increase in maximum lift coefficient and thereby allows the aircraft to further slow down. Despite of the added thrust, slowing down is possible because the very high lift coefficient leads to very high induced drag. Furthermore, if need be the wing tip propellers can continue to be operated in a windmilling configuration that both generates power and increases drag. By slowing down all the way to the blown stall speed, the aircraft is then able to achieve the desired short landing distance. Due to the low speed and the high moments generated by the wing lift about the centre of gravity, it will be difficult to keep the aircraft trimmed using the horizontal tail. Thus, to increase the effectiveness of the tail and keep the aircraft controllable, the lift augmentation for the horizontal tail will have to be activated for this third landing phase.

The final landing phase corresponds to slowing the aircraft down when it is on the ground. For the certifiable landing distance, this slowing down is purely done using the brakes on the main landing gear. In order to achieve even shorter landing distances, the pilot can chose to employ reverse thrust, which significantly increases the rate at which the aircraft decelerates to a halt. While this use of reverse thrust allows for extremely short landing distances, it must be used at the pilot's own discretion, as a failure of the energy supply during this phase would mean that the anticipated landing distance cannot be achieved.

8.2.5. Stall Procedures

For a STOL aircraft flying at very low air speeds, it's important to investigate its stall behaviour and form procedures around it. In the case of the *Twin Puffin*, the distributed electric propulsion allows for extremely low speeds, which also brings new hazards. When the aircraft is flying with lift augmentation over the main wing, the horizontal tail will lose all control authority if it is not blown by its own propellers. If the horizontal tail propellers fail, or experience a loss of power, the aircraft will enter a critical stall.

Equation 8.1 shows the non-dimensional moment equation of the aircraft. The first and second term is the wing-fuselage contribution to the moment, and the last term the contribution of the tail. Using values from Section 8.1, in the case of complete loss of horizontal tail effectiveness, the moment coefficient will be positive, $C_m = 0.666$, i.e. the aircraft experiences a pitch-up moment. This is more critical than a pitch-down moment, as a larger pitch will bring the aircraft into a continuously deeper stall. A procedure must be put in place to avoid this critical behaviour of the aircraft.

$$C_m = C_{m_{ac}} + C_{L_{A-h}}\left(\frac{x_{cg} - x_{ac}}{\bar{c}}\right) - C_{L_h}\frac{S_h l_h}{S\bar{c}}\left(\frac{V_h}{V}\right)^2 \tag{8.1}$$

It is important to quickly counter-act the pitch-up moment before it escalates into an unrecoverable stall. It is also important to quickly accelerate to past the minimum control speed, where the horizontal tail recovers control authority of the aircraft. Both the pitch-down moment, and the acceleration past the minimum control speed can quickly be supplied by the propulsion running at maximum power. When equating $M = C_m 1/2\rho V_s^2 S\bar{c}$, the total pitch-up moment will be $M = 4900$N m. The maximum thrust from all twelve tractor propellers is 6615 N, which combined with a vertical distance of 0.7 m from the centre of gravity equates to a 4630 N m pitch-down moment, close to fully counter-acting the wing-fuselage pitching moment, and naturally also quickly speeding up the aircraft. The about 300 N m discrepancy is quickly counter-acted as the aircraft speeds up and the horizontal tail recovers partial control authority.

If the horizontal tail lift augmentation fails, the pilot would have to react almost instantly as they now find themselves in an unstable flight condition. To assist the pilot in this, there are pressure sensors placed on the horizontal tailplane to quickly detect a failure of the horizontal tail lift augmentation. The engine control system is then able to react autonomously.

The proposed procedure of applying maximum thrust is not unlike conventional stall recovery and therefore does not require special pilot training. Although for this critical stall out of lift augmentation it is beneficial for the pilot not to focus on providing control inputs, as the tail will not be responsive, but rather immediately providing maximum thrust on all propellers to quickly regain control authority.

8.2.6. Aircraft Height-Velocity Diagram

Sharing characteristics with helicopters, this innovative aircraft design comes with limitations on the combination of flight altitude and velocity. When the distributed electric propulsion blows over the wing and dramatically improves the low-speed lift performance, it requires the same lift augmentation over the horizontal tailplane to ensure full controllability of the aircraft. As described in Section 6.7, this is done by two propellers accelerating the air over the horizontal tailplane. This, however, comes with the hazard of sudden loss of control authority in the event of loss of propellers or power on the horizontal tail. A critical event, as the lift augmentation will be used primarily in near-ground manoeuvres, and can turn fatal for the pilot if not properly mitigated. Combinations of height and velocity where the lift augmentation can be applied must be limited to ensure the mitigation of this hazard.

The first limit will be the velocity where above, any combination of height and velocity is possible. This is set equal to the minimum control speed for the aircraft without lift augmentation, ensuring the pilot will have full control authority over the aircraft in this regime, even in the event of engine failure. The minimum control speed can be found by following the same analysis as done in Section 6.7.1, in particular, equating Equation 6.45 with the un-augmented horizontal tail lift coefficient of $C_{L_h} = -1$, and a $C_{L_{A-h}}$ corresponding to the minimum control speed through the lift equation $C_{L_{A-h}} = W/(\frac{1}{2}\rho V_{MC}^2 S)$. Using the values of Section 8.1, the minimum control speed is equated to $V_{MC} = 24.0 m/s$.

The second limit is the upper height of the diagram. According to the Airplane Flying Handbook from the American FAA, the lowest altitude for safe training of stall recovery is set to 1500 above ground level [4]. It is assumed flying above this altitude is safe at any velocity, as a sudden stall will be recoverable by the pilot.

The third, and final, limit is the lower height of the diagram. This should be the altitude at which the lift augmentation can fail without being fatal. After implementing the procedures of Section 8.2.5, loss of control authority is not deemed a life-threatening hazard. In the Helicopter Flying Handbook from the American FAA, the assumption is done, in the context of helicopters, that an unrecoverable propeller stall above 50 ft is likely fatal. Combining this risk analysis for helicopter pilots, and considering the special procedures implemented for the aircraft, the lower limit of the diagram is set to 50 ft. When flying below this altitude the lift augmentation can be applied in a landing procedure without posing risk of significant harm to the pilot, as the pilot will be able to respond to loss of control and safely manoeuvre to the ground, as outlined in Section 8.2.5. An altitude of 50 ft also corresponds to the obstacle clearance needed during take-off and landing manoeuvres, thus providing a familiar datum for the application of the lift augmentation during approach for the pilots.

Considering these limitations, it is possible to find the height-velocity diagram as shown in Figure 8.6a. The diagram indicates the combination of velocities and altitudes for which no lift augmentation should be used. The way in which the conclusions of the velocity-height diagram affect the aircraft landing procedures is visualised in Figure 8.6b (please note that this figure is not to scale).

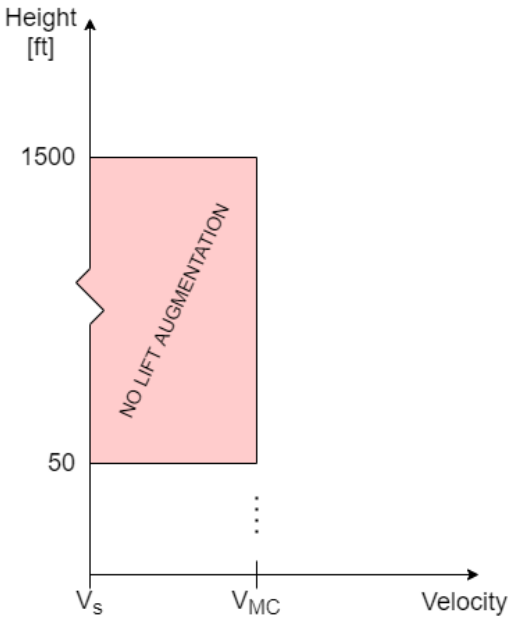

(a) The height-velocity diagram of the aircraft, showing the combination of height and velocity where lift augmentation is not possible.

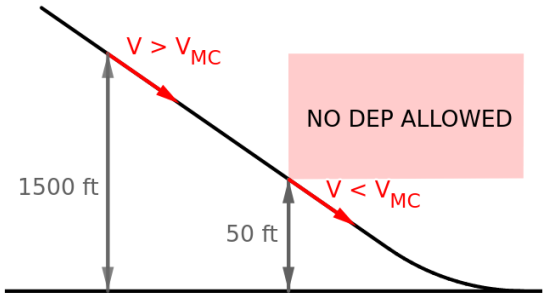

(b) The height-velocity diagram of the aircraft, with respect to the landing manoeuvre.

Figure 8.6: The height-velocity diagram visualised in different coordinate systems.

8.2.7. Loss of Power

For the loss of power, two possible scenarios have to be considered: the loss of the batteries and the loss of the generator. Due the redundant design of the aircraft, it is reasonable to claim that the two types of energy loss will not occur simultaneously (see Section 8.5 for further explanation). Thus, separate procedures are created for each scenario.

In case that the batteries fail, the effect on the aircraft operation is limited. The batteries have the prime purpose of supporting the ICE during the power surges experienced for take off and landing. The failure of the batteries means that, in order to provide the necessary energy, the ICE will have to be operated beyond its optimal conditions, which is undesirable in terms of noise and emissions. Furthermore, depending on how large of a fraction of the batteries fail, the ICE may not be able to produce all of the desired power. In that case, the takeoff and landing performance would decrease.

The scenario of the generator failing is more critical, and is similar to a single-engine bush plane losing its engine. However, the Twin Puffin has the advantage that, while the ICE is the primary power source, it is not the only one. The power stored in the batteries can be used to maintain a greater level of aircraft control during landing, as compared to the case where the aircraft would have to land completely without power and propulsion. The most critical moment at which the ICE could fail is thus the point during climb, when most of the energy stored in the batteries has been used up. However, in this case sufficient energy remains in the batteries to power the flight systems (so the sensors, the flight displays, and the communication system) during a gliding descent. During this descent, it will be possible to use the wing tip propellers in a windmilling configuration that recharges the batteries. While this will lead to an increase in drag and thus worsen the glide performance of the aircraft, the gain of generating energy that can then be used for a more controlled landing is of greater value.

8.2.8. Loss of Propellers

Conventional aircraft are severely put at risk by the scenario of losing an engine. For single engine aircraft, the loss of an engine means the loss of the only available propulsion source. For twin engine aircraft, an inoperative engine can lead to an aircraft that is difficult to control. Due to its distributed propulsion, the Twin Puffin outperforms other aircraft in this scenario.

For the Twin Puffin, two different cases have to be considered: the failure of one of the wing tip engines or the failure of multiple lift augmentation engines on one wing. The reason why these scenarios can be considered as separated and not occurring at the same time is that severe unanticipated consequences would have to arise for both the wing tip propellers and the lift augmentation propellers to be damaged simultaneously. Firstly, the two sets of propellers do not operate at the same time and are folded up when not in use (an exception is during the third phase of landing, but there the wing tip propellers are only used for windmilling). Thus, if the aircraft where to, for instance, fly into a flock of birds, the retracted propellers would be significantly less likely to be hit than the operating ones, and consequently only one set of engines would reasonably be expected to

fail. Secondly, the large spatial separation between the inboard-located lift augmentation engines and the wing tip engines means that damage sources such as bird flocks are significantly less likely to hit both propeller sets at the same time.

The engine placement so far from the aircraft centre of gravity means that in case that one of the wing tip engines fails, the aircraft has to handle a large yawing moment. The magnitude of this yawing moment is reduced by replacing the inoperative tip engine with the use of the lift augmentation propellers on the same wing. Though these propellers are not designed for high speeds and their operation will thus be less efficient, they are sufficient to generate the necessary thrust. Though the overall thrust level thus remains the same, the smaller moment arm of the lift augmentation engines on one wing, compared to the wing tip engine on the other wing, would mean that a yawing moment continues to persist. Furthermore, there would be differences in lift between the two wings, which makes the aircraft more complex to fly. To resolve these issues, it is decided that in case of either wing tip engine failing, both wings switch to being operated using only the lift augmentation engines.

In case that the lift augmentation engines on one wing fail during a phase where lift augmentation is necessary, only the engines on one wing shall be switched. Thus the wing with the broken lift augmentation engines will use only the tip engine, whereas the other wing will continue to use only the lift augmentation engines. This choice brings along several disadvantages such as the lift imbalance between the wings. This imbalance leads to both a rolling moment and an increase in drag on the wing with lift augmentation active. The asymmetric drag increase consequently increases the yawing moment. However, these moments can be overcome using a suitable combination of aircraft control surfaces and differential throttle. While this makes flying the aircraft more complicated, this complexity can be handled by the on board electronics and it is deemed that this additional complexity is justified by the advantages of maintaining lift augmentation for one wing. Retaining part of the increase in lift by keeping lift augmentation active for one wing will allow for better performance values during the critical phases of take off and landing.

8.3. Aircraft Performance

This section describes the main aircraft performance parameters of the *Twin Puffin*. The aircraft performance was analysed using the model and the procedures explained in Section 7.2. These methods were implemented above the classical mathematical techniques due to the unconventional nature of the design.

Stall speed The stall speed is calculated as described in Section 7.2.3. It is calculated for five scenarios: take-off at 0m, take-off at 2500ft ($= 762m$), cruise at 3000m, landing at 0 m and landing at 762 m. The take-off stall speed calculations are performed in take-off configuration (take-off flaps and distributed electric propulsion on, as is present from the end of the take-off roll to the start of climb) and found to be 14.05 m s^{-1} and 14.6 m s^{-1} respectively. During cruise, only the main engines are on, resulting in a stall speed of 24.3 m s^{-1} at the corresponding ISA density. During landing (full flaps and distributed electric propulsion on) the stall speed is 13.9 m s^{-1} at 0 m and 14.4 m s^{-1} at 762 m.

Rate of climb When using the optimal climb, from an emissions point of view, the power available is approximately 75 kW. This power comes from the ICE but also the batteries which are used during climb. With this power setting, a derated ”green” rate of climb of 2.16 m s^{-1} is achieved at an altitude of 2500 ft.

When increasing the power output to 100 kW, by increasing the generator RPM, the maximum rate of climb increases significantly. The maximum rate of climb in this configuration is 3.59 m s^{-1}. The pilot can opt for this climb procedure, it is however not recommended as it increases the green house emissions and the noise.

To estimate the climb performance of the aircraft under one engine inoperative condition the power available for one of the cruise engines is set to zero. This leads to a climb speed of 0.73 m s^{-1} with an estimated power available of 50 kW

Climb angle The climb angle at take-off with both cruise engines and DEP active is 7.11°. Without distributed electric propulsion on, the climb angle is 2.14°. The climb angle at take-off with one cruise engine inoperative and DEP active is 0.88°. Without DEP active, the aircraft is not able to maintain a positive climb angle.

Cruise velocity The cruise velocity of the aircraft is 54.9 m s^{-1} or 106.7 kts. The power required to maintain this velocity at cruise altitude is found as described in Section 7.2.3. The found power required is 53 kW at 3000 m altitude.

Cruise range The mission cruise range of the aircraft is 1247 km with 400 kg of payload and 106 kg of fuel. The ferry range of the aircraft is 2020 km with 100 kg of payload (mostly the pilot) and 130 kg of fuel. The ferry range can be increased further when the pilot is replaced by a remote piloting system. The range of the aircraft

is then 2234 km with 0 kg of payload and 130 kg of fuel. These results are also visually presented in the payload range diagram, Figure 8.7.

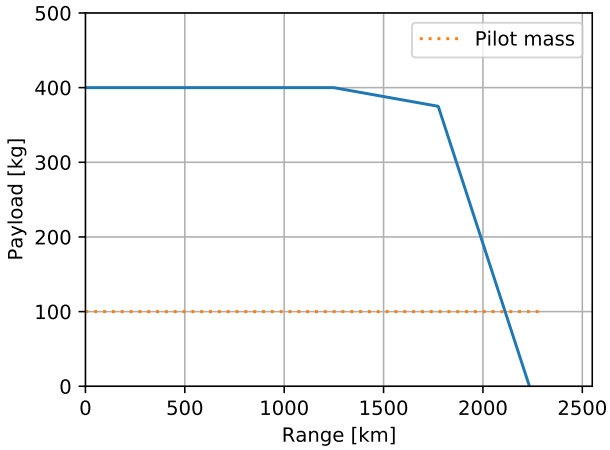

Figure 8.7: Payload-range diagram.

Take-off roll The take-off roll of the aircraft is estimated using the procedure described in Section 7.2.3. It is estimated at both sea level and at 762 m altitude, as per the requirements. The aircraft is capable of take-off after 61.0 m with a take-off run of 275.5 m. At 762 m altitude the aircraft is capable of take-off after 65.2 m with a take-off run of 282.7 m.

Landing roll The landing roll of the aircraft is estimated using the procedure described in Section 7.2.3. At sea level the landing roll without reverse thrust is 87.8 m and with a reverse thrust of 900N the landing roll becomes 20.86 m. The value of 900N, equivalent to a throttle of 20% was chosen as a conservative estimate of the available reverse thrust. At 2500 ft (=762 m) the landing roll becomes 94.5 m without reverse thrust, and with 900N of reverse thrust it becomes 23.4 m.

8.4. Aerodynamic Characteristics

This section outlines the key aerodynamic characteristics of the aircraft. First, the selected wing airfoil is presented, before the effects of lift augmentation are discussed. Then the drag values are explained and the results of the wing aerodynamic centre and moment analysis are provided.

8.4.1. Selected Airfoil

Using the method explained in Section 6.5, the airfoil selected for the wing is the USA 40-B. Being drag efficient across a wide range of lift coefficients, this airfoil has a design lift coefficient of 0.52. It is thus very close to the aimed for design lift coefficient of 0.469. Furthermore, the USA 40-B, which is displayed in Figure 8.8, is desirable for its geometric as well as its other aerodynamic characteristics.

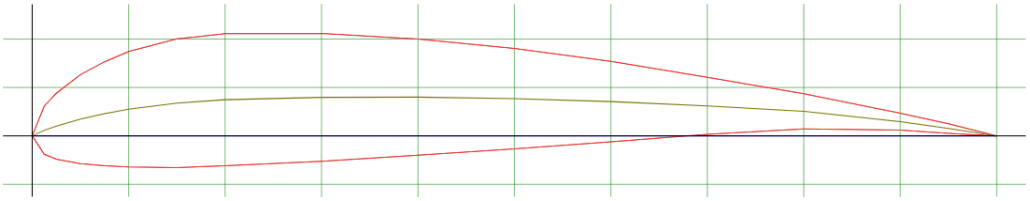

Figure 8.8: The USA 40-B airfoil selected for the wing of the Twin Puffin.

The rather high thickness to chord ratio of 13.6% makes the airfoil well performing in terms of structural performance: the high achievable moment of inertia lowers the required mass of components such as the wing spars. Furthermore, this thick airfoil accommodates the easy placement of the fuel tanks in the aircraft wings.

Aerodynamically, the USA 40-B is desirable because of its high maximum lift coefficient of 1.85. This subsequently facilitates high lift coefficients for the aircraft as a whole. Furthermore, the high stall angle of almost $15\,\mathrm{deg}$ is desirable as well. The airfoil zero lift angle of attack is $-5\,\mathrm{deg}$.

8.4.2. Lift Characteristics

Fundamental for the high STOL performance of the Twin Puffin is the generation of very high lift forces. The aircraft achieves this through the high maximum lift coefficient of the clean wing, the use of single slotted flaps across most of the wing trailing edge, and the use of lift augmentation. The achievable wing lift coefficients alongside the calculated lift slopes for the different aircraft configurations are presented in Table 8.4. Values for the augmented lift coefficients and lift slopes are provided for landing and takeoff at both sea level and an altitude of 2500 ft, the altitude from which the aircraft must still be able to take off and land within the set requirements. The lift slopes are expressed in terms of change in lift coefficient per radian angle of attack. Figure 8.9 presents the lift slope data in a visual way by showing sections of the lift curve for the different wing configurations (taking sea level as the reference altitude). As the precise plotting of the non-linear section at the end of the lift polar goes beyond the used models, this region is omitted from Figure 8.9.

Table 8.4: Achievable maximum lift coefficients for different aircraft configurations.

Configuration	*Maximum Lift Coefficient*	*Lift Slope*
Clean	1.67	4.99
Flaps in take off position	2.42	4.99
Flaps in landing position	2.61	4.99
Lift augmentation with flaps in take off position at sea level	5.32	9.86
Lift augmentation with flaps in take off position at 2500 ft	4.67	9.35
Lift augmentation with flaps in landing position at sea level	4.48	8.32
Lift augmentation with flaps in landing position at 2500 ft	3.98	7.97

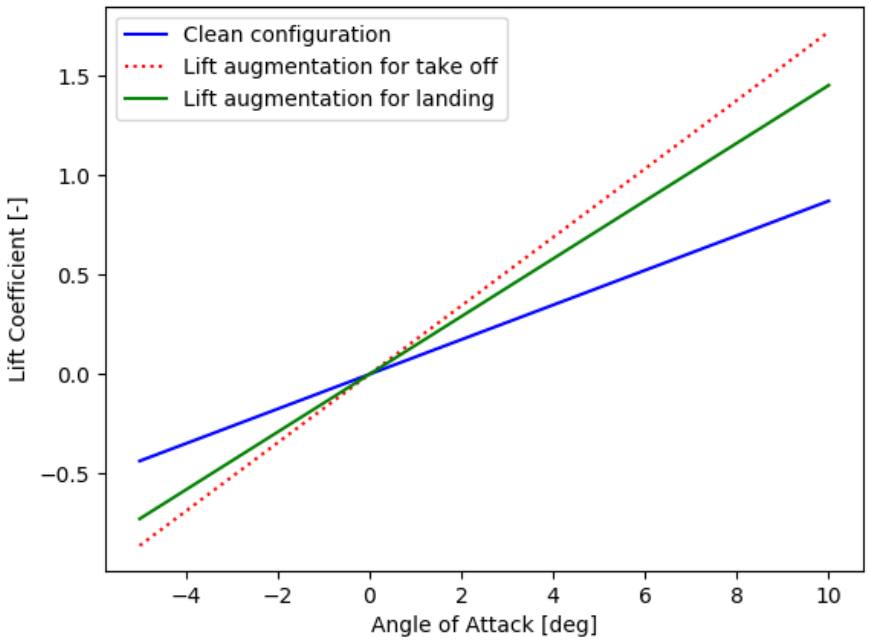

Figure 8.9: Wing lift curves for different configurations.

From Table 8.4 and Figure 8.9 it can be seen just how large the impact of the distributed propulsion along the wing leading edge is. The maximum achievable lift coefficient at sea level is more than twice of what is achievable without lift augmentation and even for landing at altitude the lift coefficient almost reaches four. These high lift coefficients are paramount to the high STOL performance of the aircraft and are only made possible by the innovative principle of distributed propulsion. An interesting observation to make for the values in Table 8.4 is that even though the flaps are not fully deployed for take off, the blown lift coefficients at take off are higher than the blown lift coefficients at landing. This is because of the higher thrust that is used for take off.

The precise way in which both the use of high lift devices and the distributed propulsion lift augmentation affect the lift generated by the wing are shown in Figure 8.10. Here a half wing and the lift distribution over it is depicted for three scenarios of interest: the clean wing, the wing with flaps fully deployed, and the wing with flaps fully deployed and lift augmentation active at sea level. The vertical dotted lines indicate the position of the high lift leading edge propellers. It must be noted that, in reality, the transition between blown and unblown sections of the wing will not be as harsh and is likely smoothened by aerodynamic effects that go beyond the scope of the employed lift augmentation model.

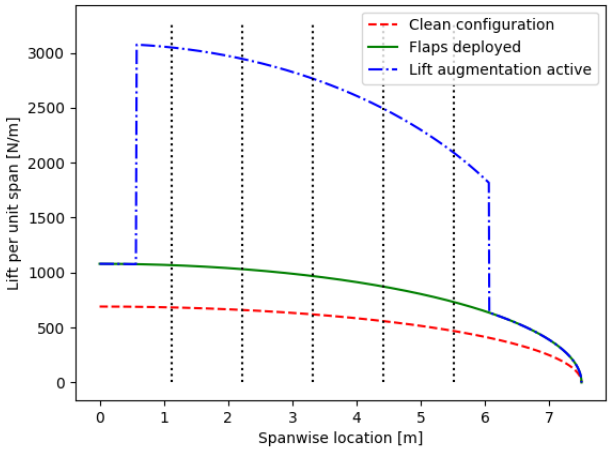

Figure 8.10: Half wing lift distribution for different high lift configurations.

8.4.3. Drag Characteristics

Relevant for the aircraft drag characteristics are the zero lift drag coefficient, the geometric and effective aspect ratio, the Oswald efficiency factor, and the cruise lift coefficient. These parameters are summarised in Table 8.5, which also provides the induced drag coefficient and the total drag coefficient for cruise.

Table 8.5: Key drag parameters for the Twin Puffin.

Parameter	*Value [-]*
Zero lift drag coefficient	0.0287
Geometric aspect ratio	8.00
Effective aspect ratio	8.91
Oswald efficiency factor	0.795
Cruise lift coefficient	0.469
Cruise induced drag coefficient	0.0099
Cruise total drag coefficient	0.0386

Several conclusions can be drawn from the values in Table 8.5. For one thing, the wing tip engines are an effective means of increasing the effective aspect ratio. During cruise, when the wing tip engines are used and efficient flying is most desired, an increase of 11.4 % is found for the effective aspect ratio. With 0.795 the Oswald efficiency is on the upper end of anticipated values. Together, the effective aspect ratio, the Oswald efficiency factor and the relatively low cruise lift coefficient lead to the low induced drag coefficient.

Based on the identified aircraft drag characteristics it is also possible to plot the aircraft drag polar. Figure 8.11 shows the plot that represents the aircraft lift and drag characteristics during cruise. As the used model of lift and drag is not able to predict reliably predict the drag polar at high lift coefficients, the diagram is limited to a range of low lift coefficients. The vertical dotted lines indicates the cruise condition.

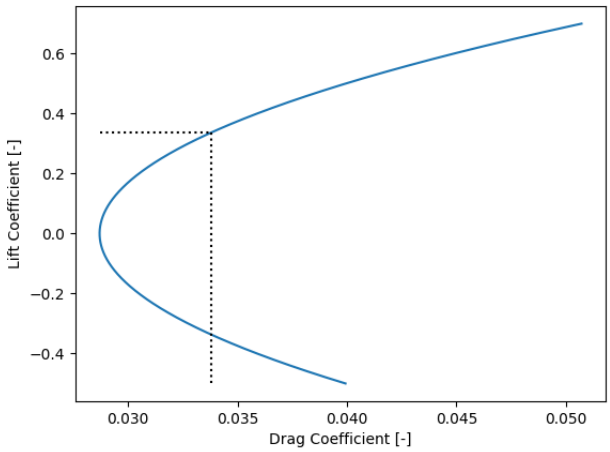

Figure 8.11: Drag polar for the aircraft.

Using the parameters in Table 8.5, a value of 12.16 is found for the cruise lift-over-drag ratio. While good, this value is not exceptionally high in comparison to reference aircraft of similar size. However, it must be noted that this is a result of the market-driven optimisation process. While other aircraft configurations where found to lead to lift-over-drag values of around 15, it appears that these configurations came with other disadvantages which made them less favourable than the final Twin Puffin configuration discussed here.

8.4.4. Aerodynamic Centre and Moments

As discussed in Section 6.5, the straight leading edge of the wing means that there is only negligible variation in the position of the aerodynamic centre as a function of the aircraft velocity. However, the aerodynamic centre shifts as a result of using flaps. Table 8.6 presents the location of the aerodynamic centre as well as the moment coefficient for the aircraft without the tail. The values are provided for three different wing configurations. As is expected, the use of flaps has a significant impact on the moment coefficient. For landing, where the flaps are deflected more than at takeoff, the effect is most pronounced. Note that the location of the aerodynamic centre is given as a percentage of the mean aerodynamic chord.

Table 8.6: Aerodynamic centre locations and wing moment coefficients.

Configuration	$(x/c)_{ac}$	$c_{m_{ac}}$
Clean	20.1	-0.0812
Take off	21.9	-0.319
Landing	22.3	-0.346

8.5. Propulsion and Energy Source Characteristics

As outlined in Section 6.6, the propulsion system is part of what makes this aircraft unique. Through the adoption of electric power and motors, it is possible to reduce noise as well as emissions while allowing the use of distributed propulsion. This state-of-the-art technology will allow the aircraft to achieve high performance STOL characteristics to allow operation in unprepared landing areas by increasing lift. Overall the propulsion system is a major system on the aircraft and the characteristics of this system will be outlined in this section. As it was decided during the design process of the final design, the *Twin Puffin* will have top level system comprising two energy sources, namely, diesel ICE and supportive lithium-ion NMC battery. Furthermore, with respect to the propulsion it will include ten distributed propulsion propellers and two 2 wing tip mounted cruise optimised propellers.

This section will cover comprehensively and in-detail how the subsystems of the propulsion and energy acquisition are integrated and what are their characteristics. It begins with presenting the power budget, which serves as an apt overview and introduction to the energy and propulsion systems. It is consequently followed by ICE, batteries and electric motors for both cruise and distributed propulsion.

However, prior to delving into details of the systems, firstly, a look at the bigger picture is in order. That is provided by the Table 8.3, which summarises the most important values obtained for the propulsion system.

Table 8.7: Final design values = Propulsion subsystem data.

Parameter	*Value*
Cruise propeller diameter	1.7 [m]
Distributed propulsion propeller diameter	1.1 [m]
Thrust of one of the high lift motors during landing	303.3 [N]
Thrust of each of the tail mounted propellers	48.2 [N]
Thrust of one of the high lift motors during take off	469.9 [N]
Power needed for cruise	52.7 [kW]
Battery mass	52.09 [kg]

8.5.1. Power Budget

Now the power that each of the aircraft elements need for they required functioning at each of the stages of the flight is looked at. This is shown in Table 8.8. The mission profile is here divided into six main phases, according to what is stated on Section 8.2.

It needs to be noted that the power required by the motors computed here comes from the thrust required at every phase. Moreover, it is assumed that the flight systems and the autopilot are constantly working, and hence constantly requiring the same amount of power. For the flight systems, the Garmin G1000[1] was used as reference, finding that it needs around 6.5 kW of power. On the other hand, the augmented autopilot system is divided into two main components: the actuators and the autopilot itself. It is estimated that the power required per actuator is of about 56 W, and the aircraft would require three of them (for the ailerons, horizontal stabiliser, and rudder); and the autopilot system is estimated to require around 100 W of power.

Table 8.8: Power required by the different aircraft components at every flight phase.

	Power Required per Flight Phase [kW]					
Aircraft Component	Take-off Phase I	Take-off Phase II	Climb	Cruise	Descent	Landing
Wing tip motors	32.2	0	99.9[2]	52.7	-8.7	30.5
High-lift motors	0	157.8	0	0	0	0
Tail motors	0	4.7	0	0	0	4.7
Flight systems[1]	6.5	6.5	6.5	6.5	6.5	6.5
Augmented autopilot	0.3	0.3	0.3	0.3	0.3	0.3
TOTAL	39.0	169.3	106.7	59.5	-1.9	42

Then, the power supplied by the different sources is also estimated, as shown in Table 8.9. When comparing it to the power required presented in Table 8.8, it can be observed that those values are lower than the power provided. However, this is due to the fact that the power needed is purely propulsive effective, meaning that no efficiencies have been included yet. This is why a margin between the required and supplied power values is required. Another thing to be noted is that, as explained in Section 8.2, the ICE is designed in order to provide the required power for cruise, and then the batteries add up to that value when needed. This will be mostly during take-off and climb, in case there are no exceptional circumstances occurring during the flight.

[1] URL `https://buy.garmin.com/en-US/US/p/6420` [cited 22 June 2021]
[2] Most critical, last phase of climb.

Table 8.9: Power supplied at every flight phase.

	Power Supplied per Flight Phase [kW]					
Aircraft Component	**Take-off Phase I**	**Take-off Phase II**	**Climb**	**Cruise**	**Descent**	**Landing**
Generator (ICE)	65	65	65	65	65	65
Batteries	0	110	50	0	0	0
Wing tip motors	0	0	0	0	8.7	0
TOTAL	65	175	115	65	73.7	65

8.5.2. Choice of the Appropriate ICE

The main source of power on the aircraft is the ICE generator which runs at peak efficiency throughout flight to produce a constant base power. During peak power operations such as take-off and climb, the ICE is helped by the battery to provide power levels larger than its output. In emergency situations the ICE should have, even if it's at sub-optimal efficiency and fuel consumption, reserves in terms of power to either charge the battery during flight, provide sufficient power to continue flying, or continue take-off operations at lower performance. This in combination with the requirement for the aircraft to be EASA certified to CS-23 means that a certified engine that runs on fuel that's most frequently available and produces at least sufficient cruise power, which would be 52.7 kW, at 60% throttle.

Based on these criteria and trying to minimise weight at the same time, from Table 6.7 the best option would be the Continental CD-155[1], as it shares the lowest weight weight the CD-135 but has a higher peak power at 114 kW. Additionally, the realistic power at FL100 and a 65% power setting is sufficient to meet the cruise power requirement including the inefficiencies of the generator, propeller, and electric motor, which are 90%, 86% found in Section 8.5.4, and 96% respectively.

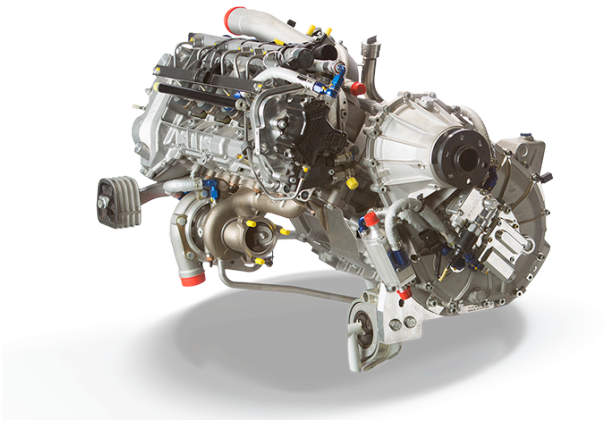

Figure 8.12: Final choice of ICE for power generation, the Continental CD-155.

Further design details relating to the engine include its positioning and packaging in the top of the fuselage as well as the constant power setting. In order to minimise the effect on the shape of the fuselage, specifically the bulbous engine cowling above the cabin. For this reason the engine will be rotated further, past the 40 degree angle it is already meant to be mounted at to further reduce its vertical footprint. Making this change will be unlikely to have major consequences on the continued EASA certification of the engine or drastically change it's design. What will likely have to be altered is the oil sump which is currently still at the bottom end of the engine, an additional oil pump or a different container may be necessary to grantee continued reliable oil supply to the engine even when it is laid flat.

8.5.3. Battery Characteristics

Based on the battery type analysis of Section 6.3.2 it can be determined that in order to have a battery that is both energy dense and on the safe side, while maintaining the benefits of lithium-ion battery types, the battery will be a lithium nickel manganese cobalt oxide based battery. As stated in Table 8.7 the battery will weigh 52.09 kg meaning that it will contain roughly 11.44 kW h of energy to provide the extra power required during climb. This can power the aircraft for 12 minutes during cruise when charged completely.

[1]URL `http://www.continental.aero/diesel/engines/cd155.aspx` [cited 22 June 2021]

8.5.4. Electric Motor Sizing

In sizing the electric motors, it was found that the existing family of motors by Emrax[2] are sufficient for use on both the tip, cruise optimised, and the high lift, low speed optimised, propellers. In both situations the motor will require a small planetary gear gearbox in order to step down the RPM range from slightly above the propeller operating speed to the ideal operating rotational speeds. The motors chosen for the task were the Emrax 188 for the high lift propellers, and the Emrax 108 for the cruise propellers. Their peak powers are 52 kW and 68 kW respectively which may look high for individual motor power, but in reality they may only be operated at lower power levels when aiming for the peak efficiency of 96%. Furthermore, they will also be air cooled further decreasing their peak power to avoid complexities effecting reliability and ease of maintenance by taking advantage of their exposed position for cooling. Overall, Table 8.10 summarises the characteristics of the two motors used for lift enhancement and cruise which are powered by one or both of the internal combustion engine and battery, Emrax 188[3] and Emrax 208[4].

Table 8.10: The chosen electric motors and their characteristics. The efficient continuous power was chosen such that the maximum efficiency of 96% is achieved. These performance values were derived using motor specific efficiency maps.

	Emrax 188	***Emrax 208***
Peak Power [kW]	52 at 6500 RPM	68 at 6000 RPM
Efficient Continuous Power [kW**]**	23 at 4000 RPM	33 at 4000 RPM
Weight [kg**]**	7.0	9.1
Dimensions ⌀ x W [m**]**	0.188 x 0.077	0.208 x 0.085
Type	Air cooled, high voltage, for distributed propulsion motors	Air cooled, high voltage, for wing tip motors
Motor Controller	AC power, specifically for the motor	AC power, specifically for the motor

8.5.5. Propeller Sizing

Firstly, the cruise propellers will be sized. These propellers will be sized based on the information given in Table 8.7, a blade number and rotational velocity based on the theory of Section 6.6. The cruise propeller will have the following characteristics described in this section, to which a JavaProp analysis was done to return the initial propeller sizing shape and performance data.

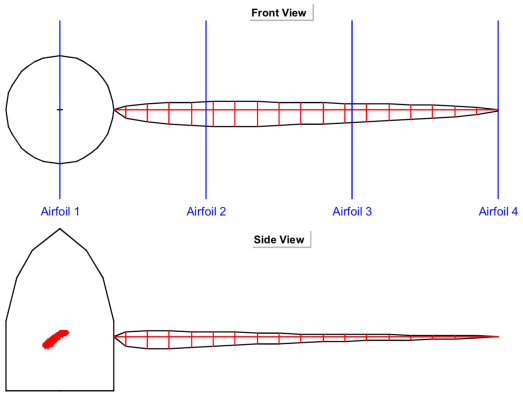

Figure 8.13: Main propeller geometry designed with Martin Hepperle's JavaProp.

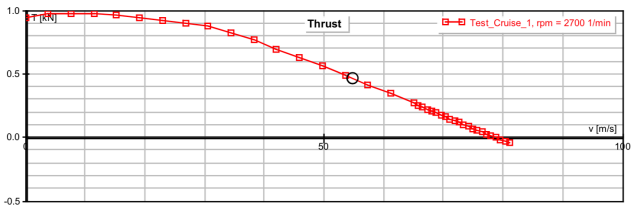

Figure 8.14: Thrust of the propeller due to the airspeed at constant pitch and RPM.

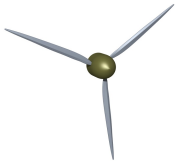

Figure 8.15: Side View of CAD Drawing of Cruise Propeller.

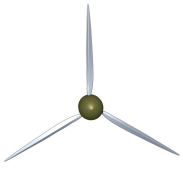

Figure 8.16: Front View of CAD Drawing of Cruise Propeller.

[2]URL https://emrax.com/e-motors/ [cited 22 June 2021
[3]URL https://emrax.com/e-motors/emrax-188/ [cited 22 June 2021]
[4]URL https://emrax.com/e-motors/emrax-208/ [cited 22 June 2021]

The cruise propellers are shown in side and in front view in Figure 8.15 and Figure 8.16 respectively. Based on the analysis done by the JavaProp, the propeller blade geometry from the Figure 8.13 was achieved. One observation that can be made initially is that the blade is rather thin. This is because the propeller was sized to

Second conclusion that can be made based on the JavaProp results, is the number of blades. It was determined that the cruise propellers will comprise three blades, as this provides a compromise between noise and performance. For lower number of blades, the noise is significantly higher however, the flow is more uniform and thus, the propulsion may be more efficient.

Another design decision that was done based on the results of the simulation concerns the pitch of the blades and the rotational velocity, RPM. It was decided that the rotational velocity as provided by the electric motor will be set to a constant value of 2700 RPM. However as the Figure 8.14 portrays, the thrust of the propeller is dependant on the airspeed velocity of the aircraft, thus in order to compensate that and preserve higher thrust for higher airspeed, with the same RPM, varying aerodynamics of the blades will be required. Hence, in order to achieve that the pitch of the propellers was decided to become a variable.

In addition, to the aforementioned features, the cruise propellers will also take advantage of their placement. By mounting them on the tips of the aircraft, certain desired aerodynamic properties can be achieved. As at the conventional wing tips (without winglets) severe tip vortices occur highly increasing the drag, the use of tip mounted propellers can counter this effect. The propellers are therefore designed to spin outboard, in counter direction to vortices at each wingtip.

In addition, the propellers offer a solution for a scenario when they can no longer provide thrust. Such scenario can occur during take-off where the cruise motors, energy produced and/or stored is not sufficient to spin the propellers so that they actually contribute to the thrust. In such case, if the propellers would work at their highest setting they would still only hinder the take-off as they would generate drag. For that reason, a design decision was made to enable them to become idle at such scenarios. The, they would generate negligent amount of drag and the energy that would be otherwise wasted can be preserved for other phases of the flight.

Lastly, the propellers will be also equipped with an option to generate power. At scenario of landing, the aircraft needs to slow down significantly. Thus, in order to collect some of the dissipated energy during air-braking, the propellers can perform a role of generators and work as windmills. It was found through a research that there exists a most efficient RPM for a given propeller for which it can generate the highest amount of power through windmilling. The relation was found to scale with the airspeed of the aircraft and the diameter of the propeller as given in the Equation 8.2. The J factor is a given constant and for the most efficient power production it needs to be equal to 1.6[57]. Thus, being able to evaluate those three parameters, the ω can be achieved and translated into RPM.

$$J = \frac{V_\infty}{\omega \cdot D} \tag{8.2}$$

Having determined the desired RPM for the highest amount of power, the efficiency that can be achieved is equal to 8.5%, which for the decent during landing phase amounts to 8kW of power. Arguably, this is a high value considering it is basically recycled from the dissipated energy.

Next, comes the initial design of the high lift, also referred to as distributed propulsion, propellers. These were sized and placed in accordance to the aerodynamic lift augmentation optimisation. In order to achieve the optimal airflow over the wing and reduce noise an odd number of blades is preferential for this propeller providing reduced noise levels. Additionally, a trade had to be made in number of propeller blades, which can reduce the radius required to output the same amount of power while decreasing noise and approach the assumption of an actuator disc, which was used for optimisation, more closely with more homogeneous exhaust flow behind the propeller. But more blades also have disadvantages. They increase complexity, cost, and maintenance while reducing reliability and availability of suitable off-the-shelf products [44]. For this reason it was decided that, as the propellers are highly specific in their use and they aren't required to perform at higher speeds, more blades may be used than on the cruise propeller but the number should stay realistic and odd; 5 bladed propellers were chosen.

The chord of the propeller was additionally designed to be slightly longer than usual due to the requirement for low speed performance of the propeller, the larger chord causes a lower propeller efficiency but this just means that the airspeed behind the propeller will be larger than normal and for this high lift propeller that is its main purpose to blow the wing surfaces[5]. Current predictions allow for a roughly 100% increase airspeed after the propeller as visible in Figure 8.18. In order to further decrease complexity, these propellers are also constant pitch, variable RPM propellers.

This is aided by the placement of the propeller. As seen in Figure 8.1, the propellers are very close to each other and placed in front of the wing. The reasoning behind this is that by slightly staggering the propellers, it is possible to have a continuously blown wing surface behind them without gaps. Additionally, placing them in

[5]URL `https://www.mh-aerotools.de/airfoils/jp_propeller_design.htm` [cited 22 June 2021]

front of the leading edge by the length of the propeller radius gives two advantages. Firstly, the distance allows the propellers to fold in with a softly spring loaded system when they are not in use. A hinge at the root of the propeller will allow it to fold onto the fairing containing the gearbox and electric motor to drastically reduce the drag that could occur from the propeller blades due to windmilling. Secondly, the distance in front of the leading edge allows the majority of the air layer at the wing surface to be accelerated to it's maximum propeller exit speed. This phenomena is visible in Figure 8.18 where at a distance of about half a meter behind the propeller the airspeed at the simplified wing shape is almost fully yellow, or at peak $\frac{V_a}{V}$ which is twice as fast as the free stream velocity.

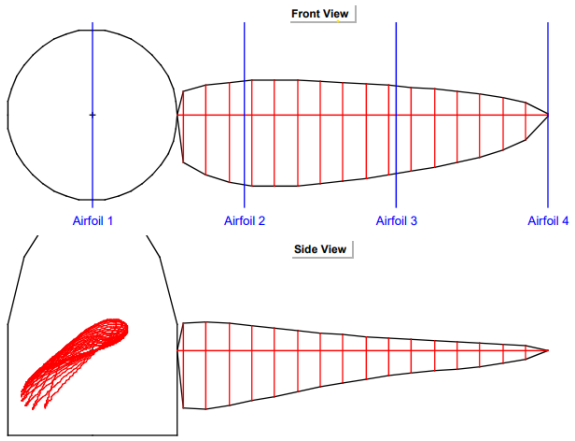

Figure 8.17: Preliminary high lift propeller geometry designed with Martin Hepperle's JavaProp.

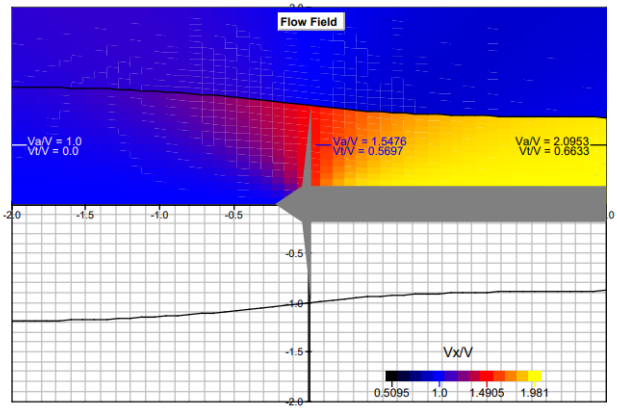

Figure 8.18: Preliminary high lift propeller flow diagram produced with Martin Hepperle's JavaProp.

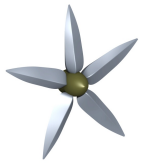

Figure 8.19: Side View of CAD Drawing of High Lift Propeller.

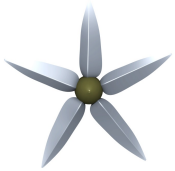

Figure 8.20: Front View of CAD Drawing of High Lift Propeller.

Lastly, two further, high lift propellers will also be placed on the ends of the horizontal tail section. These are meant to keep the airflow over the tail sufficient for controllability during STOL operations. These propellers will have the same rough geometry as those designed for the blowing of the wing in Figure 8.17. A side view and front view of the high lift propellers are shown in Figure 8.19 and in Figure 8.20 respectively.

8.6. Structural Characteristics

Following the methods in Chapter 6, this section shows the results for the final aircraft design. The structural analysis is based on the values found in Section 8.1, with a maximum load factor of $n = 6$. In Section 8.6.1, the properties of the chosen material are provided. Section 8.6.2 describes the shear flow acting on the fuselage. Section 8.6.3 provides the structural design and internal loading diagrams of the wing.

8.6.1. Material Properties

As described in Section 6.2.2, the rule of mixture is used to calculate the properties of the flax fibre composite, using a natural epoxy [6] as resin. The volume fraction of the fibres was taken to be 40%. Note that for calculations, the average of the two ultimate values of the property are taken.

Table 8.11: Material properties of flax fibre, epoxy and flax fibre composite.

Material	*Density* $[kgm^{-3}]$	*Young's Modulus* $[GPa]$	*Yield Stress* $[MPa]$
Flax fibre	$1.42 \cdot 10^3$ - $1.52 \cdot 10^3$	27-80	150-338
Epoxy	$1.18 \cdot 10^3$ - $1.24 \cdot 10^3$	2.83	57.9
Flax fibre composite	$1.314 \cdot 10^3$	22.9	130.7

[6] URL https://ecopoxy.cdn.prismic.io/ecopoxy/ba9819ca-f76e-40fe-838c-88b62db8954a_TDS-BioPoxy-36.pdf [cited 25 June 2021]

8.6.2. Fuselage Shear Flow Distribution

The shear flow through the fuselage gives insight in the internal stresses acting on the airframe. Figure 8.21 shows the calculated shear flow distribution around one transverse frame of the fuselage. The maximum shear flow appears along the vertical sections of the skin, and has an absolute value of $|q_s|_{max} = 2.26\text{N mm}^{-1}$.

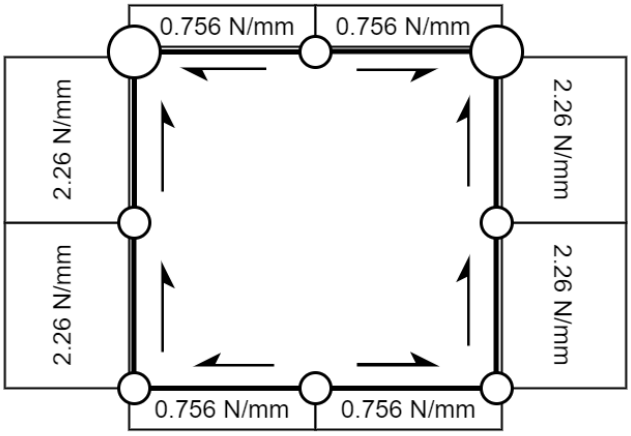

Figure 8.21: The calculated shear flow distribution around the idealised fuselage cross-section.

8.6.3. Wing Structure and Loading

The wing of the final design, as seen in Figure 8.22, features a central wing box built from two spars, connected by the wing skin at the top and bottom, highlighted in Figure 8.23. The first spar is placed at $0.20\bar{c}$ to allow for the electric motors of the propulsion system. The aft spar is placed at $0.55\bar{c}$ to allow for aircraft mobile surfaces. As the spars run across the fuselage, intersecting with the location of the ICE, the aft spar will compare its location to the dimensions of the ICE, and move aft if necessary. The volume between the two spars is $V_{wing} = (0.55 - 0.20)\bar{c} \cdot b/2 \cdot 0.13\bar{c} \approx 1200l$.

A wing-strut is in place, 3 m down the wing span, connecting the wing to the base of the fuselage and reducing the effective length of the wing to only the length beyond its attachment-point on the wing. The whole wing planform can be seen in Figure 8.22, featuring two spars, and visible control surfaces. The mobile surfaces are divided in two, where the inner-most surface is a single-slotted flap, and the outer-most surface a single-slotted flaperon, also providing roll control.

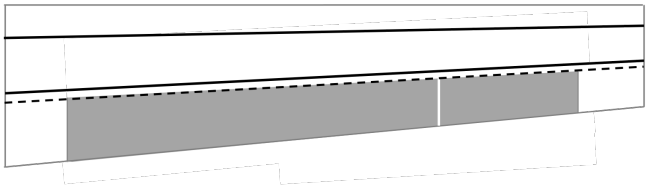

Figure 8.22: The wing planform of the final aircraft design.

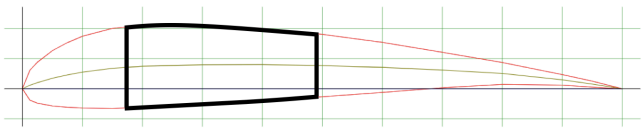

Figure 8.23: Wing cross-sectional area, showing the load-carrying wing box.

Following the values in Section 8.1, the augmented wing lift distribution in Figure 8.10 induces the internal shear force diagram shown in Figure 8.24, which in turn induces a bending moment diagram as seen in Figure 8.25. It is this internal moment diagram that is used in the calculation of the deflection of the wing. The wing is braced by a strut connecting the bottom of the fuselage to the wing, 3 m out from the wing-root, reducing the effective length of the wing.

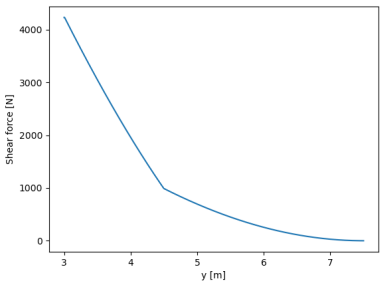

Figure 8.24: The internal shear force diagram of one wing of the final aircraft design, starting at the attachment point of the strut.

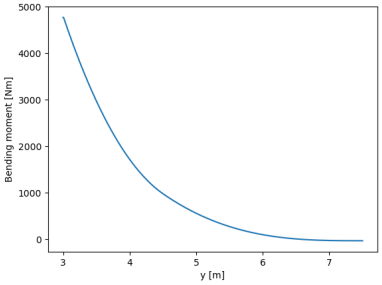

Figure 8.25: The internal bending moment diagram of one wing of the final aircraft design, starting at the attachment point of the strut.

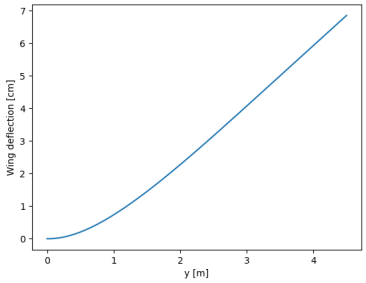

Figure 8.26: The deflection of the wing during level flight with lift augmentation, as a function of the span-wise location.

By combining the material properties in Section 8.6.1 with the geometric dimensions of the wing cross-section, the deflection of the wing can be calculated. The deflection of the wing is seen in Figure 8.26. The maximum deflection of the wing is $v_{max} = 6.9$cm.

8.7. Stability and Control Characteristics

Following the methods in Section 6.7, the stability and control are key aspects of this design, as the extreme STOL performance puts large requirements on the empennage performance. The following section highlights how the final aircraft design fulfils these requirements on stability and control, before expanding on the analysis by estimating dynamic characteristics of the aircraft.

8.7.1. Compliance with Static Stability

When an aircraft is statically stable, its response to a disturbance on its attitude is to counteract this change. This is the desired behaviour of a system, as then its control becomes easier for the pilot. The *Twin Puffin* was designed to be statically stable. This can be observed when looking back at Section 6.7, where the sizing of the vertical and horizontal tails are tackled. Three main types of static stability are discussed here: longitudinal, directional and lateral.

Longitudinal Static Stability The sizing of the horizontal stabiliser was performed in order to ensure that the aircraft is longitudinally statically stable. As explained in Section 6.7.1, the surface area of the horizontal tail is computed by using the centre of gravity range of the aircraft, together with the limits for stability and controllability of the aircraft (illustrated in a so-called scissor plot). In the initial iterations, an unrealistically large horizontal tail area was required to ensure controllability of the aircraft. This was because of the extremely low speeds, where the horizontal tail lost control authority, and would compensate by requiring a very large tail. To prevent this, the same lift augmentation applied to the main wing, and explained in Section 6.4, was applied to the empennage in the way of two propellers mounted in the intersection of the horizontal and vertical tails. This way, the empennage keeps control authority even at the critically low speeds.

With this, a sufficiently large horizontal stabiliser is obtained such that the aircraft can be trimmed at all points during flight, while designing for a not-too-large surface area, which would increase significantly the weight and drag of the empennage.

Directional Static Stability This type of static stability is ensured thanks to the design of the vertical tail, defined in Section 6.7.3. It was sized accounting for different scenarios that could compromise the stability of the aircraft (crosswind, stability, and one-engine-inoperative), where the static directional stability at cruise was the most critical, requiring the largest vertical tail area. This way, it is ensured that the bush plane is directionally statically stable throughout the whole flight, even in emergency situations such as when the loss of an engine occurs.

Lateral Static Stability Finally, static stability due to a roll angle disturbance is also ensured. This is basically inherent for all aircraft, due to the wing going down generating more lift because of the effective angle of attack increasing [36]. Hence, not many checks should be performed for this one, also realising that the large wingspan will cause the change to be counteracted in a smaller time, because of the larger moment created.

8.7.2. Dynamic Stability Analysis

While the aircraft is designed to be statically stable, it is also important to assess its response to dynamic motions. The assessment of dynamic stability at this stage is difficult as it often requires extensive testing and experimental data. Therefore, in this section, only a crude estimation is done that can only give initial hints to the dynamic responses of the aircraft.

The approach is to use certain selected methods from the ”USAF Stability and Control DATCOM”, further referred to as the DATCOM methods, to get an early estimation of the dynamic stability parameters [21]. Table 8.12 shows the parameter, a reference to the method used to estimate it, and the estimated value rounded to two decimal places. The subscripts n and l refer to yawing moment and rolling moment, respectively. The subscript β, r, p, α, and q refer to the sideslip angle, yaw-rate, roll-rate, angle of attack, and pitch rate, respectively.

Table 8.12: A selection of dynamic stability parameters, the associated section of the DATCOM method, and its estimated value.

Symbol	*DATCOM Section*	*Value [-]*
C_{Y_β}	5.6.1.1	-0.86
C_{l_β}	5.6.2.1	-0.02
C_{n_β}	5.6.3.1	0.13
C_{l_p}	7.4.2.2	-0.45
C_{l_r}	7.4.3.2	0.08
C_{n_r}	7.4.3.3	-0.29
C_{n_p}	7.4.2.3	-0.05
$C_{m_{\dot{\alpha}}}$	7.4.4.2	-2.46
C_{m_α}	4.5.2.1	-0.61
C_{m_q}	7.4.1.2	-6.05

Table 8.13: The computed eigenvalues per eigenmotion, following the stability parameters.

Eigenmotion	*Estimated eigenvalue*	*Period [s]*	*Time to half amplitude [s]*
Short period oscillation	-0.121 ±0.05j	4.34	0.20
Phugoid oscillation	-0.0004 ±0.011j	19.73	59.9
Spiral motion	0.0051	-	-4.69
Aperiodic roll	-0.405	-	0.059
Dutch roll	-0.551 ±0.827j	0.26	0.04

The spiral motion of the aircraft is characterised by a slow increase in roll angle, leading to increasingly larger sideslip, roll angle, and an eventual dive of the aircraft. Whilst critical, the motion is often slow and easily counter-acted by the pilot. The dutch roll is characterised by a rotational motion of the nose, caused by the interconnection of aircraft yaw and roll. A quicker motion, but also easily prevented by pilot intervention, or by mechanical systems such as yaw dampers [36].

The requirement for a stable spiral eigenmotion is given in Equation 8.3, derived from the linearised lateral equations of motion of an aircraft. The damping ratio of the dutch roll eigenmotion is derived from a simplification of the same equations of motion, and are given in Equation 8.4 [36]. The value of K_Z^2 is taken from literature for a comparable aircraft, namely the DHC-2 'Beaver', and is assumed as $K_Z^2 = 0.02$ [36, Tab. D-14]. The non-dimensional mass parameter is equated as $\mu_b = m/(\rho S b)$.

$$C_{l_\beta} C_{n_r} - C_{n_\beta} C_{l_r} > 0 \qquad (8.3)$$

$$\zeta = \frac{-C_{n_r}}{4\sqrt{2\mu_b K_Z^2 C_{n_\beta}}} \qquad (8.4)$$

Using the results given in Table 8.12, the aircraft is estimated to have slightly unstable spiral motion in the landing flight condition, while the dutch roll is a damped motion for all stages of the flight. It is clear that a relatively large value of C_{n_β}, following the requirements on static stability at very low speeds, causes this spiral instability. Because static stability is more critical than the dynamic stability, and because the unstable spiral eigenmotion is a very slow motion, a slight unstable spiral eigenmotion is deemed acceptable, as is the case also for other aircraft.

The values $C_{l_\beta} < 0$ and $C_{n_\beta} > 0$ also mean the direction of control surface deflection is equal to the direction of the deflection in the ultimate steady flight condition of a dynamic lateral motion [36]. This is a desirable control characteristic, making the aircraft easy and smooth to control, with no necessary back-and-forth input of the control stick to induce a motion.

Inspecting the eigenvalues in Table 8.13, it is clear the dutch roll is a heavily damped motion. This corresponds well with the analysis of slight spiral instability, and the large value of C_{n_β} is likely the reason for the large damping ratio. Also interesting to note is the negative value for the spiral motion time to half amplitude. It can be interpreted as the spiral motion doubling in amplitude every 4.7 seconds, a slow motion, as expected. The phugoid has a comfortable period of nearly 20 seconds, but a large time to half amplitude. It takes over three periods for the phugoid to half its amplitude, a slow damping which can be interesting to investigate further in the future design stages.

The final aircraft design looks to exhibit near-critical dynamic stability behaviour. Although the estimated characteristics are not unusual for similar aircraft, the influence of the driving vertical tail requirements on the dynamic stability, following the very low air speeds, should be investigated closely in further design iterations.

8.8. Electric Power Distribution

With the design of the Twin Puffin built upon the use of multiple electric engines, the reliable supply of power to the propulsion system is of utmost importance. Furthermore, for the aircraft to function properly, power must also be provided to the aircraft flight systems. Shown in Figure 8.27, the power distribution diagram divides the system into three subsystems: the power generation and management, the propulsion, and the flight systems. The meaning of the used colours as well as the design of the power distribution for each of these subsystems is explained in greater detail below.

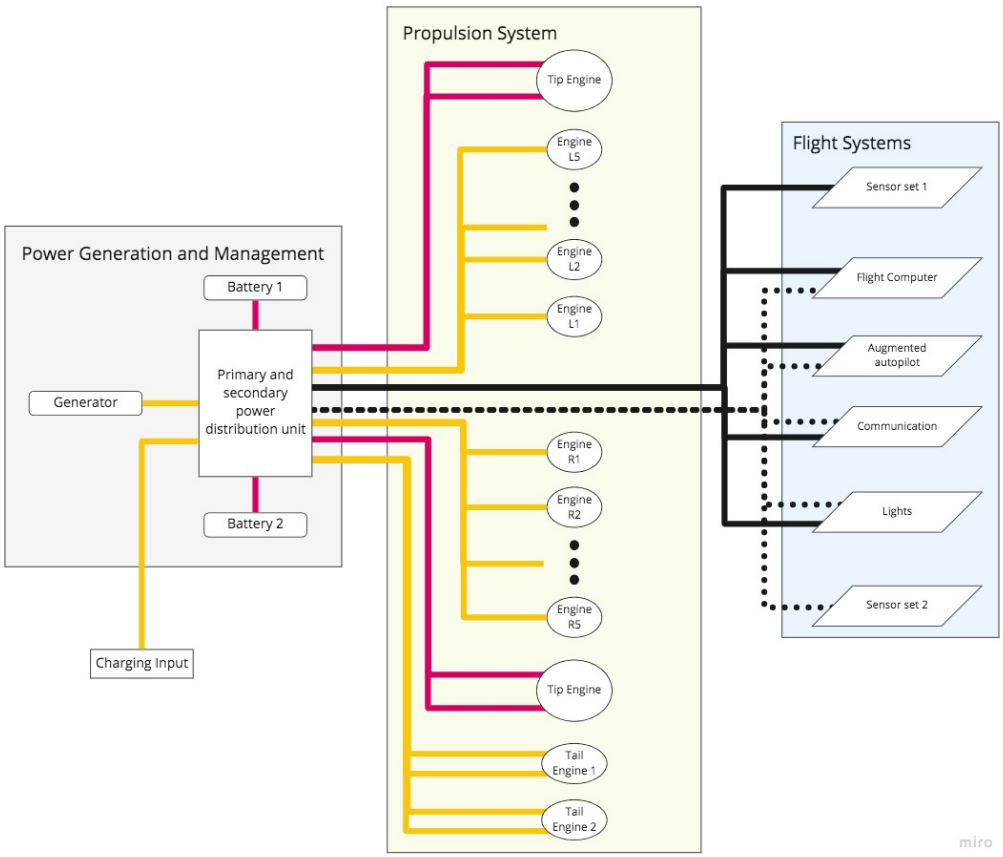

Figure 8.27: Power distribution diagram.

In the diagram, yellow lines are used to indicate those electric connections that are used for the uni-directional flow of high power, Red lines show connections intended to facilitate the flow of high power in both directions, and black lines (both dotted and continuous) represent low power flow in one direction.

8.8.1. Power generation and management

The first part of Figure 8.27 is the power generation and management. Both the fossil fuel generator and external charging (which is only possible while the aircraft is on the ground) act as primary sources of power. These power flows are directed into the box representing the primary and secondary power distribution units. The reason why both a primary and secondary power distribution system are included is for redundancy. Though it comes with notable additional mass and cost, it is deemed that this level of redundancy is required for the power distribution system as it is such a crucial component: if the power distribution system were to fail completely, neither the power from the batteries, nor the power from the generator can be accessed and the aircraft is left in a fully unpowered state.

From the (either primary or secondary) power distribution system, the electric power is directed towards where it is necessary. During external charging on the ground, when the generator produces more energy than necessary, or when the wing tip propellers are used in a windmilling power-generating configuration, the power distribution system diverts energy into the batteries. During takeoff and landing, when additional power is required, power flows back out of the batteries. When any part of the propulsion system is in use, the power

distribution system directs high power towards the relevant electric engines. The system furthermore constantly passes low power electricity to the aircraft flight systems.

The reason why the power generation and management system includes two batteries rather than a single one is for the sake of redundancy. In case that an individual battery cell fails, for instance by catching fire, the splitting of the batteries means that half of the stored power supply remains unaffected. As the battery packs are themselves composed of multiple, easily divided cells, the additional reliability from using two batteries comes at only a very small increase in mass, cost, and complexity.

8.8.2. Propulsion System

The use of electric engines means that the propulsion system is the primary consumer of electric power on board the Twin Puffin. Through a set of high power lines, energy is supplied to each engine individually. Though, for the sake of simplicity, the engine high power lines are mostly shown as one bundled connection in Figure 8.27, in reality the connections run through separate wires such that no single point of failure can lead to the loss of large parts of the propulsion system at once. Furthermore, the use of separate wires means that already at the centralised power distribution system, each engine can be set to a different power setting and thus be throttled individually.

Due to their great importance throughout the majority of the mission profile, additional redundancy is desired for the large wingtip cruise engines, which are thus connected to the power distribution unit using a redundant double connection. The same redundancy is applied to the lift augmentation engines on the vertical tail. As their failure could potentially lead to a loss of controllability and an aircraft crash. Due to the high number of leading edge lift augmentation propellers, it has been decided that wiring redundancy is not necessary for them: in case the connection to one engine fails, a sufficiently large number of engines remains to continue safe operations.

The final point of interest regarding the power supply of the propulsion system is that the high power connections to the wing tip engines are specifically designed in such a way that they facilitate the two-way-flow of power. During certain flight phases, the big wingtip engines are used in a wind-milling configuration that generates power and can be used to recharge the aircraft batteries. Thus, it is necessary to ensure that power can efficiently flow from these engines back to the power distribution units.

8.8.3. Flight Systems

Though relative to the propulsion system the flight systems require only a low level of power, the reliable provision of this power is essential. When the aircraft is manually piloted, the powered flight systems are necessary in guaranteeing proper aircraft operations. When using remote piloting, failure of the power provision to the flight systems is very likely to lead to the aircraft crashing.

For the flight systems, the balance between reliability and efficient design is found by using two separate central connections that carry the power from the power distribution units to the flight systems. For the sake of clarity, Figure 8.27 displays one of these connections using dotted lines, the other using continues lines. The first central wire branches off to serve sensor set one and all other flight system components apart from sensor set two. The second central wire mirrors this distribution in that it serves all components apart from sensor set one. This wire setup means that, apart from the two sensor sets, no component of the flight systems is put at risk by a single point of failure. For the sensors, only one connection is used per set as the inclusion of two sets already results in sufficient redundancy. The flight computer and augmented autopilot are provided with a redundant backup power connection as their failure would make flying less optimal in case of manual piloting, and would lead to the aircraft crashing in case of remote piloting. Redundant power supply is also justified for the communications system, as here a loss of power would lead to potential safety risks in case of manual piloting, and would lead to aircraft loss in case of remote piloting. Finally, the lights too are deemed to be sufficiently important to have a redundant power supply, as flying during the night or in bad weather without proper lighting would be a dangerous scenario for both those on board the plane and for others.

8.9. Hardware and Data Flows

This section examines the designed interactions between the different hardware components of the aircraft. Thus, it explains which data flows exist, which information is passed on in which ways, and how all of these flows interact to ensure the functioning of the Twin Puffin as a whole. Shown in Figure 8.28, the hardware and data diagram facilitates both the option of a pilot being present on board, and the option of the aircraft being remotely piloted. First, the use of symbols and colours shall be explained, before a discussion of each of the three main blocks of the system is presented. Finally, a note will be made on reliability.

In the diagram, the blocks represent the different physical components (mostly the hardware) and the arrows indicate data flows. The text in the diagram indicates which components are shown and which data is passed on from one component to another. For the physical components, rotated squares are used for the primary decision making agents, so the pilot and externally located remote pilot. Rounded rectangles represent sensors,

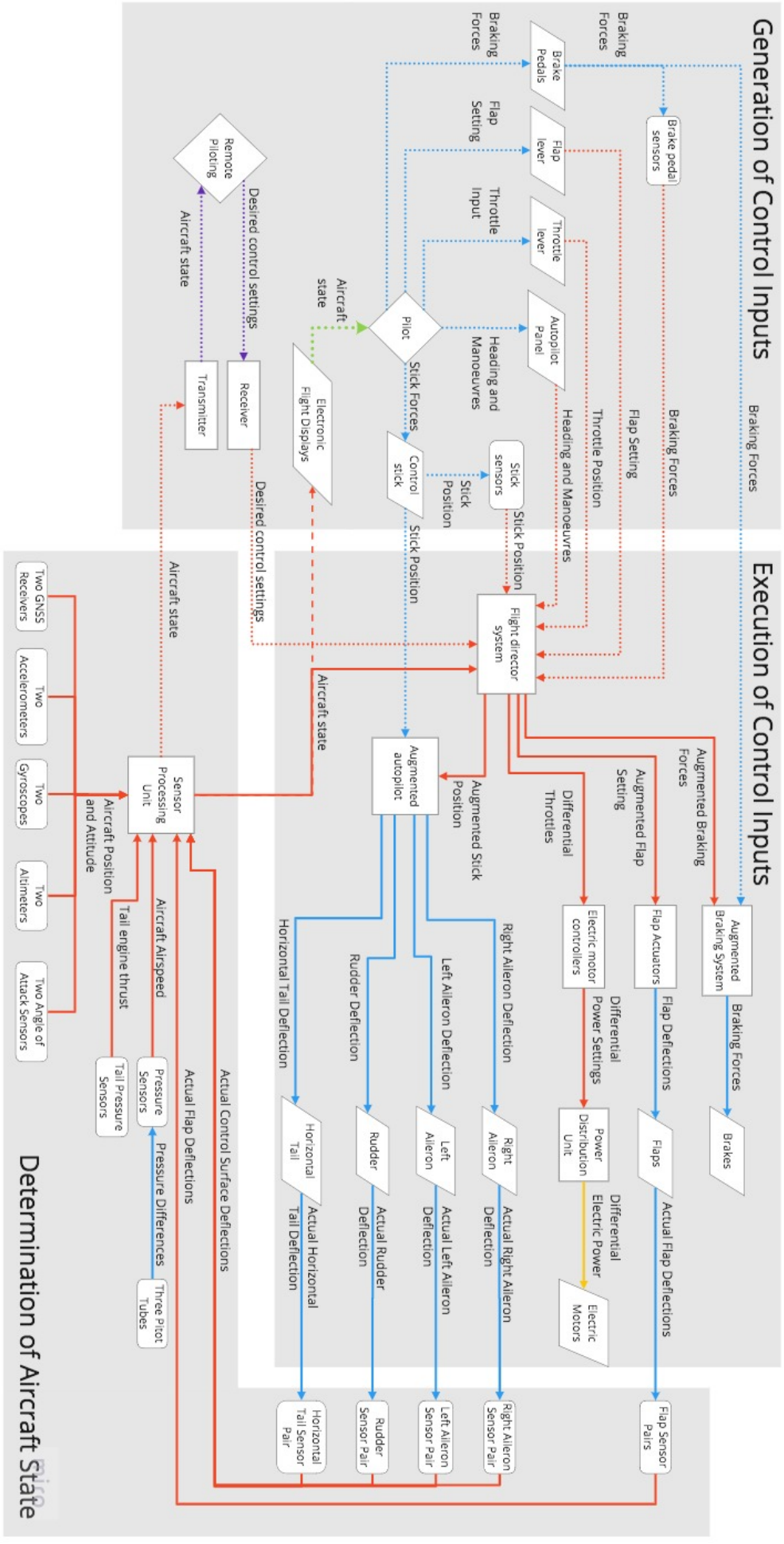

Figure 8.28: Hardware and data flows diagram.

rectangles indicate electronic components, and rhombuses are used for all other hardware. The direction of the arrows linking the hardware blocks shows the direction of the data flow. Predominantly used for the data flow are blue and red arrows. Blue arrows represent the physical transfer of data, for instance through forces applied by one component on another. Red arrows indicate that data is passed on as an electronic signal. Furthermore there are purple arrows, indicating the data flow via telecommunication signals, a yellow arrow representing that data is passed on through the level of electric power, and a green arrow symbolising a visual transfer of information. In addition to differing in colour, the arrows also differ in type: whereas continuous lines indicate a data flow that is always present, the presence of the dotted connections depends on which type of piloting is used.

8.9.1. Generation of Control Inputs

Block one of the hardware and data flow diagram is predominantly focused on the generation and communication of control inputs. First considering the case of the aircraft being controlled by an on board pilot, one sees that the pilot can generate five different data flows: the stick forces, the desired heading and manoeuvres, the throttle input, the flap setting, and the braking forces.

The stick forces, which here include the forces exerted on the pedals, are the way in which the pilot inputs the desired deflections for the aircraft control surfaces. These forces are passed on via physical connections to two places: the augmented autopilot (which is discussed further in block two) and the stick force sensors, which convert the physical data into an electric signal. An almost identical flow is seen for the braking forces, used to slow down the aircraft on the ground after landing. Here too, the physical forces are directly passed on to the destination system (the braking system) as well as to sensors converting them into electronic data flows.

The flap, throttle, and autopilot setting allow the pilot to use high lift devices, change the thrust provided by the engines, and set the aircraft on a course to follow a certain heading or execute specific manoeuvres. For these data flows, one sees that no additional sensors are needed. This is because the input hardware, so the flap lever, the throttle lever, and the autopilot panel, directly convert the input data into electronic signals. Unlike with the stick and braking forces, here there is no need to pass on the physical data flows, i.e. the force used to move a lever or press a button, to any other piece of hardware. For the sake of simplicity, the diagram only indicates one throttle lever. However, for the pilot flying the aircraft, two levers will be available, one to adjust the throttle of the wing tip cruise engines, one to adjust the throttle of the inboard lift augmentation engines. The data flow in the diagram encompasses the combined information from these two throttle inputs.

All the inputs that can be generated by an on board pilot can also originate from a remote pilot. In this case, all of the data about the desired aircraft control settings is transmitted to the aircraft via telecommunication signals. A receiver then directly translates this data into electrical signals.

For both the options of manual and remote piloting, the decision-making pilot must be provided with certain information on which they can base their choice of inputs. In the on board pilot scenario, the aircraft state is communicated visually via the flight displays in the cockpit. In case of remote piloting, the aircraft state is communicated to the external pilot via a transmitter.

8.9.2. Execution of Control Inputs

The second block of Figure 8.28 is concerned with the execution of the control inputs generated by the relevant pilot. All of the electronic data flows discussed for the first block flow directly into the flight director system, the main on board computer of the Twin Puffin. The flight director system uses the pilot inputs in combination with the aircraft state to determine which combination of braking, flap setting, individualised throttle, and control surface deflections provides the optimum way of executing the wishes of the pilot. This is one of the key advantages of distributed propulsion: rather than viewing aircraft propulsion and aircraft control as two separate domains, the system is able to combine the two in a way that maximises how efficient and pleasant the aircraft flies. With the optimum combination of control actions determined, the flight director system passes on electronic data to four different pieces of hardware.

The augmented autopilot, which is defined as discussed in Section 6.9, takes both the electronic signal from the flight director system and the physical forces from the pilot (if one is present) as data inputs. Using the electric motors of the augmented autopilot, the physical forces are decreased or increased before being passed on to the four different control surfaces: the pair of ailerons, the rudder, and the horizontal tail. Characterising the augmented autopilot system is that these data flows to the control surfaces are transferred using a physical system of struts and cables that directly push and pull on the control surfaces without the need for any additional actuators. In case of remote piloting, the blue dotted arrow flowing into the augmented autopilot is non-existing and all control forces are generated, rather than just adjusted, by the system.

Looking at the data flows concerned with the braking of the aircraft, one finds a system that is very similar to the one presented for the aircraft control surfaces. Both the physical braking forces applied by the pilot (in case that one is on board) and the augmentation signal from the flight director system flow into the augmented braking system, which adjusts or creates the physical forces as necessary. These physical forces then actuate

the breaks, slowing the aircraft down.

Both the flap actuators and the electric motor controllers are different from the augmented autopilot and braking systems in that they only take electronic signals but no physical forces as inputs. The flap actuators directly convert this electronic signal into a physical force that moves the flaps into the desired position. The electric motor controllers, however, take the electronic information about the desired differential throttles and turn it into a different electronic signal. They determine which specific power setting is required for each of the many aircraft engines and pass this information on to the power distribution unit previously discussed for Figure 8.27. Based on this data, the power distribution unit then provides different levels of power to the different engines. While also based on the flow of electricity, this transfer of data is of a different nature to the transfers indicated using the otherwise used red arrows.

8.9.3. Determination of Aircraft State

The final block of the hardware and data flow diagram focuses on the determination of the aircraft state. As seen in the discussion of the first two blocks, the information about the aircraft state is a necessary input on which the pilot (for wither piloting option) as well as the flight director system base their actions. In addition to the stick and brake pedal sensors discussed in block one, there are two groups of sensors employed for the Twin Puffin. These two groups relate to the different parameters measured by the sensors and should not be confused with the two sensor ”sets” discussed for the power distribution diagram described in Section 8.8. There the number two referred to the double inclusion of the same type of sensor, a concept that is seen here for each of the sensors in the two groups.

The first group of sensors, located on the right edge of Figure 8.28, is used to measure the actual deflections of the different mobile surfaces. In theory these actual deflections should simply equal those input by the augmented autopilot and the flap actuators. In reality, however, varying friction levels, the jamming of actuators or cables, or changes in aerodynamic forces are likely to lead to differences between the expected and anticipated deflection values. Determining these differences using sensors is essential if, as is desired, an electronic feedback loop is to be used to support the piloting of the aircraft.

The other group of sensors, which is found in the bottom part of the diagram, measure the aircraft position, attitude, and airspeed. For position and attitude, a standard set of sensors is used to receive GNSS signals, measure linear and angular acceleration, and determine altitude and angle of attack. For the airspeed, classic pitot tubes are used, which output a physical data flow of pressure differences that is then translated into electrical signals by a set of pressure sensors. As the pitot tubes must unavoiably be placed on the outside of the aircraft, they are more likely to be damaged or affected by dirt. Thus, instead of using a pair of sensors, as is the case for all other measurements, a total of three pitot tubes and corresponding pressure sensor sets shall be used.

Another sensor pair shown in the bottom part of Figure 8.28 are the tail pressure sensors. These are essential as they measure whether or not the engines on the aircraft horizontal tail are active. Thereby, they allow the system to detect a possible failure of the horizontal tail lift augmentation, a scenario in which the stall prevention protocol discussed in Section 8.2.5 must immediately come into action.

The outputs of all sensors are passed on as electronic data flows to the sensor processing unit. Here, a computer system is used to filter the received data for noise and outliers before combining the results into one coherent data set about the aircraft state. With this data then being passed on to the on board or remote pilot as well as the flight director system, the loop between all three blocks of the diagram is closed.

8.9.4. Reliability

As explained in the design methodology of Section 6.9, safe and reliable operation of the aircraft electronic systems is of utmost importance. For the sake of simplicity, not all of these reliability measures are displayed in Figure 8.28. Thus, the main steps taken to ensure this reliability shall be presented here.

Firstly, all data flows are transferred via a redundant pair of connections. This primarily holds for the electric signal data flows, where two wires are used in parallel, but is also true for physical data transmitters such as the cables used for the actuation of the control surfaces. To avoid the design being over-redundant and thus heavier and more expensive than is necessary, an exception from the principal of double connections are the sensors. Here, the use of two sensors for each measurement of interest is already sufficiently redundant such that one connection per sensor is sufficiently reliable.

Secondly, redundancy is included in all three main computing units: the flight director system, the electric motor controllers, and the sensor processing unit. Here, both the hardware and the software shall be designed in such a way that the overall functioning of the systems is protected against failures. Amongst other things, this means that the systems have to be able to detect and handle faulty input data. For the sensor processing unit, redundancy is further increased by using the ”CAN bus” protocol, which allows for the failure of individual components without risking the functioning of the system as a whole.

Another aspect making the operation of the Twin Puffin more reliable is that the use of the augmented

autopilot system continues to allow for aircraft operations in case that the power supply to the augmented autopilot or to the flight director system is lost. Given an on board pilot is present, the blue arrow connecting the control stick to the augmented autopilot means that the pilot is still able to deflect the control surfaces as desired (provided that a sufficient level of force is applied). However, it must be considered that this redundancy does not hold for the case of remote piloting: then the failure of the flight director system or the augmented autopilot would mean that the aircraft can no longer be controlled by the remote pilot.

To further increase the safety of operations when a pilot is present on board of the aircraft, two emergency switches shall be included. If need be, these will allow the pilot to manually override the augmented autopilot system and the energy supply to the engines. This means that if a software error or some other kind of failure should occur, the systems can manually be turned off. Such an intervention may be necessary if, for example, software errors cause the augmented autopilot to jam or the engines to provide unsafe levels of thrust.

Finally, to increase the reliability of flying the aircraft using remote piloting, redundancy is important for both the receiver and the transmitter. If the receiver where to fail, the remote pilot could no longer communicate the desired control settings to the flight director system. If the transmitter where to fail, the remote pilot would no longer receive the necessary information about the aircraft state. In both cases, failure would most likely lead to the aircraft crashing. Thus, including a both a backup receiver and a backup transmitter is deemed to be necessary.

With all of the reliability measures outlined here, the aircraft is sufficiently redundant that safe operation of the Twin Puffin can be guaranteed in all reasonably anticipated flight scenarios.

8.10. Aircraft Software

The non-standard features of the aircraft and corresponding functional flows (to be implemented in software) are presented in this subsection. Figure 8.29 shows the behaviour of the systems during the different flight phases, Figure 8.30 shows the special features that are enabled by the design of the aircraft, and Figure 8.31 shows how the aircraft is to react to different failures.

Take-off The take-off procedure, as outlined in the top of Figure 8.29, starts with generator startup. Then, depending on the type of take-off, a certain amount of energy is ensured to be in the battery, if necessary this involves recharging the batteries using the generator. Then, the aircraft can take-off, following the procedure described in Section 7.2. Once an altitude of 100m is reached, the distributed propulsion is turned off, turning on the main engines. Until cruise altitude is reached, the batteries provide the power that the generator cannot (as it always runs at its fixed power level).

Cruise During cruise, the generator is chosen to provide the required power while running at its maximum efficiency. This means that any excess power it produces will be used to charge the batteries. When the batteries are charged, and there is still excess power, the engine will be throttled down. This means it will no longer be running at its maximum efficiency, but will still use less fuel.

Landing During the landing, the interplay between energy and thrust needs to be managed. During descent, the main engines can be used as generator (at a very low efficiency), which can be used to charge the batteries. Once an altitude of 100m is reached, the distributed propulsion is turned on, so that the aircraft can start slowing down (while staying out of the height-velocity diagram explained in Section 8.2.6). Once the aircraft touches down, depending on the landing distance needed, reverse thrust can be turned on, on top of the brakes.

Stall If a stall is nearing, the aircraft can take mediating steps to insure passenger safety. After producing an audible and visual stall warning, the aircraft will turn on the tail propellers to increase controllability (which can also be done manually). If this is insufficient, the aircraft increase thrust (potentially turning on more engines) which creates a pitch down moment.

Remote Piloting The aircraft can be remotely piloted, through a process explained at the top of Figure 8.30. After setting up the aircraft (by a human), a remote connection can be initiated. When this happens, warning sounds and lights are produced. The emergency shutoff buttons are also activated. Then, the remote operator obtains control of the aircraft. The signals from the remote user go through an autopilot or stabilisation software, after which the actuation is performed.

Yaw stabilisation/rudder augmentation As the propellers are distributed along the leading edge of the wing, their thrust can be distributed to produce yawing moments. The throttle levers set the total value of thrust that is to be delivered by the engines, which can be distributed asymmetrically when a yawing moment is required. This yawing moment can be created to stabilise the aircraft (electric engines can react very quickly, and are

thus suitable actuators for stabilisation) or increase the total possible yawing moment for more aggressive manoeuvres (hereby augmenting the rudder).

Centre of gravity sensing As the aircraft has shock-absorbers (needed for the aircraft and passengers to overcome 5g landing), these can be used as force sensors (by measuring the distance the springs are deflected using a simple laser). With a sensor on each landing gear, the position of the centre of gravity can be estimated, as well as the total aircraft weight.

Tip-over protection A disadvantage of conventional taildraggers is the risk of a tip-over during landing or other ground manoeuvres. However, reverse thrust can also be used to pitch the aircraft back up. When the aircraft is on the ground, and the accelerometer measures a pitch angle of $> -10deg$, reverse thrust is activated.

Minimum noise take-off In urban airports, aircraft noise is of utmost importance, much more than take-off distance. Therefore, any further reductions in noise are helpful. For this, a low-noise take-off procedure is provided. It works by spinning up all engines, which can therefore rotate slower since each single engine needs to produce less thrust, dramatically reducing noise.

Bird strike A partial loss of power, for example a bird strike, can result in performance degradation. The top of Figure 8.31 shows the troubleshooting process and corresponding mitigating steps.

Loss of electrical systems When all electrical power is lost, the aircraft is designed to be able to perform a safe emergency landing. This would only occur if the generator and both independent batteries fail, or both redundant power system, and is thus much less likely than in a conventional general aviation aircraft. In the event of the total power loss, the augmented autopilot clutches should automatically detach. If this fails, the coupling can be manually overpowered. Hereby, full manual control is always available to the pilot in case of power failure. During this emergency, the aircraft will attempt to recover power and find an emergency landing strip that suits the reduced STOL capabilities of the aircraft.

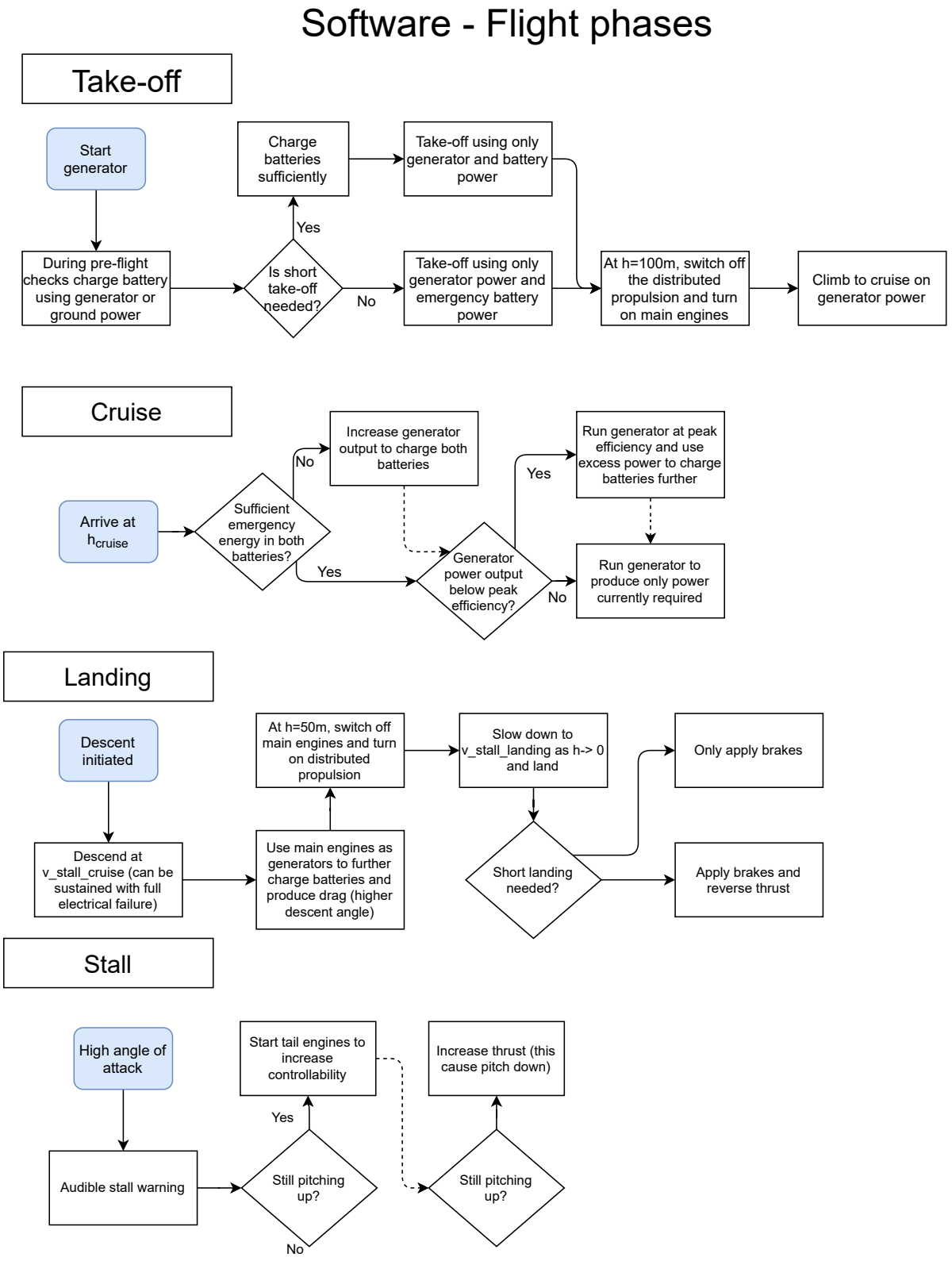

Figure 8.29: Software function flow - Flight phases.

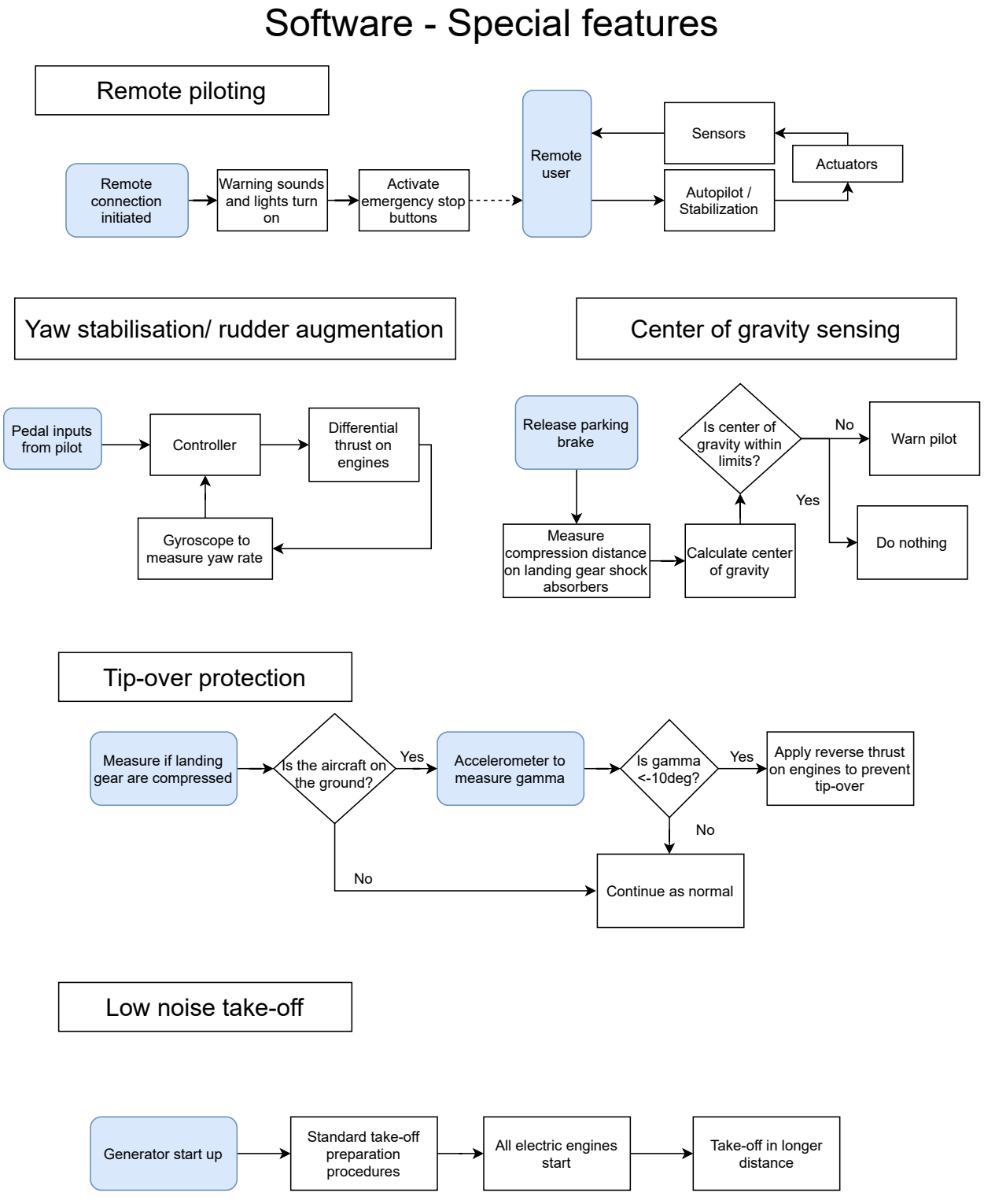

Figure 8.30: Software function flow - Special features.

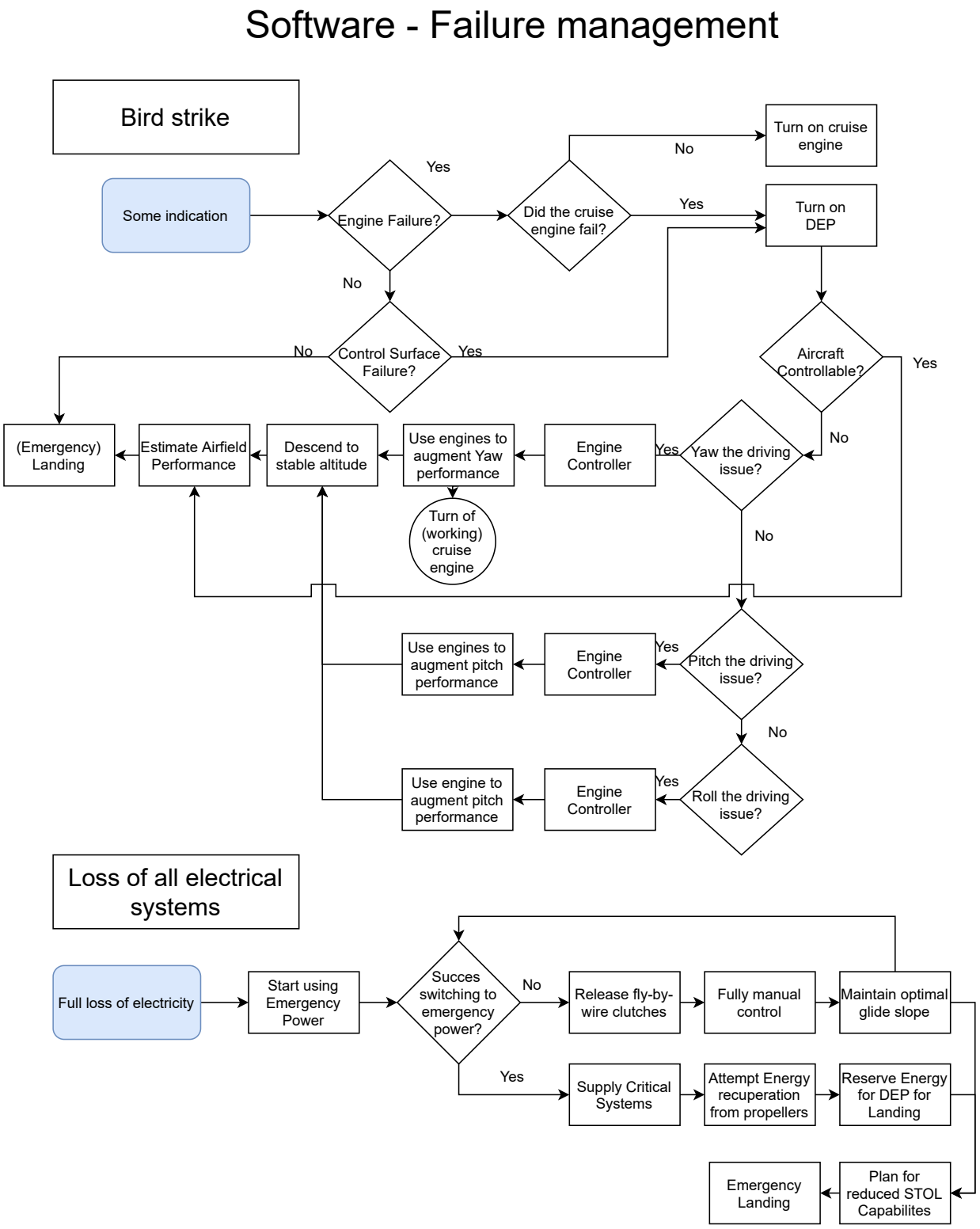

Figure 8.31: Software function flow - Failure management.

9
Assessment of Aircraft Design

The following chapter will perform an assessment of the aircraft design. First, a sensitivity analysis of the final design is performed, assessing the solution of the constrained optimisation. Next, Section 9.2 discusses the future-readiness of the *Twin Puffin*, talking about its modular design, and the possibilities for autonomous controls. Then, the sustainability of the design is assessed, by first considering the recyclability of the aircraft after end-of-life, and secondly comparing the emission performance to the comparable CubCrafters Top Cub, in Section 9.3, before outlining a future strategy to improve the sustainability.

In Section 9.4, a risk assessment is done for the aircraft mission, first identifying risks before outlining mitigation strategies to limit the risk and consequences of the identified hazards. Section 9.5 is next, assessing the required infrastructure and logistical operations to allow the aircraft to remain functional throughout its life-time. In the same vein, Section 9.6 assess the RAMS characteristics of the design, i.e. the long-term characteristics of the system, as an indicator of quality.

Finally, Section 9.7 assesses to what degree the design complies with its requirements, before comparing its performance to competing aircraft on the market in Section 9.8.

9.1. Sensitivity Analysis

This section explains the aspect of the aircraft design performed to ensure a robust solution was found. The main technique employed for this was the optimisation, whose ensures that the aircraft designed provides the highest value to the customer. The optimisation performs the task of a conventional sensitivity analysis: change parameters and see how the result changes. The main problem that can emerge is that the optimisation finds local and not absolute maxima.

The goal of the optimisation is to find the input parameters that lead to the design with the highest value to the customer. The danger stems from the highly nonlinear nature of the aircraft design and analysis process, which means that the process that takes high level design inputs and delivers the design value is highly non-linear. As result, the optimisation is prone to falling into local maxima, while the absolute maximum is sought.

To prevent the final design being in a local maximum, the optimisation was run ten times, each with different starting parameters. All function calls and resultant outputs were saved. Figure 9.1 present the wing area, take-off thrust and value (from objective function) of all the function calls. Note that the wing area and take-off thrust are not the only high-level input parameters, but they are arbitrarily chosen as examples for visualisation (as the eight dimensions of parameters cannot easily be displayed in two dimensions).

Interesting to observe from Figure 9.1 is that the optimisation converges on local maxima. A possible explanation for the straight lines is that the optimisation saw a larger gradient (hereby offering a larger potential increase in value function) in other dimensions and therefore walked in a (on this plot seeming like) straight line. The result from the optimisation is that, after combining all points from all optimisation runs, the point with the highest value was taken as the design point.

By doing this optimisation, many different variations of the design parameters have been considered, and the final point found is the optimal solution to maximise the optimisation function.

9.2. Future-Readiness

To ensure the success of the *Twin Puffin*, there should be a possibility to adjust to newly-developed technologies and market demands without the need of a major re-design. When achieving this goal, it can be guaranteed that the same airframe can be used throughout the years, without significant modifications, as it is the case for the Cessna 172. Due to the latter, re-design and re-certification costs can practically all be eliminated, bringing down the cost of the aircraft in long terms. In order to ensure the readiness of the aircraft for the future, several aspects were taken into account when designing the aircraft, as discussed in this section.

9.2.1. Modification of the Main Energy Source

As defined in the first stages of the design, the *Twin Puffin* is designed to be a hybrid aircraft, which energy source is a combination of an ICE and batteries. Although this resulted from the trade-off as the best option from the ones considered in terms of mass, volume, and sustainability, it is of course not the perfect choice. Due

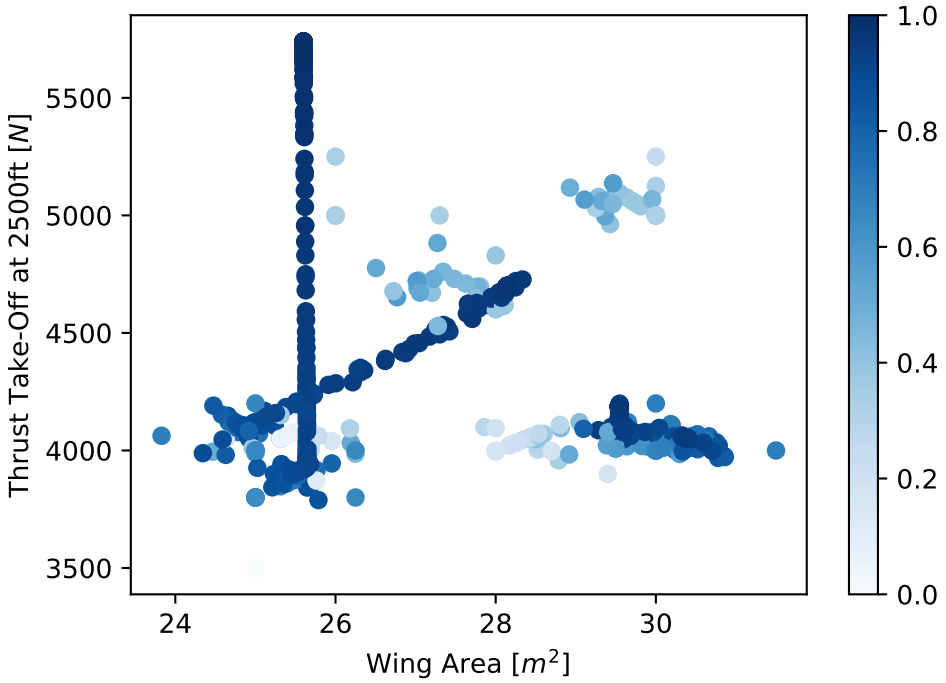

Figure 9.1: Optimisation results.

to the ICE using diesel in order to be able to generate the required energy, CO_2 is released to the atmosphere, increasing the levels of emission of the aircraft. In order to improve these, more sustainable energy sources can be considered, as listed below. However, they have not reached yet the level of development required for them to be used right now on this bush plane, but they have to be taken into account for future implementation.

Batteries as Energy Source The current problem with using batteries as the main energy source of the aircraft is linked to their low properties (specific energy and energy density). These cause the choice of batteries to be unfeasible for the bush plane design, due to the significantly high mass and volume required to achieve the needed energy.

Moreover, using this energy source will significantly reduce the noise level during flight. This decrease will be possible thanks to the elimination of the ICE, which is the main source of noise throughout the mission. Thanks to this improvement, if a noise level lower than 50 dB[1] is achieved, the market could be further expanded to short-distance low-altitude transport over highly-populated areas.

For this option to provide an improvement to the design, it needs to be made sure that the batteries are sustainable both in terms of production and operation. Hence, the majority of the energy carried by the batteries should be produced by low-carbon energy sources. Apart from this, the materials used for building them have to be obtained in a sustainable manner, causing no or minimal damage to the environment.

Hydrogen as Energy Source The idea of implementing a hydrogen fuel cell was already eliminated in the first design steps. This decision was made mainly due to its high cost and low availability. However, it is known that this type of energy sources is already being implemented on some aircraft models[2], which means that hydrogen availability could further increase in the coming years, also significantly lowering its price. Hence, this could then be considered as a viable option for the future.

Quantifying the point at which hydrogen would become a better option for the *Twin Puffin* in terms of availability is a difficult task. However, it can be expected that, once the cost of hydrogen goes down, its availability will increase considerably.

Another of the problems that this energy source has is certification, as there is no aircraft using fuel cells that has been certified up until now. Due to this reason, the costs linked to aircraft certification increase enormously. However, a reduction in this price could be possible in the long term, increasing the viability of this energy source option for the bush plane, thanks to other aircraft manufacturers which are developing hydrogen-powered aircraft and will act as precedent.

[1]URL `https://www.eea.europa.eu/airs/2018/environment-and-health/environmental-noise` [cited 15 June 2021]
[2]URL https://www.airbus.com/innovation/zero-emission/hydrogen/zeroe.html cited 15 June 2021

Alternative Fuels as Energy Source Apart from batteries and fuel cells, there exist other options which also reduce considerably the carbon emissions of the aircraft. While still generating energy with an ICE, fuels such as biodiesel or hydrogen-based e-fuels could be used. When doing so, the emissions of the engine are offset. However, these kind of fuels are not widely available away from airfields, such as diesel, which makes them not an option for the current bush plane design. In case that their availability increases in the future, this option will then become a viable one, and could be implemented.

Biodiesel is obtained from organic fats and oils[3], and it is possible to use it in engines in which diesel is normally used. This fuel is able to reduce CO_2 emissions by up to a 74 % when comparing it to petroleum diesel[4], as it is made from organic matter which captures carbon dioxide while growing.

On the other hand, in order to produce e-fuels, renewable energy is utilized in order to obtain hydrogen and capture CO_2 from the atmosphere. This results in an energy-dense fuel, which is easy to store [62]. In case that the energy used throughout the production process is carbon neutral, the fuel will be so as well (it does not produce additional carbon oxides).

Implementation of a New Energy Source Of course, the bush plane was designed in such a way that it allowed for implementing these modifications in a quick and easy manner. This way, whenever any of the above options becomes viable, improving the current hybrid design, the aircraft can be adapted in an efficient manner, so that it can be ready for operation in the shortest time possible.

For aiding in the implementation of the first two alternatives, being these the batteries and the hydrogen fuel cell, a modular design was chosen for the energy source. This means that the ICE and the batteries are not fully integrated into the airframe, such that they can be replaced by a new option, similar to building blocks. And although this substitution cannot be done by the customer, the design iteration required for it gets easier and more time-efficient.

Lastly, alternative fuels could also be used in the current ICE, following the same hybrid energy source design. In order to ensure this will be a viable option, an aviation Diesel engine was chosen. This engine will allow for biodiesel or e-fuels to be utilised once their availability in remote areas increases, without this meaning a significant decrease in the performance of the ICE.

9.2.2. Modular Design

Another aspect to consider for future-readiness of the *Twin Puffin* is an increase in demand from different types of mission. In order to achieve a better adaptability of the aircraft without the need of full interior renovation, a modular design has been implemented. This allows for the inside of the bush plane to be modified depending on the customer demand. Again, same as for implementing the batteries or the fuel cell, this design will act as building blocks, which can be interchanged in accordance to the mission.

As an example, in Section 6.1 the switch from transportation to medical/rescuing missions is tackled. It has been defined that two of the lateral seats can be easily removed, making enough space for carrying a stretcher.

9.2.3. Autonomous Vehicle

Finally, the possibility of making the *Twin Puffin* fly autonomously is considered. It needs to be noted though that, as specified in Section 6.9, the bush plane already has the option of being piloted remotely. Thanks to the augmented autopilot chosen as the control system for the aircraft, as explained in Section 6.9, little modifications will be need to be made to the system in order to remove the pilot. However, it is known that certification will be harder for these kind of systems, and hence the redundancy of all systems in case of failure will need to be ensured.

One of the few things that would still need to be implemented on the aircraft would be electronic brakes, which are not a feature of the design right now. Also, a robust data link is required, as the bush plane will be controlled from the ground. Hence, the aircraft should contain several redundant sensors which communicate the information detected, together with the augmented autopilot which will control the aircraft in the desired way.

The main advantage that the current design has which will make it easier for switching to a auto-piloted system is the redundancy in the power sources. As described in Section 6.1, the *Twin Puffin*'s energy source is composed of an ICE and two different sets of batteries. This means that, in case of one of these failing, the others can take up the power generation until it is safe to land.

9.3. Sustainability

One of the most important aspects of the *Twin Puffin*, and the reason behind many of the choices made throughout the design process, is its sustainability. The main characteristics looked at when assessing the sustainability

[3]URL https://afdc.energy.gov/fuels/biodiesel_basics.html [cited 15 June 2021]
[4]URL https://afdc.energy.gov/fuels/biodiesel_benefits.html [cited 15 June 2021]

of the aircraft are related to the environmental impact of the aircraft (CO_2 and noise pollution, production, and end-of-life). Moreover, social sustainability is also taken into account during the creation of the production plan.

This section is divided into two main parts. Firstly, the design is analysed, identifying all criteria which make it stand out from the other aircraft in terms of sustainability. Then, the aspects to be considered in future design steps are listed, following from some of the design characteristics that can be improved or are still to be defined in more detail.

9.3.1. Sustainability Analysis of the Current Design

As it can be observed throughout the report, the design of the *Twin Puffin* has been directed towards improving its sustainability as much as possible, while still maintaining the same performance levels. Almost each of the design choices took into account at least one aspect related to the sustainability of the bush plane such as noise and emissions, starting from the aircraft concept selection, performed in the Midterm Report [17] and presented as well in Chapter 5. This means that the current design already takes many sustainability considerations into account, which are shown here.

Gas Emissions Currently, aviation accounts for 2.5% of the global CO_2 emissions, and for about a 1.9% of the total greenhouse gases emissions[5]. This is why special attention was put on designing an aircraft that could reduce its gas emissions to a minimum. In order to achieve this, a hybrid system is considered, which includes both batteries and an ICE for power generation. So as to reach minimum contamination levels, the ICE will always operate at its optimum condition (as it is designed for cruise level) while the batteries will aid whenever there is an increase in the demand of power (Section 6.6).

Moreover, the ICE uses two types of filters for reducing these emissions even more. The first one is a Diesel Particulate Filter (DPF)[6], which retains the larger particles in order to prevent them from going to the atmosphere. The other filter used is a catalytic converter. This is a device helping to convert harmful compounds on the fuel such as carbon monoxide (CO), hydrocarbons and nitrogen oxides (NO_2) into carbon dioxide (CO_2), carbon dioxide (CO_2) and water (H_2O), and nitrogen (N_2) and oxygen (O_2), respectively[7].

The emission levels of this bush plane were directly estimated from the required fuel mass, and considering diesel for obtaining the necessary values. Here the emissions for two different gases are quantified: CO_2 and NO_x. They are both given in grams per passenger per kilometre, accounting for the aircraft to be able to carry four passengers and having a range of 1247 km, as predefined.

The CO_2 emissions of this bush plane have been estimated by using Equation 9.1. The amount of CO_2 emitted by a kilogram of diesel was taken as 2.67 kilograms[8], and from the aircraft design it is known that 106 kg of fuel are required. By using these values, together with the number of passengers and the range, a value of 56.76 grams of CO_2 per passenger per kilometre was outputted.

Similarly, the NO_x emissions of the aircraft were also computed by means of Equation 9.2. Here, instead of using a direct conversion from kilograms of fuel to kilograms of gas emitted, the amount of NO_x was given per amount of energy, having a value of 250 kg/TJ for all fuels [19, p.3.64]. Hence, the Net Calorific Value (NCV) of diesel was used, which was found to be of 42.91 MJ/kg [9]. By inserting these numbers into the equation, the NO_x emission value for the *Twin Puffin* was found to be of 0.23 grams per passenger per kilometre.

$$m_{CO_2} = m_{fuel} \cdot \frac{m_{CO_2/fuel}}{n_{pax} \cdot R} \qquad (9.1)$$

$$m_{NO_x} = m_{fuel} \cdot \frac{NCV_{fuel} \cdot m_{NO_x/J}}{n_{pax} \cdot R} \qquad (9.2)$$

In the same manner, the gasses emitted by direct competitors such as the *CC Top Cub* can be estimated. From research, it is known that the fuel mass of this aircraft is equal to 136.3 kg[10]. Moreover, the Top Cub operates with AVGAS 100LL fuel, which is estimated to have CO_2 emissions of 3.13 kilograms per kilogram of fuel [66], a NCV of 43.5 MJ/kg [11], and again, a NO_x factor of 250 kg/TJ [19, p.3.64]. Finally, this bush plane carries up to two passengers, and has a range of 917 km[12]. By using all these values, it was estimated that the *CC Top Cub* releases a total amount of 232.7 and 0.81 grams per passenger per kilometre of CO_2 and NO_x, respectively.

[5] URL https://ourworldindata.org/co2-emissions-from-aviation [cited 18 June 2021]

[6] URL https://www.autoevolution.com/news/how-the-diesel-particulate-filter-works-90866.html [cited 18 June 2021]

[7] URL https://auto.howstuffworks.com/question66.htm [cited 18 June 2021]

[8] URL https://ec.europa.eu/environment/enveco/taxation/pdf/Annex%205%20-%20Calculations%20from%20the%20case%20studies.pdf [cited 18 June 2021]

[9] URL https://www.claverton-energy.com/wordpress/wp-content/uploads/2012/08/the_energy_and_fuel_data_sheet1.pdf [cited 18 June 2021]

[10] URL http://cubcrafters.com/topcub [cited 28 June 2021]

[11] URL https://www.exxonmobil.com/en-us/commercial-fuel/pds/gl-xx-avgas-series [cited 18 June 2021]

[12] URL http://cubcrafters.com/topcub [cited 28 June 2021]

With these results, the two aircraft can be compared. As shown in Table 9.2, the CO_2 emitted by the *Twin Puffin* is estimated to be about 76% less of what the *CC Top Cub* emits. Something similar is also observed for the NO_x emissions, where the ones current design are computed to be 75% lower than the ones from the reference bush plane. Hence, the *Twin Puffin* is thought to present a considerable improve in sustainability with respect to similar aircraft.

Table 9.1: Comparison between the gas emissions of the *CC Top Cub* and the *Twin Puffin*.

Aircraft	*CO_2 Emissions* $[g/pax/kg]$	*NO_x Emissions* $[g/pax/kg]$
CC Top Cub	232.7	0.81
Twin Puffin	56.76	0.23
Difference	-175.94 (-76%)	-0.61 (-75%)

These reductions are significantly beyond the required 50%. Hence, even if the level of accuracy showed up to be not enough in further design steps, the high margin allows for some increase in emission levels without it compromising the compliance with this requirement.

Noise Pollution As aforementioned, the design of the propulsion subsystem is based on a hybrid energy source. It consists mainly of an Internal Combustion Engine (ICE), which is designed for cruise and always operates on its optimum RPM setting, as well as a set of batteries, which provide the extra power needed at some points during the mission (e.g. take-off). Although the presence of the ICE itself increases the noise levels when compared to a fully-electric or a fuel cell option, the use of auxiliary batteries allows for the engine to be smaller and operated at lower RPM settings, reducing the noise. Furthermore, the positioning of the internal combustion engine over the wings in a more complete enclosure also allows the use of increased noise insulation and sound diversion away from the ground.

Overall, this aircraft generates thrust by using many electric propeller and motor combinations which have a smaller diameter and higher blade count than average, this presents a significant noise reduction with respect to regular engines used in general aviation. This can be observed when looking at the Sound Pressure Level (SPL) estimated at a one-metre distance of the aircraft, which has a value of 126.4 dB at takeoff and 128.7 dB at cruise. Moreover, the noise level at 2500m down-range at minimum climb rate is estimated to be 84 dBA which surpasses the ICAO airport noise requirement.

Table 9.2: Comparison between the noise levels of the *CC Top Cub* and the *Twin Puffin*.

Aircraft	*SPL at one metre* $[dB]$	*SPL during climb for ICAO* $[dBA]$
CC Top Cub	140.9	91.9
Twin Puffin	128.7	83.6
Difference	94%	85%

Flax Fibre Composite In Section 6.2.2, it is concluded that the material to be used for the main structure of the *Twin Puffin* is a flax fibre composite with natural epoxy resin. Apart from proving to have sufficiently good mechanical properties for it to be used in the structural components of the bush plane, this material also stood out from the rest due to its superior sustainability characteristics.

Natural fibres are capable of absorbing CO_2 when growing [46]. This aspect makes them a perfect candidate to further reduce aircraft emissions, as it contributes in lowering the overall CO_2 produced by the aircraft. Also, during the production of the fibres, flax seeds produce linseed oil as a by-product. Linseed oil can be used as building material for the natural epoxy, making the production process even more efficient. This also increases the biodegradability of the composite.

Recyclability One important characteristic of the *Twin Puffin* design is its recyclability. This comes linked to the requirement which states that at least 80% of the materials used on the aircraft shall be recyclable (TP-USER-12, in Table 4.1). Here, each component making up the aircraft is identified, together with its computed mass. Then, a recyclability percentage is estimated, providing an explanation for each of them. All can be found in Table 9.3. However, it needs to be taken into account that due to the components of the aircraft not being fully detailed-designed now, these are very rough estimates, mainly based on literature.

Table 9.3: Recyclability budget of the *Twin Puffin*.

Aircraft Component	*Mass* $[kg]$	*Recyclability Percentage*	*Explanation*
Battery	52.1	90 %	Lithium-Ion batteries can be fully recycled. However, this can be a lengthy and costly process [26]. It then needs to be ensured that it is followed correctly in order to achieve the stated recyclability percentage.
Electric Engines	151.7	100 %	The electric engines are assumed to be fully-recyclable, as they are mainly made of metallic parts[13].
Empennage	221.4	90 %	The main structure of the aircraft has been chosen to be built out of flax fibre composite, which can be recyclable [32].
Fixed Equipment	103.0	60 %	The fixed equipment includes the control, de-icing, and emergency systems, together with the instrumentation, avionics, and electronics. It is difficult to estimate how much of this equipment will be recyclable, as it has not been designed in detail yet. Hence, a conservative percentage was chosen here. However, it is known that wires can be recyclable[14], and it is also expected that as many components as possible are chosen to be built out of fully-recyclable materials.
Fuselage	168.6	90 %	Most of the fuselage is made out of flax fibre composite, which is fully recyclable. However, due to its matrix being epoxy (thermoset), a two-step recycling process is required [32]. Special care needs to be taken when applying coatings to the aircraft, as this would increase the difficulty of the recycling process [38].
Generator	150.8	70 %	Due to the ICE being made of aluminium[15], it is assumed that it will be possible to recycle most of its structure.
Landing Gear	54.3	70 %	The landing gear can either be made out of metal or flax fibre composite (as the main structure), both thought to be fully-recyclable. However, the rubber from the wheels (in case of having it) cannot be easily recycled, although it can be ground and repurposed.
Wing	368.2	90 %	Again, similar to the fuselage, the majority of the structure of the wing is built of flax fibre composite. This can be recycled, although not through an easy process [32].
TOTAL	1270.1	85.5 %	

End-of-Life Once the *Twin Puffin* reaches the end of its operational life, its safe disposal needs to be ensured. Although not every aspect of this procedure can be known yet, some things have already been considered, as it will be further specified in Section 9.5.5.

It should be ensured that, when the aircraft is stripped-down, all parts are recycled correctly. This needs to be done by following the recyclability budget presented above, which needs to be updated in future design phases. Moreover, specialised recycling companies should be hired for this purpose, in order to make sure that this process is carried out with the minimum environmental impact.

[13]URL https://intercotradingco.com/recycling-electric-motors/ [cited 21 June 2021]
[14]URL https://www.conserve-energy-future.com/can-you-recycle-electrical-wires.php [cited 21 June 2021]
[15]URL `http://www.continental.aero/diesel/engines/cd155.aspx` [cited 21 June 2021]

9.3.2. Future Strategy to Improve Sustainability

Although the current design, as identified in the previous subsection, already includes many aspects that make its sustainability greater than direct competitors, there are still several aspects to consider in further design steps.

Gas Emissions Although the current estimate of the emissions of the aircraft shows that the required levels are met, this calculations will need to be refined in order to constantly checked these values. Moreover, in future design steps, more accurate values of the characteristics of the bush plane will be known, which facilitates increasing the accuracy of the estimations.

Noise Pollution Similar to the aircraft emissions, the calculations performed to estimate noise level will also need to be further refined as well as validated with experimental results. Other aspects of the aircraft such as the oversized landing gear or the possibility of using low noise propellers will also need to be taken into account in the noise measurements.

Once the aircraft has been designed in more detail, on of the last steps will be to measure the SPL in an experimental setting to confirm previous estimates and make corrections if necessary.

Flax Fibre Composite As aforementioned, this material presents many characteristics that make it the best choice in terms of sustainability. However, it is still not clear whether this benefits also exist in terms of eutrophication and ecotoxicity, these being caused by nutrients, fertilisers, and pesticides applied in flax cultivation [16]. Hence, in order to extract all possible benefits of the flax fibre composites, the origin of this natural fibre will need to be checked before its purchase. This should be done so as to avoid using flax cultivated under non-sustainable conditions.

Aircraft Production As all the details for the design are still to be known, it is not possible to make a specific production plan yet. This is why some aspects to be taken into account in the creation of this plan are listed here.

First of all, it needs to be noted that when defining all production steps of the aircraft, two different types of sustainability need to be taken into account: environmental and social. The former refers to the process meeting the requirements without posing a hazard to the environment, while the later is more focused on the management of the process (direct or indirect).

When considering environmental sustainability, two main elements which contribute to the levels of pollution are contemplated. The emissions throughout the aircraft production need to be reduced to a minimum. Any process that considerably contributing to atmosphere, soil, or water contamination will need to be eliminated. In case that this cannot be avoided, another alternative for the manufacturing of the specific element should be defined, even if it involves the re-design of such part.

Special attention will need to be put into the production of the batteries, as the levels of pollution throughout the process have proved to be significantly high, and the conditions for the obtention of the necessary rare-Earth-metals are not ensured to be sustainable [16]. Apart from this, the source from which the energy to recharge the batteries comes from has to be identified. This is because, in case that the energy comes from, for example, coal, it will take longer for the aircraft to surpass the emission levels of a conventional diesel engine [17].

Lastly, as mentioned, the social sustainability regarding the production process is also examined. With this, it will mainly be ensured that the whole chain is performed in an ethical way. From the purchase of the materials, to the final assembly of the aircraft, all steps need to follow sustainable international standards.

End-of-Life Together with the increase in detail of the aircraft design, the end-of-life strategy will need to be updated. This needs to be more specific after each design step, once more and more characteristics of the *Twin Puffin* are known.

Something to be considered when building this disposal plan is that decommissioning of the bush plane should not lead to a significant level of extra pollution. For this, aspects such as possible oil spillage, or what to do with non-recyclable materials and batteries, will need to be tackled. In case that the end-of-life pollution of any of the components is deemed considerable, the design may need to be modified to account for this.

Furthermore, it will need to be checked at all times that the requirement stating that 80% of the aircraft shall be recyclable (TAG) is still complied. This was estimated in (Section 9.3.1), but it needs to be refined whenever more specific material or component choices are known. For this, every element on the aircraft will need to be tracked, establishing a volume/mass and recyclability of such. In case this is not guaranteed at some point in the design process, the research of new materials or components will need to be performed.

[16] URL https://www.greentechmedia.com/articles/read/lithium-ion-battery-production-is-surging-but-at-what-cost [cited 19 June 2021]

[17] URL https://www.industryweek.com/technology-and-iiot/article/22026518/lithium-batteries-dirty-secret-manufacturing-them-leaves-massive-carbon-footprint [cited 19 June 2021]

Future Improvements Moreover, as explained in Section 9.2, this aircraft is also prepared for the relatively easy implementation of future technologies which will increase the overall sustainability of the design (and more specifically, in terms of emissions). These modifications include aspects such as the replacement of the current hybrid energy source by a cleaner one, like a fuel cell, or more efficient batteries. Also, there is the possibility of using more sustainable fuels in the ICE once these become highly available.

9.4. Risk Assessment

Once the final *Twin Puffin* design is presented, a risk assessment needs to be performed in order to make sure that none of the characteristics of the aircraft acts as a possible hazard to the mission. Risk management is a dynamic process, meaning that a continuous identification, evaluation, and handling of risks is required at every design step. Previously, the risks relating to the design phase of the aircraft were discussed in the Baseline Report [18]. Here, a risk analysis based on the current design of the aircraft and its future operation is performed. Although this was already tackled in the Midterm Report [17], now the final design parameters are known and hence it is possible to achieve a more specific risk assessment of the bush plane. Many of the risks presented in the previous report will be re-assessed in this section, while also new ones will be added to the analysis.

This section is structured in two separate parts. As a first step, all risks are identified and their consequence and likelihood is also estimated. Then, these parameters are lowered for some risks by presenting a risk mitigation strategy, which needs to be implemented in future steps of the design process.

9.4.1. Risk Identification

In Table 9.4, the main risks of the aircraft's design are listed. These are presented with a tag identifying the risk, some reasoning explaining why that risk exists, and a likelihood-consequence score. They are all divided into six different groups, each of them corresponding to a different tag: risks regarding market issues (*MKT*), others related to the general design of the aircraft (*GEN*), the ones caused by the failure (or degradation) of technical components (*TECH*), those presenting a threat to the environment (*ENV*), risks that arise from the operation of the aircraft (*OP*), and finally the ones related to mission logistics (*LOG*).

Each of the risks is quantified with a Likelihood-Consequence (L,C) score with numbers ranging from one to four, which defines how critical these are. The first parameter, the likelihood, measures the probability of the risk happening, which can be very low (1), low (2), moderate (3), or high (4). On the other hand, the consequence of the risk evaluates its impact as being marginal (1), notable (2), critical (3), or catastrophic (4). The higher this score is for a risk, the more criticality it presents.

Table 9.4: Main identified risks.

Tag	*L,C*	*Risk*	*Reasoning*
		Market Issues	
RSK-MKT-01	3,4	Low demand for high-tech bush planes	In case of the market not being open to this new alternative, the project itself may fail.
RSK-MKT-02	3,3	Issues with purchase and production of flax fibre composites	Will most probably cause an increase of cost and delays.
		Related to the General Aircraft Design	
RSK-GEN-01	1,2	Engines ingest rubble and dirt	Will cause engine failure. Lower likelihood due to high-wing configuration.
RSK-GEN-02	2,1	Strong, poorly damped eigenmotions	Will lead to passenger discomfort.
RSK-GEN-03	2,4	Failure of structural components in-flight	Could have catastrophic consequences depending on the damaged part.
RSK-GEN-04	2,3	Trapped moisture and corrosion	If not properly taken into account and maintained, could lead to structural failure.
		Arising from the Failure of Technical Components	
RSK-TECH-01	2,2	Battery degradation or failure	Although with some performance loss, the ICE can take up the required power deficit.
RSK-TECH-02	1,2	ICE failure	The batteries are sized for take-off and some climb. Failure could be dangerous when the batteries are drained and insufficient power for landing operations is available.
RSK-TECH-03	1,4	Failure of all energy sources	The aircraft may be able to land (depending on the location), but performance will decrease.

Table 9.4: Main identified risks.

Tag	*L,C*	*Risk*	*Reasoning*
RSK-TECH-04	1,3	Brake failure	Will increase considerably the landing distance, which may be an issue when flying in remote areas.
RSK-TECH-05	1,3	Cruise propeller failure	The probabilities of one of the main engines failing are very low, but it could mean the end of the mission, without catastrophic results although asymmetric thrust will endanger controllability.
RSK-TECH-06	2,1	Auxiliary propeller failure	The take-off and landing performance will be reduced, potentially causing an unexpected stall or loss of control.
RSK-TECH-07	2,3	Multiple propeller failure	The aircraft may be able to end the mission, but with a reduction in performance. Asymmetric thrust can endanger controllability.
RSK-TECH-08	2,4	Tail propeller failure	When landing, may lead to loss of control of the aircraft at low speeds.
RSK-TECH-09	2,4	Control system failure	Will lead to loss of control of the aircraft. Without proper handling, consequences are catastrophic.
RSK-TECH-10	3,3	Sensors failure	It could lead to failure of the augmented autopilot, and will confuse the pilot/instruments.
RSK-TECH-11	2,3	Electronics failure	Leads to the augmented autopilot failing. Moreover, it can lead to propeller failure or fire.
RSK-TECH-12	2,2	Augmented autopilot failure	It would lead to manual control of the aircraft. Safety and redundancy will be reduced.
		Threats to the Environment	
RSK-ENV-01	2,2	Oil spills	Although not directly affecting the mission, a small oil spillage already has a significant environmental impact.
RSK-ENV-02	2,3	Battery fire	May have catastrophic consequences if not insulated and shielded appropriately. May release toxic fumes or particles
RSK-ENV-03	1,3	Failure of emission reduction systems	Emissions will no longer be filtered and can release toxic fumes, NOx, and methane. Can also lead to fire.
RSK-ENV-04	3,2	Propeller damage	The noise level will increase significantly.
		Arising from Aircraft Operation	
RSK-OP-01	2,2	Frontal tip-over	Increased likelihood in taildraggers. Will lead to structural damage of the aircraft.
RSK-OP-02	2,3	Lateral tip-over	The likelihood is low for a correctly designed landing gear, but it can cause wing and propeller damage. May also occur due to side-gusts.
RSK-OP-03	1,2	Damage to tail landing gear during landing	In case the tail wheel is highly-loaded, this could lead to its failure, making subsequent ground operations difficult.
RSK-OP-04	1,2	Sinking of the landing gear	Will lead to abruptly halting the aircraft, which can also cause tip-over.
RSK-OP-05	2,2	Flat tyre	Decreases landing performance. Return to the airport could be necessary.
RSK-OP-06	1,4	Pilot health issues	May lead to an aircraft crash.
RSK-OP-07	3,2	Aircraft entering deep stall conditions	The horizontal tail is designed such that the aircraft can still be controllable in such circumstances.
RSK-OP-08	2,2	Aircraft entering spin	It is checked that enough part of the rudder is outside the wake of the horizontal tail so that the aircraft is recoverable.

Table 9.4: Main identified risks.

Tag	L,C	Risk	Reasoning
		Related to the Logistics	
RSK-LOG-01	1,2	Fuel runs out in-flight	Reduced performance and range, emergency landing required. Leads to ICE failure.
RSK-LOG-02	1,2	Fuel runs out in wild area	There is low likelihood due to the availability of diesel and the expertise of the pilots.
RSK-LOG-03	3,1	No electricity available for battery recharging	The ICE could take up the power generation, but emission and noise levels will increase.
RSK-LOG-04	1,3	No diesel available for refuelling	Diesel is chosen because of its wide availability. In case of no other fuel available, the electric range is probably not enough.
RSK-LOG-05	1,3	The maximum take-off weight of the aircraft is exceeded	Fuel consumption increases, and performance is decreased. Extreme wing and structural loading
RSK-LOG-06	2,3	Unsecured cargo	Could lead to an undesired shift on the centre of gravity. Can result in instability or loss of control.

When comparing the criticality of some of the risks with what was presented in the Midterm Report [17], it can be observed that either their likelihood or consequence (or enev both for some specific cases) has been reduced. This comes from the fact that the risks listed in Table 9.4 are the result of the design steps carried out so far. Many of the risk entries have already received some attention in previous sections of this report. Hence, when arranging these risks on a risk map (as the one shown in Figure 9.2), it is observed that a risk level, defined by the product of likelihood and consequence, higher than 9 cannot be found.

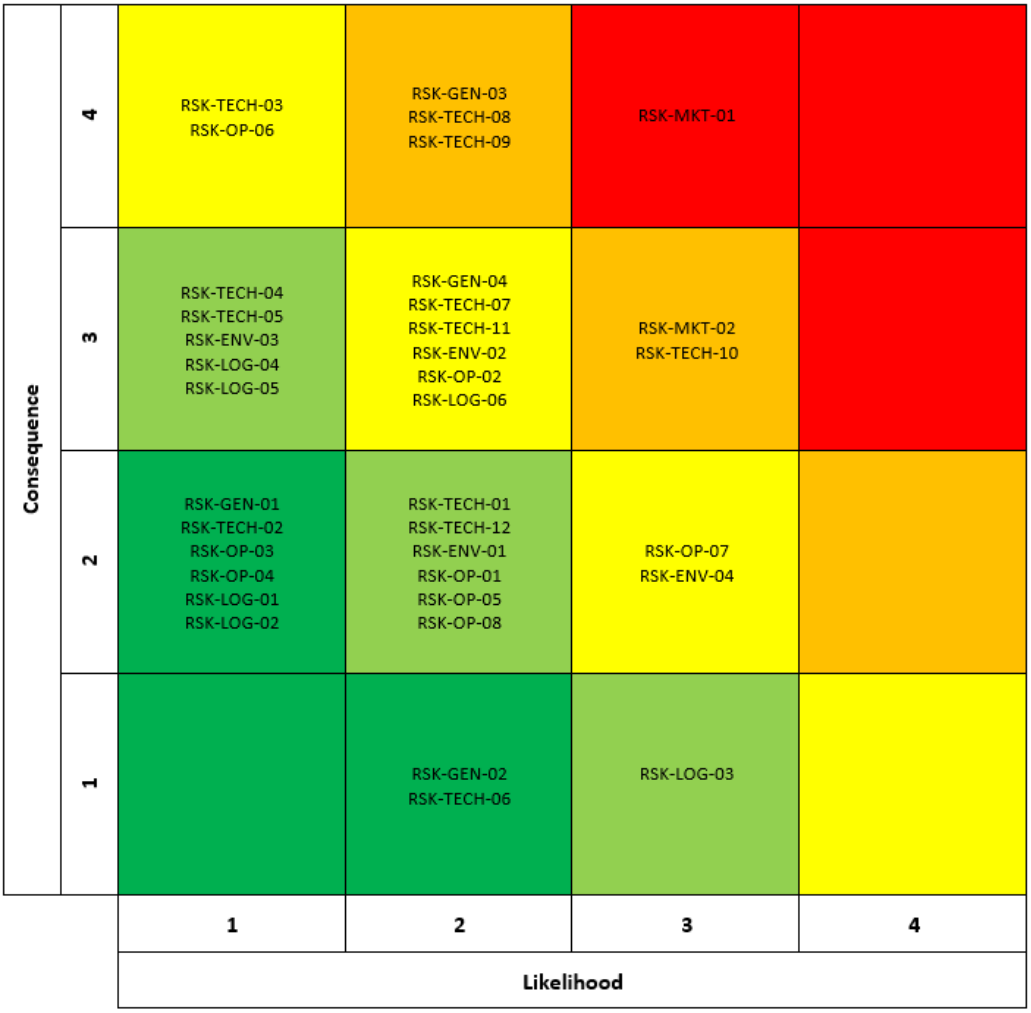

Figure 9.2: Risk map corresponding to the identification of risks.

9.4.2. Risk Handling

Once all risks have been identified, a mitigation strategy needs to be created for those presenting the highest criticality (shown in yellow, orange, and red in the risk map). This is shown in Table 9.5, where the tags are presented again together with their old likelihood-consequence score, and a way of lowering this value is explained followed by their new score.

Table 9.5: Handling of the most critical risks.

Tag	*L,C*	*Risk Mitigation Strategy*	*New L,C*
		Market Issues	
RSK-MKT-01	3,4	A thorough market analysis has to be performed so as to guarantee a place for the *Twin Puffin* on the market. In case that this cannot be ensured, the design should be modified in order to account for the market demand.	1,4
RSK-MKT-02	3,3	The production plan will need to be very well-defined to make sure that all steps can be properly followed in order to produce the main structure of the aircraft.	2,3
		Related to the General Aircraft Design	
RSK-GEN-03	2,4	During the design, appropriate safety factors should be used, and a fail-safe strategy has to be followed, reducing the fatal consequences. Moreover, once built, regular checks and maintenance of the structure needs to be performed in order to avoid its failure. Hence, the likelihood can also be brought down.	1,2
RSK-GEN-04	2,3	The detailed design of the structure needs to be performed in such a way that fluids are not trapped so that moisture and/or corrosion are minimised. Moreover, when constantly flying in humid environments, regular checks would need to be performed.	1,3
		Arising from the Failure of Technical Components	
RSK-TECH-03	1,4	Improving the static and dynamic stability of the aircraft throughout the design process will avoid having catastrophic consequences in case of all energy sources failing. The aircraft could then glide safely until the most appropriate location for landing under such circumstances can be reached.	1,3
RSK-TECH-07	2,3	It needs to be checked throughout the whole design process that the vertical tail is able to produce enough moment to counteract the loss of multiple engines, and hence the controllability of the aircraft is not significantly affected. Also, the electrical system should be designed in a way such that the loss of one engine does not act as a hazard to the correct functioning of the rest.	1,2
RSK-TECH-08	2,4	In order to avoid the loss of control of the aircraft due to a failure on a tail propeller, the pilot should follow the guidelines stated on the dead man's curve presented in Figure 8.6a in Section 8.2.6.	2,2
RSK-TECH-09	2,4	The control system of the aircraft needs to be designed with sufficient redundancy, following the fail-safe philosophy. Hence, if one wire or rod fails, the connection between the pilot and the control surface is not lost.	1,3
RSK-TECH-10	3,3	The sensors configuration on the aircraft need to be redundant enough so that the failure of any of them does not cause a loss in control of the vehicle.	3,1
RSK-TECH-11	2,3	An emergency system needs to be installed on the aircraft which accounts for the augmented autopilot failing, and provides manual control of the bush plane.	2,1
		Threats to the Environment	
RSK-ENV-02	2,3	Proper insulation should be included on the final design of the aircraft in order to account for the batteries caching fire. This reduces the consequence of the risk.	2,2
RSK-ENV-04	3,2	Regular maintenance, where the emission level is checked reducing the risk of possible environmental damage	2,2
		Arising from Aircraft Operation	
RSK-OP-02	2,3	It should be checked at all times that the clearance angle between the tip of the most outboard propeller and the landing gear is sufficient.	1,3
RSK-OP-06	1,4	Designing the augmented autopilot system in such a way that the aircraft can be remote-piloted in this extreme conditions will decrease the consequence of this risk.	1,3

Table 9.5: Handling of the most critical risks.

Tag	*L,C*	*Risk Mitigation Strategy*	*New L,C*
RSK-OP-07	3,2	The likelihood of the aircraft entering deep stall can be reduced by including the appropriate sensors and a warning system on the cockpit. Moreover, it should be constantly checked throughout the design process that the horizontal tail is outside of the wake of the wing (and the fuselage if required) in deep stall conditions, so that the bush plane can still be controllable.	2,1
		Related to the Logistics	
RSK-LOG-06	2,3	So as to avoid a centre of gravity shift due to unsecured cargo, several checks should be performed before the start of the mission in order to reduce the likelihood of this event. Moreover, some physical barriers can be installed in the interior of the fuselage that prevent loose objects from moving around, decreasing the consequence.	1,2

With this risk handling strategy settled, a new risk map can be created in order to assess the effectiveness of this plan. By looking at Figure 9.3 it can be observed that only one of the risks remains now on the yellow zone, while all others have been mitigated, and their risk level has been brought down to (less than) four points.

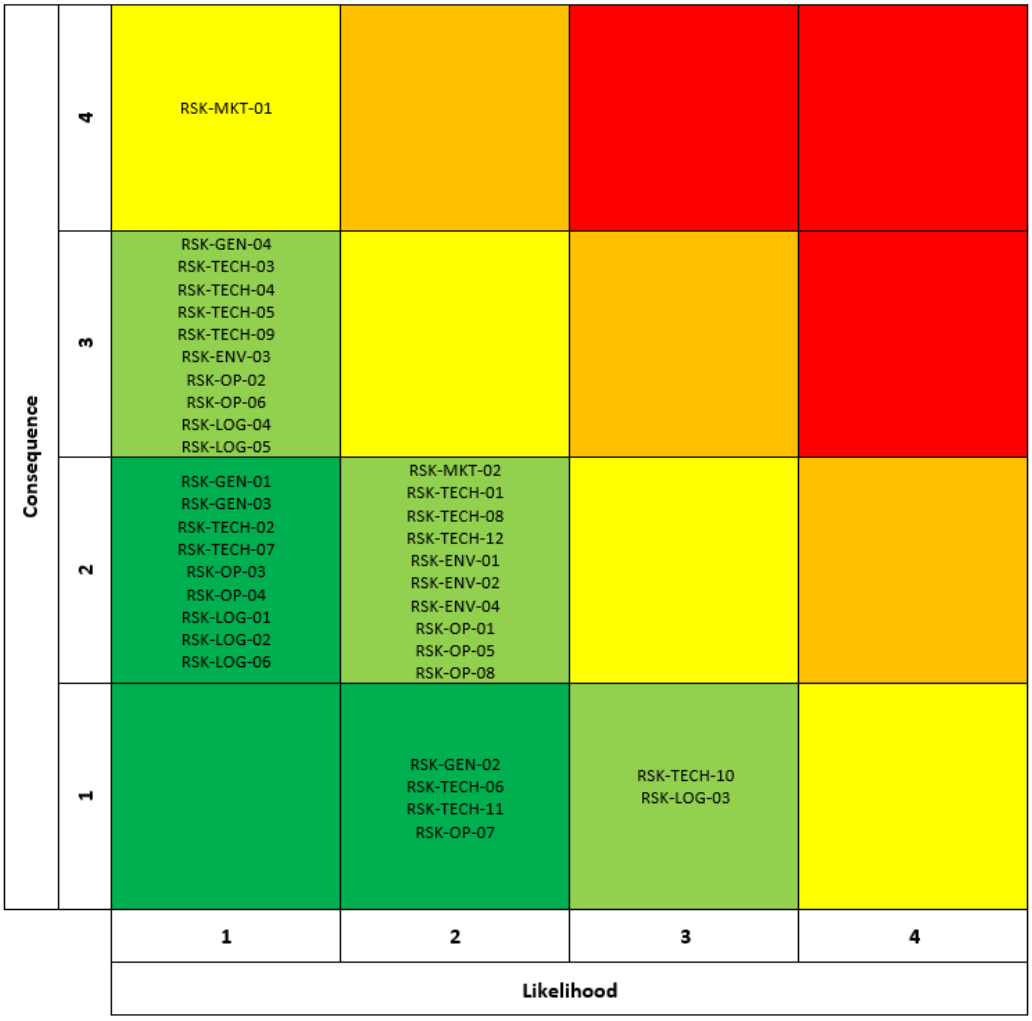

Figure 9.3: Risk map corresponding to the likelihood and consequence of the risks after handling.

Of course, the risk assessment of the *Twin Puffin* does not end here, but it must continue throughout the whole design process. In the following steps of more detailed design, new risks should be added and a risk mitigation strategy will need to be created for these as well. However, it needs to be taken into account that the risks which have been identified until now cannot be avoided, and their criticality should also be checked at all times.

9.5. Operations and Logistics

An aircraft is only functional when paired with a system of infrastructure and logistics which are required to make it fly, and still be able to do so for an extended time. Therefore, this section presents the relevant aspects of operations and logistics which relate to the use cases specified for the *Twin Puffin*. In Figure 9.4, the operations and logistics flow diagram illustrates the use of the aircraft, from its purchase to the end of its operational life.

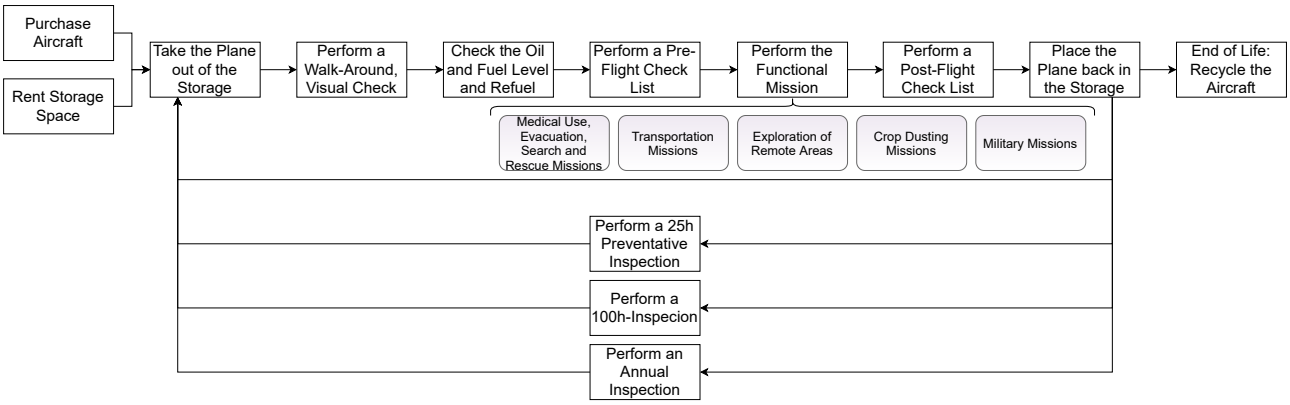

Figure 9.4: Operations and Logistics diagram for the *Twin Puffin*.

It needs to be noted that the aircraft can also fly without a pilot, being remotely guided. For the *Twin Puffin*, this can be done in case of transportation missions (with no passengers onboard). The only case in which the aircraft is allowed to use its remote control in cases in which the pilot suffers from any health condition during the flight, as already explained in Section 9.4.

Relevant aspects in terms of operations and logistics of an aircraft include the basic functional operations, the storage and maintenance of the aircraft, and the end-of-life procedure. Compared to typical commercial aircraft, the processes pertaining to a bush plane with advanced distributed propulsion systems may vary significantly in terms of aspects including storage, airport and refuelling or charging operations as well as life expectancy, maintenance, and disposal, and these differences are here noted.

9.5.1. Storage Infrastructure

At the instances in which the aircraft is not on operation (on ground), proper storage is required in order to avoid major harm from happening. For this, a storage infrastructure is required, which will vary mainly depending on the use case of the aircraft.

There exist many options for storing small aircraft. The main ones include outside storage, and shared or private hangars. Of course, it is preferred that the *Twin Puffin* is stored on the inside, as weather conditions can affect the structure of the bush plane, especially considering that the material used for building the structure (a flax fibre composite) is sensitive to moisture.

However, if this cannot be possible, an appropriate mooring of the aircraft is required so as to ensure that it remains stationary in case of extreme weather phenomena, such as strong winds, occurring. Due to the aircraft being designed under the principle of distributed propulsion, the propeller engines present a smaller diameter (and hence a less stiff blade structure) than the ones used in conventional bush planes, especially the auxiliary engines. This is why Special caution will need to be put on the propellers when storing the aircraft outside. Lastly, in order to minimise the impact of weather conditions, a cover could be used.

Regarding the location of the storage, for all cases it is preferred that the aircraft is situated close to the infrastructure used for take-off and landing. By doing this, taxiing time is reduced, which at the same time contributes to the saving of energy. Now, depending on the use case, the facilities surrounding the storage point may vary. In case of transportation or tourism, the shorter the distance from the runway the better, as then the distance in which the aircraft needs to carry all the payload is reduced. For medical or rescuing services, however, a storage infrastructure located close to a medical facility is required.

In touristic missions, a place in which the passengers can board the bush plane safely needs to be provided as well. This spot may coincide with the storage location, which would be the optimum. However, if this cannot be guaranteed, a boarding position closer to the runway is preferred, again, to reduce the energy required while taxiing.

Normally, a mission will start and end on the same location, and preferably at a (rural or urban) airport. However, in case that the aircraft needs to be stored in the bush for a longer period of time, the same considerations as for outside storage apply.

9.5.2. Take-off and Landing Infrastructure

One of the main advantages of a bush plane is that a proper take-off and landing infrastructure is not required, as these aircraft are designed for being able to operate on unprepared, rough terrains. However, runways should always facilitate the start and end of the mission, and decrease wheel wear and tear. Thus, they are expected to be used whenever possible. Additionally, care has to be taken in rough terrain as the wing tip propellers are prone to prop-striking when the aircraft is at a roll angle close to the ground and the wings are very long.

In case of transportation missions, the bush plane is expected to at least take-off from an airport with (relatively) regular runways. This allows for an easier start with the aircraft loaded at its maximum weight. However, it may happen that the landing site is located in some remote area without proper infrastructure. The landing would then need to be performed on an unprepared runway, which may cause some harm to the landing gear. Here it needs to be also noted that the landing is slightly less critical than the take-off, as the aircraft would have already burned some fuel during the flight, decreasing its weight.

For flights related to medical, search, and rescuing missions, it will be required that the last landing location is relatively close to a hospital or medical centre, which will shorten the transportation time of a patient. Moreover, the runway should be of easy access for ambulances, which then means that rough terrains should be avoided in these cases. For the other take-off and landing locations, the preparation of the runways is not of such importance. Also, it is expected that the site in which medicine is delivered, or a person is rescued, will lack the level of infrastructure necessary to contain a well-prepared runway.

Lastly, for touristic routes, different options are viable. On the one hand, the aircraft could be not required to land (air tourism). In this case, the only runway in which it would be operated is the one closest to the storage location. On the other hand, in case that the passengers need to be transported from one place to another, two scenarios can take place. Firstly, it could be possible that, for pre-defined routes, the tourism companies have already installed small runways in locations close to the points of interest. Otherwise, the bush plane may be required to land in the wild. This will not pose a problem, as stated before, but will increase the damage on the landing gear and structure of the vehicle.

Another aspect that can be considered is the use of heliports. Due to the STOL characteristics of the design, it could be the case that already-built heliports can provide with the sufficient infrastructure for take-off and landing in some areas, decreasing hence the need for the construction of new runways.

9.5.3. Charging and Refuelling Infrastructure

Due to the energy source of the aircraft being designed as an hybrid system, both charging and refuelling infrastructures are required prior to take-off in order to ensure the correct operation of the vehicle. Here different options for each of them are considered, accounting also for the fact that the aircraft may operate on remote locations.

Obtaining fuel throughout the mission is not expected to be a major issue. An engine running on diesel was selected due to the widespread geographical availability of this fuel, even in remote areas. However, in case that diesel is not accessible, other kerosene-based fuels such as Jet-A can be considered, without them affecting the performance or airworthy certification of the engine.

One of the aspects that characterises the *Twin Puffin* is its use of batteries. In order to recharge them, appropriate infrastructure could be required. However, this is not a requirement, as they can be recharged during flight. Another possibility would also be to charge the batteries on ground by operating the ICE. However, this option will consume fuel, not making it the most desirable one. In case of the batteries being charged with external energy, it will need to be ensured that this energy comes from renewable and sustainable sources (as explained in Section 9.3.

9.5.4. Maintenance

Two main types of regular or scheduled maintenance exist: pre- and post-flight checks, and mandatory. Here each of them are tackled, explaining the procedure to be followed so as to ensure the correct functioning of the aircraft and prevent accidents.

Before and after every flight, the pilot should perform small maintenance actions. These checks can be in the form of walk-arounds, making sure that there are no major issues that could act as a hazard to the safety of the aircraft. Prior to take-off, a checklist should be performed, ensuring the correct functioning of electronics, engines, and control systems. Moreover, the oil and fuel levels need to be checked before the start of every mission, and refilled if necessary. Finally, after landing and before storing the aircraft, a post-flight check needs to be carried out in order to identify any possible issues that would require maintenance before the start of the next mission.

Regarding the mandatory inspections, component checks shall be performed regularly by qualified staff. The maintenance manual for the Cessna 206[18] provides different time intervals after which an inspection needs

[18]URL https://www.cessnaflyer.org/media/kunena/attachments/1805/Chap5206MXmanual.pdf [cited 20 June 2021]

to be performed for each of the components of the aircraft in flight hours, which are used as an estimate for the maintenance times of the *Twin Puffin*. However, these are given for aircraft operating at average weather conditions. In case that the aircraft is operated in extremely humid or cold areas, these time will be reduced. In Table 9.6, the inspection time intervals for the main systems forming the aircraft are presented.

Table 9.6: Maintenance time intervals for different aircraft components.

Inspection Time Interval	***Component(s)***
50h	Electric system, propellers, and ICE.
100h	Structure, heater, batteries, seats, emergency systems, flaperons, rudder, horizontal stabiliser, fuel tank, landing gear, brakes, doors, and empennage.
200h	Communications system, wiring, control system, sensors, and wing.
400h or 1 year	Ventilation system.
1000h or 1 year	Autopilot.

Furthermore, there should also be a scheduled general check of the whole aircraft. Its frequency would depend on the owner/operator of the bush plane and the amount of hours that the *Twin Puffin* is operational, but annual inspections are often performed.

Apart from this, there is also a third type of maintenance: unscheduled. This needs to be carried out when an aircraft component unexpectedly fails or is not functioning correctly. Non-regular maintenance shall be minimised as much as possible by performing regular checks of the aircraft, as it hampers the operational availability of the bush plane.

9.5.5. End-of-Life

Once the *Twin Puffin* reaches the end of its operational life, an end-of-life plan should be followed in order to ensure its correct disposal. There are many possibilities to be considered, and some of them are explained here in more detail.

Firstly, one option would be to reuse the aircraft for a totally different purpose. This would mean, for example, refurbishing the aircraft and converting it into a restaurant, hotel, or children playground. This would be the most optimal strategy, as little effort and energy would be required. However, due to the small number of opportunities, not every unit will be able to end up this way, and hence other possibilities need to be considered as well.

Another alternative would be to recycle the aircraft. For this, the bush plane needs to be stripped down and, thanks to the compliance with the requirement stating that at least 80% of the materials used shall be recyclable, many parts of the aircraft could safely be disposed. Specialised recycling companies should be chosen for this purpose, in order to ensure the minimum environmental impact of this end-of-life procedure. On the other hand, it would also be possible to use some still-functioning elements (as parts of the structure, engines, or batteries) in other similar aircraft still on operation, as spare parts.

9.6. Aircraft RAMS Characteristics

The Reliability, Availability, Maintainability, and Safety (RAMS) of an aircraft is a long-term characteristic of the system, and it is used as an indicator of the quality and quantity of the system's functionality and availability.

9.6.1. Aircraft Reliability

The reliability of a system refers to the probability that it has to perform its function as required for a given time. A complex system, such as an aircraft, is made up of several elements, which affect the reliability of the whole entity. Its value can be computed from the failure rates of all the different components comprised by the system. By using Equation 9.3, the failure rate of the complete system λ_{sys} can be computed when knowing the failure rate of each individual element λ_i and the number of similar elements in the system N_i. From this number, the reliability R_{sys} can be computed with Equation 9.4.

$$\lambda_{sys} = \prod_{i=1}^{i=n} \lambda_i^{N_i} \tag{9.3}$$

$$R_{sys} = e^{-\lambda_{sys} t} \tag{9.4}$$

Similarly, the reliability of a single component R_i can also be computed as $e^{-\lambda_i t}$, by using the failure rate of just that specific element λ_i. Then, the reliability of the complete system could be derived using a similar relation to Equation 9.3, but including the component reliabilities instead of failure rates.

In order to find the reliability of the *Twin Puffin*, two different approaches can be followed. The first one would be to use already-computed failure rates of different components. Such data can be obtained from collections as

the 'Nonelectronic Parts Reliability Data (NPRD-2016) [49]' publication for mechanical components, and 'MIL-HDBK-217F, Military Handbook: Reliability Prediction of Electronic Equipment'[19] for the electronic elements composing the system. When obtaining all necessary values, the reliability of the system can be calculated.

Another way to assess the reliability of the aircraft, although a less accurate one, would be to estimate it based on previous flight data. The Federal Aviation Administration (FAA) contains a record of all civil aircraft accidents and incidents[20]. Inside of this dataset, the specific causes of the event are also documented. By making use of these, together with the total number of flights, a statistical estimate of the failure rate of the different subsystems and/or components of the aircraft can be obtained. Again, once these values are known, Equations 9.3 and 9.4 can be used in order to compute the reliability of the bush plane.

Due to the design being on its early stages of the design and the poor availability of data in some cases, it has not been possible to obtain all numbers necessary to quantify the reliability of the *Twin Puffin*. For future design steps, once more detailed characteristics of the aircraft are defined, a proper reliability analysis would need to be carried following the procedure specified above.

9.6.2. Aircraft Availability

The availability of a system is its ability to perform some specific function under given conditions at a definite point in time (or over a time interval). For an aircraft, this would mean its ability to safely perform a mission under an allocated schedule. There exist three main levels of aircraft availability [7]:

L1. ***Total Unavailability.*** All the aircraft grounding due to maintenance or non-technical events.

L2. ***Maintenance Unavailability.*** The period of time that an aircraft is on ground in a non-airworthy condition (in need of maintenance). Both planned and unplanned maintenance activities are included there.

L3. ***Operational Unavailability.*** Only takes into account all the aircraft grounding due to maintenance that affect the operations of the aircraft.

Special attention needs to be put on the last level, the operational unavailability. This type of availability impedes the correct functioning of the aircraft, and prevents it from performing its scheduled missions. Although it cannot be completely avoided, some actions can be performed in order to bring it to a minimum. Regular maintenance and checks, as defined in Section 9.5, will help in noticing any kind of issues on time, before the actual failure occurs. Also, operating the aircraft under the conditions as indicated by the designing team and the manufacturer will increase the lifetime of the different aircraft elements.

Moreover, because of the energy source system being hybrid and hence containing batteries, time for recharging is also required. From their volume and charging capacity, it is estimated that they need about an hour before reaching full charge . Hence, proper planning and logistics need to be ensured in order to give the batteries the sufficient time to charge, without this posing an issue for the mission. However, it needs to be taken into account that this charge time has been computed assuming the batteries are completely empty. If this is not the case, then this time is (significantly) reduced.

9.6.3. Aircraft Maintainability

Here the maintainability of an aircraft refers to the probability that a specific maintenance action can be performed as predefined (using the required procedures and resources) under given conditions and within a prespecified time interval. This includes the availability of the required resources, as well as the correctness of the procedures applied. Three main types of maintenance exist: scheduled, unplanned, and refurbishment. The latter is rarely needed. However, when required, this process is deemed to be lengthy and costly[21].

The second kind, unplanned or unscheduled maintenance, can cause delays or cost increases, and should be avoided. Similar to what happens with operational unavailability, it can never be fully eliminated, as unexpected conditions can sometimes lead to the failure of components or parts. However, this type of maintenance is strongly linked to the former one, the regular and scheduled checks. By performing these as indicated, the reparation time can be significantly decreased in case of a minor issue being found, when compared to the time to repair a complete failure.

An important aspect to consider for the design of the aircraft is its maintainability. It needs to be made sure that the parts that are prone to failing or getting damaged can be repaired as efficiently as possible. This should also take into account that, in order to repair one element, others which are perfectly functional should not be disposed as well due to the way in which the structure is designed. For instance, when part of the flax fibre composite is damaged, a quick repair is be required. The use of paper-sheets based epoxy composites is then proposed. These epoxy composites are designed so they can be used for field repairs on composites with

[19] URL https://www.quanterion.com/wp-content/uploads/2014/09/MIL-HDBK-217F.pdf [cited 20 June 2021]
[20] URL https://av-info.faa.gov/dd_sublevel.asp?Folder=%5CAID [cited 20 June 2021]
[21] URL https://nbaa.org/aircraft-operations/maintenance/time-upgrade-need-know-aircraft-refurbishment/ [cited 20 June]

epoxy resins [28]. The advantages of using paper based composites are low cost, biodegradability and low environment impact.

9.6.4. Aircraft Safety

In this context, safety refers to the freedom of an aircraft from the occurrence of an unacceptable risk. This concept is significantly related to the risk assessment performed in Section 9.4.

In order to assess the safety of the *Twin Puffin*, it needs to be made sure at all times throughout the design process that there exists no risk critical enough that could cause the catastrophic failure of the mission. This is why it is important to constantly perform risk analysis, reassessing the likelihood and consequence of older risks, and coming up with new ones. Moreover, this analysis should always come together with a risk mitigation strategy, which would point future design steps in the right direction.

Moreover, in the later stages of the design, extensive testing should be performed so as to ensure the safety of the whole system. To start with, safety checks of smaller elements and components can be performed once more detailed specifications of the aircraft characteristics are known. Moreover, off-the-shelf products can be assumed to be certified (or at least this needs to be ensured), and hence it will not be necessary to test the element individually, but its interaction with other parts. Finally, once the first model of the aircraft is built, several tests will need to be carried out, some of which will also be part of the certification process.

9.7. Compliance with Requirements

One of the main steps on the assessment of the *Twin Puffin* design is to check its compliance with the pre-specified requirements (as presented in Chapter 4). In Table 9.7, all different requirement tags are listed, together with a brief explanation of the verification process followed for each of them. In case that a specific requirement has been verified, a check mark (✓) will indicate so. Otherwise, there is a cross (✗) instead.

Table 9.7: Verification of requirements.

Tag	*Verification Procedure*	*Verified*
	STAKEHOLDER REQUIREMENTS	
TP-AP-01	Inspection of the dimensions of the design indicates that the length and width of the aircraft do not exceed 15 metres.	✓
TP-MA-01	The number of seats of the aircraft is checked to be four by inspection.	✓
TP-MA-02	The aircraft is designed so that it is able to carry a usable mass of at least 500 kilograms. Moreover, in the simulation it is checked that the bush plane is able to take-off while carrying this amount of payload + fuel.	✓
TP-USER-01	By performing a simulation of a mission, it is checked that the bush plane is able to take-off in less than 100 metres.	✓
TP-USER-02	By performing a simulation of a mission, it is checked that the bush plane is able to land in less than 100 metres.	✓
TP-USER-03	It is checked by inspection that the wheels are capable of operating in rough terrains so that it is ensured that the aircraft can take-off from unprepared runways.	✓
TP-USER-04	It is checked by inspection that the wheels are capable of operating in rough terrains so that it is ensured that the aircraft can land in unprepared runways.	✓
TP-USER-05	The design of the *Twin Puffin* does not contemplate any other equipment to be used during pre-flight actions other than for refuelling.	✓
TP-USER-06	The aircraft has been designed for having a cruise speed of at least 100 knots ($51.44\,\mathrm{m\,s^{-1}}$), and the simulation carried out has computed that the cruise velocity is $54.9\,\mathrm{m\,s^{-1}}$.	✓
TP-USER-07	With the mission simulation the range of the aircraft has been computed to be of 1247 kilometres, which exceeds the required 500 nautical miles (926 kilometres).	✓
TP-USER-08	By inspection, it is checked that indeed the aircraft is designed for it to use distributed propulsion.	✓
TP-USER-09	The engines used by the aircraft are checked to be electric.	✓
TP-USER-10	When looking at the interior dimensions of the fuselage, and as specified in Section 6.1, it can be seen that an stretcher can perfectly fit.	✓
TP-USER-11	Although all aspects included in the current design of the aircraft comply with EASA CS-23 requirements, not all of them have been able to be checked yet.	*NA*

Table 9.7: Verification of requirements.

Tag	*Verification Procedure*	*Verified*
TP-USER-12	A recyclability budget is obtained, as stated in Section 9.3.1, and it is found that approximately 85% of the aircraft mass is recyclable, which exceeds the required 80%.	✓
TP-USER-13	In Section 9.3 an assessment of the levels of emission of the aircraft is performed, determining that, both in terms of CO_2 and NO_x, the *Twin Puffin* has more than a 50% emissions reduction when compared to the *CC Top Cub*.	✓
TP-USER-14	An analysis has been performed to assess the noise level of the aircraft, proving that there is a 70% reduction when compared with the CC Top Cub.	✓
TP-USER-15	By performing a financial analysis, presented in Section 10.2.2, the aircraft is estimated to cost around 350,000€.	✓
	SYSTEM REQUIREMENTS	
	Structure	
TP-SYS-01	Inspection of the dimensions of the design indicates that the width of the aircraft does not exceed 15 metres.	✓
TP-SYS-02	Inspection of the dimensions of the design indicates that the width of the aircraft does not exceed 15 metres.	✓
TP-SYS-03	In this report, the structure has been designed in order to be able to withstand loads of up to an ultimate load factor of 6, which is considered to include a sufficient safety factor.	✓
	Noise	
TP-SYS-04	In the noise analysis it is checked that, in initial climb configuration, the peak SPL at one metre away from the aircraft has a value of 130.7 dB, which is less than the required 135.7 dB.	✓
TP-SYS-05	The noise level 2500m down range at minimum climb rate is computed to be 83.6 dB. This value is less than the required value of 88 dB, taking into account the maximum take off mass.	✓
	Emissions	
TP-SYS-06	An analysis of the aircraft emissions is performed in Section 9.3, proving that the CO_2 emissions are of 0.057 kg/pax/km (less than the required 0.095 kg/-pax/km).	✓
	Usable Mass	
TP-SYS-07	The aircraft is designed so that it is able to carry a usable mass of at least 500 kilograms. Moreover, in the simulation it is checked that the bush plane is able to take-off while carrying this amount of payload + fuel.	✓
TP-SYS-08	With the required fuel mass being 106 kg, this leaves 394 kg for payload, which exceeds the required value of 380 kg.	✓
	Performance	
TP-SYS-09	By performing a simulation of a mission, it is checked that the bush plane is able to take-off in less than 100 metres.	✓
TP-SYS-10	By performing a simulation of a mission, it is checked that the bush plane is able to land in less than 100 metres.	✓
TP-SYS-11	The vertical climb speed is obtained from an analytical expression to be $3.59\,\mathrm{m\,s^{-1}}$ at a velocity of $28.9\,\mathrm{m\,s^{-1}}$ (Section 8.3), which exceeds 1.2 times the take-off stall speed.	✓
TP-SYS-12	Using the simulation carried out, it can be checked that the climb gradient of the aircraft with all engines operative is of 7.11 degrees (12.5%), exceeding the 8.3% required.	✓
TP-SYS-13	The vertical climb speed with one wing tip engine inoperative is obtained from the simulation to be $0.73\,\mathrm{m\,s^{-1}}$ at a horizontal velocity of $26\,\mathrm{m\,s^{-1}}$ (Section 8.3), which exceeds 1.2 times the take-off stall speed.	✓
TP-SYS-14	With the simulation, it is checked that the aircraft has a positive climb gradient when flying at 1.2 times the take-off stall speed.	✓
TP-SYS-15	The aircraft has been designed for having a cruise speed of at least $51.44\,\mathrm{m\,s^{-1}}$, and the simulation carried out computed a value of $54.9\,\mathrm{m\,s^{-1}}$, exceeding this requirement.	✓

Table 9.7: Verification of requirements.

Tag	*Verification Procedure*	*Verified*
TP-SYS-16	The stall speed of the aircraft is confirmed to be lower than 25 m s^{-1} at all times, having its maximum value at cruise of 24.3 m s^{-1}.	✓
TP-SYS-17	By using the simulation, the range of the aircraft has been computed to be of 1247 km, which exceeds the required value of 926 km.	✓
	Aerodynamics	
TP-SYS-18	By analysis, it is found that the L/D ratio with engines inoperative is 11.8, which exceeds the required value of 7.	✓
	Stability & Control	
TP-SYS-19	By simulation, it is checked that the aircraft is trimmable and can be controllable at all points during the mission.	✓
TP-SYS-20	The horizontal tail is designed in such a way that longitudinal static stability of the aircraft is guaranteed.	✓
TP-SYS-21	As the horizontal stabiliser is designed for longitudinal stability of the aircraft, C_{m_α} is known to be negative. Moreover, this is also checked by performing moment equilibrium of the bush plane.	✓
TP-SYS-22	The vertical tail has been designed for the aircraft to be vertically statically stable (even with the loss of one engine). This is then proved again when estimating the coefficient C_{Y_β}, which is found to be negative, as required.	✓
TP-SYS-23	(Almost) All aircraft inherently possess lateral static stability (correction on a disturbance of the roll angle). Moreover, in the dynamic stability analysis of the aircraft (Section 8.7.2), the coefficient linked to this stability type (c_{l_p}) is estimated to be negative.	✓
TP-SYS-24	It is checked that, for deep stall conditions, the horizontal stabiliser is not located inside of the wake of the main wing. Due to its span being larger than the distance between the booms, it is assumed that there will always be enough part of it outside the wake of the fuselage.	✓
TP-SYS-25	Due to the empennage configuration, more than one third of the rudder is free in case of the aircraft entering spin, which allows it to be able to recover from such condition.	✓
TP-SYS-26	The landing gear of the bush plane is designed following preliminary design processes, and hence it is assumed that controllability on ground is achieved by having the correct angles and distances between the centre of gravity and the landing gear location.	✓
	Cost	
TP-SYS-27	A financial analysis is performed (Section 10.2.2) the cost of the aircraft is estimated to be of around 350,000$, which is less than the required 500,000€.	✓
	Energy	
TP-SYS-28	The batteries are designed in such a way that, in case of an ICE failure, they can continue to provide power to the flight systems and (given that they are recharged during descent) also provide the power necessary for the aircraft to perform an emergency landing.	✓

As it can be observed, all requirements have been verified by now except for TP-USER-11. This one has to do with the certifiability of the aircraft. Although all steps followed up until now point towards the compliance with this requirement, not all aspects in the EASA CS-23 have been tackled yet, and hence it cannot be fully ensured that this requirement is completely met.

9.8. Comparison with Competitors

The last step for the assessment of the design is to check the performance of the *Twin Puffin* against other existing reference aircraft, such as the *CubCrafters Top Cub* and the *Cessna 172 Skyhawk*. Table 9.8 shows the characteristic values of the three models. These values were graded on a scale from one to five, using the *CubCrafters Top Cub* as reference and giving it a score of three for all its characteristics. These scores are then used to construct two radar charts, shown in Figure 9.5, one for comparing the bush plane design to each of the other aircraft.

Table 9.8: Comparison of the *Twin Puffin* with reference aircraft.

		AIRCRAFT MODEL					
		Twin Puffin		Top Cub		Cessna 172	
AIRCRAFT CHARACTERISTICS	Unit	Value	Score	Value	Score	Value	Score
Take-off Roll	$[m]$	65.2	4	82.3	3	221.0	1
Landing Roll	$[m]$	94.5	4	121.9	3	207.3	1
Cruise Speed	$[m/s]$	55	4	38.7	3	63.9	5
Range	$[km]$	1250	5	920	3	1289	5
Climb Rate	$[m/s]$	3.6	2	4.1	3	3.4	1
Usable Mass	$[kg]$	500	3	500	3	333.0	2
Noise	$[dB]$	128.7	5	141.0	3	142.7	2
CO_2 Emissions	$[g/pax/km]$	57	5	232.7	3	92.7	4

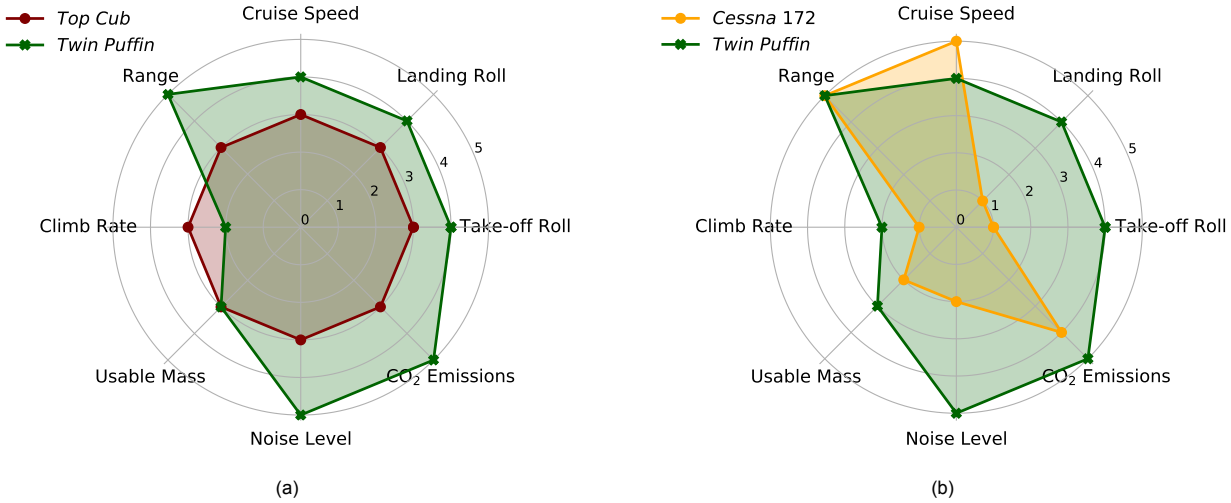

Figure 9.5: Radar charts showing the comparison between the *Twin Puffin* and other reference aircraft.

From Figure 9.5 it is seen that the *Twin Puffin* is, without a doubt, able to compete with the two reference aircraft in terms of performance. The *Twin Puffin* outperforms the *Top Cub* in all manners apart from the climb rate, and even there it does not fall behind significantly. Compared to the *Cessna 172*, the *Twin Puffin* again demonstrates an overall superior performance, going beyond the *Cessna 172* in all categories apart from the range, where the two aircraft score equally well, and the cruise speed, where the *Cessna 172* maintains a slight advantage. It is thus reasonable to claim that the *Twin Puffin* does not need to fear the comparison with the established competition on the market.

10
Continuation of the Project

The following chapter outlines the steps necessary to continue the project. First, a product validation plan is created, Section 10.1, then a financial analysis is performed in Section 10.2, which outlines the proposed investment, return on investment and direct operating cost. Then, in Section 10.3 the post-dse plan is explained, followed by the production plan Section 10.4.

10.1. Product Validation

For the aircraft to be of a high quality and airworthy, product validation is needed. This consists of subsystem validation, explained in Section 10.1.1 and certification, explained in Section 10.1.2

10.1.1. Subsystem Validation

To check if the final product that is of high quality, multiple product validation examinations should be executed. The system validation can be performed through tests, inspections and analyses for the different subsystems. The examinations that will be performed at later stages of the design, are listed and explained in Table 10.1.

Table 10.1: Subsystem Validation Methods.

Tag	*Validation Method*	*Type*
	Wing Group	
TP-SYS-WNG-01	The desired roll of the aircraft shall be provided by the ailerons.	Test
TP-SYS-WNG-02	The mass of the wing shall not exceed 400 kg.	Test
TP-SYS-WNG-03	The Lift Augmentation (as measured with propellers and put to test in a wind tunnel) shall comply with the theoretical model.	Test
TP-SYS-WNG-04	Improvement of the effective aspect ratio due to tip mounted propellers shall decrease the drag as expected. To be measured in a wind tunnel.	Test
TP-SYS-WNG-05	High Lift Devices shall provide sufficient CL increase and shall work with and without the Lift Augmentation.	Test
	Structure Subsystem	
TP-SYS-STR-01	The aircraft length *(fuselage + booms)* shall not exceed 15 m.	Inspection
TP-SYS-STR-02	The fuselage shall have the capacity for carrying at least four seats.	Inspection
TP-SYS-STR-03	The fuselage shall be able to carry a stretcher.	Inspection
TP-SYS-STR-04	The usable volume of the fuselage shall be of at least 2 cubic metres.	Inspection
TP-SYS-STR-05	The structure of the aircraft shall be able to withstand a maximum loading of 6g.	Analysis
TP-SYS-STR-06	The structure of the aircraft shall be able to withstand a minimum loading of -4g.	Analysis
	Propulsion and Energy Acquisition Subsystem	
TP-SYS-PROP-01	The thrust due to torque measured in a wind tunnel shall be compliant with the theory that was used to size the propellers.	Test
TP-SYS-PROP-02	Airspeed after the propeller shall be measured in the wind tunnel to validate if it is sufficient for the Lift Augmentation.	Test
TP-SYS-PROP-03	ICE and generator shall be subjected to endurance and abuse tests.	
TP-SYS-PROP-04	Propellers shall be tested under noise requirements.	Test
TP-SYS-PROP-05	The emissions of the ICE shall be below 190 g/pax/kg.	Test
TP-SYS-PROP-06	Batteries shall have the required capacity and shall be subjected to stress-testing.	Test
	Aircraft Stability	

Table 10.1: Subsystem Validation Methods.

Tag	*Validation Method*	*Type*
TP-SYS-STB-01	The empennage size and area of the aircraft shall not deviate more than 10% from empennage size and area of comparable general aviation aircraft.	Inspection
TP-SYS-STB-02	The range of the centre of gravity shall be within limits.	Analysis
TP-SYS-STB-03	Landing gear position shall not cause propeller or tail strike.	Analysis
TP-SYS-STB-04	Cm_α shall be negative for stabiilty	Test
TP-SYS-STB-05	Dynamic stability shall be tested	Test

10.1.2. Certification of the Aircraft

Further validation of the aircraft is required by official authorities. For the design to be approved, a 'Type Certificate' is to be obtained in the country of use. The aircraft is designed and manufactured in Europe, and following the CS-23 regulations. Therefore, the EASA is in charge of the certification of this aircraft [1]. However, when flown in the United States of America, a FAA certificate shall be requested and approved. Fortunately, the latter seems not to be an issue as the EASA authorities and FAA authorities collaborate closely together and have harmonised their regulations. When the aircraft certifications are requested simultanuously, the EASA is the primary authority responsible for the certification and the FAA serves as a secondary authority and its role is mainly to review, observe and confirm the work of EASA. Further than the 'Type Certificate', also an 'Aircraft Certificate', which is a Certificate of Airworthiness (CoA) is needed, before the aircraft can be flown. Each individual aircraft is required to have such aircraft certificate, containing the approval that the aircraft conforms to the certified design. In the aircraft certification, it is said whether the aircraft is properly built and maintained. When the aircraft obtains both the design certification and the aircraft certificate, it is officially approved to fly the *Twin Puffin*.

10.2. Financial Analysis

The financial analysis is important to determine whether the product that is developed is viable financially. First, the proposed investments are outlined, the return on investments is investigated and finally the direct operating hours are estimated.

10.2.1. Investment in the project

It can take years for a product to start creating money for the company. Before that, large amount of money has to be invested first. To create an estimate of the investment costs, a Cost Breakdown Diagram is created first to identify the sources that generate cost at this stage of financial life of the product. The Cost Breakdown Diagram is presented on Figure 10.1.

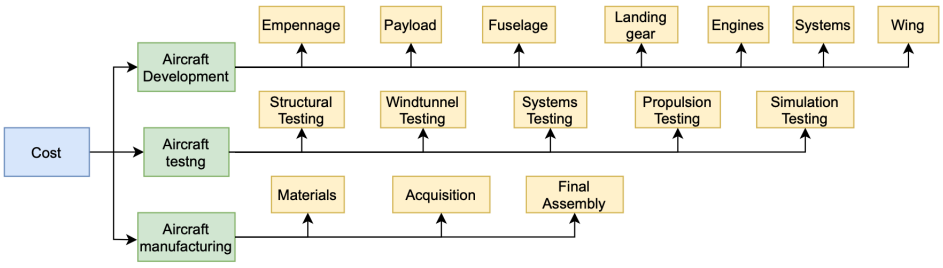

Figure 10.1: The Cost Breakdown Diagram.

As it can be seen on Figure 10.1, the three identified contributors to the investment cost of the aircraft are programme development cost, aircraft manufacturing, and aircraft testing which would be discussed below. Each of those three categories can then split down further. For example, aircraft development cost concise of development cost of each subsystem of the aircraft, while aircraft testing consists of testing each of the subsystems on its own but also together to see how the system works together. For the manufacturing costs, the cost of material has to be taken into consideration, alongside the cost necessary to acquire or create the tools which will be used for final assembly. The cost of human work of production engineers and technicians is also taken into consideration in that part.

Below, a method to estimate the costs of each of the three components is explained.

[1] URL: https://www.easa.europa.eu/domains/aircraft-products/aircraft-certification [cited 19/06/2021]

Development Costs For the programme development cost, a method developed by Markish and Willcox [33] is used. It estimates the programme development cost for the aircraft by summing up the engineering programme development costs of specific subsystems based on cost per kilogram of mass of each of the subsystems. That is presented on Table 10.2. The total development cost for the *Twin Puffin* programme was found to equal 43 million USD in 2021 using that method.

Table 10.2: The engineering cost of each of the components per kilogram in USD.

	Wing	*Empennage*	*Fuselage*	*Landing Gear*	*Installed Engines*	*Systems*	*Payload*
cost per kg [$]	15637	4599	28301	2202	7665	30254	9491

It is nonetheless recommended to perform a more detailed research work into estimating that cost and assessing the margins of uncertainty. That exercise is nonetheless exceeding the scope of this DSE Project.

Manufacturing Cost For the manufacturing cost, again the method developed by Markish and Willcox [33] is used. It estimates the manufacturing cost for the aircraft by summing the manufacturing costs of specific subsystems based on cost per kilogram of mass of each of the subsystems. The manufacturing cost contribution per kilogram of each of the subsystems can be seen in Table 10.3.

Table 10.3: Manufacturing cost of each subsystem per kilogram of mass in 2002 US Dollars.

	Material	*Labour*	*Other*	*Total Cost per kg [$]*
Wing	1343	450	194	1986
Empennage	3558	1067	514	5139
Fuselage	1497	419	216	2132
Landing Gear	236	216	35	487
Installed Engines	547	201	79	827
Systems	694	201	101	996
Payloads	893	220	130	1243
Final assembly	128	9	7	143

The total cost of manufacturing of the aircraft can then be calculated using the values of masses of each of the subsystems. Those were obtained as a result of using the design procedure explained in Chapter 6 and running the optimisation code outlined in Chapter 7. They can be found in Appendix A. The final cost of manufacturing the first aircraft was found to be 430 thousand USD in 2021.

However, the effects of the learning curve shall also be taken into consideration at this point. That refers to a reduction of production cost related to more experience and thus capability to work faster and more efficient of the production crew. For a typical aircraft manufacturing process, it was found that the production cost is reduced by a factor 0.9 every time the production is doubled [64]. For that reason, the variation in production cost can be accurately represented with Figure 10.2.

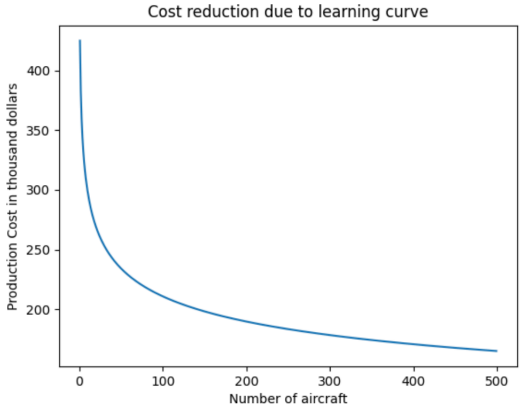

Figure 10.2: The variation in production cost due to the effect of learning curve.

Testing Cost The method for estimating the cost of testing the new aircraft is based on Roskam [51]. Test scenarios include those from the Cost Breakdown diagram Figure 10.1 and include the following: windtunnel testing, systems testing, structural testing, propulsion testing and simulation testing (flight software). The testing cost can be found using Equation 10.1.

$$C_{\text{test}} = 0.008325 \cdot W_{\text{ampr}}^{0.873} \cdot V_{\text{cruise}}^{1.890} \cdot N_{\text{test}}^{0.346} \cdot IC \cdot F_{\text{diff}} \tag{10.1}$$

In this equation, W_{ampr} can be estimated using Equation 10.2, V_{cruise} is the speed of the aircraft during cruise expressed in knots, N_{test} is the number of prototypes built for the purposes of testing, which for a small general aviation aircraft as the Twin Puffin is often selected as two [51], IC is the inflation index with respect to 1970 which was found to be 6.91 [2], and F_{diff} is the parameter which translates to the difficulty level of the project (how novel this design is). It was decided to set it to the highest one possible, ”2”, meaning that the *Twin Puffin* is a programme that involves ”very agressive use of new technologies” [51]. The total testing cost for the *Twin Puffin* was found to be 2.5 million USD in 2021.

$$W_{ampr} = inv \log [0.1936 + 0.8645 \log (W_{TO})] \tag{10.2}$$

10.2.2. Return on Investments

Return on investment outlines how much money the programme shall ultimately bring for the investors. It can be calculated as the difference between the total profit and total cost, where the total cost can be found by summing the development, testing, and production cost, and the total profit can be obtained by multiplying the total number of aircraft sold by the price of each one.

Break even point is a measure to determine the point in time and in terms of number of aircraft sold when the total cost covered by the investors is surpassed by the profit due to selling of the aircraft.

Two selling strategies are analysed for the Return on Investment. One assumes that all the aircraft will be sold at a fixed price, whereas the second strategy makes uses of the idea that it can be beneficial for the aircraft manufacturer to sell first few items of his product at a reduced price to immediately get some market share and ”validate” the product in the days of future customers by receiving positive feedback from the pilots and companies who decided to buy one of the first few items of the aircraft.

The market value price of the ”Twin Puffin” was found using the cost function outlined in Section 7.3.2. Here, the market price function used the inputs labelled as important for the bush plane operators. Those were take-off and landing distance, and the climb rate. The total final market price using that method was found as approximately 350000 US Dollars in 2021.

Regarding the production rate, it is assumed to be 15 at the beginning of production and then, due to the effects of the learning curve, it is assumed to increase to 30 per year very late in the production process. This is to consider the fact that a small company like the *Twin Puffin* will be unable to produce more than 15 aircraft per year, especially at the beginning of its operation.

Regarding the total production volume , using the estimate of 60 aircraft presented in ”Market for the *Twin Puffin*” 3.4, and considering the production rate, it seems that the production capabilities are actually the limiting factor in terms of supply. For that reason, the total production is set at 500 aircraft. It shall be noted however, that if the company grows quickly, the total production volume can increase.

Therefore, given the beginning of production scheduled for 2029 (Figure 10.6), the average later production rate assumed at 22 aircraft per year, the total production time for the Twin Puffin is estimated at 23 years, until 2052.

Regarding the expected number of aircraft sold, and thus the percentage share of the market, it is a number that is very difficult to estimate, mostly due to the fact that a lot of small general aviation aircraft, and especially bushplanes, have been produced long time ago. Nevertheless, using the estimate of 60 aircraft presented in ”Market for the *Twin Puffin*” 3.4, the total estimation of 500 aircraft sold has been derived and is used for the purposes of Return on Investment Calculation.

The first selling scenario assumes the same price of 350 thousand USD (the market value as found by the objective function) for each of the aircraft sold. In that scenario, the break-even point is achieved in 2044, after 318th aircraft sold. The total Return in Investment in that scenario is estimated at 33 million USD.

[2] https://www.inflationtool.com/us-dollar/1970-to-present-value

(a) Equity during selling phase with number of aircraft sold.

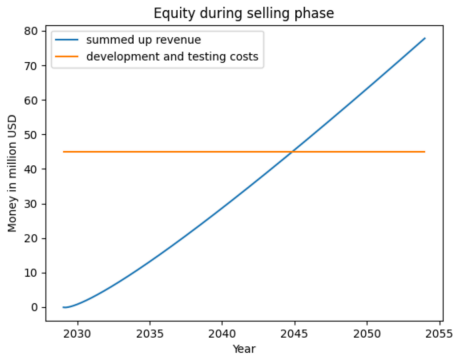

(b) Equity during selling phase over the years of selling period

Figure 10.3: Equity during selling phase with selling scenario 1.

The second selling scenario is considered below. In here, it is decided to sell the first 100 aircraft at a lower price of 299 999 USD in order to gain a higher and quicker market presence. Afterwards, all the remaining 400 aircraft are sold at a price of 399 999 USD. For this scenario, the break-even point is achieved in 2043, after 293rd aircraft sold, and the total Return on Investment is estimated at 47 million USD.

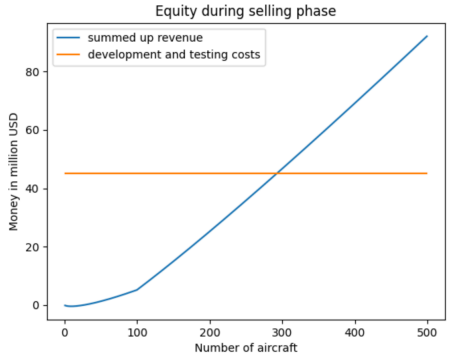

(a) Equity during selling phase with number of aircraft sold with a discount for first 100 aircraft.

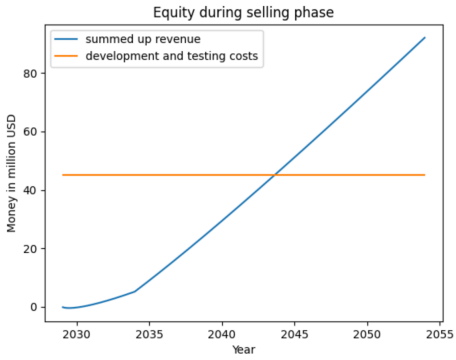

(b) Equity during selling phase over the years of selling period with a discount for first 100 aircraft.

Figure 10.4: Equity during selling phase with selling scenario 2.

10.2.3. Operating Cost

The operating cost is a measure to determine how much it will be to fly the aircraft per hour. It can be calculated based on indirect and direct costs that the owner of the aircraft has to cover every year. In Table 10.4, an overview of operating cost of three aircraft: the Cirrus SR22, the Diamond DA42 NG, and the Mooney M20R Ovation is summarised, as obtained from aircraftcostcalculator.com [3]. Because the estimates for most of the factors contributing to the operating cost of the Twin Puffin are based on estimates of those costs for different aircraft, it was necessary to select those three aircraft carefully to ensure that the cost estimate properly reflects the specifics of the design of the Twin Puffin. The first aircraft, the Cirrus SR22 was selected because it is of the same size as the Twin Puffin, and it is also a relatively new design (meaning that its market value, and thus the insurance will be relatively high). The Diamond DA42 NG twin piston engine aircraft was selected to represent the fact that the Twin Puffin has multiple engines. The increases in expenses due to that fact are visible in maintenance cost in particular. Mooney aircraft was selected for its boxy shape, similar to that of the *Twin Puffin*, meaning that the maintenance can in turn be slightly easier (due to better accessibility), and thus slightly cheaper

The Total Yearly Cost of owning an aircraft is split into five different categories: Indirect Operational Cost, the Maintenance, The Direct Operation Cost, the Airport Adaptation, and Aircraft Miscellaneous costs. All cost components of the Twin Puffin were calculated as the average of the that cost component of the other selected aircraft with a notable exception of the insurance and depreciation cost. For the insurance cost, it was found by calculating the percentage that the insurance cost is with respect to the value of the aircraft. That calculation was performed for three competition aircraft, and the found percentage of 11% was applied in calculating the insurance cost of the /textitTwin Puffin. For the depreciation, it was assumed to be 10% of the current value of the aircraft per year.

[3]Aircraft Cost calculator: https://aircraftcostcalculator.com/default?ReturnUrl=%2f

Table 10.4: Operating cost of the Twin Puffin and three representative competing aircraft.

	Cirrus SR22	*Diamond DA42 NG*	*Mooney M20R Ovation*	*Twin Puffin*
		Indirect Operational Cost [$]		
Insurance	7000	6700	1900	4765
Depreciation	57500	49500	18950	40000
Interest	0	0	0	0
Hangarage	12180	15120	11865	13055
		Maintenance [$]		
Airframe labour + material	4100	9500	6500	6700
Engine Labour + material	3500	6500	2500	4170
Maintenance burden	500	500	500	500
		Direct Operational Cost [$]		
Crew training	2900	5900	3900	4230
FAs	0	0	0	0
Landing fee	0	0	0	0
		Other [$]		
Airport Adaptation	0	0	0	0
Aircraft Miscellaneous	4700	4700	4700	4700
Total Cost	92380	98420	50815	78120
Fuel Cost for 1 hour flying	90	95	95	84

It shall be noted that some costs were intentionally left as zero. For example, the landing fee is a very individual parameter depending on the area of operations and thus its estimation would be very inconsistent. As a rough estimation, however, it can be assumed that the landing fees. The parameters that were left as zero shall be approximated by individual customers after acquiring the *Twin Puffin*.

The airport adaptation cost is labelled as zero because the *Twin Puffin* does not require any additional infrastructure on the airport for its operations.

It shall also be noted that the cost of depreciation and insurance is likely to decrease each year because the market value of a used aircraft is going to decrease, and therefore so will the yearly cost of owning the aircraft.

Finally, having done that, a comparison of the operational cost per hour can be made between the *Twin Puffin* and one of the reference aircraft. The Cirrus SR22 is selected for comparison because it has the lowest fuel cost per hour of flight among the aircraft considered in Table 10.4. Due to the fact the operational cost per hour of flying decreases with an increase in number of hours flown per year, results for three different numbers of flying hours are presented: 200, 500, and 800 hours. Those values were selected to represent potential different users of the aircraft. The lowest value is representative for a private owner of the aircraft, the 500 hours is applicable for flight clubs, and 800 hours is a very high value which could be applicable for cargo airlines in Alaska, or for example companies flying with tourists in big cities and national parks. The effects of the comparison can be seen in Figure 10.5.Thus, the *Twin Puffin* performs notably better than the Cirrus SR22. Quantitatively, cost data are presented in Table 10.5.

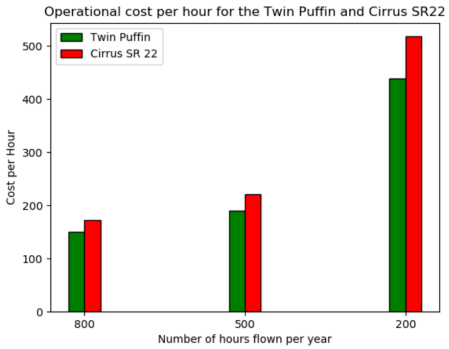

Figure 10.5: Comparison of operational cost per hour for the Twin Puffin and Cirrus SR22.

Table 10.5: Operating cost of the *Twin Puffin* and Cirrus SR22

	Cost [$]	
	Twin Puffin	***Cirrus SR22***
200 h	439	518
500 h	190	221
800 h	150	172

It shall be noted that while no direct comparison is made with the Piper Cub, the difference in operational cost per hour per year is likely to be even greater due to inferior aerodynamics and older design of the latter in comparison with the Cirrus SR22.

10.2.4. End-of-life Costs

Another important aspect for consideration of the financial analysis is the cost of aircraft disposal. Having served its lifetime the *Twin Puffin* shall enjoy a well-deserved retirement. In order to be compliant with sustainability requirements of the project as well as moral obligations towards society, there are no savings on EOL strategy that could impact the environment. The estimated costs of the entire procedure are presented in this subsection.

According to the information found in the literature, the costs of disposal of aircraft usually amount to 10% of the aircraft acquisition costs[70]. Thus, for the *Twin Puffin* the EOL costs are believed to be in the range of 35 to 40 thousand USD.

It is believed that the estimation is accurate for the *Twin Puffin* despite the unconventional material choice for the majority of the structure. It is known that the fibres are biodegradable, thus they do not require high utilisation costs. However, the resin that is used, albeit natural, is not biodegradable and for that reason it needs treatment, which result in higher costs. Lastly, because of the fact that fibres and resin need different procedures for EOL, they need to be separated from each other. This is believed to be a quite expensive process.

Thus, to conclude, despite the lower EOL costs for the biodegradable fibres, the total cost is still assumed to follow the same rule as the conventional aircraft as the costs for fibres separation and utilisation of the resin is higher.

10.3. Scheduling of Post-DSE Activities

One way to describe the continuation of *Twin Puffin* design, is by creating a Gantt chart. This Gantt chart shows the different phases for the design process in chronological order and estimates the time scheduled for these activities. These future design phases are explained in Section 10.3.1, Section 10.3.2 and in Section 10.3.3 a short explanation is provided regarding the quality assessment of the product, throughout the design process. In Figure 10.6, the Gantt chart of the future design phases of the bush plane is shown, in which the duration of the following design phases is estimated.

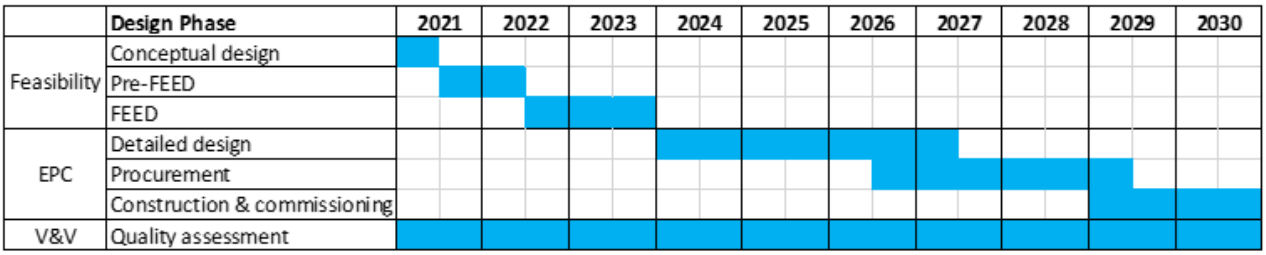

Figure 10.6: Gantt chart of the design phases of the project continuation

10.3.1. Feasibility Design Phase

The feasibility design phase is the initial design phase. During this phase, the Front-End Engineering Design (FEED) is finalised. Three phases are done to do this: the conceptual design phase, the pre-FEED phase and the FEED phase. These different phases are described below.

Conceptual Design Phase So far, the T*win Puffin* reached the end of the conceptual design phase. This stage is the first phase during the design process. During this stage, several concept ideas are listed, of which one is chosen and further developed into a complete concept design. It is important during this phase to understand the stake-holders needs and how to meet this in terms of requirements.

Pre-FEED Phase During the preliminary front-end engineering design phase (pre-FEED), various studies take place to identify the remaining technical issues and a rough investment cost is estimated, to confirm the economical and technical feasibility of the project [4]. This phase includes deciding whether the project will be continued or discarded due to the infeasible nature of the project. The block diagram in Figure 10.7, shows the order of activities to be performed during the pre-FEED phase, which is the first phase after the DSE.

[4] URL https://chiyoda-us.com/services/engineering/ [cited 11 June 2021]

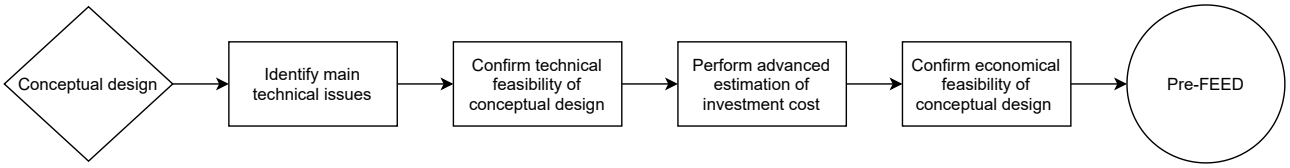

Figure 10.7: Flow diagram of tasks to be executed during the pre-FEED phase

FEED Phase The FEED phase is the second major phase to be performed after the DSE. This phase involves the optimisation of the basis of the design concept, the finalisation of the execution plan, putting the construction plan into place, receiving the funding needed and completion of any work needed to initiate the detailed engineering design [69] [41]. In Figure 10.8, the block diagram is shown, containing the tasks to be executed in chronological order during the FEED phase. This is the final stage before the design can enter the Engineering, Procurement and Construction (EPC) design phase.

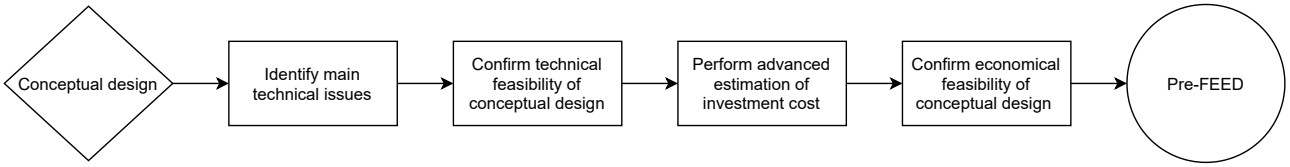

Figure 10.8: Flow diagram of tasks to be executed during the FEED phase

10.3.2. EPC Design Phase

During the Engineering, Procurement and Construction design phase (EPC), the design is fully worked out, tested and produced. In the EPC-phase, the design is completely carried out in detail, all equipment and materials are procured and the design is constructed to deliver a finished functioning product to the customers [5]. The EPC design phase consists of three parts explained below: the detailed design phase, the procurement phase and the construction and commissioning phase.

Detailed Design During the detailed design phase, the specification of both the geometry the materials and tolerances are defined of all the parts and the assembly. This is done through detailed CAD drawings of parts, specific assembly drawings and general assembly drawings that are then used for precise manufacturing and assembly. Next to that, also the construction plan is created during this phase, so the design is fully ready for construction. After this phase, all parts of the product are physically described in a complete and precise way [29]. In Figure 10.9 shows the tasks, in chronological order, that have to be executed during the detailed design phase.

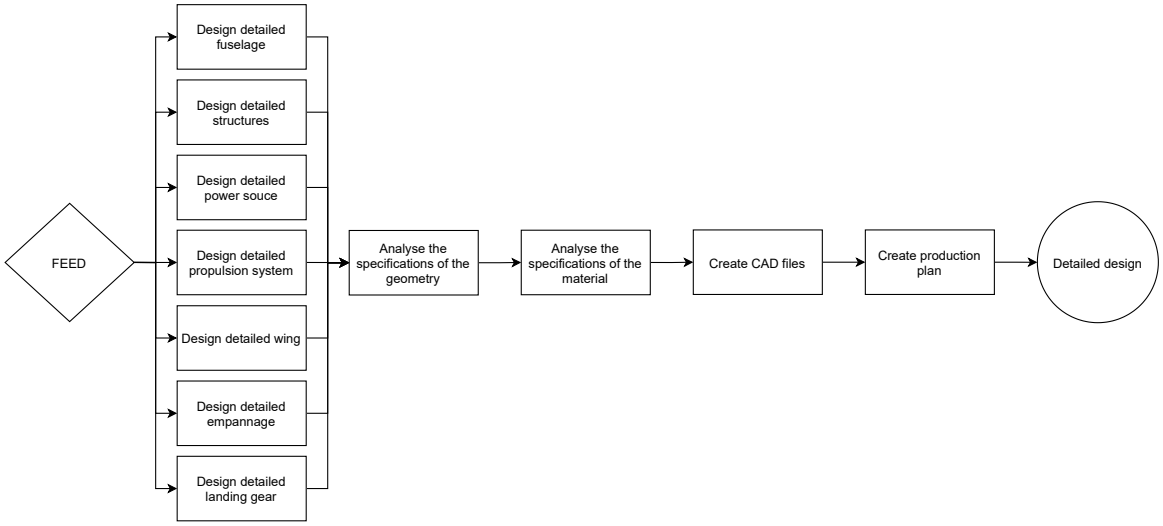

Figure 10.9: Flow diagram of tasks to be executed during the FEED phase

Procurement After the detailed design is finalised, the design enters the procurement phase. During this phase, the requirements are examined through certifications of official authorities. At first, the equipment and

[5]URL https://texvyn.wordpress.com/2015/09/26/epc-engineering-procurement-construction/ [cited 14 June 2021]

the construction materials that are based on engineering drawings are procured. Then, the main task of the procurement takes place that includes sourcing, purchasing, contracting and managing the materials [68]. During this phase, the previous mentioned steps are taken for both the materials, the parts, the sub-assemblies and the assembly. Furthermore, the aircraft needs both a design certificate and aircraft certificate, before it can be flown, as explained in Section 10.1.2. In Figure 10.10, the flow diagram is given of the activities to be performed during the procurement phase.

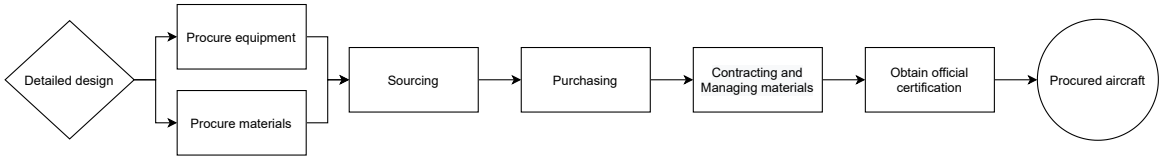

Figure 10.10: Flow diagram of tasks to be executed during the procurement phase

Construction & Commissioning In the last phase of the design of the *Twin Puffin*, the aircraft will be build to be sold afterwards. The first step is to construct the specific facilities, divided in different work packages, that was yet defined during the detailed design phase. Moreover, the equipment and material, that are defined during the procurement phase, are brought to the right facility during this phase. During the actual construction of the bush plane, the construction phase will continuously be re-evaluated, to obtain the most logical and cost-effective approach [68]. Finally, the aircraft is finished and ready to be sold. In Figure 10.11, the tasks to be executed are listed in a chronological order in means of a flow diagram.

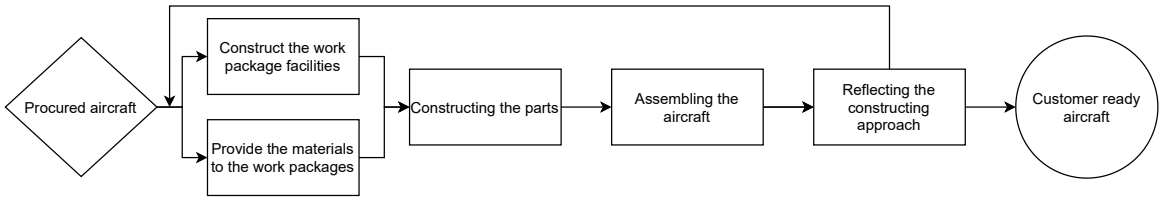

Figure 10.11: Flow diagram of tasks to be executed during the constructing and commissioning phase

10.3.3. Quality Assessment

During the complete design of the *Twin Puffin*, quality should be assured. Therefore, continuous verification and validation is required during all design phases. During the conceptual design phase, requirement verification, requirement validation and model verification are performed and as explained in Section 10.1, the steps to perform further product validation are established. For further design stages, similar approaches will be taken to ensure the quality of the final product.

10.4. Production Plan

After the *Twin Puffin* is fully certified, the construction phase can start. For this to happen in a time- and cost-efficient manner, it is important to set out a structured production plan. To have such a production plan, the production flow needs to be defined in which the different production steps are identified, the facilities for production need to be analysed and an adequate managerial method has to be specified.

10.4.1. Production Flow

Before assembling the aircraft, parts need to be produced. Therefore, the first step in producing the aircraft is the production of parts. For the production of the parts of an aircraft, dedicated workshops create batches of such parts, so there are always enough parts for the assembly of the aircraft. Afterwards, these parts can enter the assembly line. The assembly happens through an assembly line, existing of multiple sub-assembly lines that flow into the main assembly line. [55]

Part Production Main parts are made out of flax fibre composite and therefore need a labour intensive production. Using low cost Vacuum Assisted Resin Infusion (VARI) methods, those parts can be produced, to obtain the lattice cores fibre structure, as explained in Section 6.2.2 [65]. First, the dry fibres, that have the lattice core structure, need to be positioned the right in the mold way using manual lay-up. After vacuum pressure is used such that, the resin is infused into the structure [59]. Note that the production of the parts, using VARI is time-consuming and labour intensive. The parts are produced in different dedicated workshops and are usually produced in batches to be stored in warehouses afterwards. The batch production repeats itself,

when the number of parts in the warehouse reached a critical value. Simultaneous to the production of a batch, the parts are removed one by one from the warehouse for assembly. [55]

Assembly line One way to assemble an aircraft efficiently, is through line production. All parts are then assembled in a ordered way into sub-assemblies and then into the main assembly. For this to happen in a time-efficient and cost-effective way, different tasks are divided into work stations of equal sized work. Each work station contains the same work, the same crew and the same duration as other work stations. One advantage of using the line production method is that the time needed at every work shop decreases over time, due to the crew obtaining more expertise.

This decrease in working time can be described by the means of a learning curve, as presented on Figure 10.2. This curve is an exponential function relating the experience and production cost which is directly related to reduction in production time as well [55].

10.4.2. Facilities needed

To allow for easy production of parts and assembly, many facilities are required. First, tools regarding the production of parts, like vacuum tools and tools to create moulds are necessary to facilitate the resin infusion. Moreover, as not all parts will be directly produced in the factory, some small parts need to be purchased, e.g rivets, bolts etc.

Secondly, to facilitate the assembly, tools like assembly jigs are required. these assembly jigs are used to hold the parts to ease the assembly. Main functions of the assembly jigs are providing support, and is therefore a very rigid and stiff structure, and to position the parts precisely. This jig should allow for easy accessibility and easy detaching to assure the quality of the assembled structures.

Thirdly, having skilled employees is crucial during the entire production phase, to assure quality. Employees are needed who are in charge the production of specific parts, as well as employees who have experience with the manual lay-out of fibres, for the production of the materials through vacuum assisted resin infusion. Furthermore, for the assembly line, employees are needed at each work shop and to ease the assembling itself, who remain at the same workshop to allow for decrease of work hours due to the learning curve. [55]

10.4.3. Lean Manufacturing

Definition To have the maximum efficiency during the production phase of the *Twin Puffin*, lean manufacturing is used. Lean manufacturing is a production philosophy based on the production system of the company *Toyota*. Murman E. et al. defined lean manufacturing as a dynamic, knowledge driven and customer-focused process, through which all people in a defined enterprise continuously eliminate waste with the goal of creating value [37]. Instead of a push market, a pull market is created, where the production of the aircraft is focused on the demand, rather then producing and selling the product. The main characteristic of lean manufacturing is the reduce of waste, which is defined as 'anything that uses resources but does not add any value to the final product' by Sinke [55]. There are two main types of such waste: actions that are required for the product but do not add any value e.g. transport of the parts, and actions that are not required and do not add any value. The latter should immediately be eliminated in order to achieve lean manufacturing. Moreover, adding value is defined by the stakeholder itself, so direct profit is generated. Lean manufacturing however is a dynamic way of thinking as the mindset requires continuous evolving and improving [42][55].

Applying lean manufacturing There are multiple ways to achieve lean manufacturing within the production of the *Twin Puffin*. One of the most common methods for lean manufacturing is by using the *5S* method, where five steps are to be performed for the elimination of waste First, during the 'Sort'-phase, all items within the work space are divided into two categories: necessary and unnecessary items, where the latter is immediately removed from the work space. Secondly, 'during the 'Simplify' step, the items with random locations are re-organised to have a logic place. Thirdly, the work space and the tools used should regularly be cleaned as a visual control, during the 'Scrub' phase. The fourths S stands for 'Standardise', where all the improvements are clearly documented to see which are more effective than others and which shall be eliminated. During the final 'Sustain' phase, the effort of the employees is recognised, to keep the people motivated.

Other than the *5S* method, the JIT method is used for the production of the bush plane where in the assembly line, the product is delivered, just in time, so storage space and therefore costs and time are minimised.

Load levelling is another method that is applied to obtain lean manufacturing where the work load is based on the demand of the customers and based on that the team has to work synchronous with equally distributed tasks.

Cellular manufacturing is another way to apply lean manufacturing during the production of the *Twin Puffin*, where the positioning of the tools and employees are ordered following the production flow, to minimise the transport. By applying the aforementioned strategies and by reflecting those, the production of the *Twin Puffin* will be done as time- and cost-efficient as possible [42] [55].

11

Conclusion and Recommendations

The goal of this report is to convey the design process and final design of the *Twin Puffin*, the design project of DSE Group 12. The midterm report presented the result that a twin-boom, taildragger, hybrid-electric, distributed propulsion aircraft would best suit the market needs. This final report focuses on the further design and specification of the design.

Figure 11.1: CAD-render of the *Twin Puffin* in cruise.

The aim of this report was to showcase the design process and results of the further design of the *Twin Puffin*. In the end, by following systems engineering principles, DSE Group 12 implemented verified methods for designing and assessing a state-of-the-art, high performing bush plane, that outperforms the current market, and fulfils all outlined user and stakeholder requirements. The distributed electric propulsion bush plane can carry up to four passenger, or two passengers and a stretcher, for over 1000 km, and perform take off and landing rolls of less than 100 m. Its key characteristic values are shown in Table 11.1.

After identifying competing aircraft on the current General Aviation market, the use cases of the aircraft are identified as *Transportation*, *Emergency Medical Services*, and *Tourism*. Further, an analysis is done for the new markets that will open up for a quiet STOL aircraft. It is concluded that the market share of the *Twin Puffin* is likely to be larger than previously expected.

The design process is divided in subsystem design methods, which are then combined in one central iteration and optimisation program. The considered design methods for the aircraft subsystems cover all key components of the aircraft and take into consideration how the *Twin Puffin* is affected by its use of distributed propulsion. Key aspects are, amongst others, the fuselage layout, the method of estimating the lift augmenting effects of the distributed propulsion, and the selection of the ”augmented autopilot” as control system type for the aircraft.

All of the individual design methods are combined in one iterative central program that optimises the aircraft parameters with respect to a specially defined objective function. This objective function is based on a market assessment for competitive reference aircraft and uses parameters such as the take off distance and the cruise speed to determine the value of the *Twin Puffin* for different aircraft configurations. Consequently, the most optimum combination of aircraft parameters is identified, leading to the final aircraft design.

The final aircraft is as shown in Figure 11.1. It is marked by its large wings with distributed propulsion on the leading edge, as well as by the twin boom empennage that allows for easy aft loading. The operational procedures, describing how to fly the aircraft in different mission phases and scenarios, are presented and the defining technical characteristics of the aircraft are explained. By being significantly cleaner and quieter than its competitors, the *Twin Puffin* is able to brake away from the flaws of traditional bush plane aircraft. Transcending the design results for the different aircraft subsystems is the pattern that many of the unique features of the *Twin Puffin* are a direct consequence of its innovative use of distributed propulsion.

Following the presentation of the final design of the *Twin Puffin*, the next step was to perform the assessment of the design. Here, the aircraft was assessed in terms of its sustainability, risk handling, future readiness and usability characteristics. Based on this, the compliance with all of the set requirements was identified and it was established that the *Twin Puffin* out-performs the competitive *CubCrafters Top Cub* and *Cessna 172* aircraft in many ways and only falls behind its competitors for the climb rate

The project continuation after the DSE is established and the time for the following design steps is estimated. The first phase after the DSE is the pre-FEED phase followed by the FEED phase. If this is finished, the feasibility phase is completed so the choice should then be made whether the project will be continued and

Table 11.1: Key characteristic values.

Parameter	*Value*	*Unit*
Payload Mass	400	kg
Seats	4	-
Design Range	1247	km
Cruise Speed	54.9	$m\,s^{-1}$
Take-off Roll (2500 ft)	61.0	m
Landing Roll (2500 ft)	94.5	m
Noise (2500 m downrange)	72.1	dBA
CO_2 Emissions	56.76	g/pax /km
Operating Costs 800 h	150	USD hr^{-1}
Maximum Take-off Mass	1781	kg
Operative Empty Mass	1201	kg
Design Fuel Mass	106	kg
Lift-to-Drag Ratio (cruise)	12.2	-
Stall Speed (cruise)	24.3	$m\,s^{-1}$

finished or stopped. When the project is chosen to continue, the bush plane enters the detailed design phase, procurement and construction phase (EPC). After the construction phase, that is based on the production plan that is yet preliminary established, the plane is ready for the market. Furthermore, quality is assured by continuous verification and validation.

Furthermore, the Investment Cost for the the project was found to be approximately 3 million USD. At the same time, the Return on Investement has been calculated at 70 to 80 million USD depending on the sale strategy that is going to be adopted, which is to be expected in 2050s. Finally, the break-even point has also been determined, and is expected to happen 3 years after the production of the aircraft commences.

11.1. Recommendations

The results shown in this report demonstrate that an overall aircraft design has been developed for the Twin Puffin aircraft. In order to continue this project in the future and move the Twin Puffin from theoretical design to tangible aircraft, certain aspects should be taken into consideration. This section outlines the main recommendations for the continuation of the aircraft development program.

Validation The software and models used in this DSE have been verified, but not validated. This means that while there is trust in the implementation, there is no certainty in the validity of the models and design approaches, which is what validation provides. The validation is of utmost importance not only because it determines the trustworthiness of the tools and techniques but also because it helps uncover unknown unknowns. This will be especially crucial for the lift augmentation.

Market and cost analysis The market analysis and cost estimations have provided useful guidance for the design of the aircraft. However, before millions of euros are invested into further aircraft research and development, it is crucial that a more thorough and quantitative market analysis and estimation of all costs is performed. For the market analysis, a detailed prediction regarding the future market of the Bushplanes, as well as small urban aircraft commuters would be in order to further increase the confidence in the design of the *Twin Puffin*. The part of the cost analysis that deserves extra attention is the programme development cost which has been estimated as a very low number. For that reason, that part shall be revisited to ensure the validity of the estimations there.

Auxiliary systems design During this aircraft design process, a large focus has been placed on the digital aspects of the aircraft. For the design of the aircraft systems, engineers with other area of expertise are needed. For example, the hardware and data-flows have been described, but not designed, for which electrical engineers are required. It is mostly the electronic systems that need to be designed (but have been defined).

Certification During the design process a focus has been placed on ensuring that the systems and aircraft are certifiable, rather than focusing on the specific EASA rules. As the design of subsystems and sub-subsystems progresses, designing for specific certifications becomes increasingly important. The decision of which certifications to design for must also be made.

Digital engineering Most of the aircraft design process has been performed in software. This is done, through the implementation of parametric design tools, to allow for rapid changes in the design. This is especially important for this project as there is a very large design space that needs to be considered (due to the novel nature of the design). This program would especially benefit from a continued focus on fully digital design (including embedded software, simulation of flight manoeuvres and structural loading) to find the optimal design.

Bibliography

[1] *Handbuch Verbrennungsmotor: Grundlagen, Komponenten, Systeme, Perspektiven*. ATZ/MTZ-Fachbuch. Springer Vieweg, Wiesbaden, 8. überarbeitete auflage edition, 2017.

[2] H.P.S. Abdul Khalil, I.U.H. Bhat, M. Jawaid, A. Zaidon, D. Hermawan, and Y.S. Hadi. Bamboo fibre reinforced biocomposites: A review. *Materials & Design*, 42:353–368, December 2012.

[3] Federal Aviation Administration. *General Aviation and Part 135 Activity Surveys*. United States Department of Transportation, Washington, DC, 2013.

[4] Federal Aviation Administration. *Airplane Flying Handbook*. U.S. Department of Transportation, Oklahoma, 2016.

[5] T. Alomayri, F.U.A. Shaikh, and I.M. Low. Characterisation of cotton fibre-reinforced geopolymer composites. *Composites Part B: Engineering*, 50:1–6, July 2013.

[6] Michael F. Ashby, Hugh Shercliff, and David Cebon. *Materials Engineering, Science, Processing and Design*. Elsevier Science & Technology, Cambridge, MA, 3 edition, December 2018.

[7] International Air Transport Association. *Aircraft Operational Ability*. Geneva, 1st edition, 2018.

[8] A. Athijayamani, M. Thiruchitrambalam, U. Natarajan, and B. Pazhanivel. Effect of moisture absorption on the mechanical properties of randomly oriented natural fibers/polyester hybrid composite. *Materials Science and Engineering: A*, 517(1):344–353, 2009.

[9] Isidor Buchmann. *Batteries in a portable world: a handbook on rechargeable batteries for non-engineers*. Cadex Electronics Inc, Richmond, British Columbia, 4. edition edition, 2016.

[10] Melville Byington, Jr. Piston Airplane Cruise Performance. *Journal of Aviation/Aerospace Education & Research*, pages 14–24, 1993.

[11] Sibele Piedade Cestari, Daniela de França da Silva Freitas, Dayana Coval Rodrigues, and Luis Claudio Mendes. Recycling processes and issues in natural fiber-reinforced polymer composites. In *Green Composites for Automotive Applications*, Woodhead Publishing Series in Composites Science and Engineering, pages 285–299. Woodhead Publishing, 2019.

[12] Peter A. Claisse. Chapter 32 - Alloys and nonferrous metals. In *Civil Engineering Materials*, pages 361–368. Butterworth-Heinemann, September 2015.

[13] R. Curran, S. Raghunathan, and M. Price. Review of aerospace engineering cost modelling: The genetic causal approach. *Progress in Aerospace Sciences*, 40(8):487–534, November 2004.

[14] Helmut Dahlen. *Comparison of the ICAO annex 16 chapter 10 and chapter 6 noise certification procedures on the basis of flight noise measurements of ten "light propeller-driven aeroplanes"*. Mitteilung Deutsche Forschungsanstalt für Luft und Raumfahrt. Deutsche Forschungsanstalt für Luft- und Raumfahrt, Köln, 1990.

[15] Sam Dakka and Oliver Johnson. Aerodynamic Design and Exploration of a Blended Wing Body Aircraft at Subsonic Speed Aircraft at Subsonic Speed. 6(5), 2019.

[16] Yelin Deng and Yajun Tian. Assessing the Environmental Impact of Flax Fibre Reinforced Polymer Composite from a Consequential Life Cycle Assessment Perspective. *Sustainability*, 7(9):11462–11483, August 2015.

[17] 2021 DSE Group 12. Revised midterm report. Delft, the Netherlands, . TU Delft.

[18] 2021 DSE Group 12. Revised baseline report. Delft, the Netherlands, . TU Delft.

[19] H. S Eggleston, L. Buendia, T. Ngara, K. Miwa, and K. Tanabe, editors. *2006 IPCC Guidelines for National Greenhouse Gas Inventories Chapter 3: Mobile Combustion*, volume 2. IGES, Japan, 2006.

[20] M. R. Fink. Airframe Noise Prediction Method. Technical report, Federal Aviation Administration, Washington, D.C., March 1977.

[21] R. Fink. *USAF STABILITY AND CONTROL DATCOM*. AF Wright Aeronautical Laboratories, California, April 1978.

[22] V. Fiore, T. Scalici, G. Di Bella, and A. Valenza. A review on basalt fibre and its composites. *Composites Part B: Engineering*, 74:74–94, June 2015.

[23] Vicent Fombuena, Roberto Petrucci, and Franco Dominici. Maleinized linseed oil as epoxy resin hardener for composites with high bio content obtained from linen byproducts. *Polymers*, 11(2):301, january 2019.

[24] Kevin G. Gallagher, Steven Goebel, Thomas Greszler, Mark Mathias, Wolfgang Oelerich, Damla Eroglu, and Venkat Srinivasan. Quantifying the promise of lithium–air batteries for electric vehicles. *Energy & Environmental Science*, 7(5):1555, 2014.

[25] Snorri Gudmundsson. *General Aviation Aircraft Design: Applied Methods and Procedures*. Elsevier, 2014.

[26] Gavin Harper, Roberto Sommerville, Emma Kendrick, Laura Driscoll, Peter Slater, Rustam Stolkin, Allan Walton, Paul Christensen, Oliver Heidrich, Simon Lambert, Andrew Abbott, Karl Ryder, Linda Gaines, and Paul Anderson. Recycling lithium-ion batteries from electric vehicles. *Nature*, 575(7781):75–86, November 2019.

[27] M.J. Heap, P. Baud, P.G. Meredith, S. Vinciguerra, A.F. Bell, and A.G. Main. Brittle creep in basalt and its application to time-dependent volcano deformation. *Earth and Planetary Science Letters*, 307(1-2):71–82, May 2011.

[28] M.H. Hussin. A preliminary study on paper sheets based epoxy composites designed for repairing work application and its properties – a review. *Pertanika Journal of Science and Technology*, 26(3):923–932, July 2018.

[29] Anthony Johnson and Andrew Gibson. The Tools of the Design Process and Management of Design. In *Sustainability in Engineering Design*, pages 113–180. Academic Press, February 2014.

[30] Hyun Dae Kim. Distributed Propulsion Vehicles. page 11, Cleveland, Ohio, September 2010. NASA Glenn Research Center.

[31] R. Klees and R. P. Dwight. *Applied Numerical Analysis*. Delft University of Technology, Delft, February 2020.

[32] Marco L. Longana, Vaclav Ondra, HaNa Yu, Kevin D. Potter, and Ian Hamerton. Reclaimed Carbon and Flax Fibre Composites: Manufacturing and Mechanical Properties. *Recycling*, 3(4):52, December 2018.

[33] Jacob Markish and Karen Willcox. Multidisciplinary techniques for commercial aircraft system design. *9th AIAA/ISSMO Symposium on Multidisciplinary Analysis and Optimization*, 2002.

[34] T. H. G. Megson. *Aircraft structures for engineering students*. Elsevier aerospace engineering series. Butterworth-Heinemann, Burlington, MA, 4th ed edition, 2007.

[35] Tseko Mofokeng, Paul T. Mativenga, and Annlizé Marnewick. Analysis of aircraft maintenance processes and cost. *Procedia CIRP*, 90:467–472, 2020.

[36] J.A. Mulder, W.H.J.J. van Staveren, J.C. van der Vaart, E. de Weerdt, C.C. de Visser, A.C. in 't Veld, and E. Mooij. *Flight Dynamics Lecture Notes*. Delft University of Technology, Delft, March 2013.

[37] Earll Murman, Thomas Allen, Kirkor Bozdogan, Joel Cutcher-Gershenfeld, Hugh McManus, Deborah Nightingale, Eric Rebentisch, Tom Shields, Fred Stahl, Walton Myles, Joyce Warmkessel, Stanley Weiss, and Sheila Widnall. *Lean Enterprise Value: Insights from MIT's Lean Aerospace Initiative*. Palgrave, 2002.

[38] Jose Alberto Muñiz Lerma, In-Ho Jung, and Mathieu Brochu. Thermal Decoating of Aerospace Aluminum Alloys for Aircraft Recycling. *Metallurgical and Materials Transactions B*, 47(3):1976–1985, June 2016.

[39] Gi-Dong Nam, Le Dinh Vuong, Hae-Jin Sung, Seok Ju Lee, and Minwon Park. Conceptual Design of an Aviation Propulsion System Using Hydrogen Fuel Cell and Superconducting Motor. *IEEE Transactions on Applied Superconductivity*, 31(5):1–7, August 2021.

[40] M. Nita and D. Scholz. Estimating the oswald factor from basic aircraft geometric parameters. *Deutscher Luft- und Raumfahrtkongres*, 2012.

[41] J.T. O'Conner, W.J. O'Brien, and J.O. Choi. Industrial Modularization: How to Optimize; How to Maximize. Technical report, University of Texas at Austin: Construction Industry Institute, Austin, TX. RR283-11.

[42] Taiichi Ohno. *Toyota Production System: Beyond Large-Scale Production*. Taylor & Francis Inc, March 1988.

[43] Michael D. Patterson and Brian German. Simplified aerodynamics models to predict the effects of upstream propellers on wing lift. Kissimmee, Florida, 2015-01-05. American Institute of Aeronautics and Astronautics.

[44] Michael D. Patterson, Joseph M. Derlaga, and Nicholas K. Borer. High-Lift Propeller System Configuration Selection for NASA's SCEPTOR Distributed Electric Propulsion Flight Demonstrator. In *16th AIAA Aviation Technology, Integration, and Operations Conference*, Washington, D.C., June 2016. American Institute of Aeronautics and Astronautics.

[45] Michael D. Patterson, Nicholas K. Borer, and Brian German. A simple method for high-lift propeller conceptual design. San Diego, California, 2016-01-04. American Institute of Aeronautics and Astronautics.

[46] M. Pervaiz and M. M. Sain.

[47] W. F. Phillips and D. F. Hunsaker. Lifting-Line Predictions for Induced Drag and Lift in Ground Effect. *Journal of Aircraft*, 50(4), July 2013.

[48] Vishnu Prasad, K. Sekar, and M.A. Joseph. Mechanical and water absorption properties of nano tio2 coated flax fibre epoxy composites. *Construction and Building Materials*, 284:122803, 2021.

[49] Quanterion Solutions Incorporated (U.S.). *Nonelectronic parts reliability data 2016.* 2015.

[50] Claire Quigley, Dean Southall, Martin Freer, Alan Moody, and Mark Porter. Anthropometric Study to Update minimum Aircraft Seating standards. Technical report, ICE Ergonomics Ltd, July 2021.

[51] Jan Roskam. *Airplane design*. DARcorporation, Lawrence, KS, 1986.

[52] G. J. J Ruijgrok. *Elements of airplane performance*. Delft Academic Press, Delft, 2009.

[53] Carlo Santulli. Post-impact damage characterisation on natural fibre reinforced composites using acoustic emission. *NDT E International*, 34(8):531–536, 2001.

[54] D. G. Simons and M. Snellen. *Aircraft Noise and Emission Part A: Introduciton to general acoustics and aircraft noise*. AE4431. Delft University of Technology, Delft, September 2020.

[55] Jos Sinke. *Production of Aerospace Systems (AE3211-II)*. Delft University of Technology.

[56] Tomas Sinnige, Nando van Arnhem, Tom C. A. Stokkermans, Georg Eitelberg, and Leo L. M. Veldhuis. Wingtip-mounted propellers: Aerodynamic analysis of interaction effects and comparison with conventional layout. 56(1):295–312.

[57] Tomas Sinnige, Tom Stokkermans, Nando van Arnhem, and Leo L. Veldhuis. Aerodynamic Performance of a Wingtip-Mounted Tractor Propeller Configuration in Windmilling and Energy-Harvesting Conditions. In *AIAA Aviation 2019 Forum*, Dallas, Texas, June 2019. American Institute of Aeronautics and Astronautics.

[58] Melvin H. Snyder and Glen W. Zumwalt. Effects of wingtip-mounted propellers on wing lift and induced drag. 6(5):392–397.

[59] Pavle M. Spasojevic. Chapter 15 - thermal and rheological properties of unsaturated polyester resins-based composites. In Sabu Thomas, Mahesh Hosur, and Cintil Jose Chirayil, editors, *Unsaturated Polyester Resins*, pages 367–406. Elsevier, 2019.

[60] Bing Tao Liu, Guang Yu Zhu, and Peng Ju Ding. The research progress of epoxy resin coating in building waterproof. *Advanced Material Research*, 671:1779–1782, march 2013.

[61] Egbert Torenbeek. *Synthesis of Subsonic Airplane Design*. Delft University Press, Delft, 1982.

[62] Falko Ueckerdt, Christian Bauer, Alois Dirnaichner, Jordan Everall, Romain Sacchi, and Gunnar Luderer. Potential and risks of hydrogen-based e-fuels in climate change mitigation. *Nature Climate Change*, 11 (5):384–393, May 2021.

[63] G.A.M. van Kuik. *Handbook of Wind Energy Aerodynamics*. Springer, 2020.

[64] Karen Willcox. Aircraft systems engineering: Cost analysis, 2004.

[65] Jun Xu, Xiang Gao, Chong Zhang, and Sha Yin. Flax fiber-reinforced composite lattice cores: A low-cost and recyclable approach. *Materials Design*, 133:444–454, 2017.

[66] Tara I. Yacovitch. *Exhaust emissions from in-use general aviation aircraft*. Number 164 in ACRP Airport Cooperative Research Program Research report. Transportation Research Board of the National Academies, Washington, DC, 2016.

[67] Libo Yan, Nawawi Chouw, and Krishnan Jayaraman. Flax fibre and its composites - A review. *Composites Part B: Engineering*, 56:296–317, January 2014.

[68] K.T. Yeo and J.H. Ning. Integrating supply chain and critical chain concepts in engineer-procure-construct (EPC) projects. *International Journal of Project Management*, 20(4):253–262, May 2002.

[69] Abdulrahman Yussef, Edd Gibson, Mounir El Asmar, and David Ramey. Front End Engineering Design (FEED) for Large Industrial Projects: FEED Maturity and Its Impact on Project Cost and Schedule Performance. *Construction Research Congress 2018*, April 2018.

[70] Zhao, Wim Verhagen, and Curran. Disposal and recycle economic assessment for aircraft and engine end of life solution evaluation. *Applied Sciences*, 10:522, 1 2020.

[71] L. Zhu, N. Li, and P.R.N. Childs. Light-weighting in aerospace component and system design. *Propulsion and Power Research*, 7(2):103–119, June 2018.

A
Numbers

Table A.1 presents the overall set of final aircraft parameters calculated for the *Twin Puffin*.

Table A.1: Final aircraft design

Parameter	Value	Unit	Parameter	Value	Unit
α_0 wing airfoil	-5.2	deg	power required during cruise	52.7	kW
α_{stall} airfoil	14.9	deg	propeller incidence angle	2.86	deg
$\eta_{propeller}$	0.82	-	range	1247	km
aileron chord to wing chord ratio	0.40	-	rear spar chordwise position	0.55	-
aileron inboard edge location	5.11	m	rear spar sweep	-2.78	deg
aileron inboard edge location	6.75	m	specific energy battery	180	$kW\,h\,kg^{-1}$
aircraft length	8.95	m	specific power ICE	800	$kg\,kW^{-1}$
aircraft mass at end of cruise	1640	kg	take-off roll at 0 ft	61.0	m
aircraft mass at start of cruise	1701	kg	take-off roll at 2500 ft	65.4	m
airfoil	USA-40-B	-	take-off run at 0 ft	275.5	m
airfoil lift slope	5.73	-	take-off run at 2500 ft	282.7	m
airfoil thickness ratio	0.14	-	take-off time (50 ft)	54	s
axial separation between engines	0.10	m	thrust take-off 2500 ft	4.7	kN
battery mass	52.1	kg	ultimate load factor	6	
$c_{l_{des}}$ airfoil	0.52	-	v_{cruise}	54.9	$m\,s^{-1}$
$c_{l_{des}}$ wing	0.47	-	v_{stall} cruise	24.3	$m\,s^{-1}$
$c_{l_{max}}$ clean configuration	1.67	-	v_{stall} landing 0 ft	13.9	$m\,s^{-1}$
$c_{l_{max}}$ high lift device	2.61	-	v_{stall} landing 2500 ft	14.4	$m\,s^{-1}$
$c_{l_{max}}$ landing blown 0 ft	4.48	-	v_{stall} take-off 0 ft	14.05	$m\,s^{-1}$
$c_{l_{max}}$ landing blown 2500 ft	3.98	-	v_{stall} take-off 2500 ft	14.6	$m\,s^{-1}$
$c_{l_{max}}$ take off blown 0 ft	5.32	-	vertical tail area	4.40	m^2
$c_{l_{max}}$ take off blown 2500 ft	4.67	-	vertical tail aspect ratio	1.20	-
$c_{l_{max}}$ wing airfoil	1.85	-	vertical tail chord to rudder chord ratio	0.30	-
c_{m_α}	-0.195	-	vertical tail leading edge sweep	5.73	deg
$c_{m_{ac}}$ airfoil	-0.08	-	vertical tail MAC	1.37	m
$c_{m_{ac}}$ wing	-0.0812	-	vertical tail quarter chord sweep	20.1	deg
$c_{m_{ac}}$ wing landing	-0.346	-	vertical tail root chord	1.59	m
$c_{m_{ac}}$ wing take off	-0.319	-	vertical tail span	1.63	m
cabin length	5.50	m	vertical tail taper ratio	0.70	-
cruise altitude	3000	m	vertical tail thickness to chord	0.12	-
cruise Mach	0.20	-	wing area	28.14	m^2
Cruise thrust	1.9	kN	wing aspect ratio	8.00	-
Empennage mass	221	kg	wing blown lift slope landing 0 ft	8.32	-
Fixed equipment mass	103	kg	wing blown lift slope landing 2500 ft	7.97	-
Flap hinge chordwise location	0.60	-	wing blown lift slope take-off 0 ft	9.86	-
Flap hinge sweep	-3.03	deg	wing blown lift slope take-off 2500 ft	9.35	-
Front spar chordwise location	0.2	-	wing chord MAC	1.90	m
Front spar sweep	-1.27	deg	wing effective aspect ratio at cruise	8.91	-

Table A.1: Final aircraft design

Parameter	Value	Unit	Parameter	Value	Unit
Fuel mass	106.54	kg	wing leading edge sweep	0	deg
Fuselage height	1.41	m	wing mass	368	kg
Fuselage mass	169	kg	wing quarter chord sweep	-1.27	deg
Fuselage width	1.30	m	wing root chord	2.21	m
generator power	134	kW	wing span	15	m
half chord sweep	-2.53	deg	wing taper ratio	0.7	-
High lift engines motor mass	7.30	kg	wing thickness to root chord ratio	0.136	-
High lift engines propeller mass	1.18	kg	wing three quarter chord sweep	-3.8	deg
horizontal tail area	2.23	m^2	wing tip chord	1.55	m
horizontal tail aspect ratio	6.5	-	Wing tip engine motor mass	9.21	kg
horizontal tail downwash gradient	0.20	-	Wing tip engine propeller mass	7.26	kg
horizontal tail leading edge sweep	0	deg	wing trailing edge sweep	-5.0	°
horizontal tail mac	0.585	m	x-location AC horizontal tail	7.72	m
horizontal tail root chord	0.585	m	x-location AC vertical tail	7.75	m
horizontal tail span	3.81	m	x-location AC wing	0.716	m
horizontal tail taper ratio	1	-	x-location battery	2.77	m
horizontal tail thickness to chord ratio	0.09	-	x-location cargo max	3.50	m
ICE mass	151	kg	x-location cargo min	2	m
landing gear mass	54	kg	x-location centre of gravity aft	4.67	m
landing roll at 0 ft	87.8	m	x-location centre of gravity forward	3.90	m
landing roll at 2500 ft	86.7	m	x-location centre of gravity OEW	4.63	m
landing run at 0 ft	442.5	m	x-location leading edge MAC wing	3.76	m
landing run at 2500 ft	441.4	m	x-location main landing gear	3.65	m
lift over drag cruise	12.7	-	x-location seats first row	1	m
MAC chordwise position cruise	0.201	-	x-location seats second row	2	m
MAC chordwise position landing	0.219	-	x-location tail landing gear	8.95	m
MAC chordwise position take-off	0.223	-	y-location aileron inboard	5.11	m
max aileron deflection	30	deg	y-location flap inboard	0.72	m
maximum airport altitude	762.00	m	y-location flap outboard	6.75	m
MTOW	1781	kg	y-location location MAC	3.53	m
number of engines (incl. tail)	14	-	y-location main landing gear	1.58	m
number of seats	4	-	z-location AC horizontal tail	-0.13	m
OEW	1201	kg	z-location AC vertical tail	0.38	m
Oswald efficiency factor cruise	0.795	-	z-location AC wing	0	m
passenger mass	86	kg			

Change Record

This change record provides an overview of the changes that have been done for the final report. The changes are based on the feedback received on the draft report and at the final review.

Table A.2: Documentation of the changes made to this document after the draft version.

SECTION	CHANGE	STATUS
General	To make the report and its structure easier to understand for the reader, the report has been divided into three parts: setting up the design space, the detailed design methods, and the final aircraft design	Done
General	To standardise the format of the report, the format of the tables has been adjusted across the document	Done
General	Legends have been added to certain plots where they were needed	Done
General	All aircraft renders have been updated to account for the new tail engine configuration. The wing span and distance between the booms, both initially incorrect in the images, have been corrected	Done
Blank Page	Has been included after the title page. The applicable blank page label has been added	Done
Executive Summary	Commented about how paradoxical it is that traditional bush planes go into nature but are very polluting. Remarked that jet fuel and biofuels can also be used	Done
Table of Contents	Removed subsections to make the TOC shorter and easier to read	Done
Nomenclature	Completed and reformatted. Divided it into *Abbreviations*, *Greek Symbols* and *Latin Symbols*	Done
List of Tables	Has been added to the report	Done
List of Figures	Has been added to the report	Done
Introduction	Adjusted to explain the use of parts	Done
2.1	Included number of students. Grammar fixed	Done
3.	Expanded chapter introduction to explain link between market analysis and requirements. Grammar fixes	Done
3.2	To highlight the connection to the objective function and requirements, divided the section into three subsections: *Main Competitive Aircraft*, *Analysis of Aircraft Value* and *Market Requirements*	Done
3.2.2	Moved part of the analysis originally in 7.3.2 to here. Explained how the analysis of the competition will be used for the objective function	Done
3.2.3	Highlighted the two additional requirements flowing from the market analysis	Done
3.3	Corrected incorrect claims about distributed propulsion (most notably the one in 3.3.2 which was only true for BWB aircraft)	Done
3.4	Added subsection *General Market Trends* and *Achievable Market Share* to better structure the content. Also removed the figure showing general economic effects on the aircraft market (previously figure 3.2)	Done
3.4.1	In the new section about general market trends, added remark on trends such as ”flight shaming” and how the *Twin Puffin* may partly solve this problem	Done

3.4.3	Included footnote that night flying will be limited to VFR nightflight with illuminated runways	Done
4.1	Renamed to *Stakeholder Requirements*. Linked market analysis and requirements more by explaining how requirements are a result of the stakeholder and market analysis	Done
4.2	Added missing explanations for system requirements. Rephrased noise requirements in terms of decibel	Done
5.1.3	Remarked about use of biofuels	Done
5.2	Remarked about use of biofuels	Done
6.2.1	Included wires as one of the dangers to pilots	Done
6.2.2	Switched from conventional to natural epoxy and explained the implications	Done
6.3.1	Remarked about use of biofuels	Done
6.5.2	Revised explanation of how and why lift augmentation is filtered out to find the design lift coefficient. Removed the previous figure 6.14 as it was more confusing than helpful	Done
6.5.5	Expanded explanation of which engines are active for the lift distribution shown in the figure in this section	Done
6.7	Revised the section to explain why the blowing of the horizontal tail is necessary and what its effects are. Adjusted section for new placement of horizontal tail propellers and their effect on the vertical tail. Thus also moved the vertical tail parts after the horizontal tail parts	Done
6.9	Removed the talk with Ir. Ferdinand Postema as a footnote citation. Included different source instead	Done
6.10.	Added section summarising the outcomes of the subsystem design methods. Done to more logically connect this chapter to the final design presented in Chapter 8	Done
7.	Grammar fixed. Rewrote partially for clarity	Done
7.2.3	Updated the approach used to find the possible climb rates. Extended the method to account for a ”green climb” and a maximum performance climb. Added obtaining aircraft noise	Done
7.3.2	Moved part of the content to the market analysis chapter. Commented on valid range for retail price estimate. Fixed grammar	Done
7.3.4	Updated the results of the optimisation to show the aircraft values on a relative rather than an absolute scale	Done
7.4	Reformatted this into a section without subsection as the subsection header did not add additional value	Done
8.1.3	Changed values for climb rate and noise	Done
8.1.5	Added this section to visualise the noise of the aircraft	Done
8.1.6	Added illustrations of the climate control and de-icing system	Done
8.2.1	Added subsection about general pilot-aircraft interaction. Mentioned split between manual pilot inputs and automatic control of engines and mobile surfaces	Done
8.2.6	Combined the height-velocity diagram with a time-altitude diagram for better visualisation	Done
8.3	Updated climb rate values	Done
8.5.5	Added renders of the propellers for better visualisation	Done
8.7	Emphasised effect of blown horizontal tail. Expanded on stability and control during different flight phases. Found and discussed relevant aircraft eigenvalues	Done
8.9.1	Added remark about the two types of throttle	Done
9.3.1	Revised value comparison and text for gas emissions and noise pollution. Updated to account for the use of natural epoxy. Expanded on the sustainability of flax fibre	Done
9.8	Adjusted radar plots for new climb rate values. Expanded text	Done
10.2.1	Revised method for program development cost	Done

10.2.2	Updated return on investments in line with the new development cost	Done
10.2.4	Added explanation and estimation of end-of-life cost	Done
Conclusion	Strengthened comparison to traditional polluting bush planes	Done
Bibliography	Corrected the format of certain citations	Done
Appendix	Shortened the appendix of aircraft values to remove irrelevant parameters	Done